Chapter 5

Interferometers

Michelson Interferometer

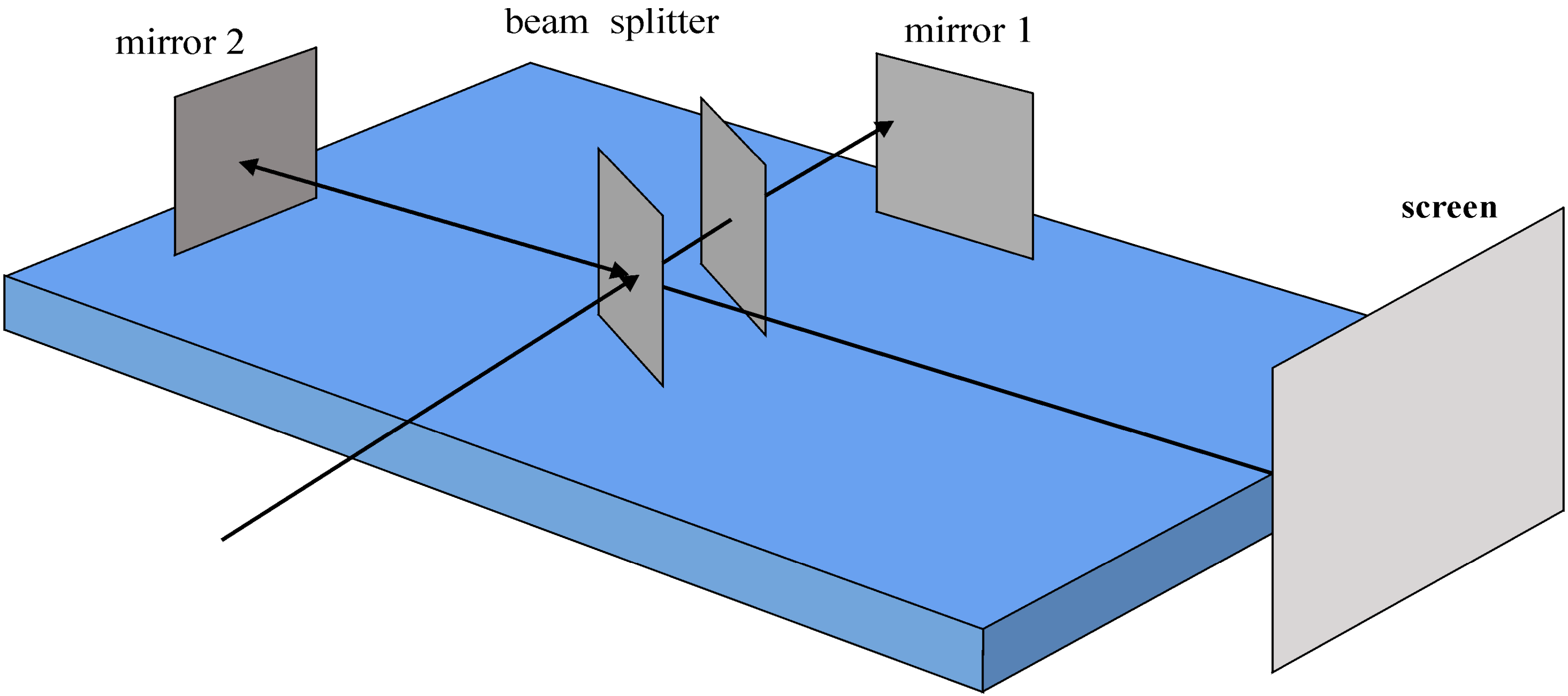

Two cases of the light interference:

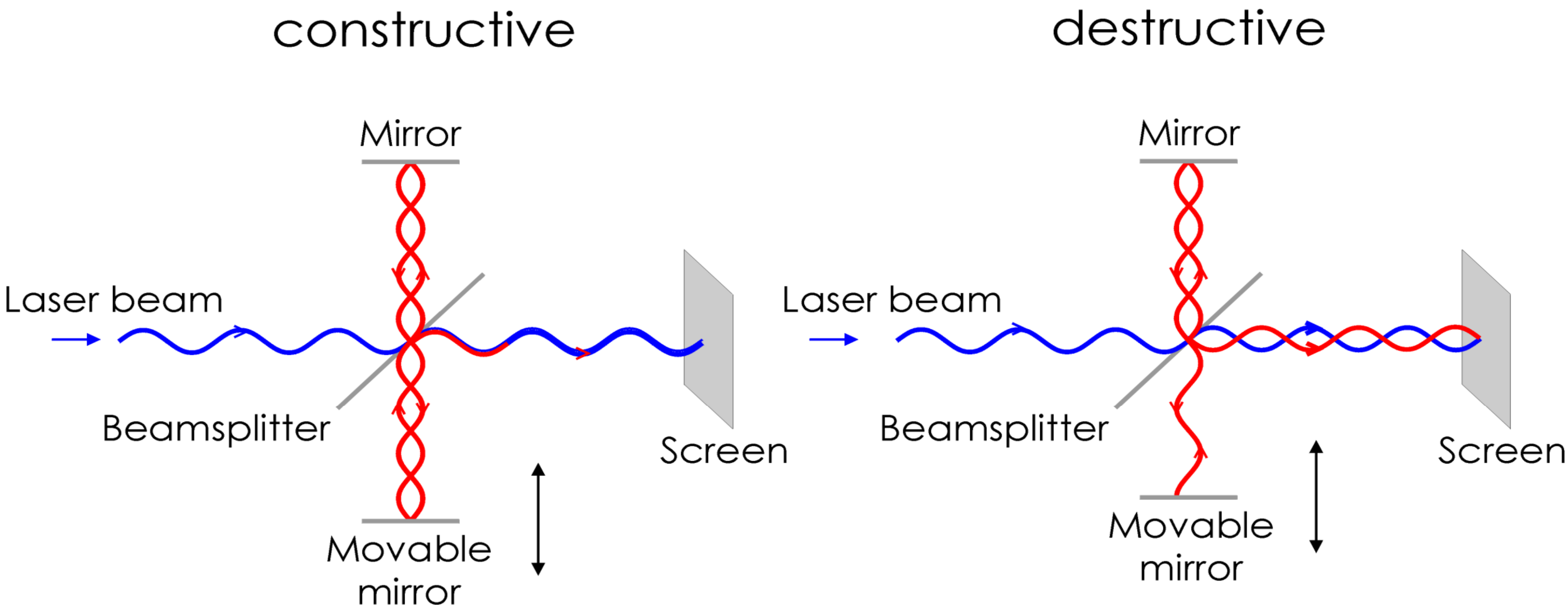

Mach-Zehnder Interferometer

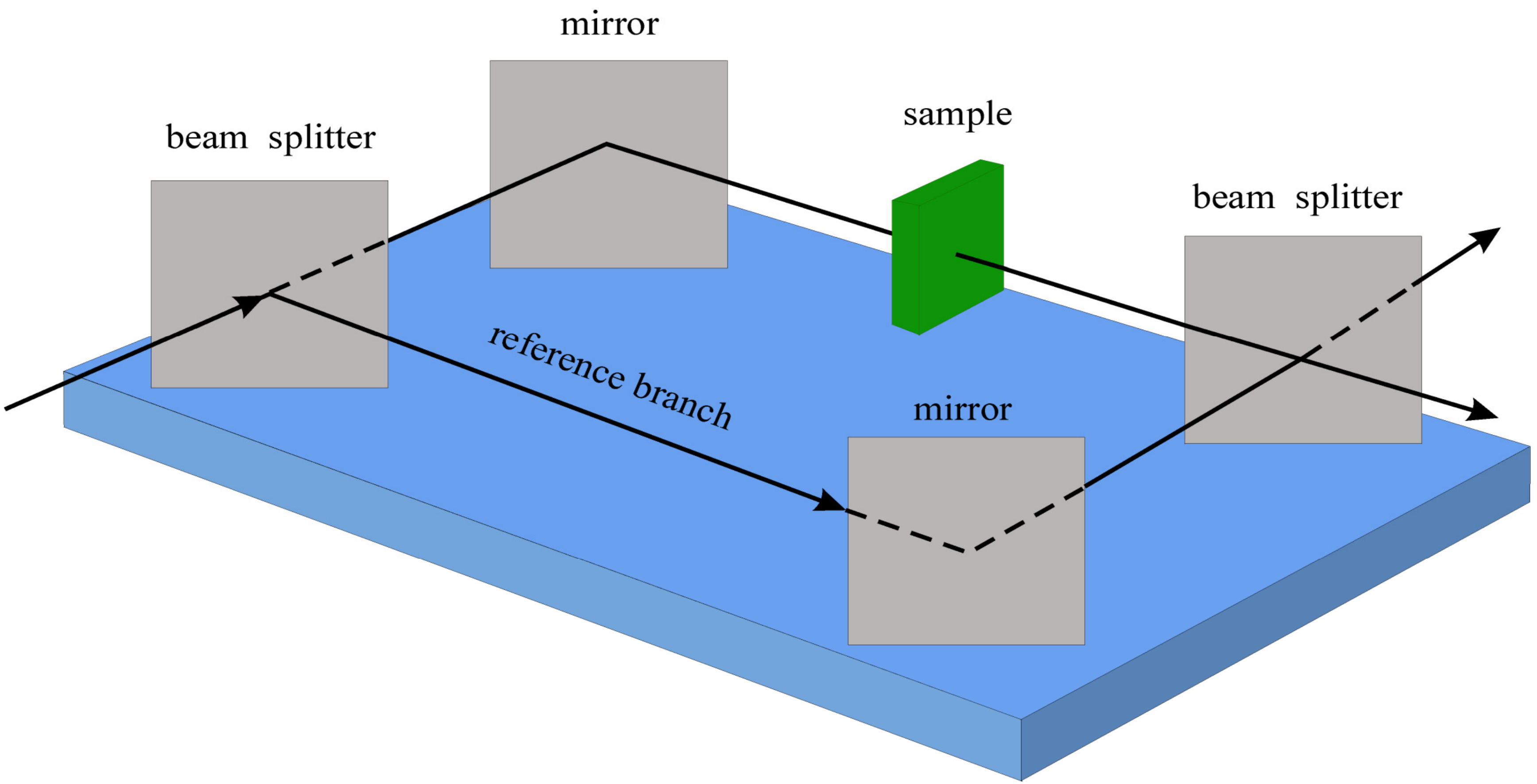

Mach-Zehnder Interferometer on a polymer basis

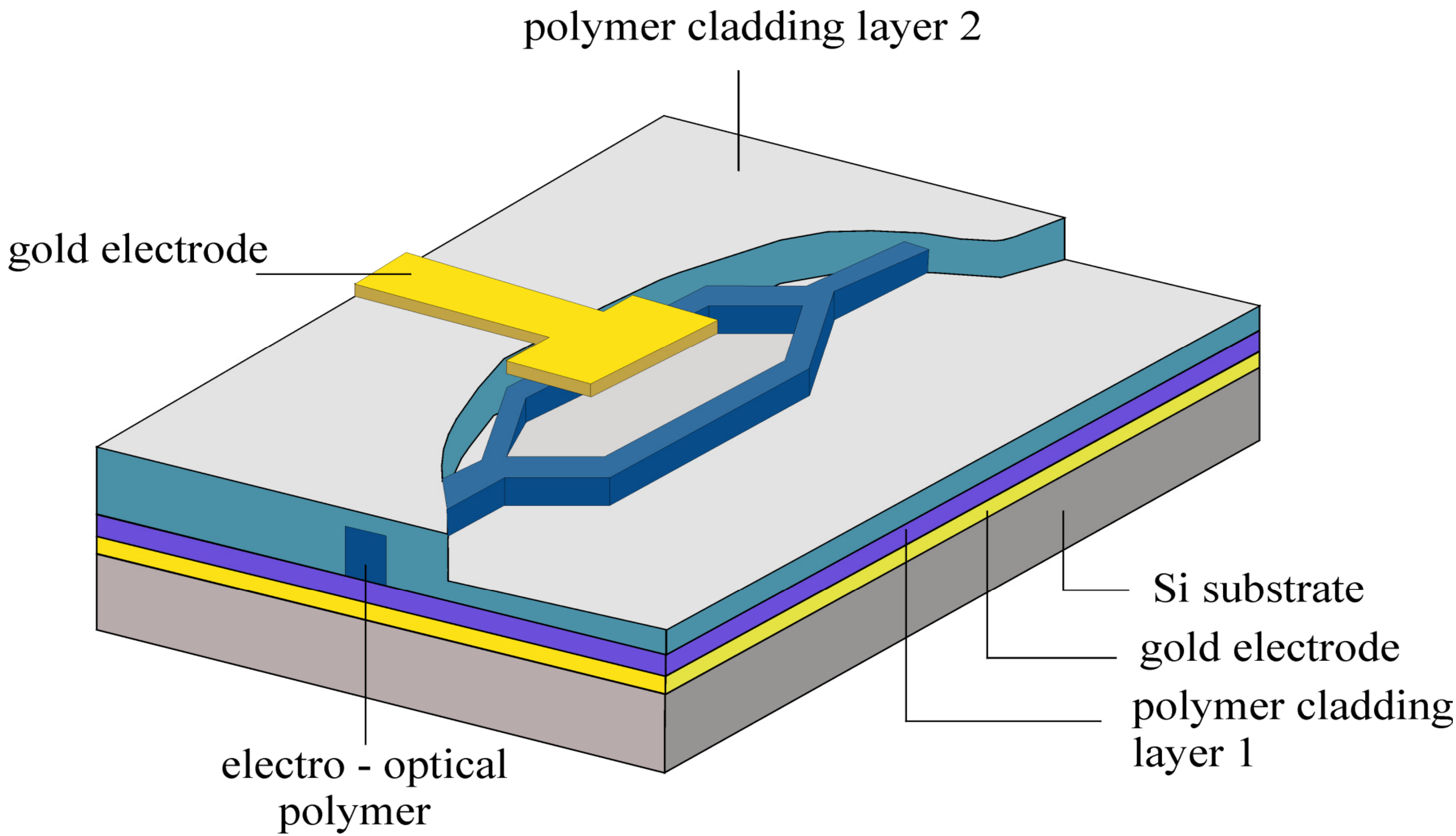

Fabry - Pérot (FP) Interferometers

- This chapter (chapter 5) handles the ideal FP interferometer
  - based on 2 ideal mirrors having no extension in z-direction
  - ideal mirrors are 2D and not 3D

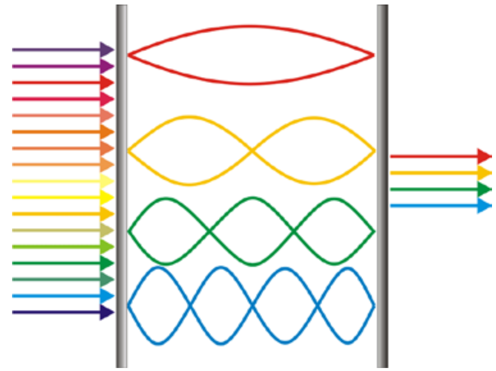

- Next chapter (chapter 6) handles real mirrors having an extension in z-direction.
  - real multilayer mirrors (DBR type) are 3D

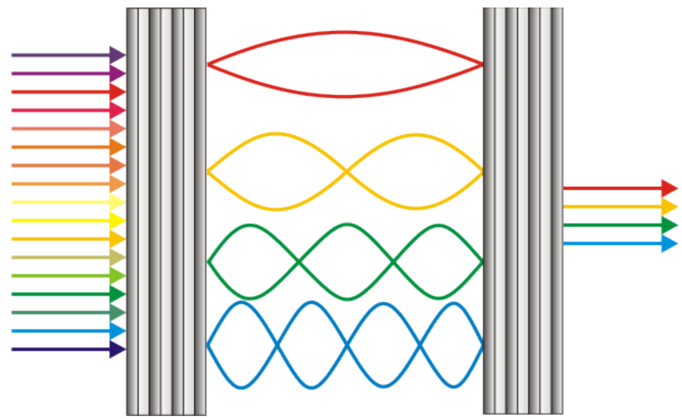

- In chapter 6, real interferometer will be treated subsequently, on the basis of these real mirrors.

Fabry - Pérot Interferometer

- Ray model with ideal unextended mirrors:

– Using two plane parallel layers (unextended 2D mirrors) with respective **electrical field** transmission and reflection coefficients (r, t)

– The angled incidence is shown here to clearly visualize the propagation flow

– We observe constructive and destructive interferences of transmitted and reflected beams

– Summing up all rays via a mathematical series:

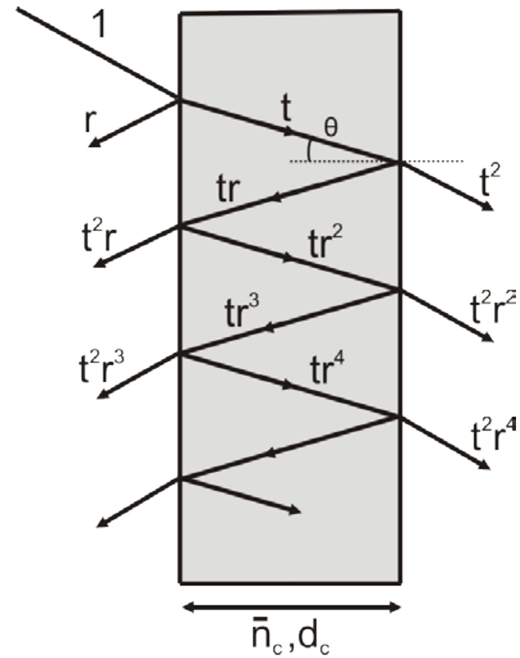

electrical field:
$$\boxed{\begin{aligned} E_r &= r(1+t^2e^{j\delta}+t^2r^2e^{j2\delta}+\ldots) \\ E_t &= t^2(1+r^2e^{j\delta}+r^4e^{j2\delta}+\ldots) \end{aligned}}$$

R and T as the **intensity** of reflection and transmission, respectively.
δ is the roundtrip phase shift. We obtain the **Airy formula.**

$$R = \mathrm{Re}(E_r)^2 = \frac{\dfrac{4r^2}{(1-r^2)^2}\sin^2(\dfrac{\delta}{2})}{1+\dfrac{4r^2}{(1-r^2)^2}\sin^2(\dfrac{\delta}{2})};$$

$$T = \mathrm{Re}(E_t)^2 = \frac{1}{1+\dfrac{4r^2}{(1-r^2)^2}\sin^2(\dfrac{\delta}{2})}$$

$$Where, \delta = \frac{4\pi n_c d_c \cos\theta}{\lambda}$$

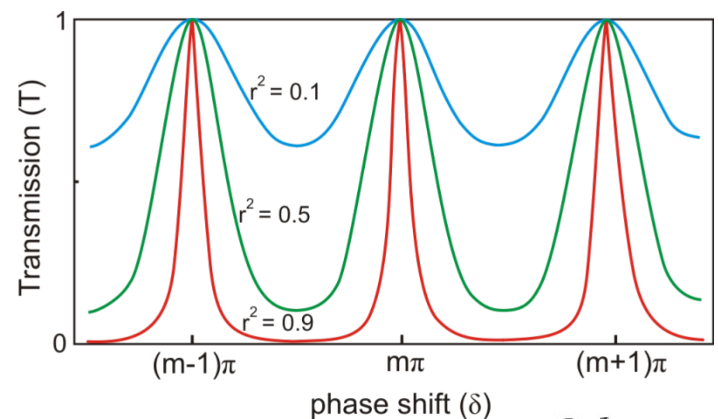

Position of maxima depends on cavity length

$$\lambda_c = \frac{2d_c}{m} \quad \text{(air cavity)}$$

Fabry - Pérot (FP) etalon including absorption

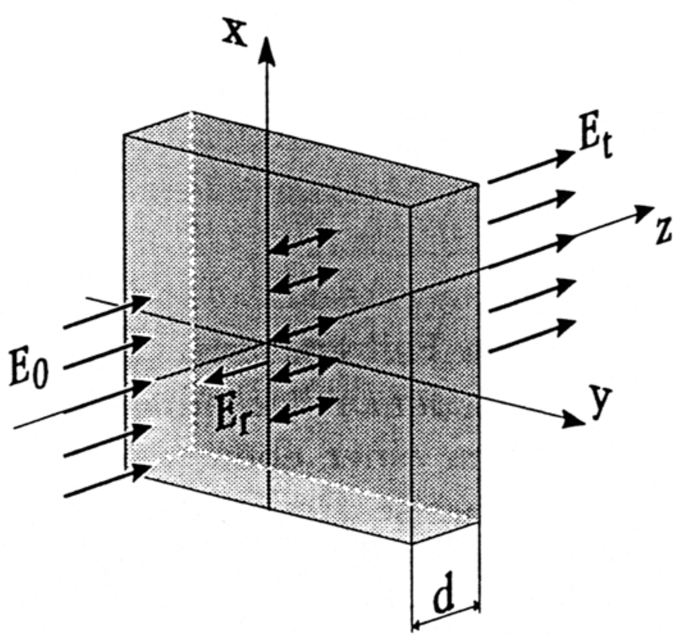

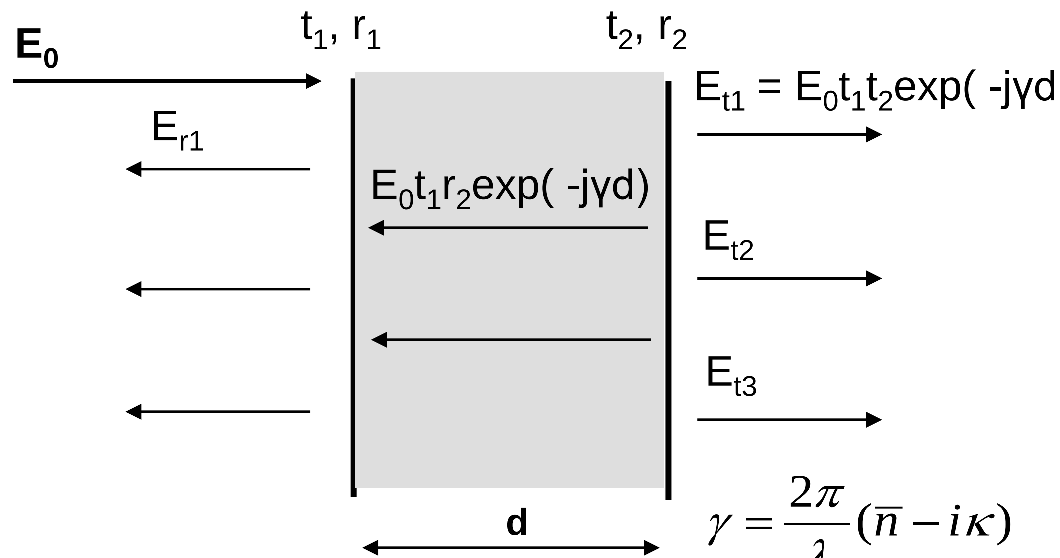

$$\gamma = \frac{2\pi}{\lambda}(\overline{n} - i\kappa)$$

κ = extinction coefficient

γ = complex refractive index

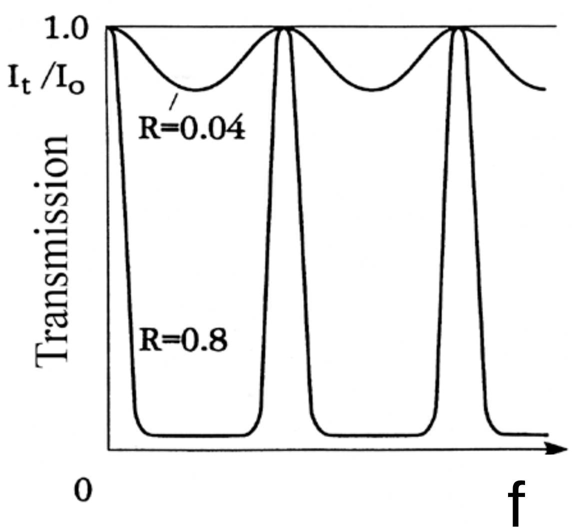

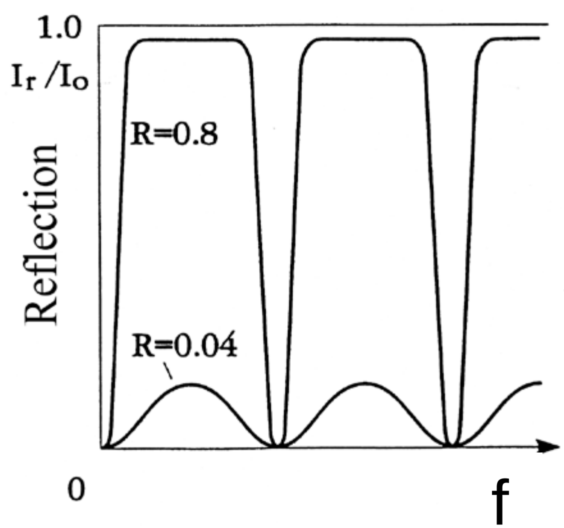

← for weak absorption

Fabry Pérot Interferometer
– ideal case, not extended mirror

1. case: large cavity thickness d

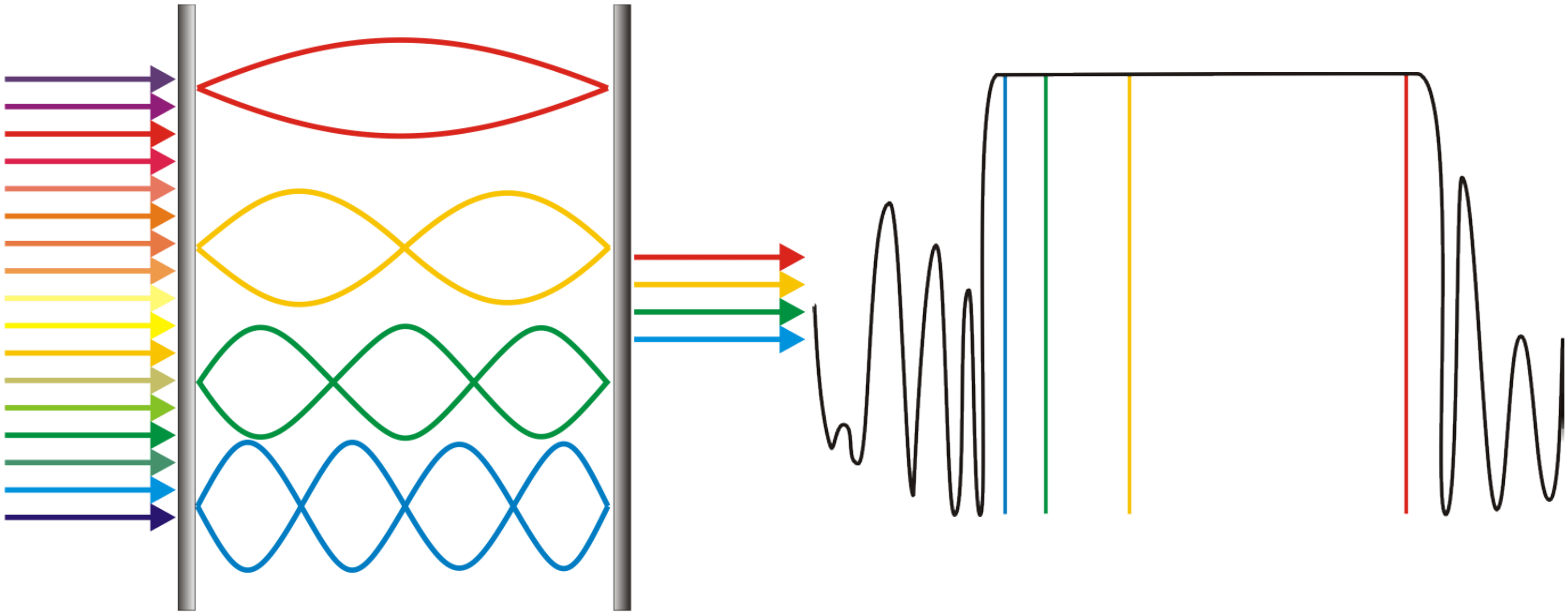

here 4 modes are located inside the spectral range of the stopband

2. case: small cavity thickness d

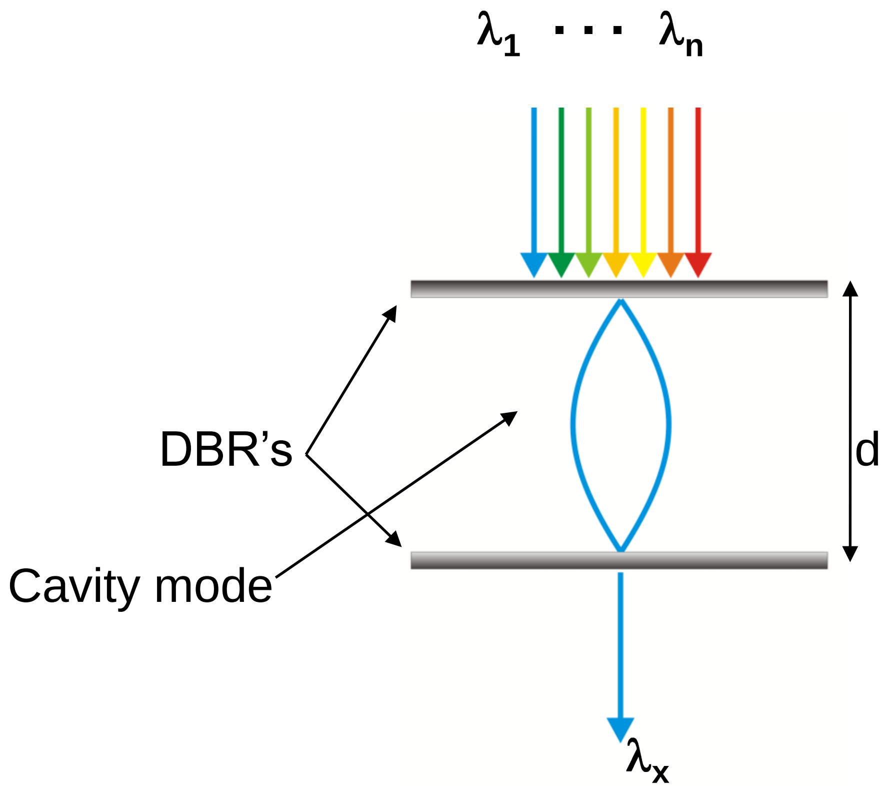

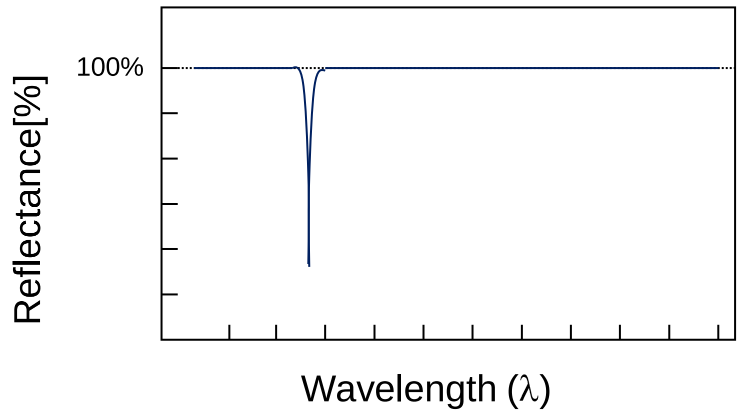

only a single mode is located inside the spectral range of the stopband

Fabry – Pérot Interferometer

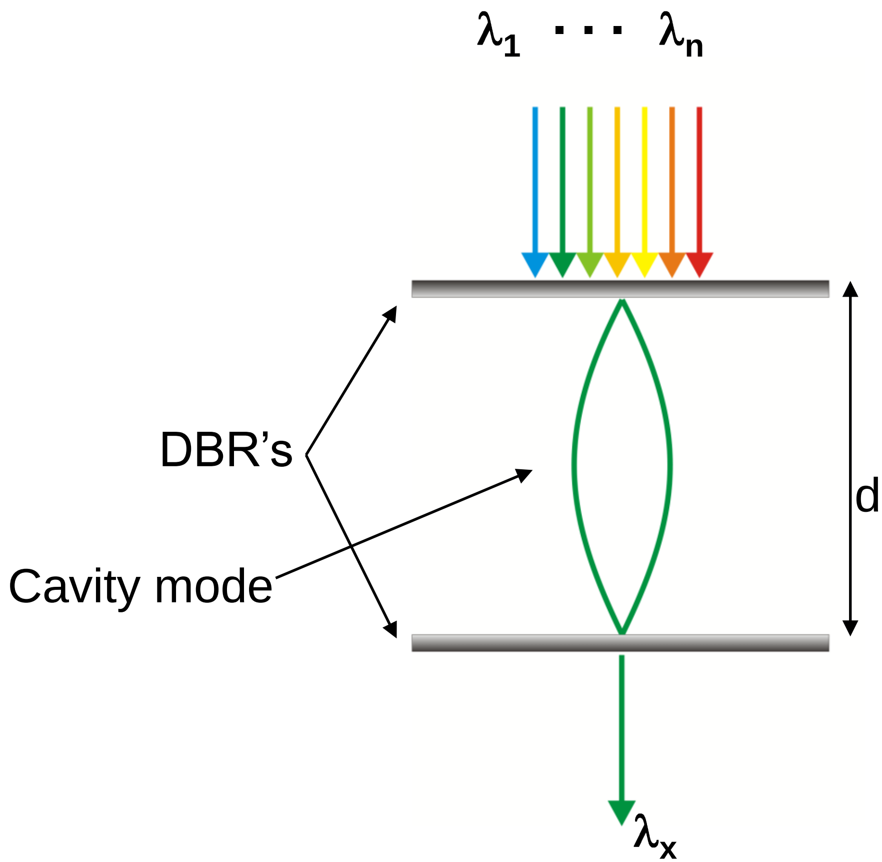

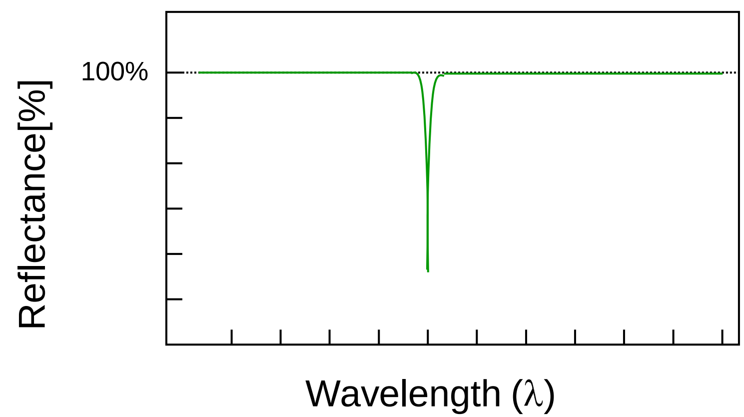

only a single mode is located inside the spectral range of the stopband

Fabry – Pérot Interferometer

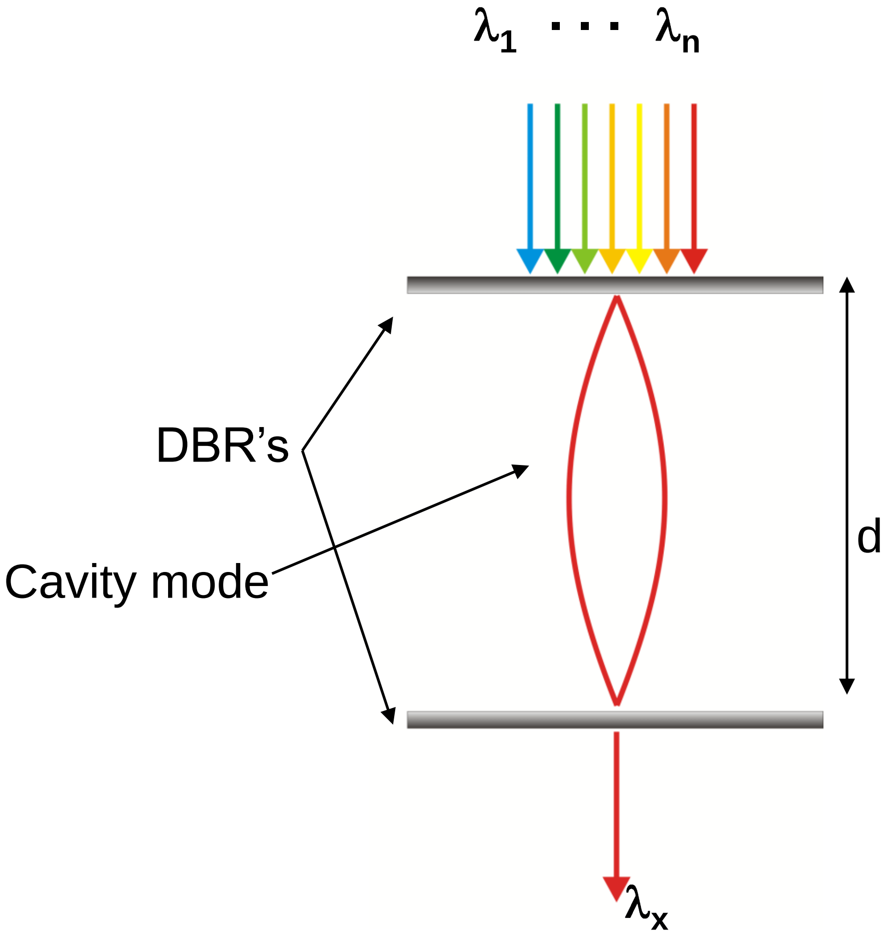

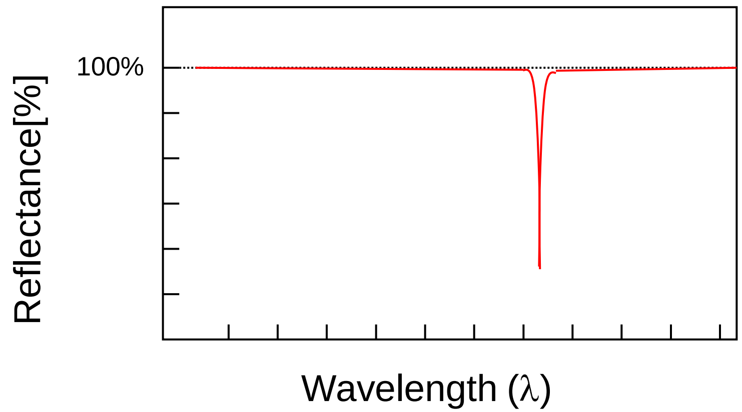

only a single mode is located inside the spectral range of the stopband

Chapter 6

Multilayer mirrors and interference filters

Distributed Bragg Reflector (DBR) mirror

A dielectric mirror including layers of high and low refractive index, alternatively.

Angled incidence

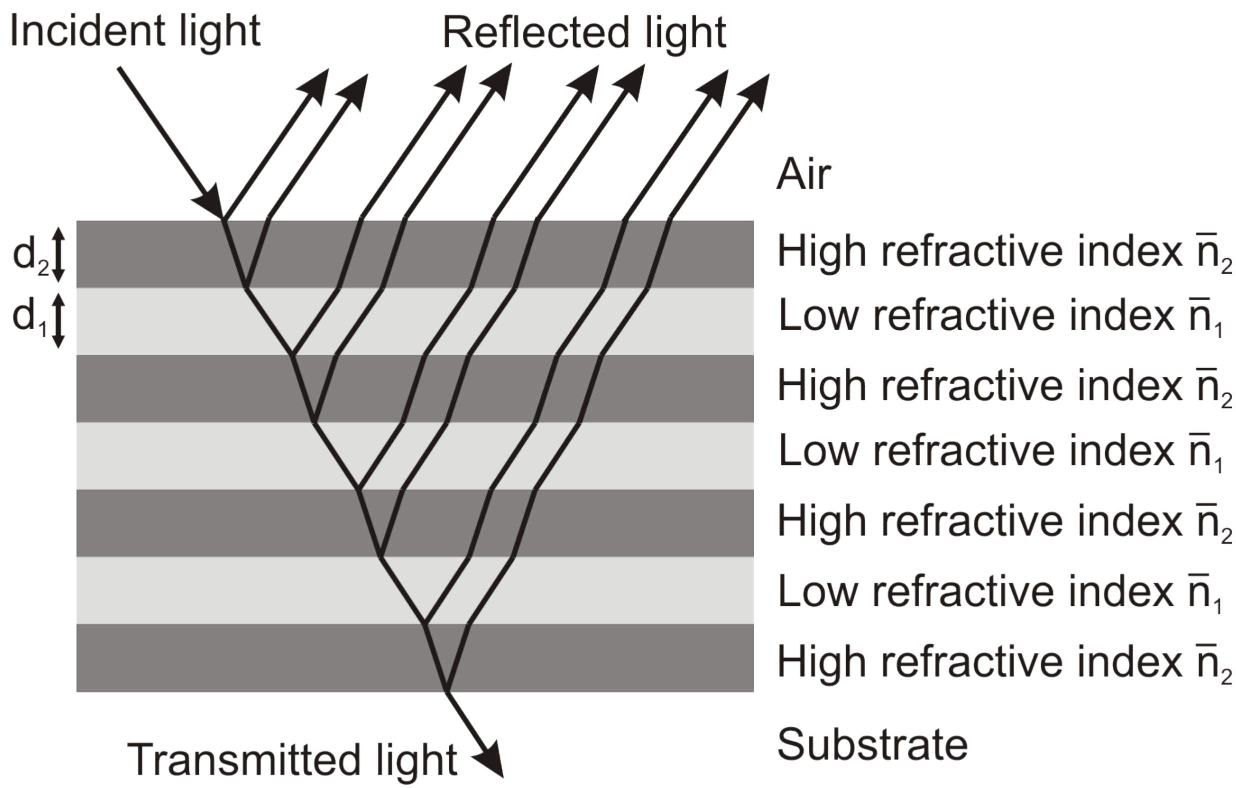

DBR mirrors can be design using tailored values for d_1, d_2, $\bar{n}_1$, $\bar{n}_2$ to obtain very high reflectivity (very close to 100%) within a desired spectral range, which we later will indicate as "stop band".

Note: in comparison, metallic mirrors (Ag, Al, Au) only reach reflectivity between 90% and 95%.

Distributed Bragg Reflector (DBR) mirrors

For constructive interference: $\Delta\varphi$ phase difference has to be 0, 2π, 4π,…

Vertical incidence

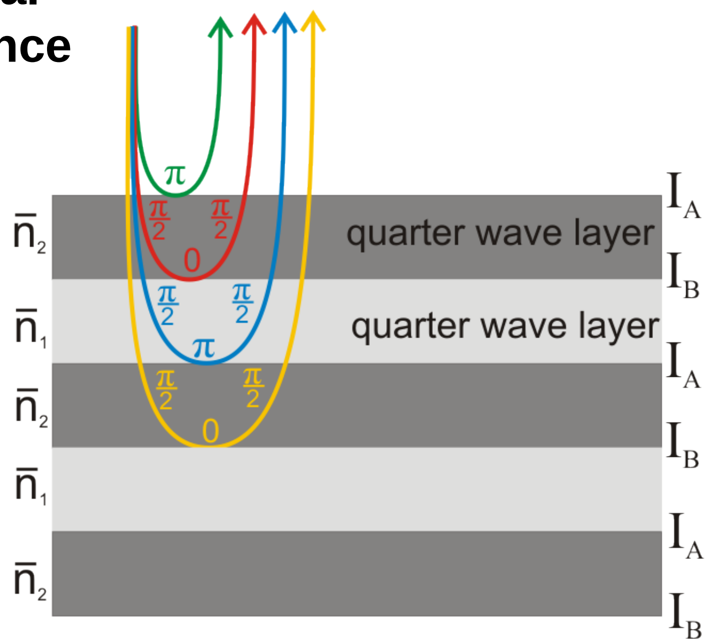

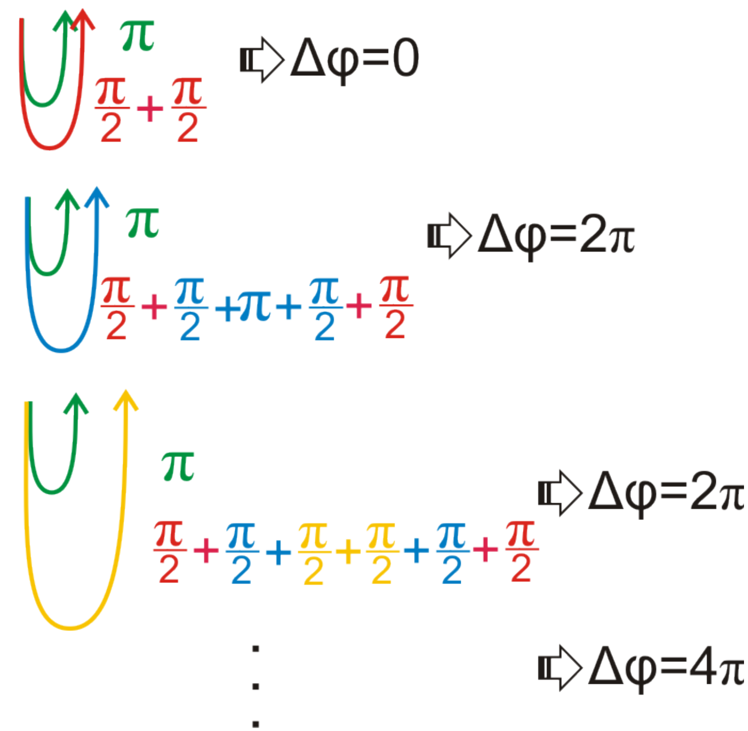

From Fresnel equations we obtain for vertical incidence a phase shift of $\Delta\varphi=\pi$ if the reflection occurs at the interface I_A (low against high refractive index).

We have $\Delta\varphi=0$ at an interface I_B (high against low refractive index)

Result for a mirror design:

e.g. $\overline{n}_1 d_1 = \frac{1}{4}\lambda$ e.g. $\overline{n}_2 d_2 = \frac{1}{4}\lambda$

(in general $d_i = \frac{\lambda}{4\overline{n}_i}, \frac{3\lambda}{4\overline{n}_i}, \frac{5\lambda}{4\overline{n}_i}$...)

A chain of two-ports in electrical engineering is treated via a matrics multiplication

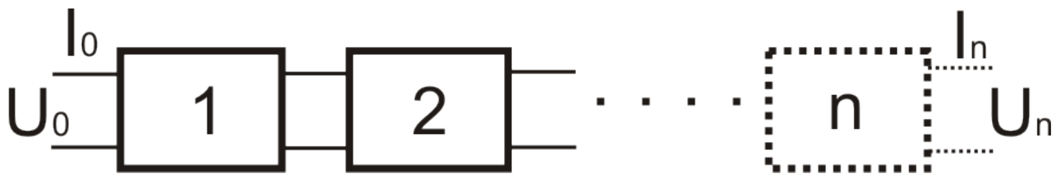

$$\begin{pmatrix} U_n \\ I_n \end{pmatrix} = \prod_{i=1}^{n} \underline{\underline{M}}_i \begin{pmatrix} U_0 \\ I_0 \end{pmatrix}$$

This can be also used in optics for a stack of dielectric layers

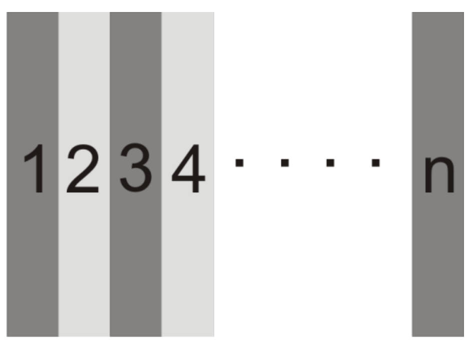

$$\begin{pmatrix} E_n \\ H_n \end{pmatrix} = \prod_{i=1}^{n} \underline{\underline{M}}_i \begin{pmatrix} E_0 \\ H_0 \end{pmatrix}$$

E_i electrical fields
H_i magnetic fields

Transmittance T, Reflectance R and Absorption A

The sum of transmittance T, reflectance R and absorption A is always one.

$$1 = T + R + A$$

First we consider
$A = 0$

$$1 = T + R$$

design wavelength
600nm

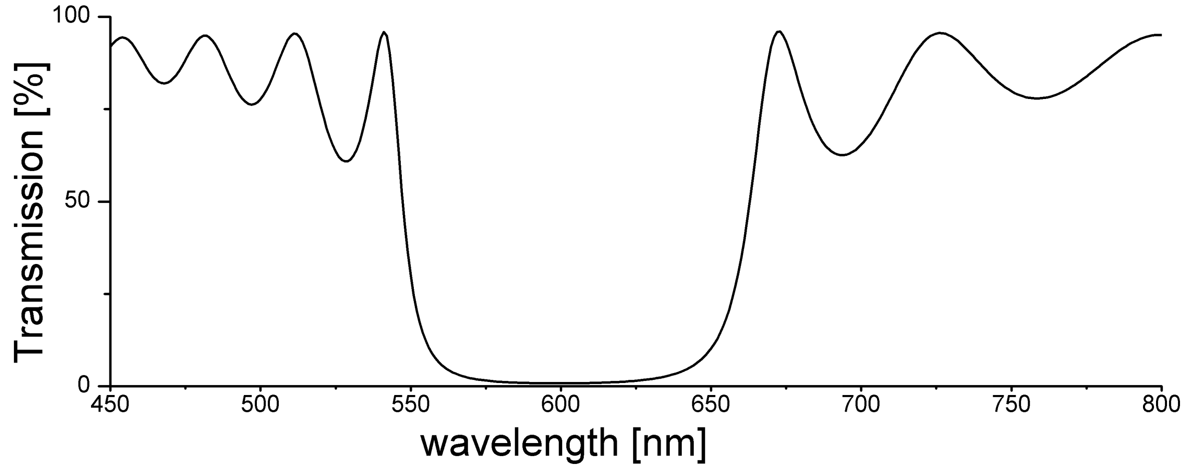

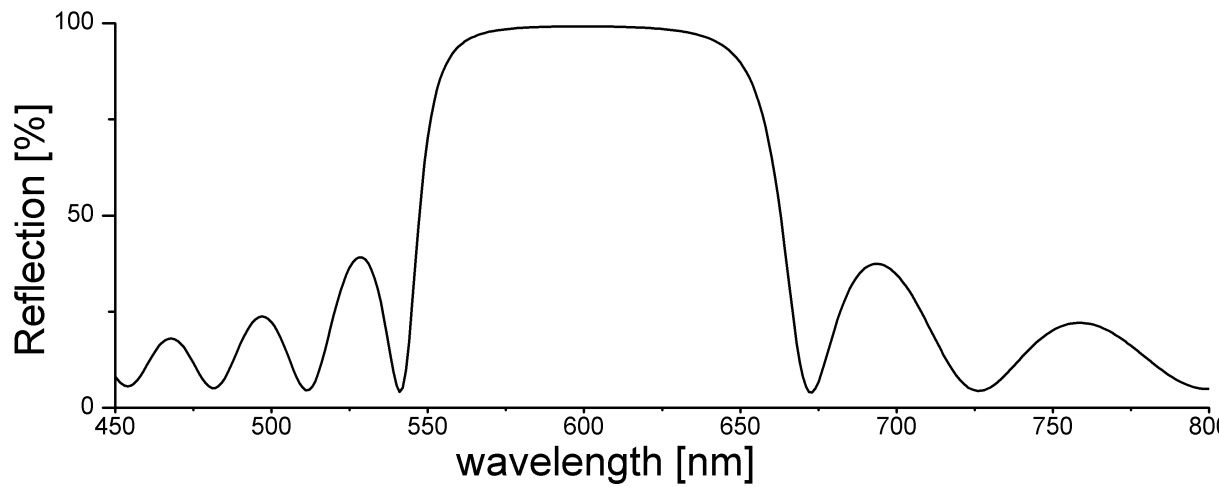

Bragg reflections of electromagnetic waves

X-ray diffraction at
lattice planes of
solid state crystals

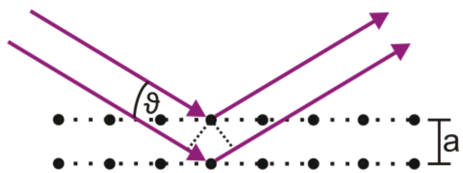

Bragg-condition:

$2a \sin\vartheta = m\lambda$

lattice parameter: $a \approx 0.3$ nm
X-ray wavelenght λ
m=1, 2, 3...

diffraction of light (IR) on periodically
aligned semiconductor layers (DBR structure)

constructive interference

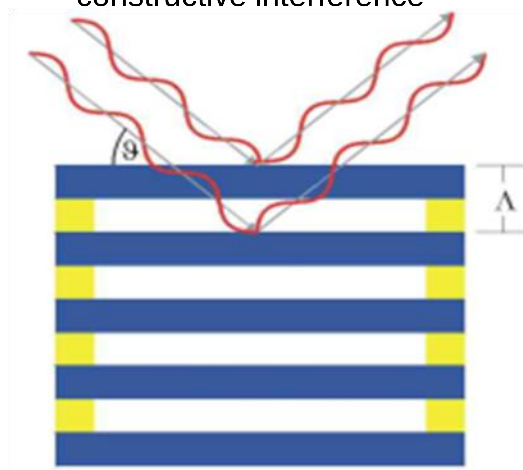

reflected lightwaves
with matching phase

destructive interference

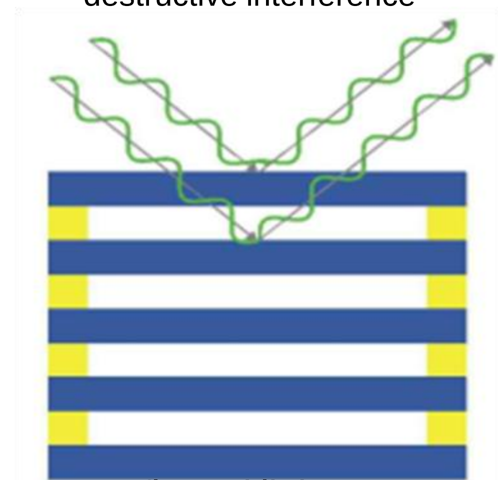

reflected lightwaves
with opposite phase

$$\Lambda = \frac{m\lambda_B}{2\,\bar{n}_{eff}\,\sin\vartheta}$$

lattice periodicity Λ= 90 ... 250 nm
Light wavelength λ_B=0.6 ... 1.5 µm (in air)

In chapter 5 we considered ideal mirrors having no extension.

In chapter 6 we now consider real mirrors of best reflectivity available.
Real mirrors are

- extended
- can have very high reflectivity
- are wavelength dependent
- have finite absorption

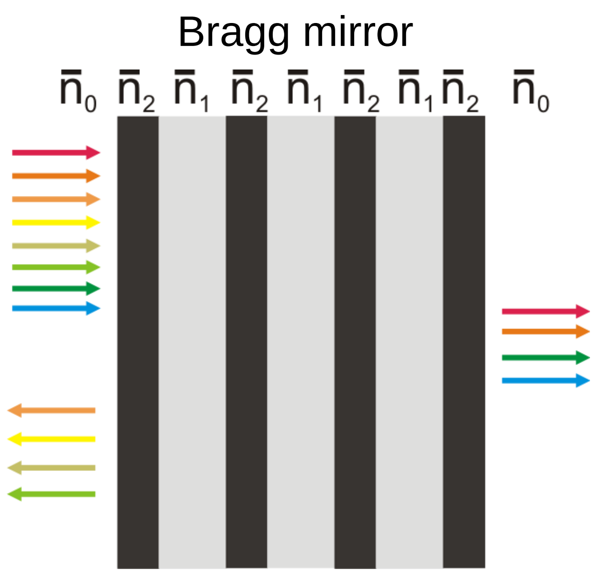

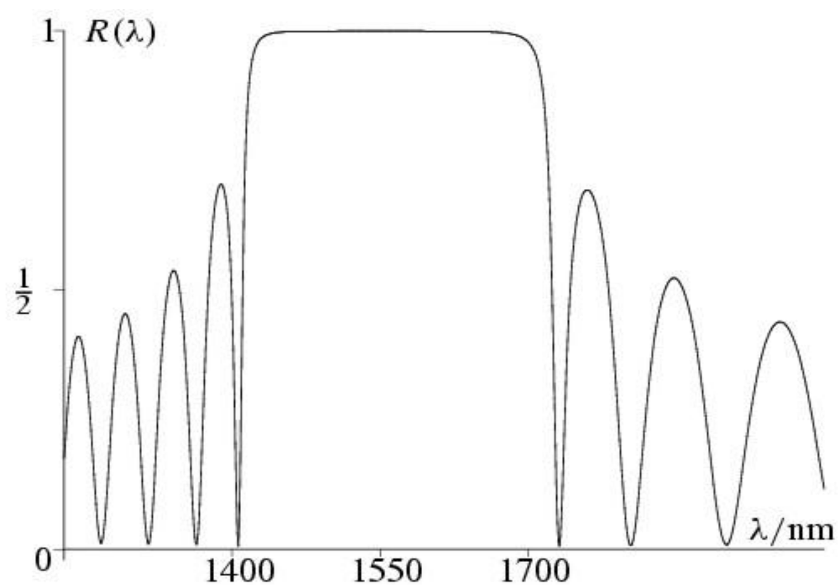

In this example the mirror is designed for a central wavelength (design wavelength) of 1.55µm.

Example: semiconductor DBR mirror

A multiple sequence as a multilayer mirror

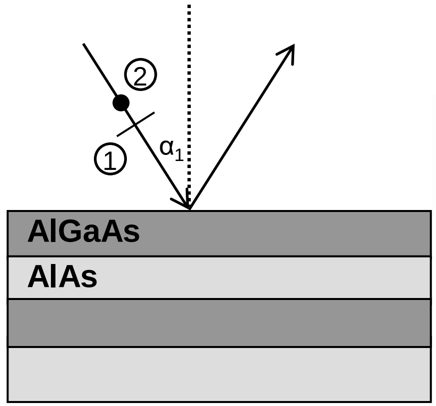

-
- In total 20 pairs
- AlGaAs / AlAs
-

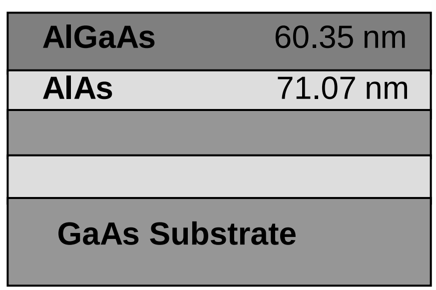

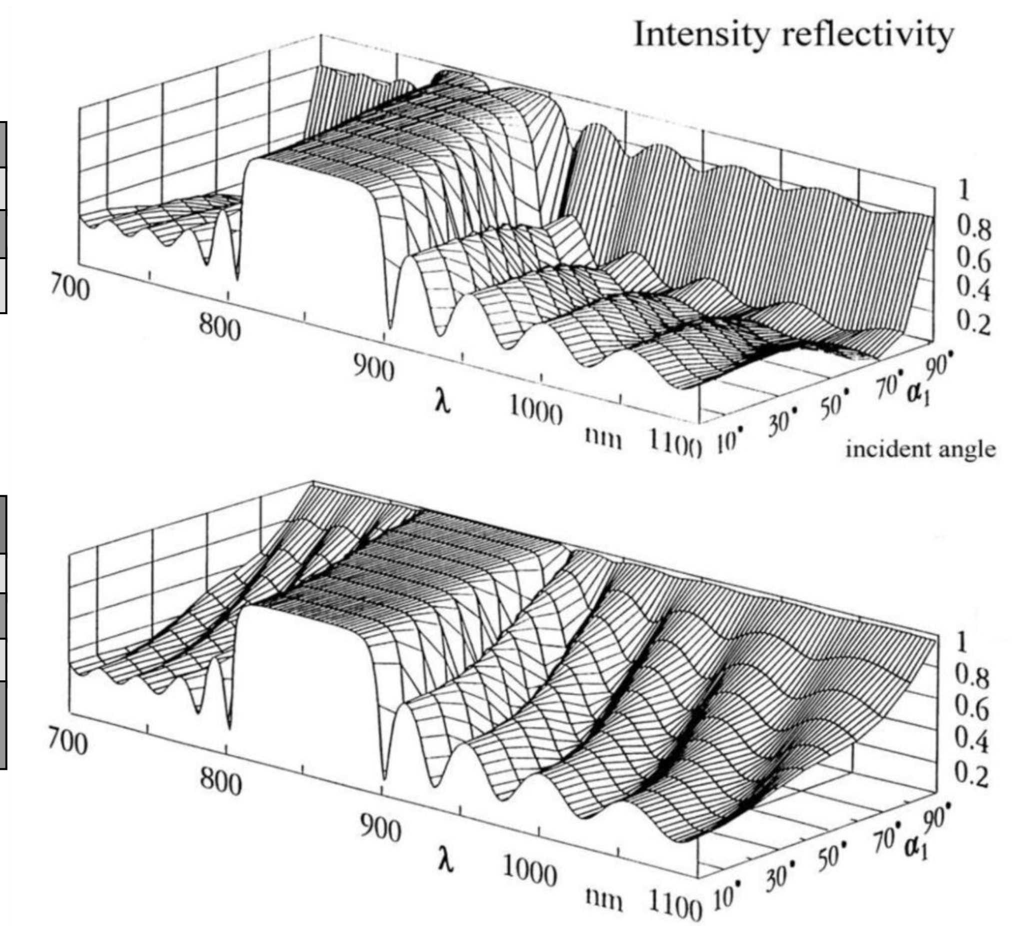

① TM mode

Electrical field is located in the plane of incidence

② TE mode

Electrical field is parallel to the Bragg mirror interface

Examples for dielectric mirrors: design wavelength 800nm

Layer	$\bar{n}_i$	d_i [nm]
Si_3N_4	1.82	109.89
SiO_2	1.47	135.91
Si_3N_4	1.82	109.89
SiO_2	1.47	135.91
Si_3N_4		
⋮	⋮	⋮
Si_3N_4	1.82	109.89
SiO_2	1.47	135.91
Si_3N_4	1.82	109.89

9.5p or **15.5p**

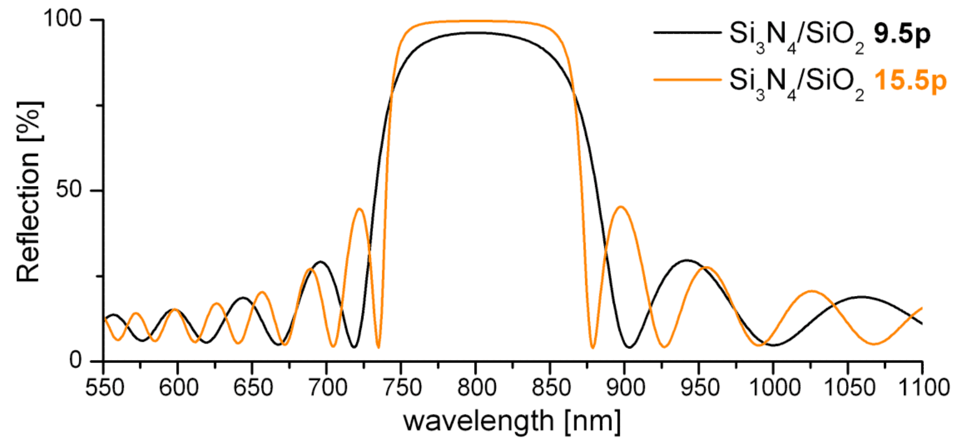

ZrO_2/SiO_2
$\Delta\bar{n} = 0.67$

$\bar{n}_i$	d_i [nm]	Layer
2.14	93.67	ZrO_2
1.47	135.91	SiO_2
2.14	93.67	ZrO_2
1.47	135.91	SiO_2
⋮	⋮	⋮
2.14	93.67	ZrO_2
1.47	135.91	SiO_2
2.14	93.67	ZrO_2

9.5p

TiO_2/SiO_2
$\Delta\bar{n} = 0.78$

Layer	$\bar{n}_i$	d_i [nm]
TiO_2	2.25	88.87
SiO_2	1.47	135.91
TiO_2	2.25	88.87
SiO_2	1.47	135.91
⋮	⋮	⋮
TiO_2	2.25	88.87
SiO_2	1.47	135.91
TiO_2	2.25	88.87

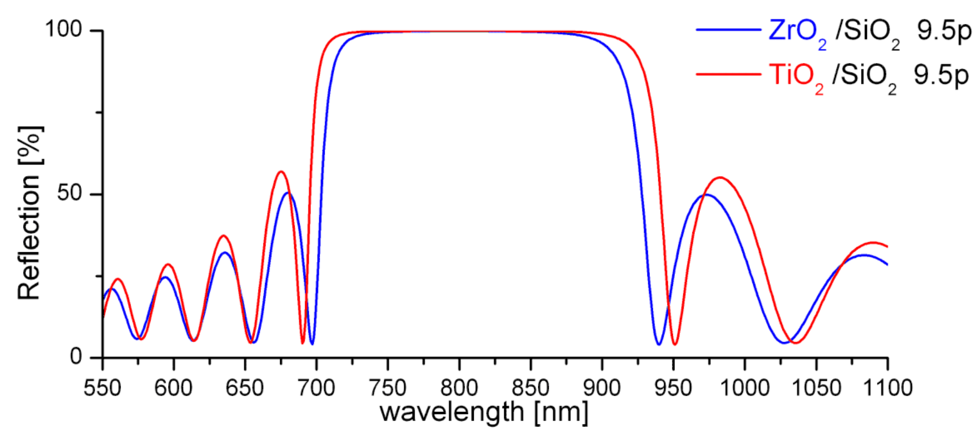

Transmittance T, reflectance R and absorption A

If $A \neq 0$ $\quad 1 = T + R + A$

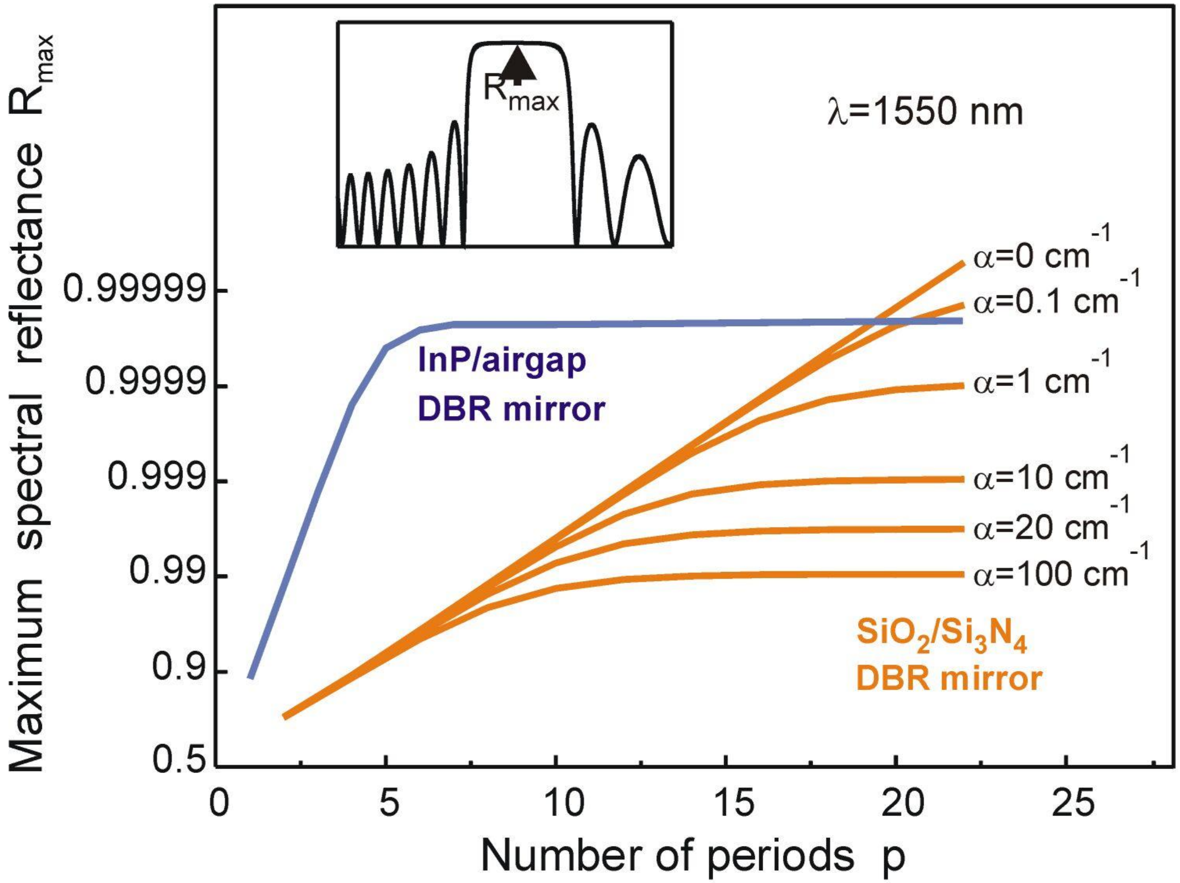

α = absorption coefficient

Bragg Mirrors for Long Wavelength VCSELs and Filters

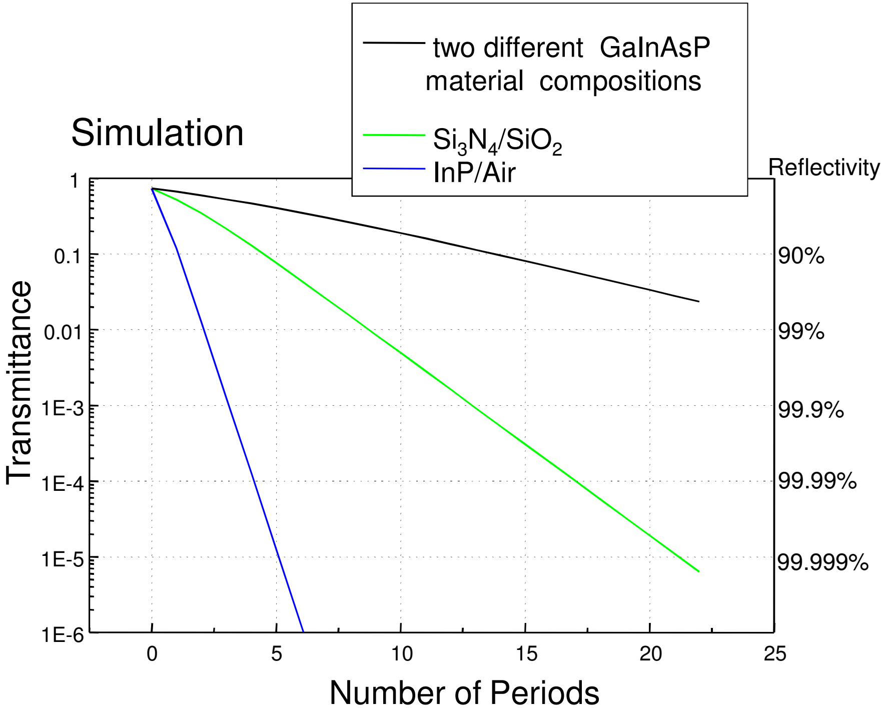

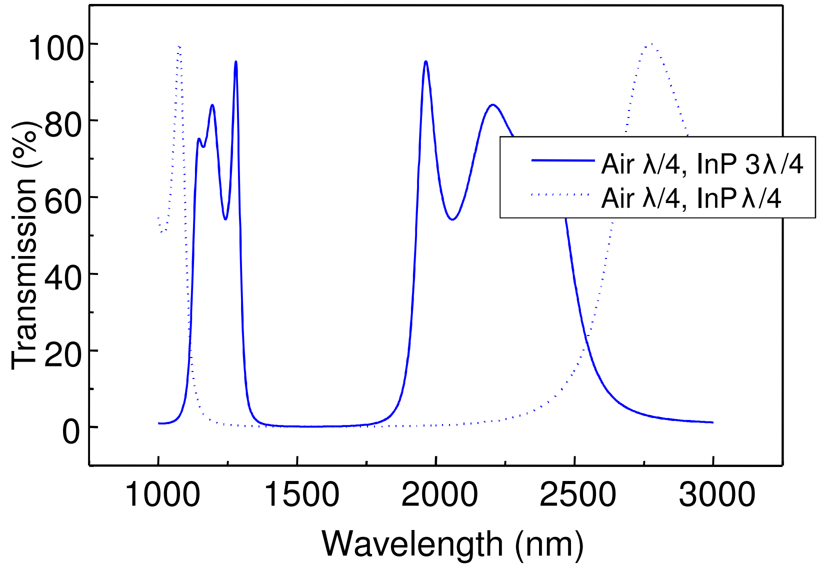

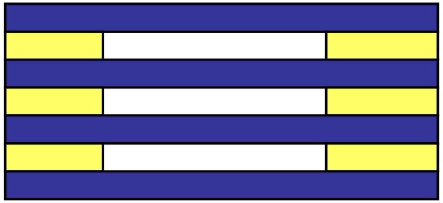

- High index contrast (>1:3)
- High reflectivity (4p: 99.9%)
- Large stop-band (>300 nm)

Real mirrors of DBR type to be used in FP interferometers

As mentioned already above:

Real mirrors are

- extended
- can have very high reflectivity
- are wavelength dependent
- have finite absorption

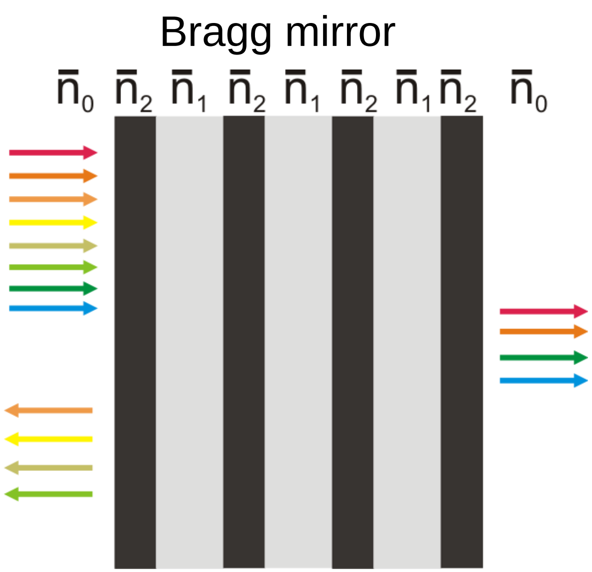

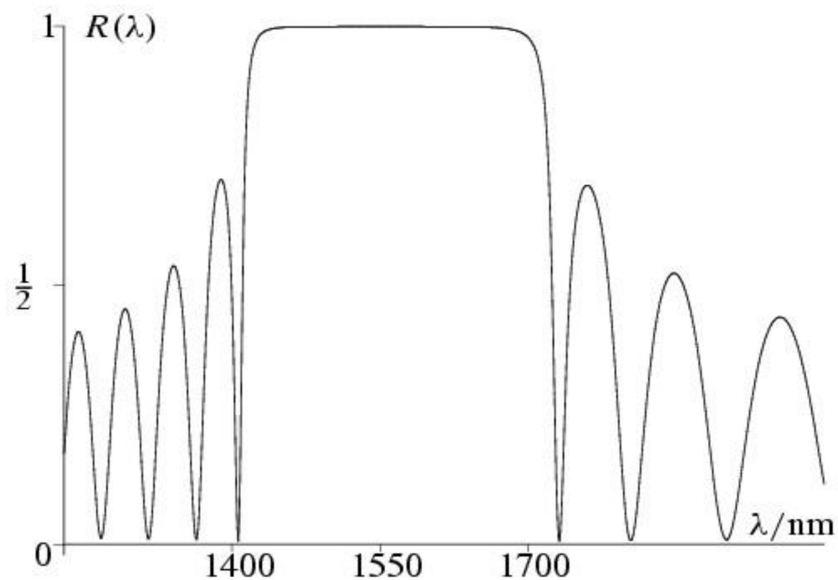

In this example the mirror is designed for a central wavelength (design wavelength) of 1.55µm.

- Replacement of the 2 unextended ideal mirror in the simple interferometer set-up (see above) by 2 Distributed Bragg Reflectors (DBRs) delivers a real Fabry - Pérot (FP) interferometer

Farby-Pérot filter with Bragg mirrors

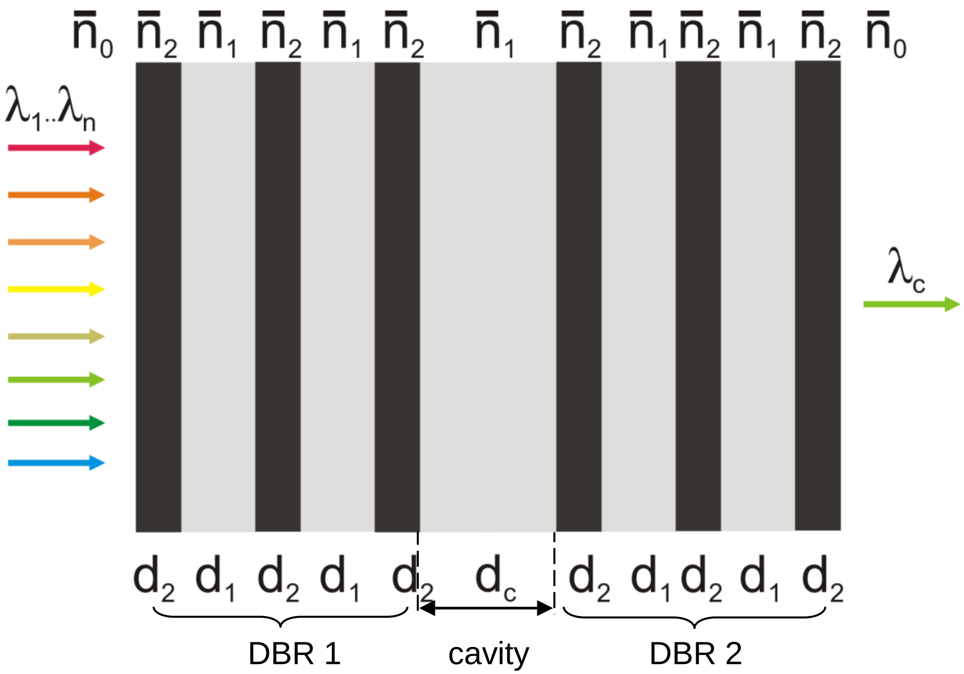

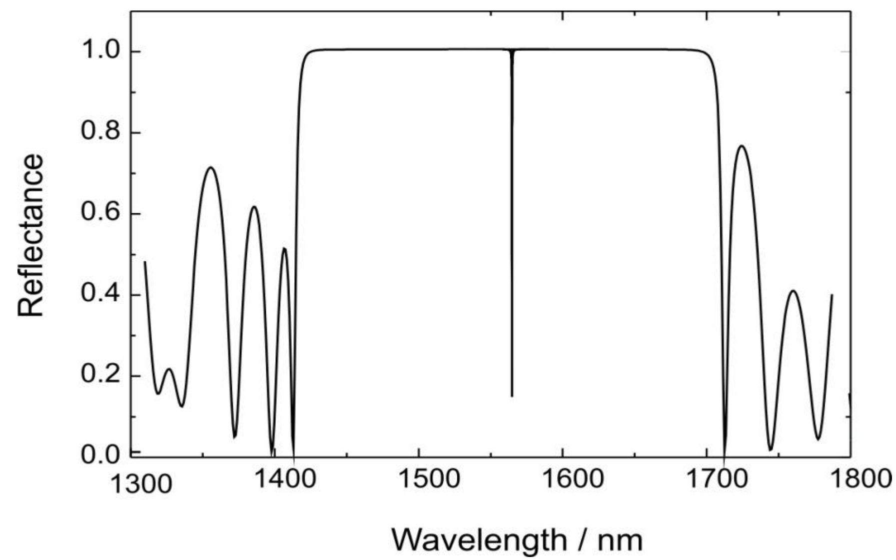

Example : Spectra of Semiconductor multiple air-gap structures

- Transmission spectra

DBR mirror InP/air 3 periods

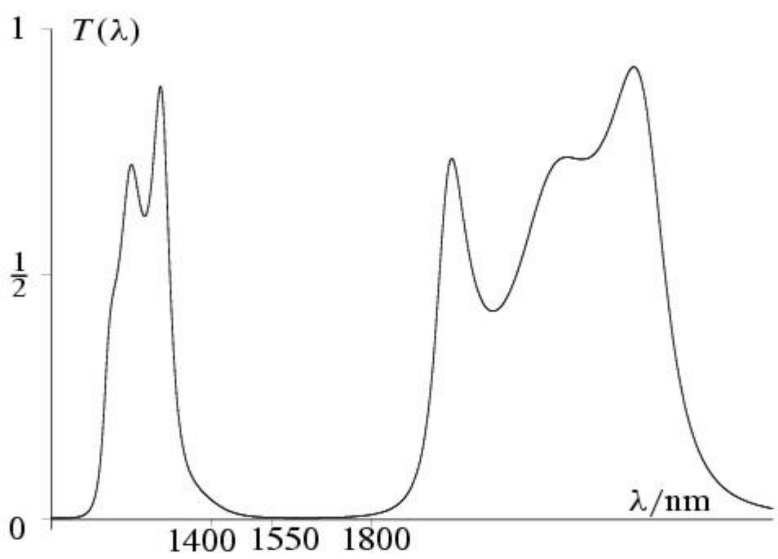

Fabry-Pérot filter InP/air
(2 DBR mirrors embedding a cavity)

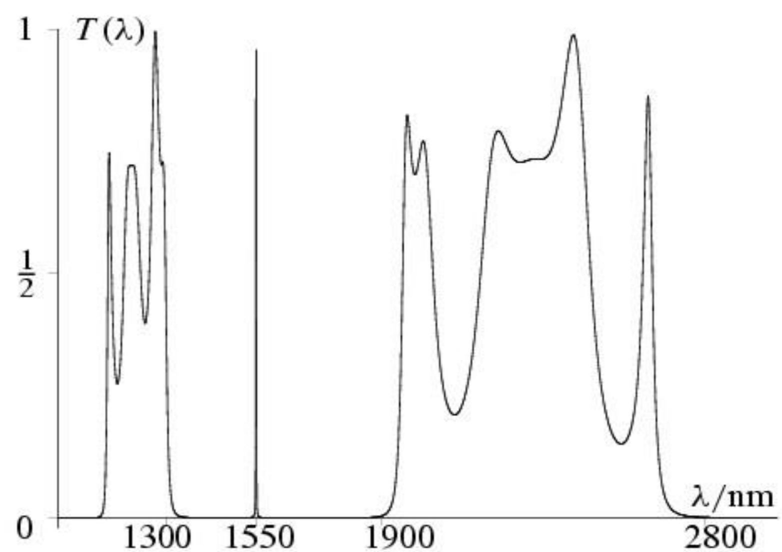

Tunable All - Air - Gap and Dielectric Mirror Filters

optoelectronic devices

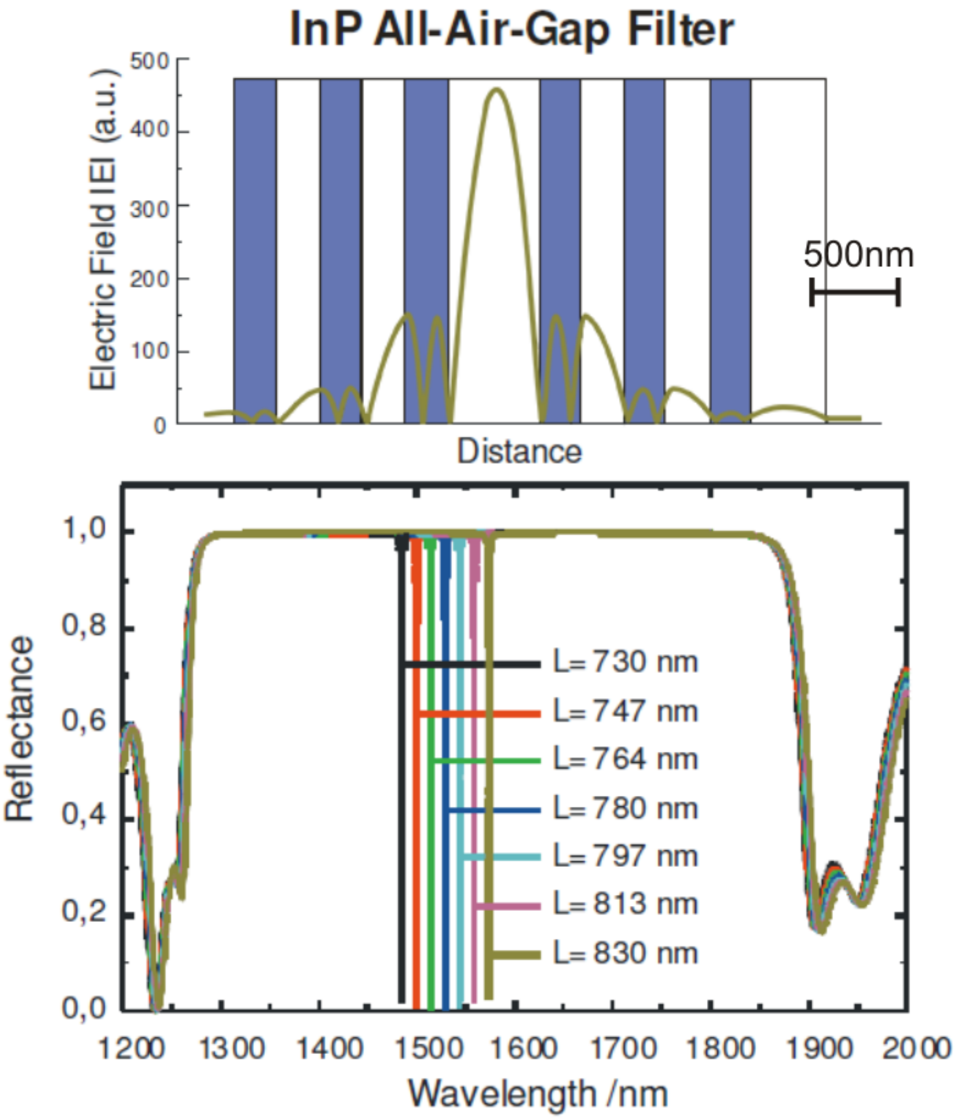

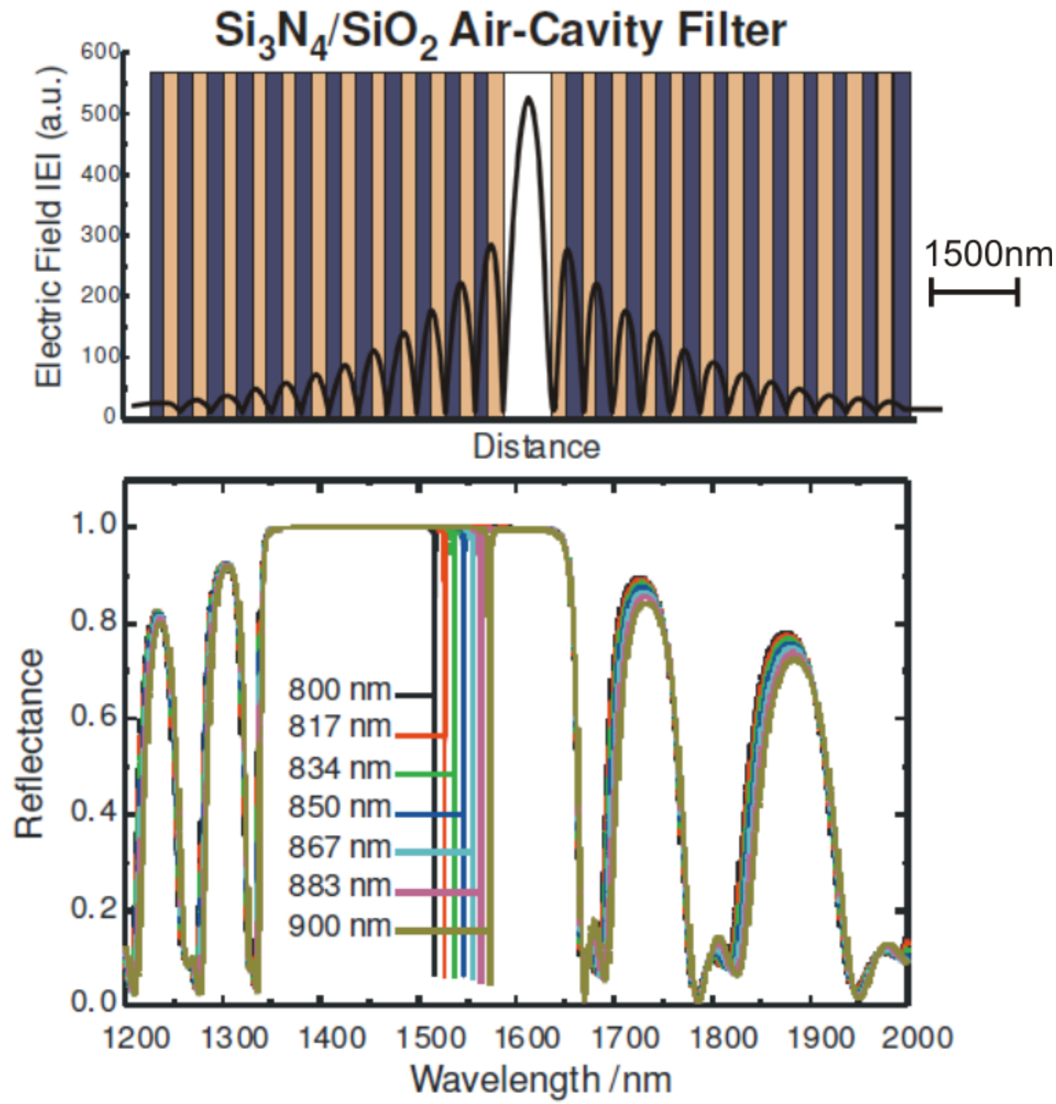

Tuning: $\Delta\lambda$ **= 89 nm,** $\dfrac{\Delta\lambda}{\Delta L}$ **= 0.89**

Tuning: $\Delta\lambda$ **= 56 nm,** $\dfrac{\Delta\lambda}{\Delta L}$ **= 0.56**

Full width at half maximum

FWHM

Free spectral range

FSR

Finesse

$\mathcal{F}$

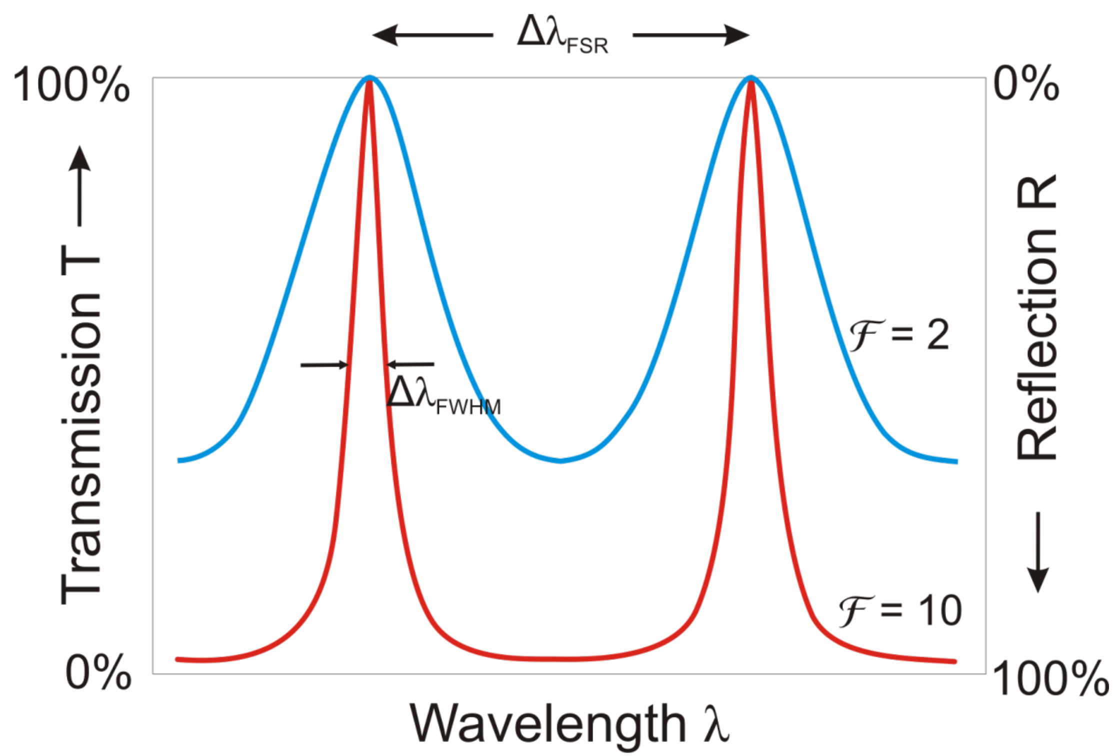

$$\Delta\lambda_{\mathrm{FWHM}} \approx \frac{(1-RA)\lambda_{\mathrm{c}}^2}{2\pi\, d_{\mathrm{c,eff}}\sqrt{RA}}$$

$$\Delta\lambda_{\mathrm{FSR}} \approx \frac{1}{2d_{\mathrm{c,eff}}}\lambda_{\mathrm{c}}^2$$

$$\mathcal{F} = \frac{\Delta\lambda_{\mathrm{FSR}}}{\Delta\lambda_{\mathrm{FWHM}}} \approx \frac{\pi\sqrt{RA}}{(1-RA)}$$

= how many modes are fitting closely neighbored to each other inside the FSR

Filter types used in telecommunication networks

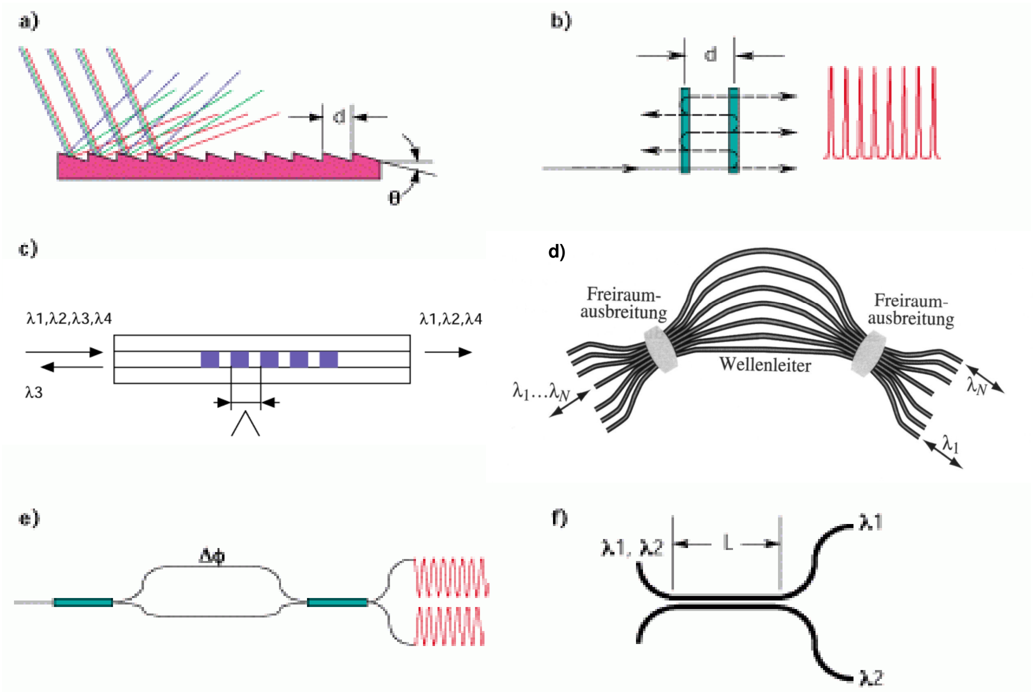

a) plane grating

b) Fabry-Perot interferometer (FPI)

c) fiber Bragg grating

d) arrayed waveguide grating (AWG)

e) Mach-Zehnder interferometer (MZI)

f) fused bionic coupler / filter

[Anderson, WDM Solutions, p97, June 2001]

Fabry – Pérot Interferometer with moving DBR mirrors

incident light with multi-wavelength

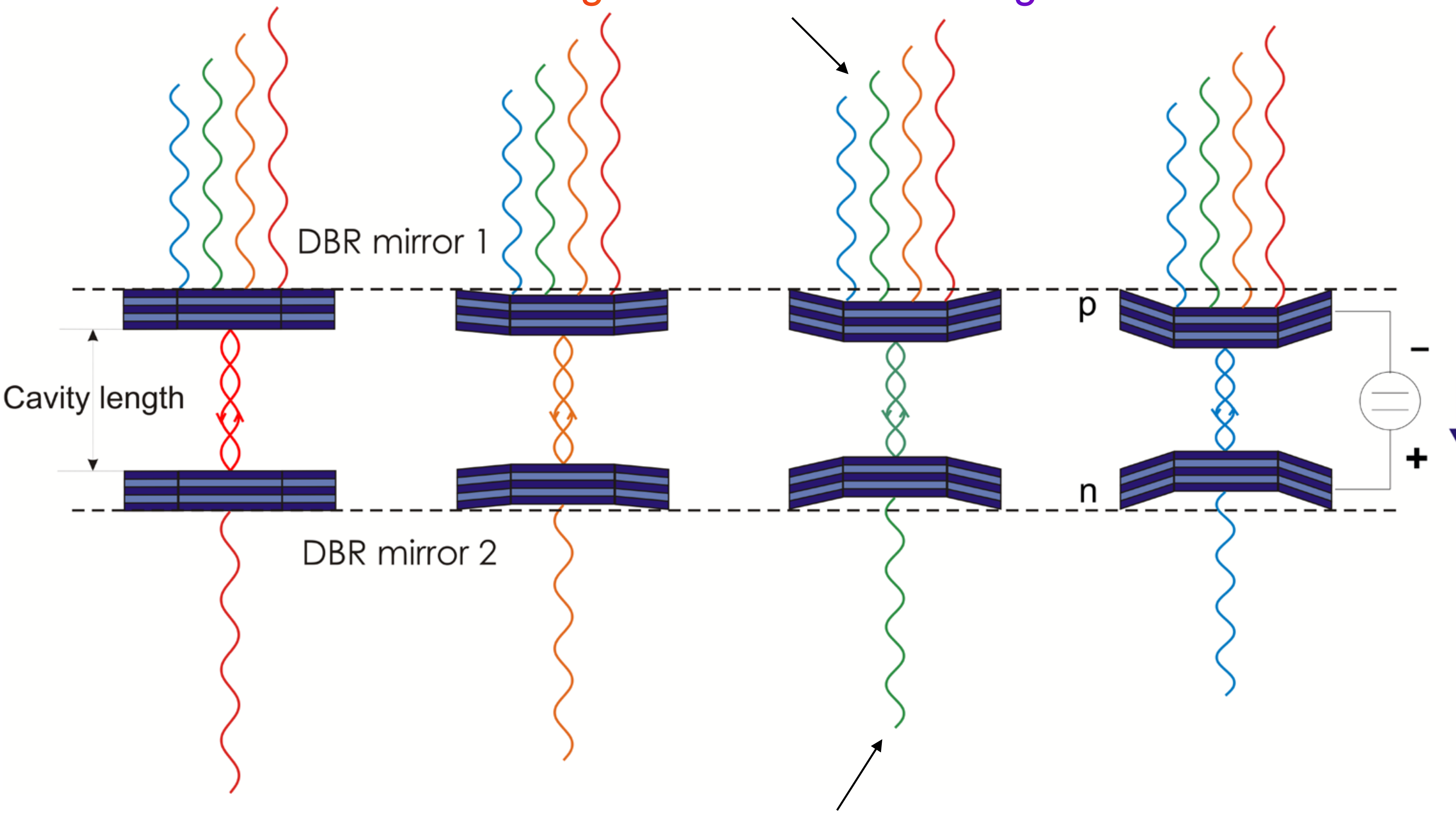

transmitted light with single-wavelength

Integration of a photo diode (PD), a semiconductor membrane multiple air-gap FP filter and a fibre

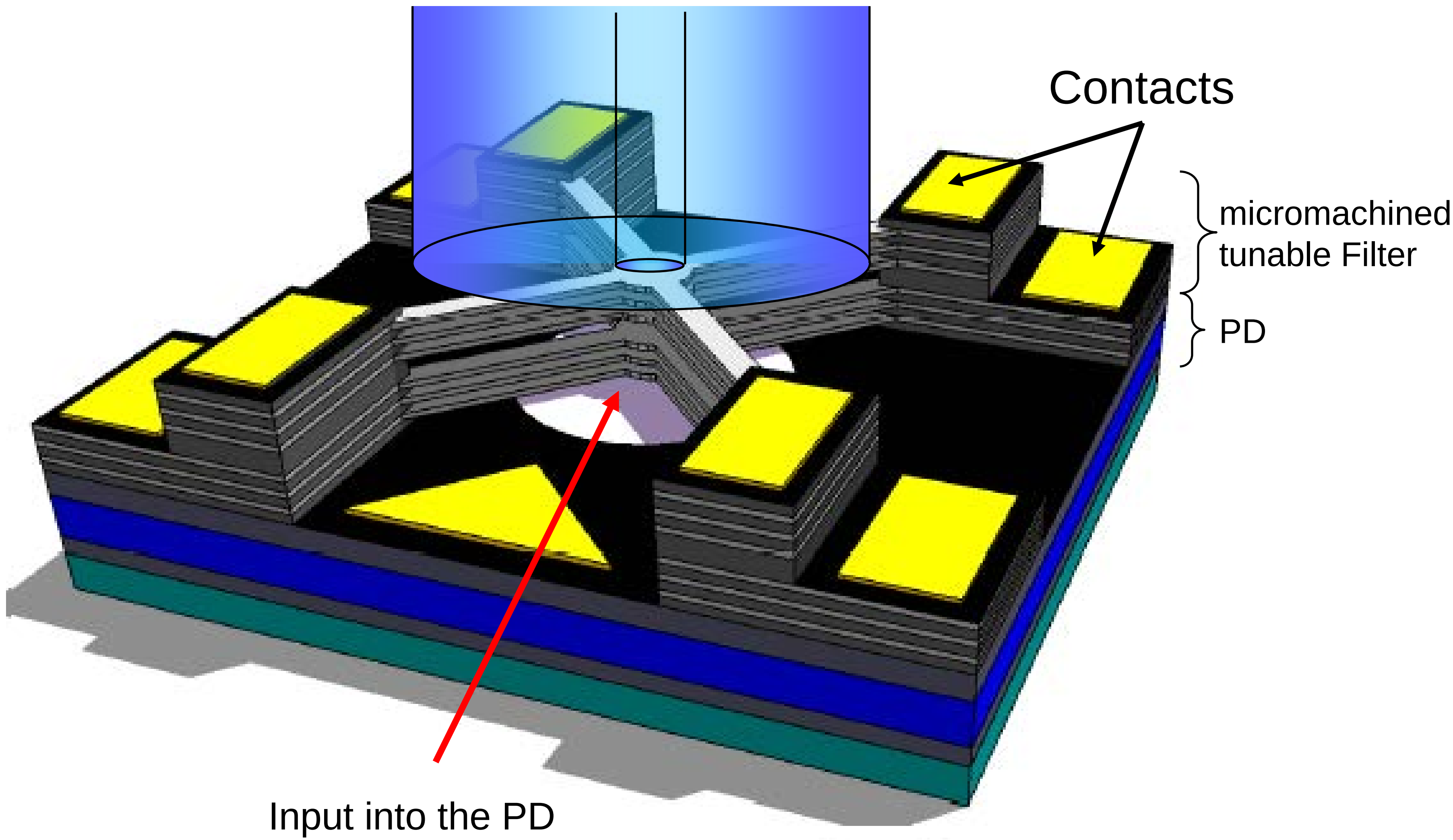

Requirements on filters

- Filters for long haul DWDM-systems
  - distance between channels 0.8 nm (ITU-T G.692)
  - sideband suppression ratio > 20 dB (ITU-T G.692)
  - FWHM < 1nm
  - FSR > 100nm
  - small loss
  - devices should be appropriate for tuning

- InP/air material module
  - high refractive index contrast
  - Bragg mirrors with high reflectivity (R > 99.9%) with only 3 periods
  - air-gap cavity makes micromechanical tunable devices possible
  - InP makes 1550 nm VCSEL possible

Optical filter applications in optical networks

- Filtering = selection of certain data channel, least change of other channels

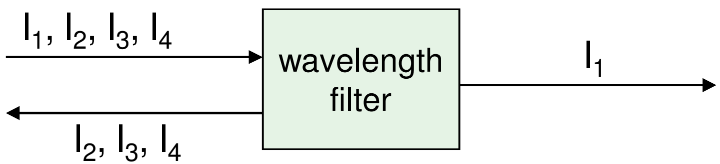

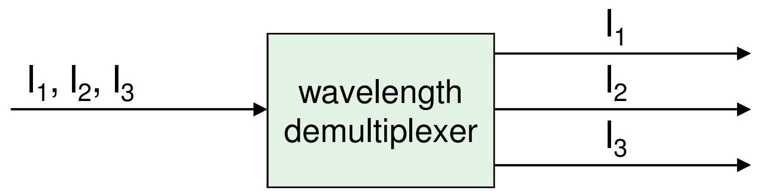

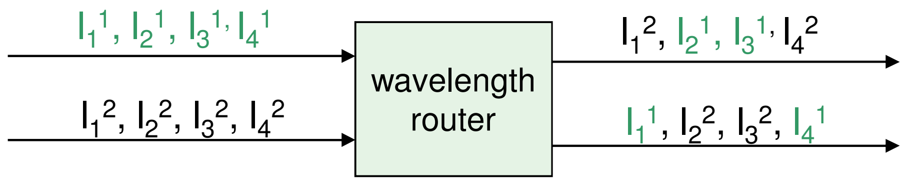

- WDM system applications

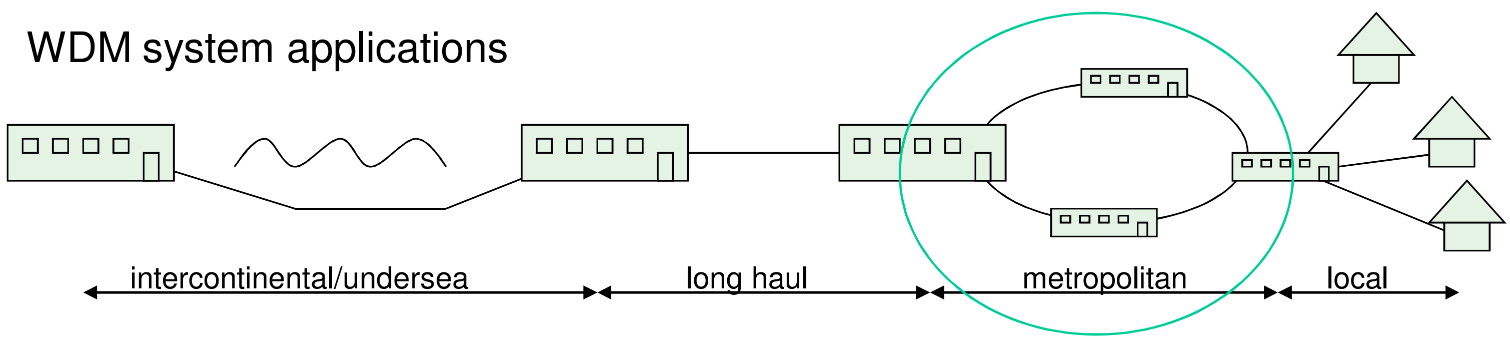

WDM systems

	Long haul	Metropolitan	B-PON (Broadband Passive Optical Networks)
Distance	>100km .. 1000km	<100km	<20km
Channels/ Traffic	uniform; 2.5GBit/s, 10GBit/s, (40Gbit/s)	highly diverse; (SONET, Ethernet, up to 10Gbit/s)	diverse, capacity adjustable (ATM, Eth. up to 622Mbit/s)
Topology	linear (point-to-point) 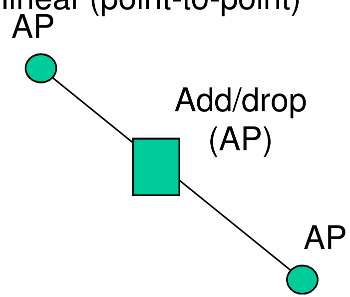 AP = access point	ring or mesh 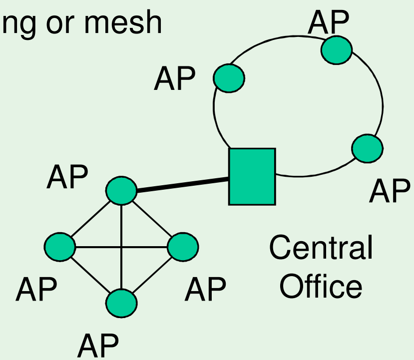	point-to-multipoint 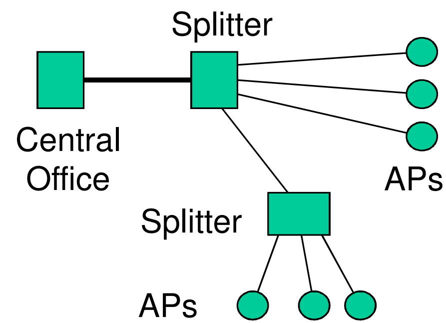
Migration	add channels (possibly)	add capacity, add new rings / connections	adjustable capacity per channel
Filter cost	high (few filters)	medium/low (high # of filters)	low (high # of filters)

Requirements on filters I (insertion loss)

- **Example: metropolitan networks**

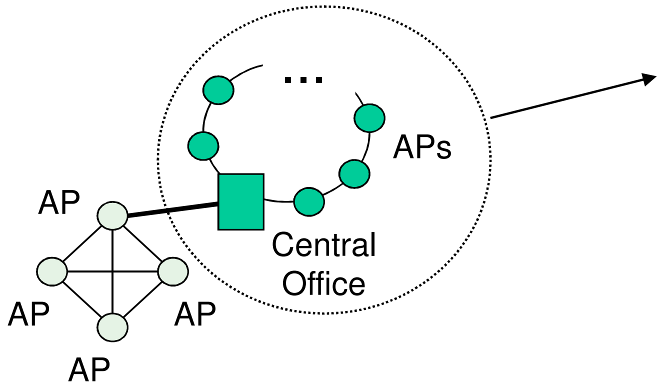

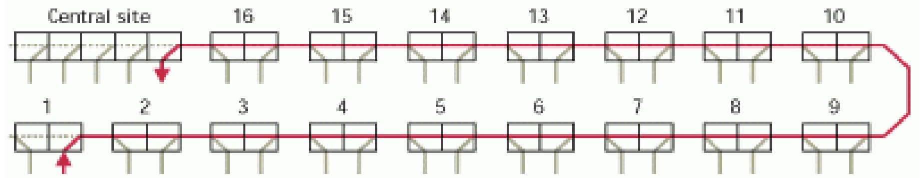

Assumptions:
2 x add/drop loss of 1.5dB, 30 x through filter count, 35dB power budget, 0.3dB/km fiber loss, no power monitor / optical supervisory channel

Through filter loss [dB]	Total loss in filters [dB]	Power budget - filter losses [dB]	Ring circum-ference [km]
0.50	18.0*	17.0**	60
0.75	25.5	9.5	34
1.00	33.0	2.0	7

[Batchellor, WDM Solutions, p49, April 2001]

* $=30\cdot 0.5dB+2\cdot 1.5dB$
$=18.0dB$
** $=35dB-18dB=17dB$

- => **Small insertion loss** needed

Requirements on filters II (crosstalk)

- **Example: metropolitan networks**

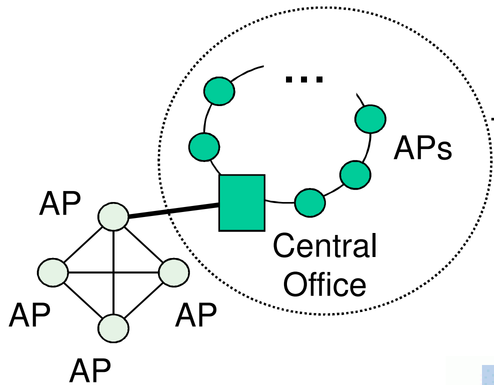

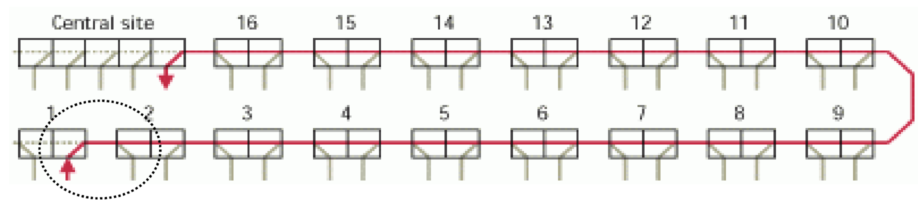

at receiver: interfering signal 15dB below data signal needed

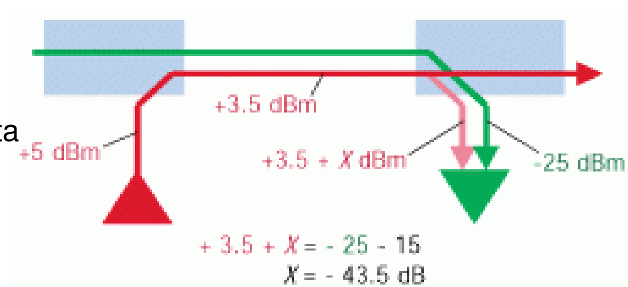

X=Amount of isolation afforded by the filter

- **=> High isolation** (**small crosstalk** = high Side Mode Suppression Ratio = **SMSR**) necessary

Requirements on filters III (FSR, FWHM, Finesse)

- **Filter principle:**
  - splitting & interference of light waves
  - constructive/destructive interference
  - => periodical filter spectrum (Free Spectral Range = **FSR**)

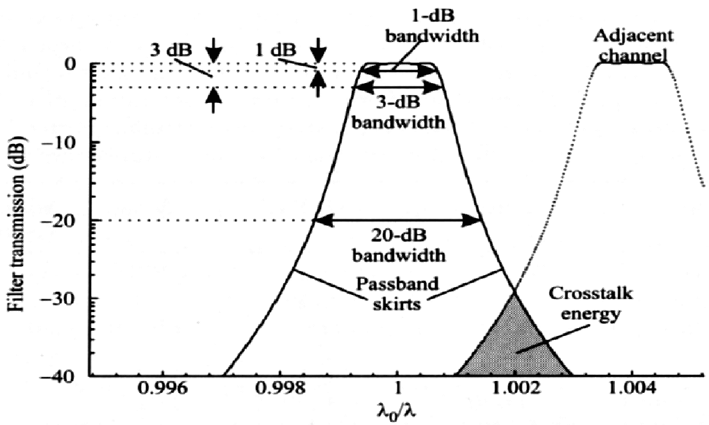

1 dB, 3dB, 20dB bandwidth of filter

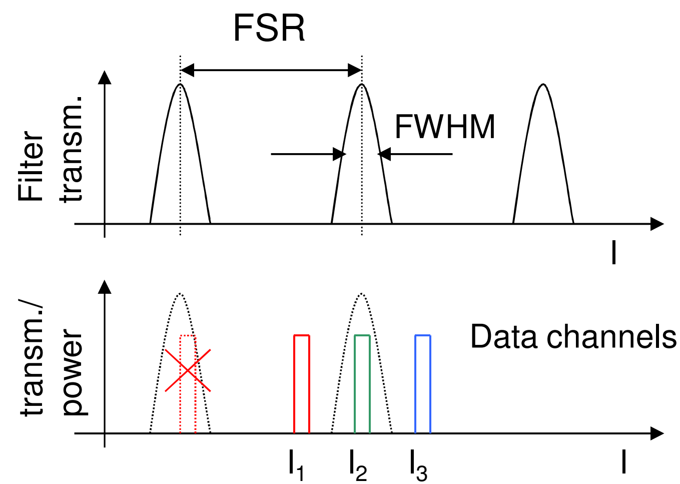

Separation of adjacent channels:
characterisation of filters by several bandwidths: 1dB bandwidth, 3dB bandwidth (**FWHM**), 20dB bandwidth

Finesse:
FSR/FWHM ≈ # of channels which can be used

Requirements on filters IV (Tunin, Distortion, …)

- **Tuning:**
  filter should be easily tunable to different center wavelength (channels)

- **Distortion:**
  change of spectrum caused by optical filtering

- **Further requirements: => least possible dependence on**
  - **temperature**
  - **dispersion:**
    different parts of spectrum should propagate with equal speeds
  - **polarisation:**
    waves with different polarisations should propagate with same speeds

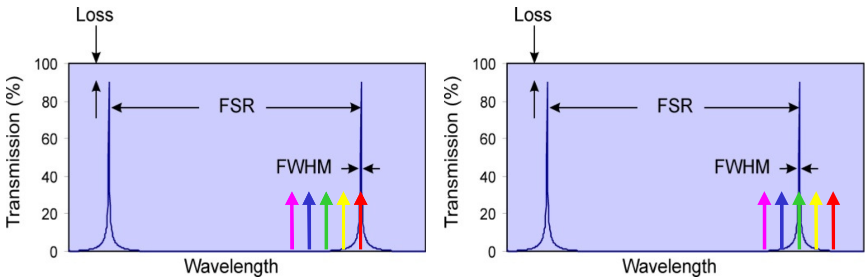

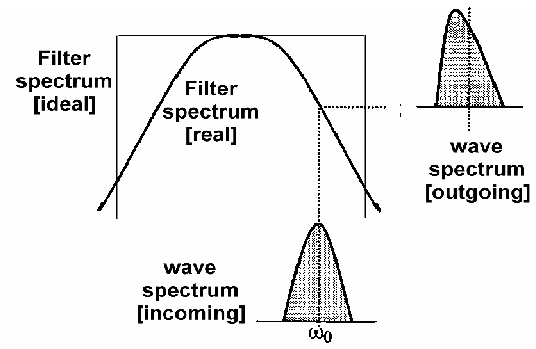

distorted wave spectrum in cause of non-ideal filtering (outgoing wave = convolution of incoming + filter function)

Filter classification (MA / AR filter)

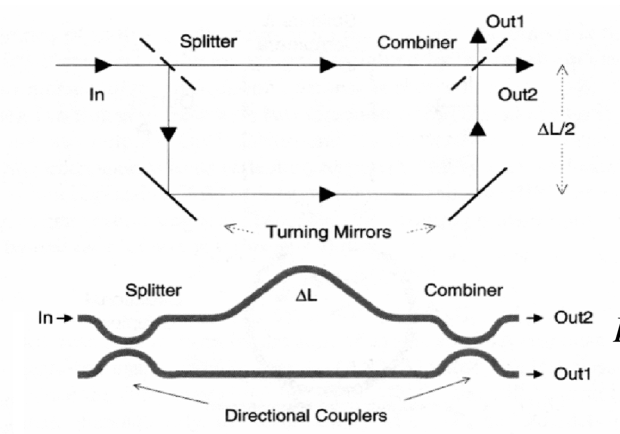

moving average filter (MA) = filters with finite impulse response (FIR)

$$H(\nu) = \sum_{n=0}^{N} \left[c_n e^{-j(2\pi\nu\tau n - \phi_n)} \right]$$

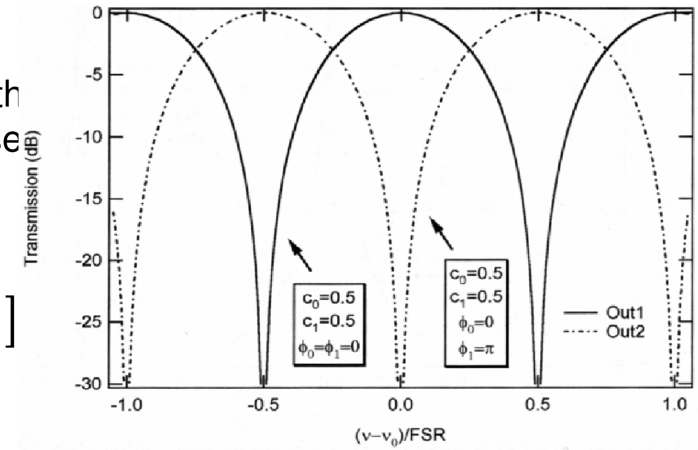

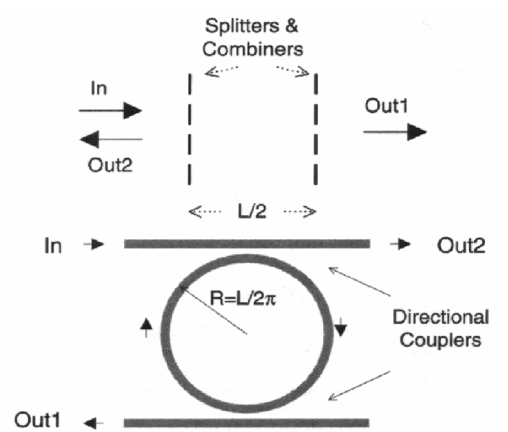

autoregressive filter (AR) = filters with infinite impulse response (IIR)

$$H(\nu) = \frac{1}{\sum_{n=0}^{N} \left[c_n e^{-j(2\pi\nu\tau n - \phi_n)} \right]}$$

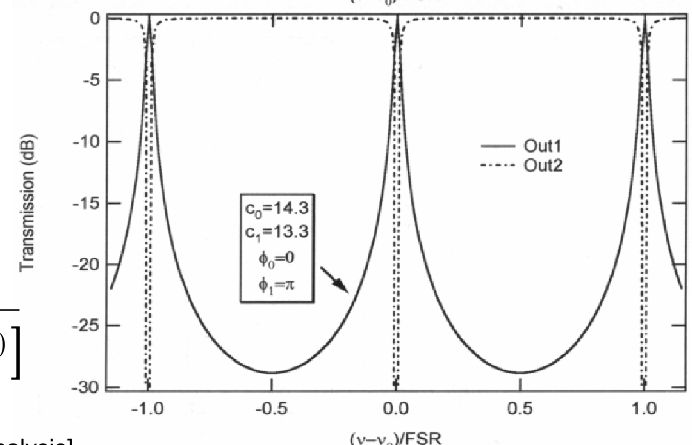

[Madsen, Optical Filter Design and Analysis]

Outlook: Tunable FPF - application

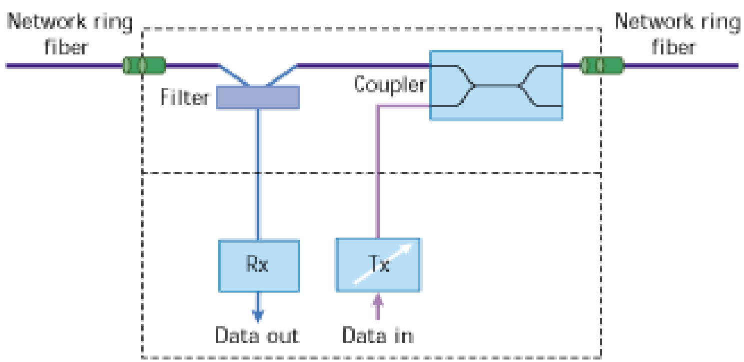

[Dhar, WDM-Solutions, p83, September 2001]

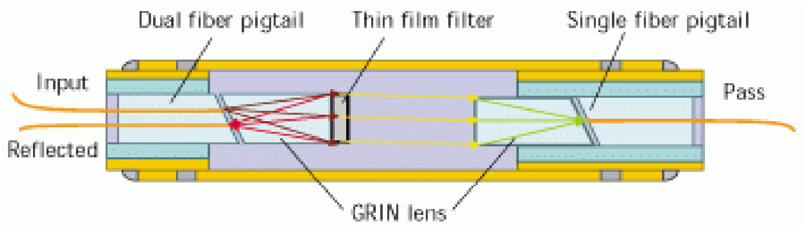

[Chun, WDM-Solutions, p39, May 2001]

Concept for application of tunable FP filters

Discovery of Gratings in Optical Fibres

- Research on nonlinear properties of germania-doped fibre.
  Discovery of a photosensitivity of optical fibre.
  [Hill, 1978]

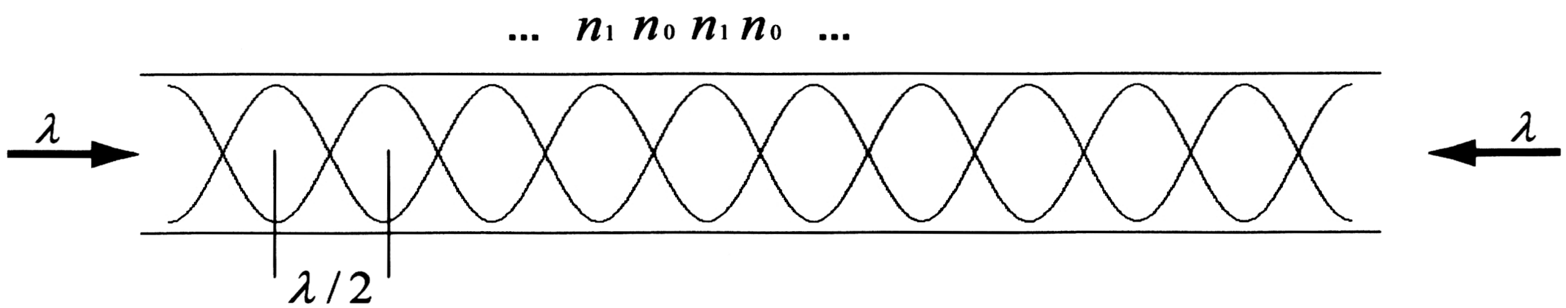

- Argon ion laser ($\lambda \approx 488\,\mathrm{nm}$)
- Exposure time of several minutes
- Permanent, very narrowband bragg reflection filters

- UV radiation leads to chemical reactions in the fibre core.
  $\lambda \approx$ 190–280 nm (absorbed only by the fibre core!)

- Refractive index change dependant on GeO_2 concentration.
  3 mol% $\rightarrow \Delta n \approx 3 \cdot 10^{-5}$
  10–20 mol% $\rightarrow \Delta n \approx 10^{-3}$

- Erbium-doped fibres have typically a high GeO_2 concentration!

- Additional doping materials can increase Δn (eg. boron, H_2 ...).

Fabrication of Fibre Bragg Gratings I

- Direct writing of gratings through the cladding by two intersecting beams of UV light. [Meltz, 1989]

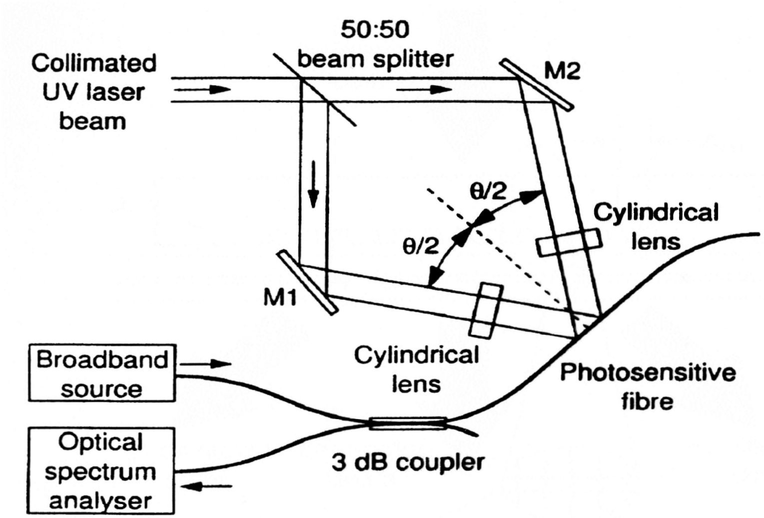

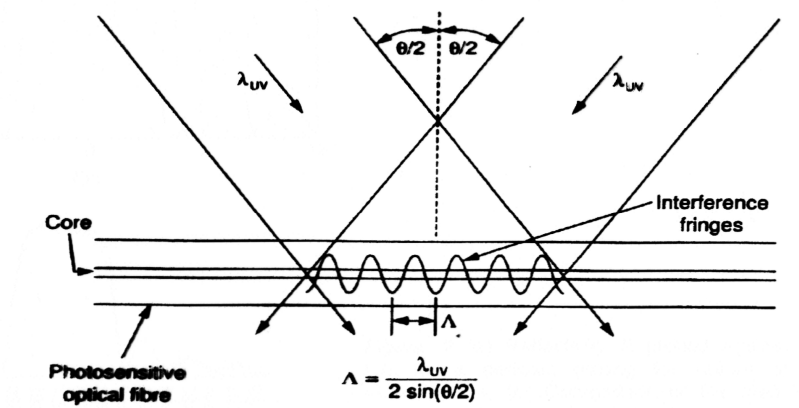

[Bennion, 1996]

- Dispersion compensation with chirped FBGs

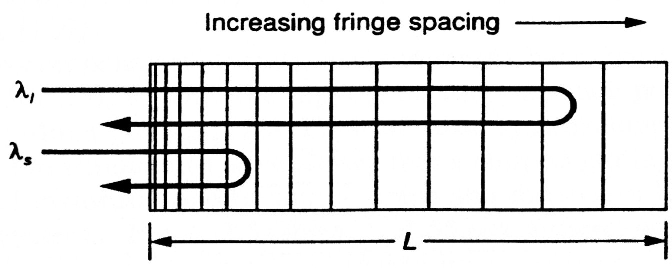

[Bennion, 1996]

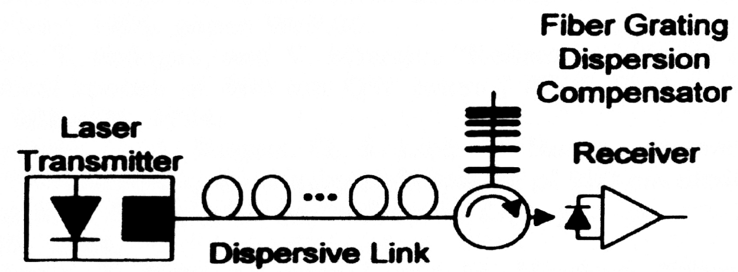

[Giles, 1997]

- e. g. 5 cm quadratically chirped gratings
  can compensate 800 km of fibre over a 1 nm bandwidth [Bennion, 1996].

Applications of Fibre Bragg Gratings II

- Phase masks for direct writing of fibre bragg gratings.
- Easy to use.
- Low demands on optical devices.
- One mask for each wavelength required.

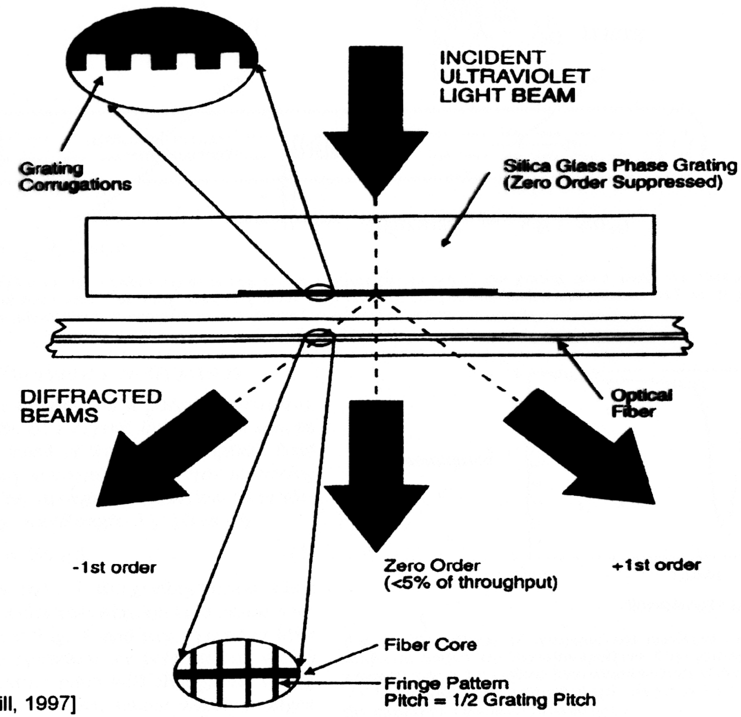

[Hill, 1997]

Applications of Fibre Bragg Gratings III

- Efficiency improvement in erbium-doped fibre amplifiers (EDFA)

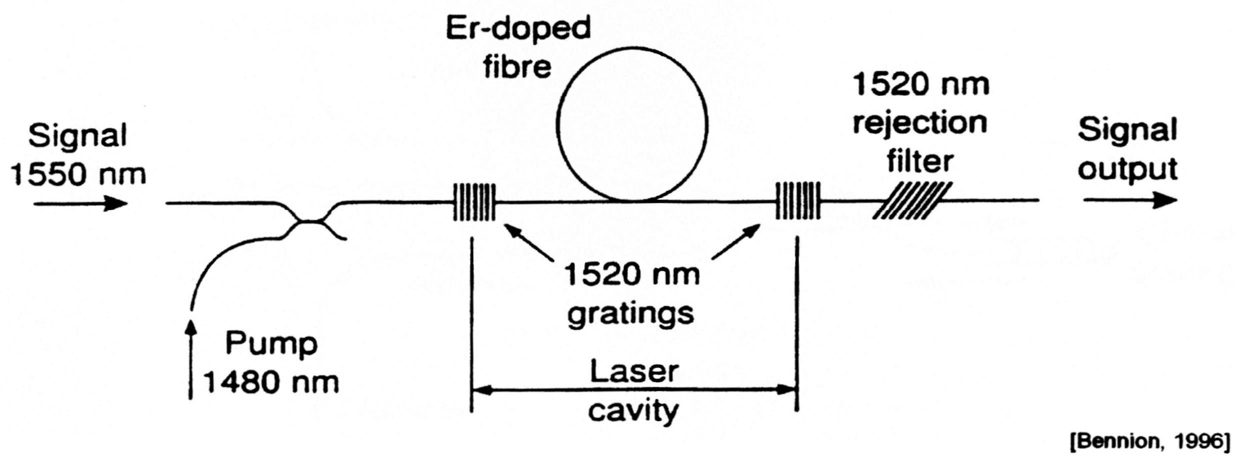

- 15,2 dB gain at 1550 nm with 80 mW pump power,
  Less than 0,2 dB gain variation for input powers up to 0,32 mW [Bennion, 1996].

Applications of Fibre Bragg Gratings IV

- Filters for WDM Systems

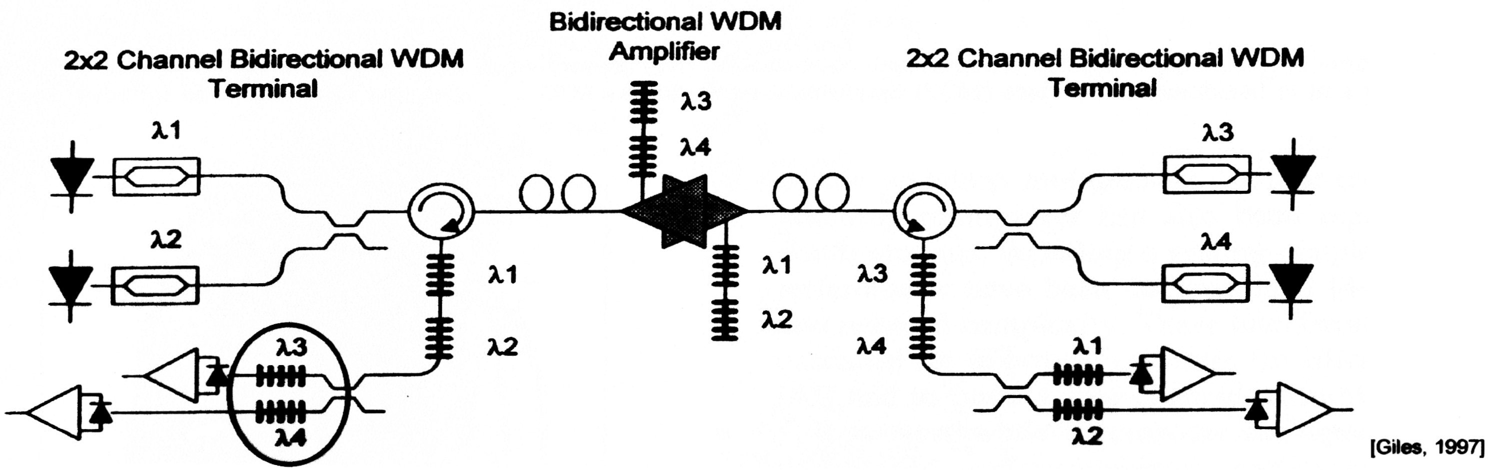

Filter type	Insertion Loss	Channel Spacing, Isolation	Bandwidth (FWHM)	Tuning Range	Tuning Speed	Tuning Mechanism
Micromachined FP	1 dB	2 nm/30 dB	< 0.5 nm	≈ 60 nm	100μs	Micromechanical
FBG [Iocco 1997]	0.1 dB	1.6 nm/22 dB	< 0.2 nm	< 10 nm	2 ms	Temp.,Stretching

Applications of Fibre Bragg Gratings IV

- Sensors for strain and temperature
- e.g. $\Delta\lambda$ = 13 pm / °C @ 1550 nm

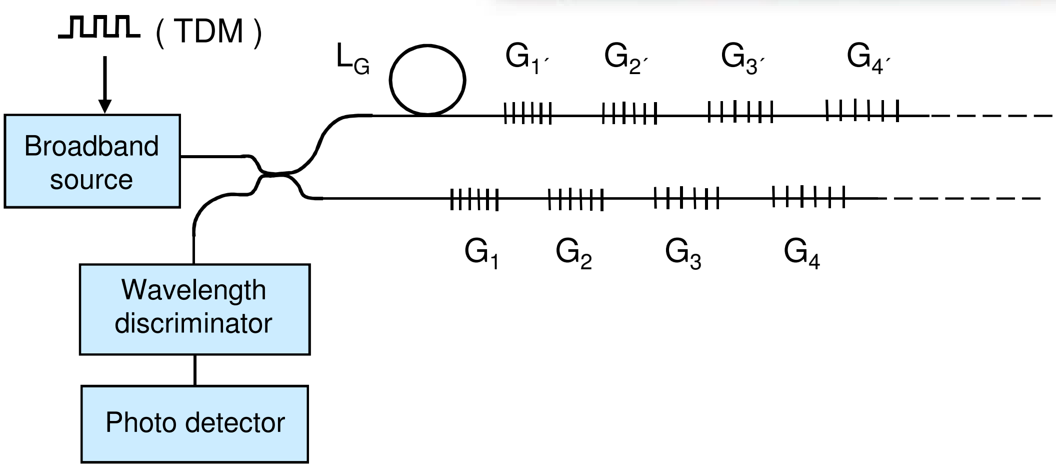

Filter types used in telecommunication networks

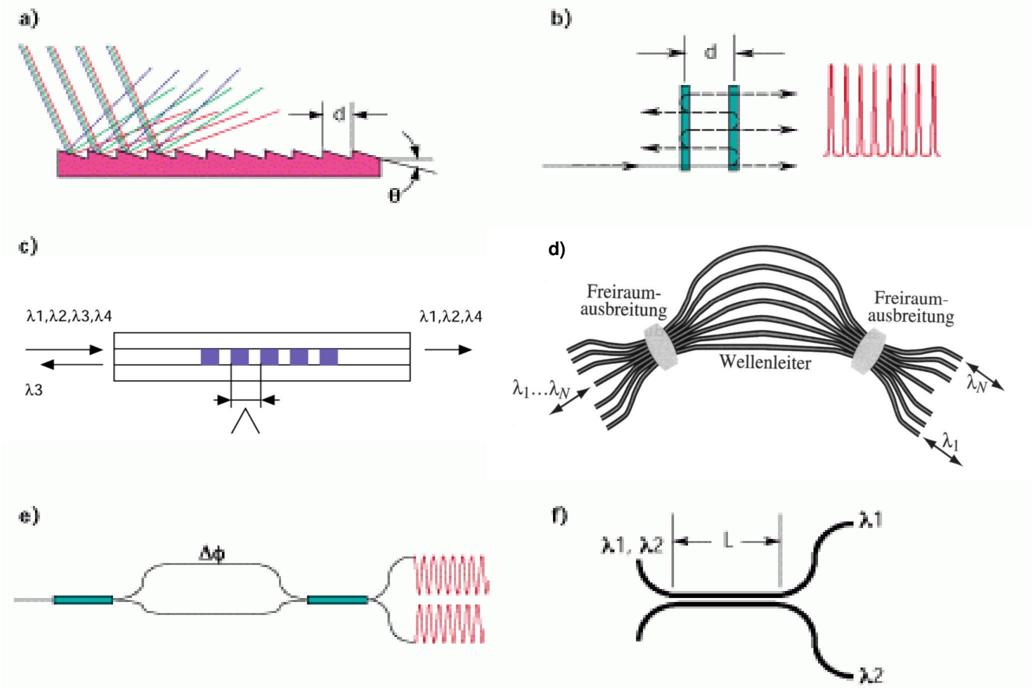

a) plane grating

b) Fabry-Perot interferometer (FPI)

c) fiber Bragg grating

d) arrayed waveguide grating (AWG)

e) Mach-Zehnder interfero-meter (MZI)

f) fused bionic coupler / filter

[Anderson, WDM Solutions, p97, June 2001]

InP - based AWG (*NTT Confidential*)

64-ch AWG
(50GHz spacing)

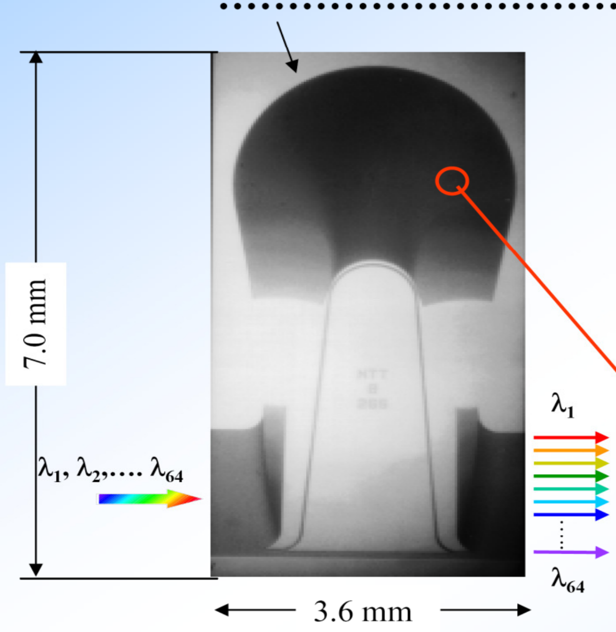

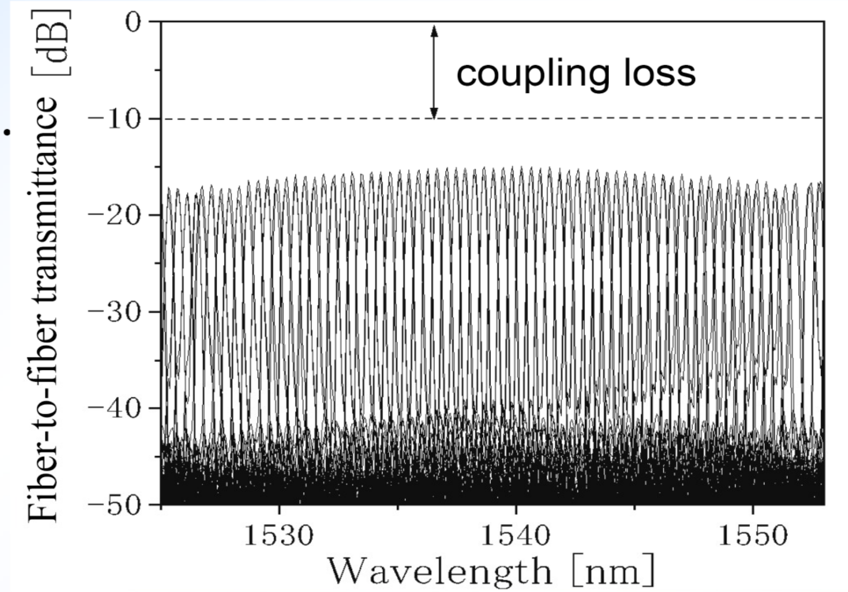

M. Kohtoku et al.

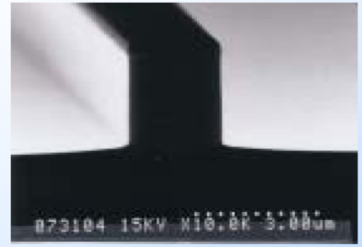

High-mesa structure

NTT Confidential

Concept: Two-step selection

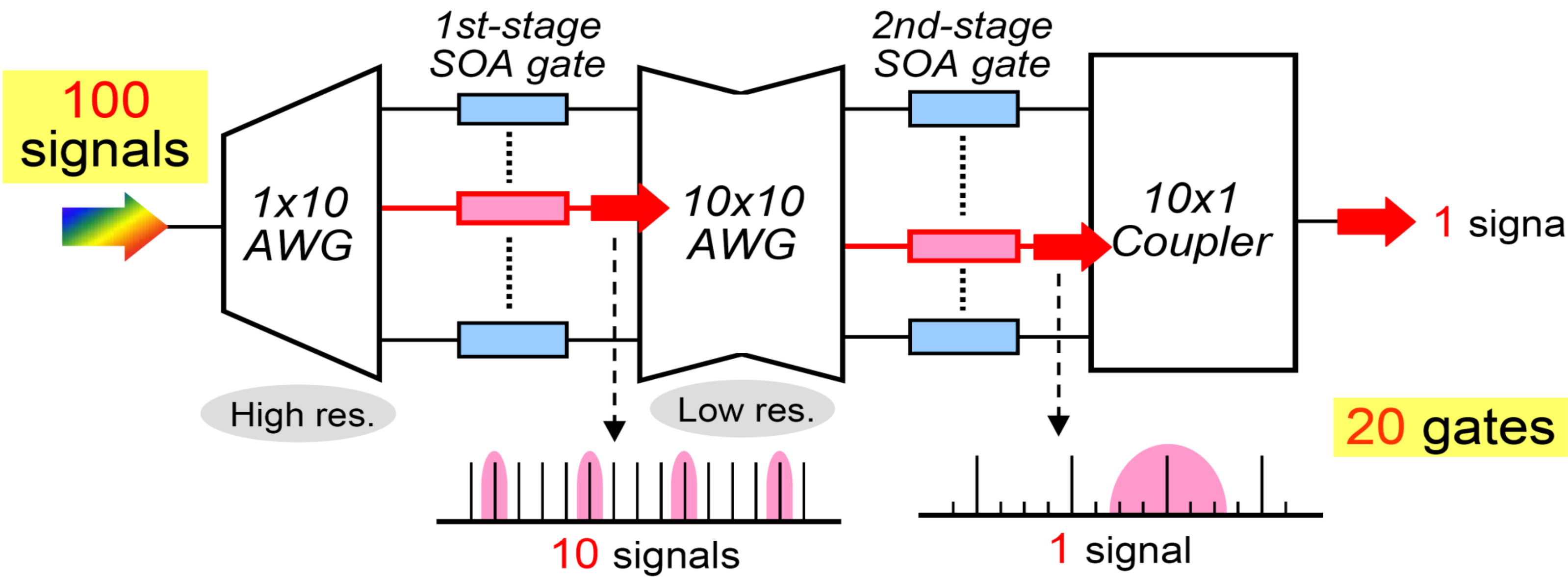

Handles "*large number of channels*" with small number of gates!

Chapter 7

Introductions to lasers

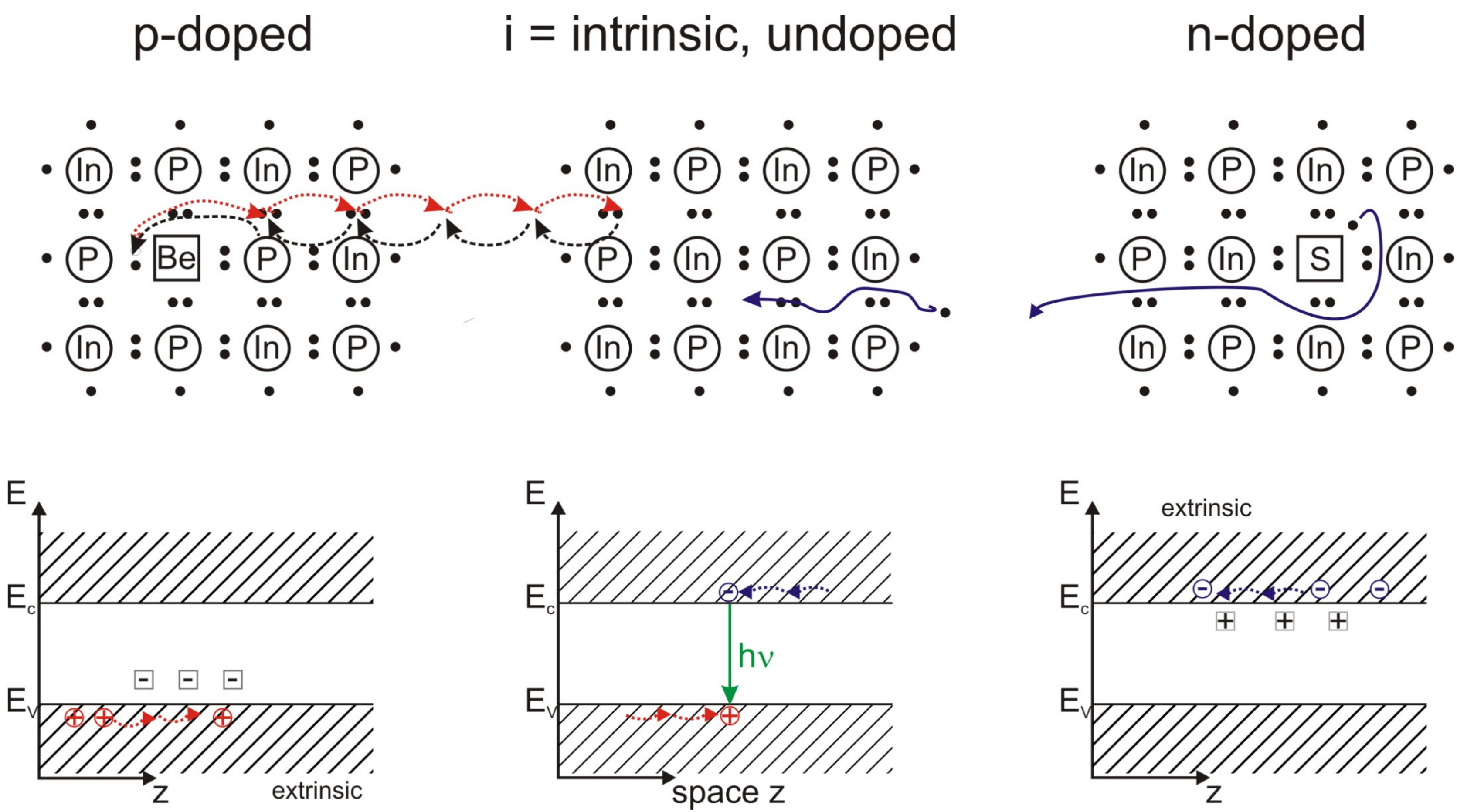
p-doped
i = intrinsic, undoped
n-doped
In
P
Be
S
E
E_c
E_v
z
extrinsic
space z
hν
extrinsic
z

Lasers

Light **a**mplification by **s**timulated **e**mission of **r**adiation

Principle of lasers

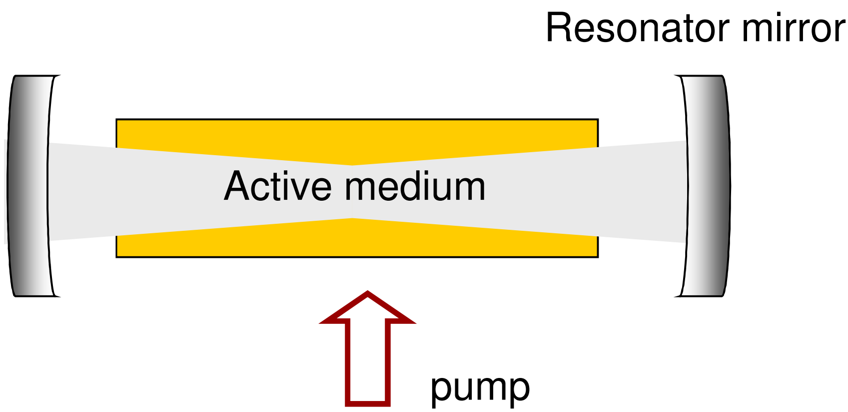

Feedback by the resonator

Light amplification by the active medium

Very strong pumping (= energy source) to obtain carrier inversion

i.e. more carriers in high energetic levels (2)

than in the low energetic levels (1)

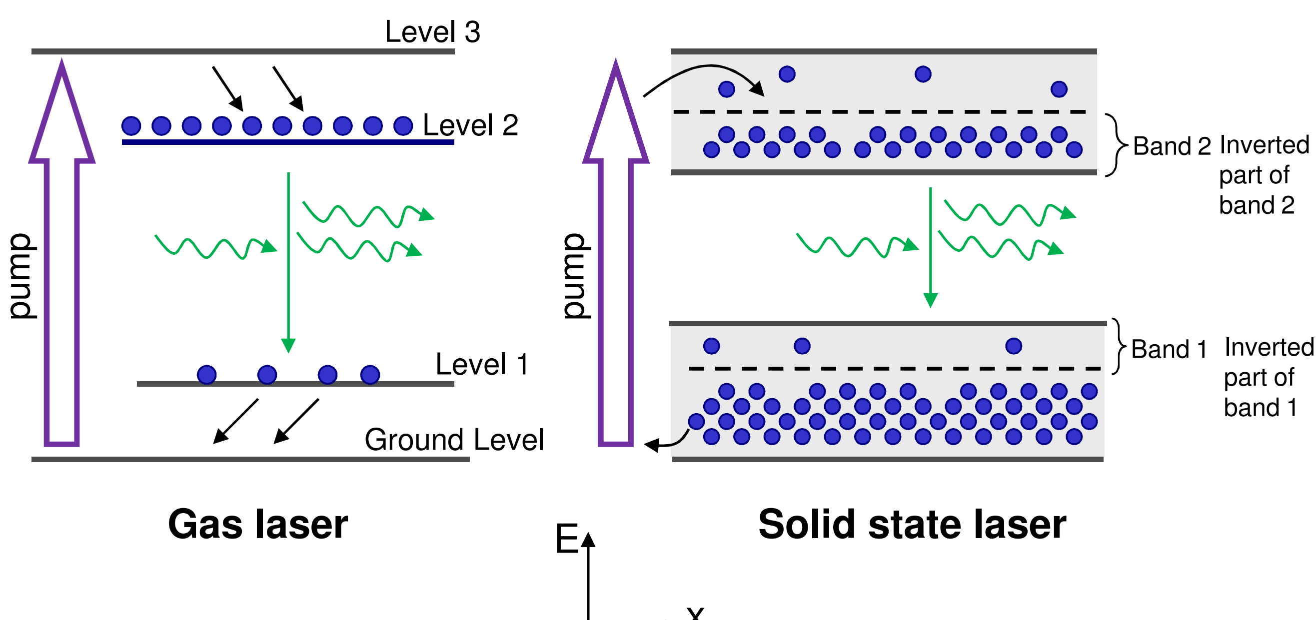

Principle of inversion

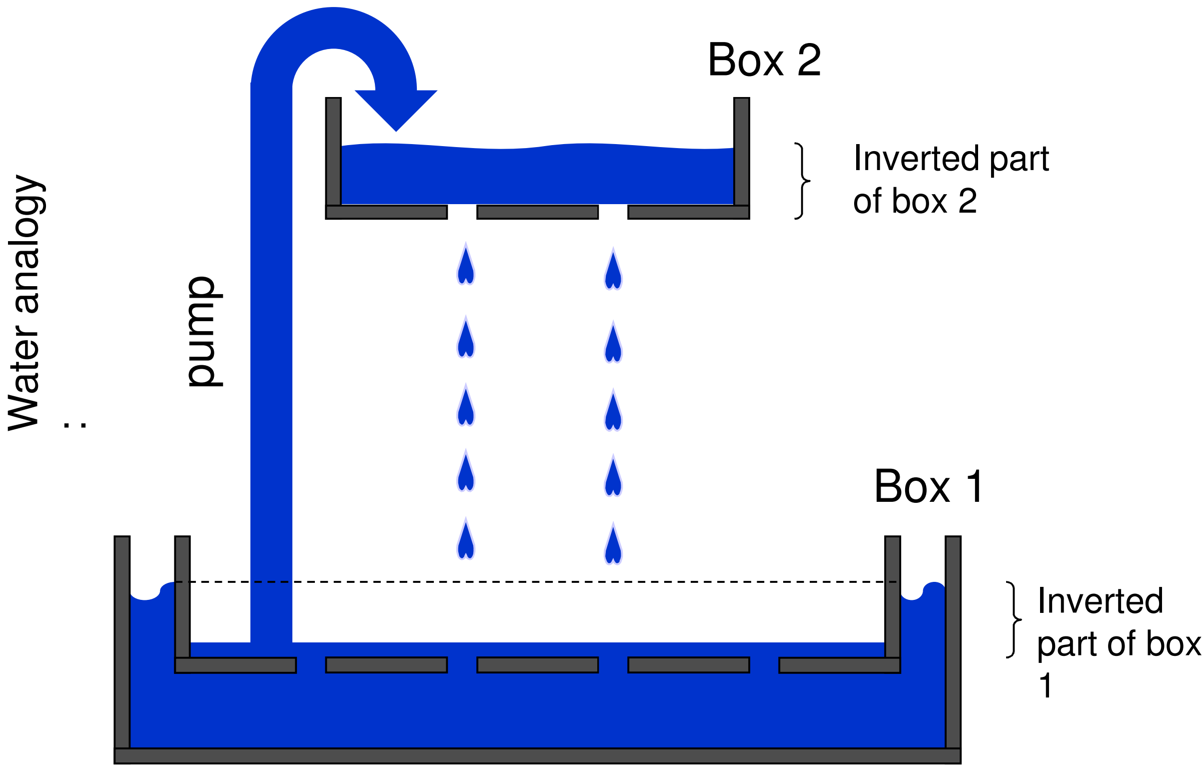

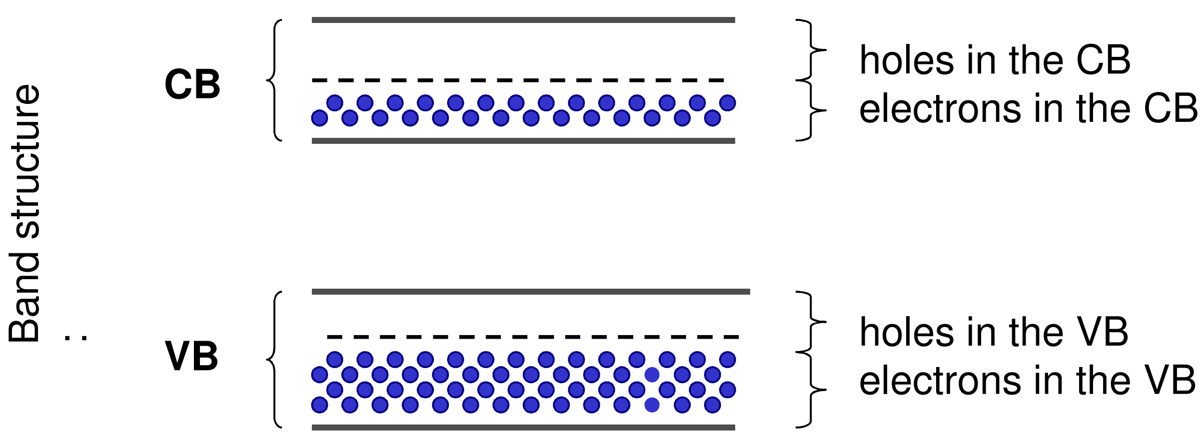

Emmision of photons by radiative recombination of electron-hole pairs

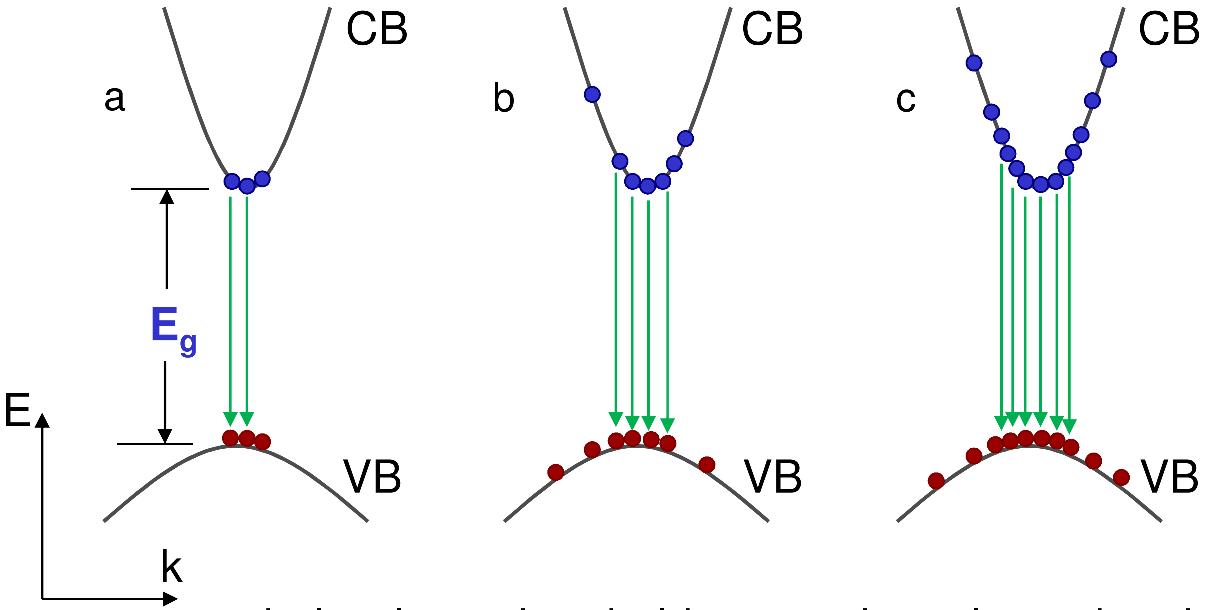

below laser threshold

above laser threshold

Corresponding band structure of the active layer in real space including the quasi Fermi levels

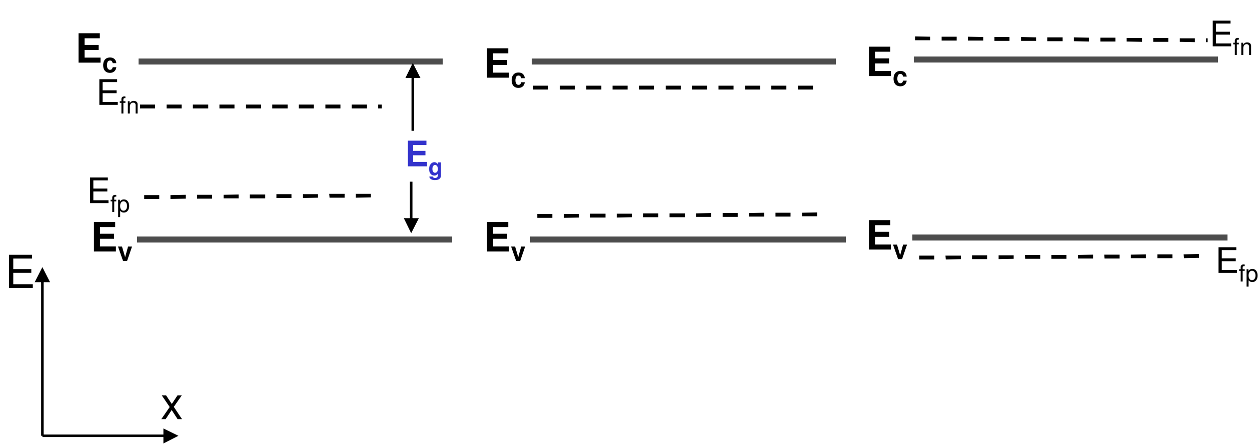

Band structure of the active layer in real space

1. Additionally a **waveguide** is required :

Active layer is surrounded by material of lower refractive index $\bar{n}$

Active layer : lowest E_g $\longrightarrow$ highest $\bar{n}$

Cladding layers : lower $\bar{n}$ $\longrightarrow$ higher E_g

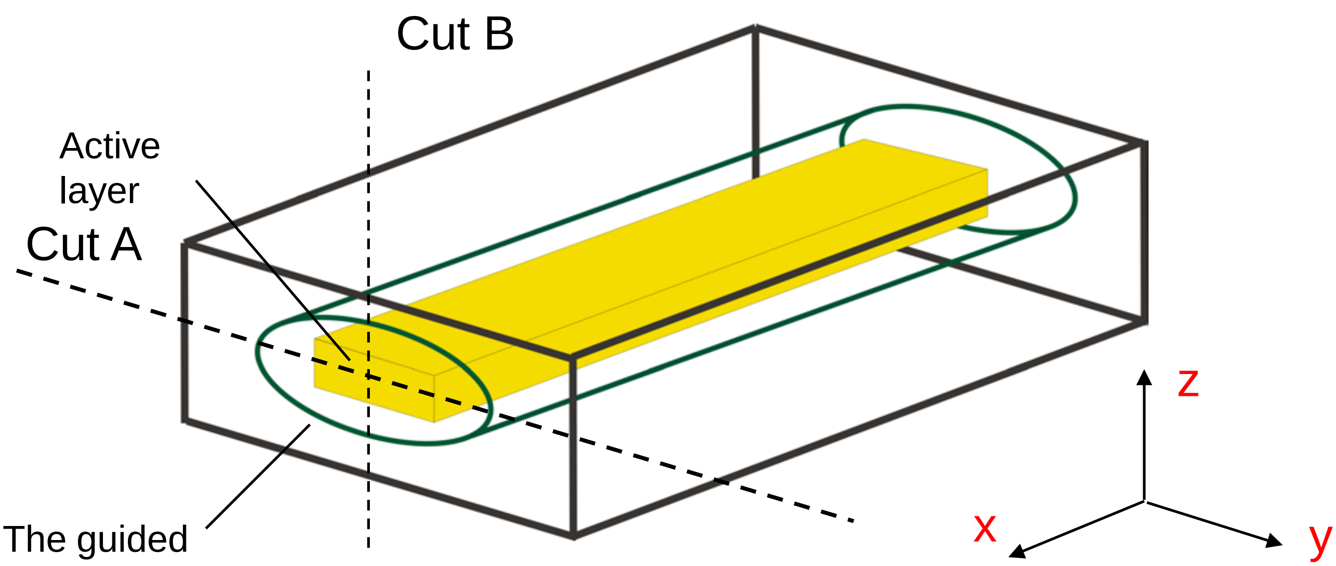

The guided optical field is schematically shown. On the ellipse all prints of a considered (constant) intensity are located details of the intensity distributions (profiles) are shown below:

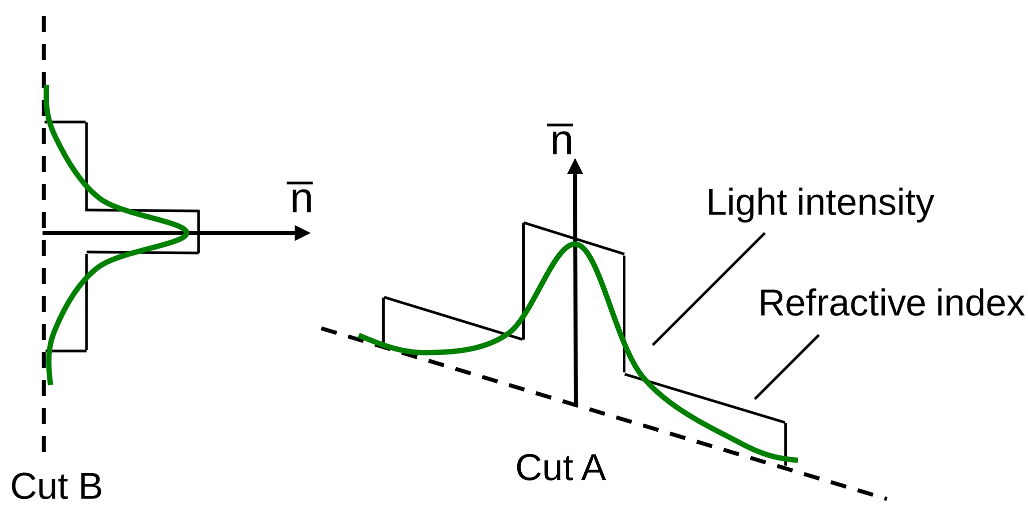

Here : the active layer is homogeneous (3D active layer)

Fabry – Pérot – Laser

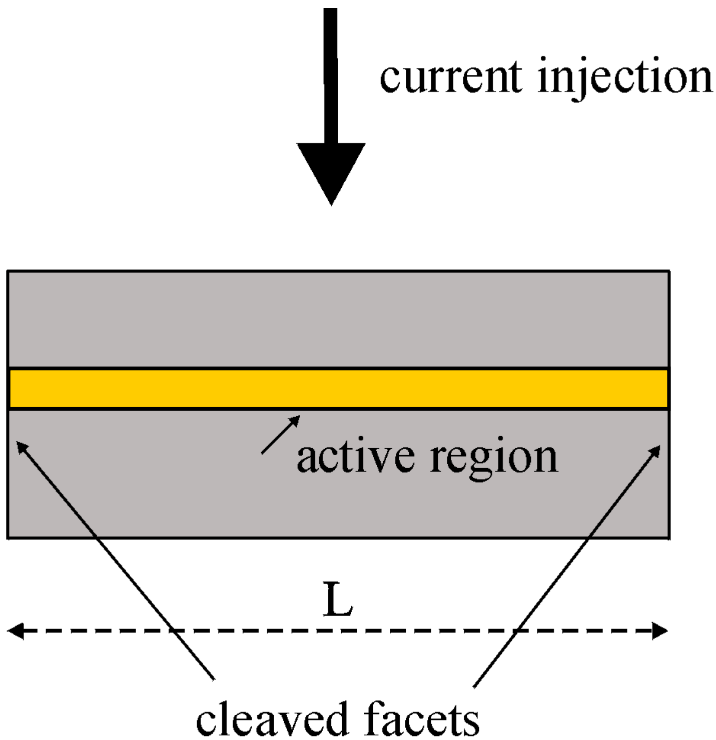

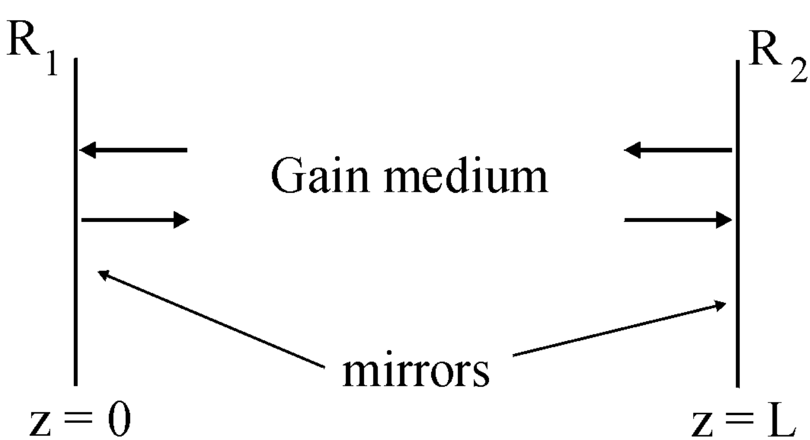

Fabry - Perot cavity

$$R \sim \left(\frac{\bar{n}_1 - \bar{n}_2}{\bar{n}_1 + \bar{n}_2} \right)^2$$

The semiconductor laser I

In modern semiconductor lasers the bulk (3D) active layer is replaced by a multiple quantum well stack (2D).

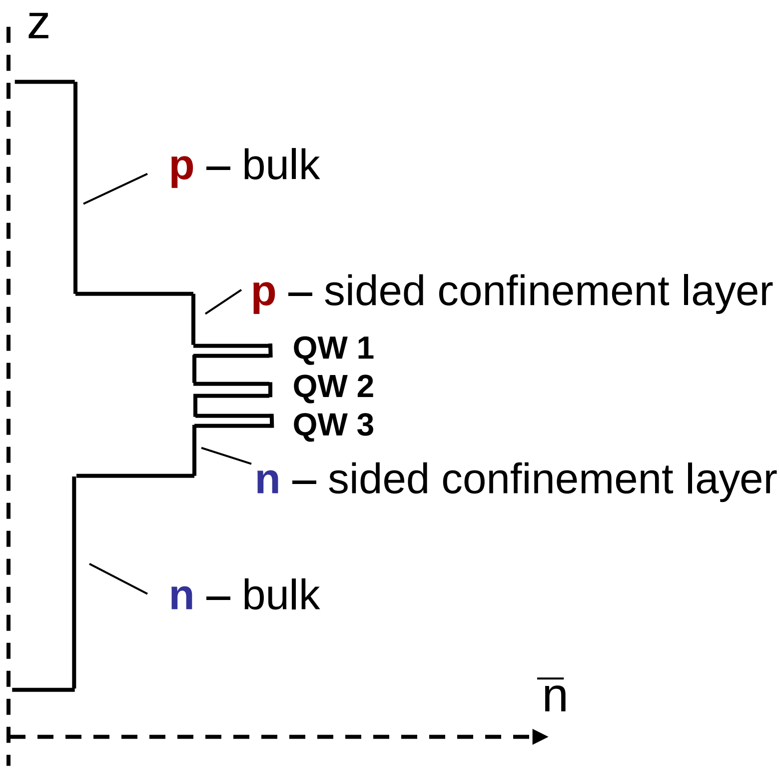

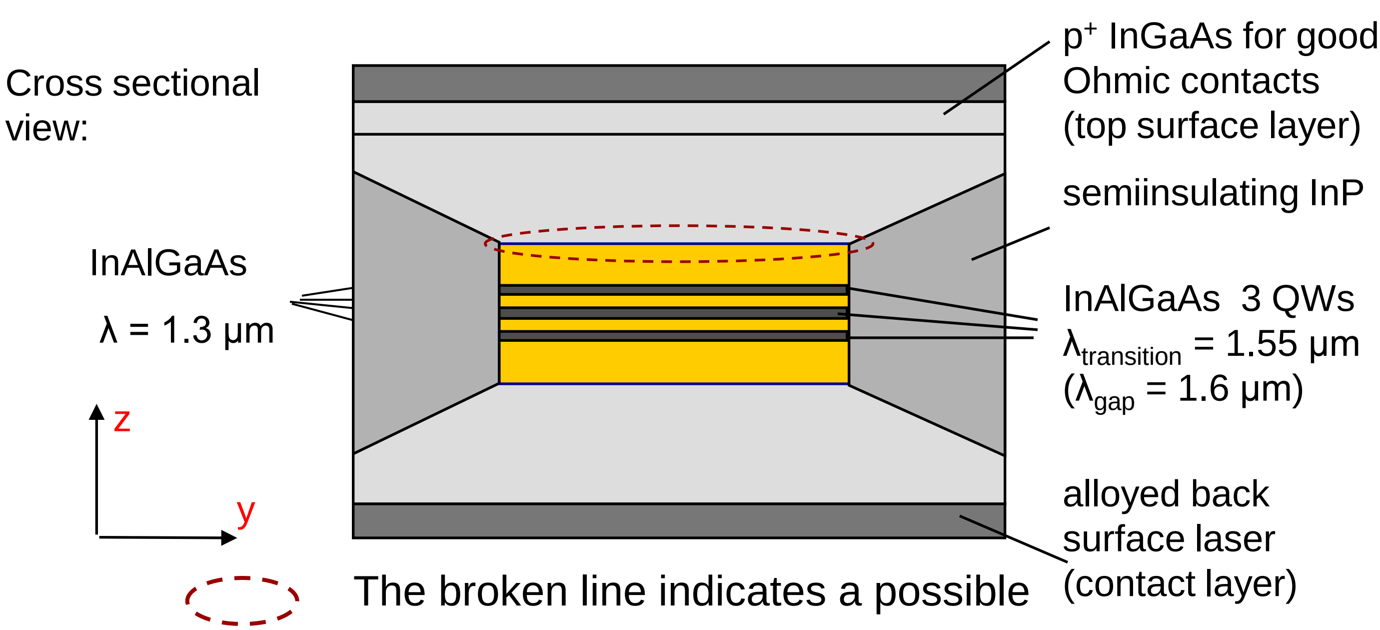

The broken line indicates a possible position of the DFB grating

The semiconductor laser II

Insulating layers on the left or right hand side of the active layer or other tricky arrangements are required to force the carriers to pass the active layer (to avoid noticeable leakage currents).

2. Pumping

A. Optical pumping:

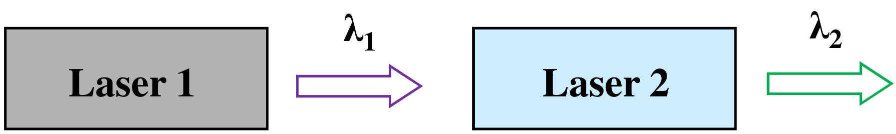

λ_2 is the designed wavelength, to be used in the application

$\lambda_1 << \lambda_2$; λ_1 is used for pumping the active layers of laser 2

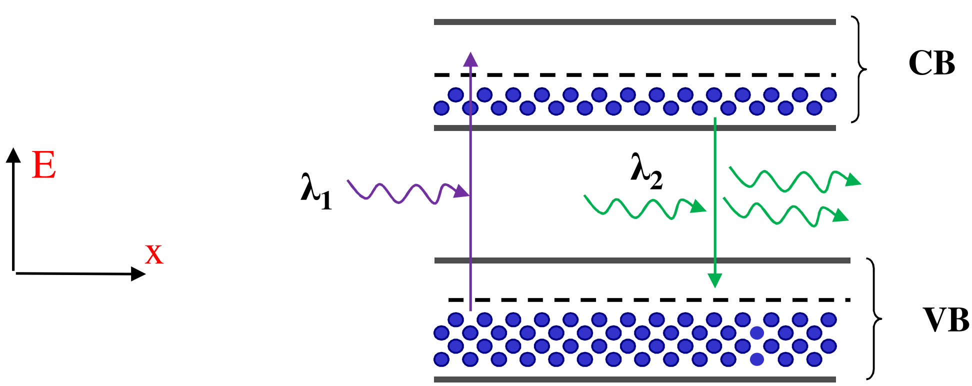

Optical pumping has to be used in the cases where no electrical pumping is possible / not yet possible. E.g. for new material systems where often p-contacts are bad or p-doping difficult.

Semiconductor materials for optoelectronics

optoelectronic devices

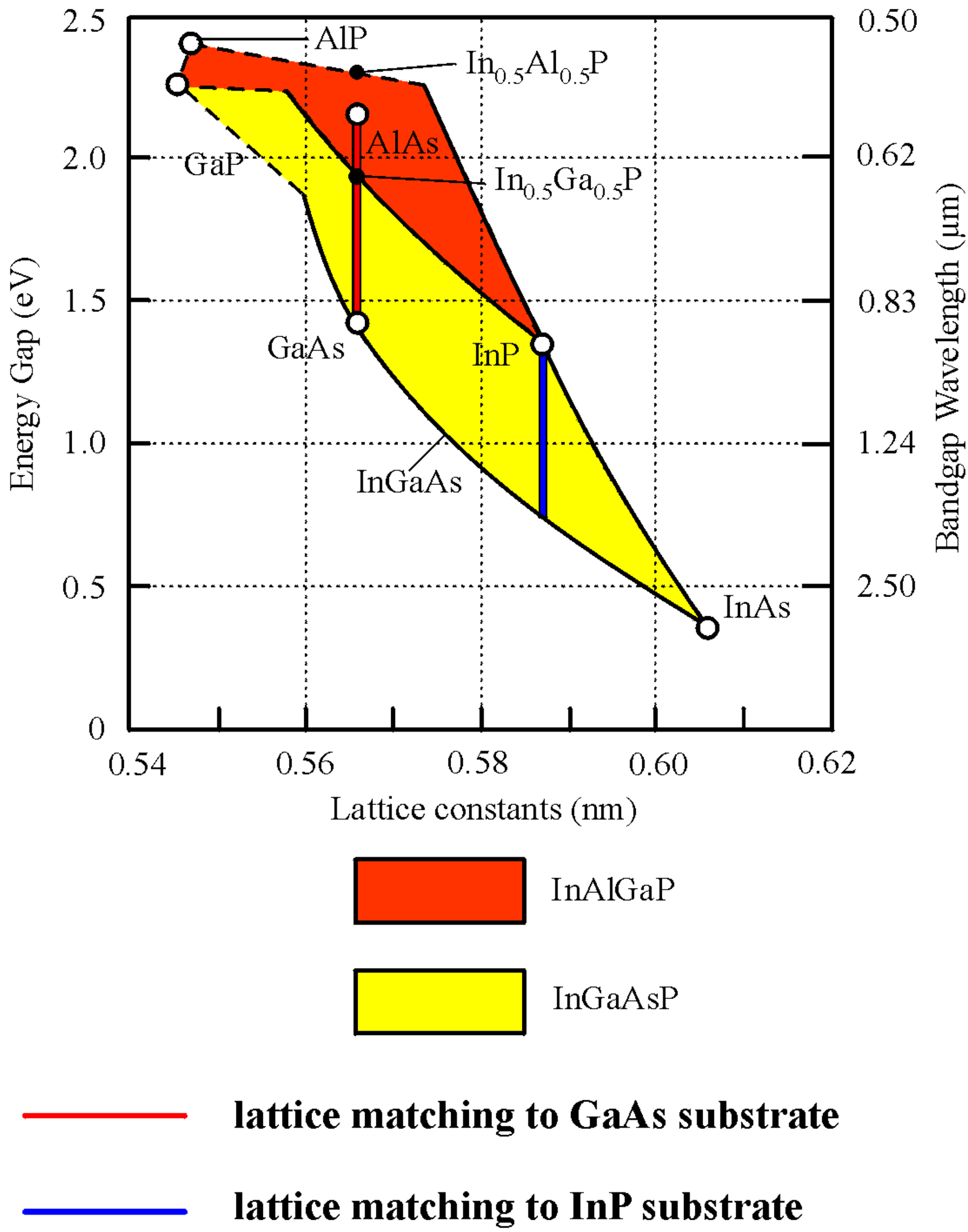

Long wavelength fiber communication lasers (λ = 1.3 - 1.55 µm) :
InGaAsP on InP substrate

Red lasers (λ = 620 - 690 nm) :
InAlGaP on GaAs substrate

Schematic diagram of an edge emitting laser

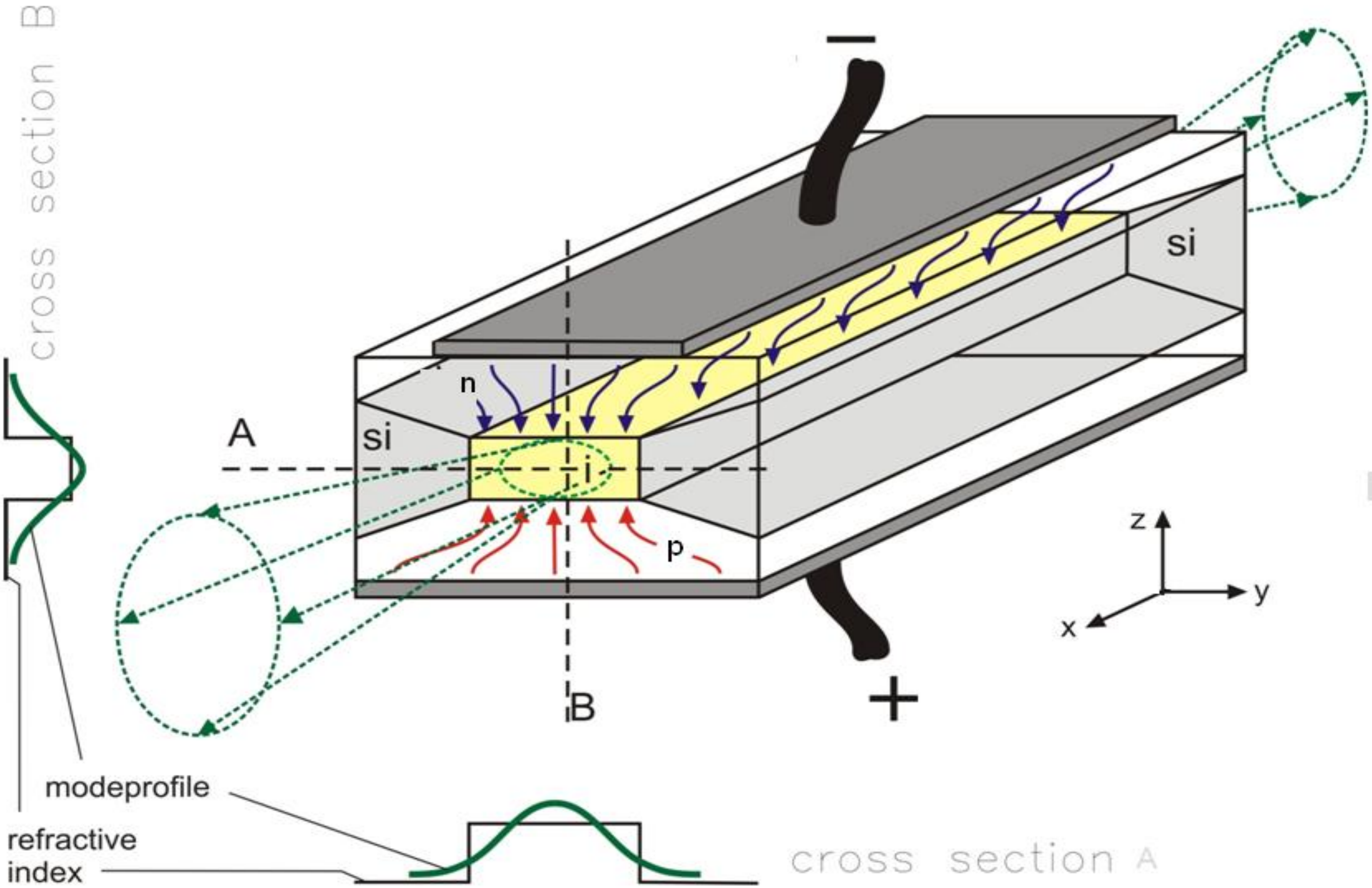

B. Electrical pumping

(in most of the cases)

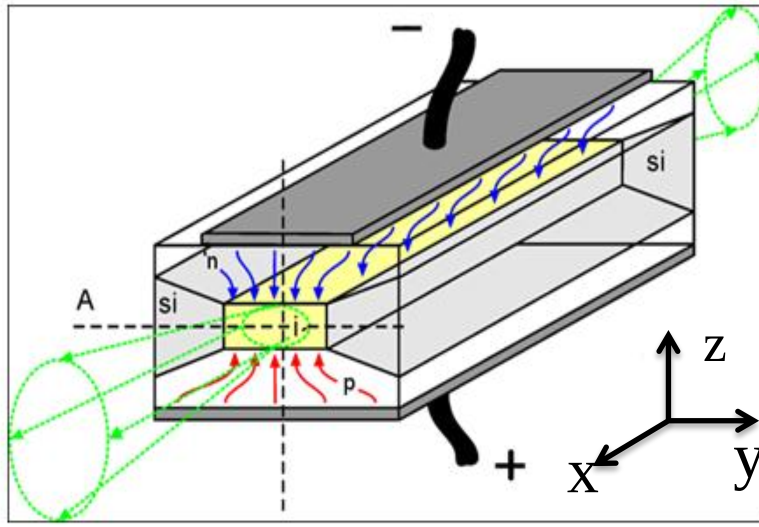

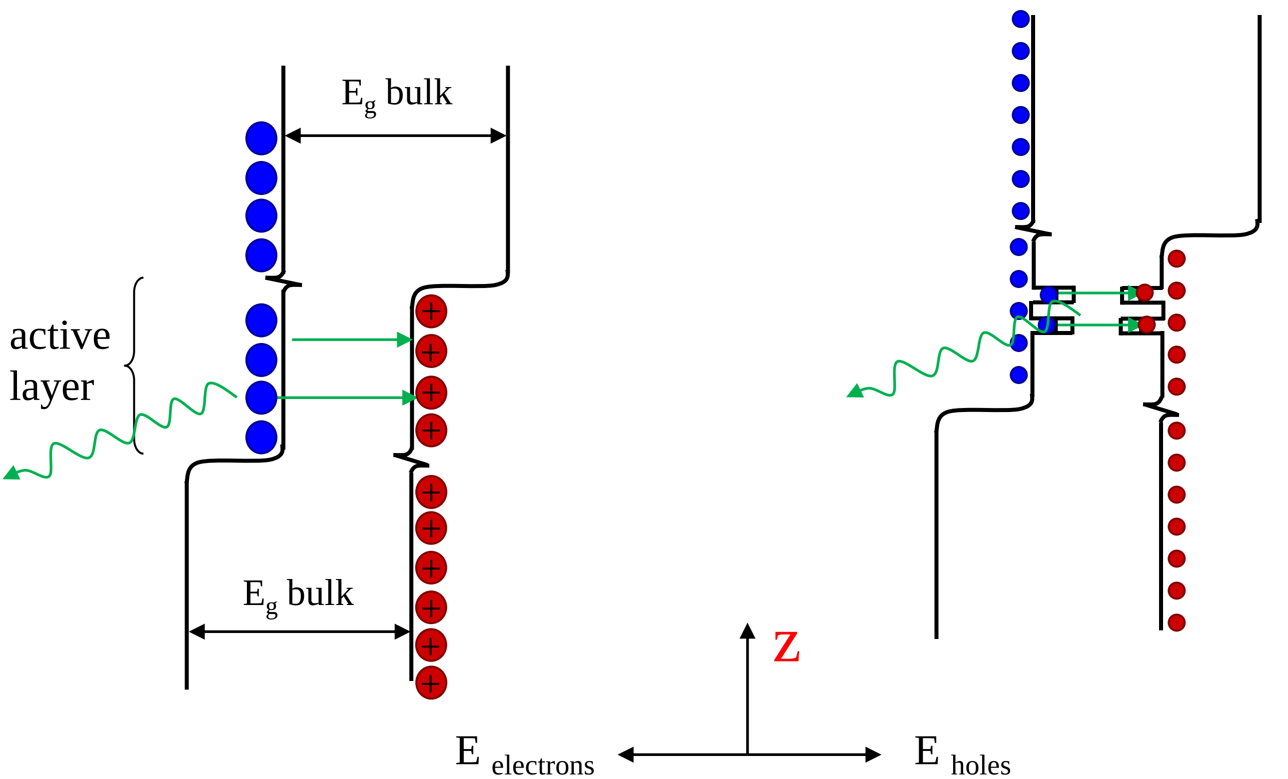

for a bulk 3D active layer

for an active layer consisting of 2 QWs

The laser transition takes place between the lowest energetic level of the CB well and the energetic lowest level of the VB well.

Simple **pn- homojunction** for **Semiconductor Lasers**

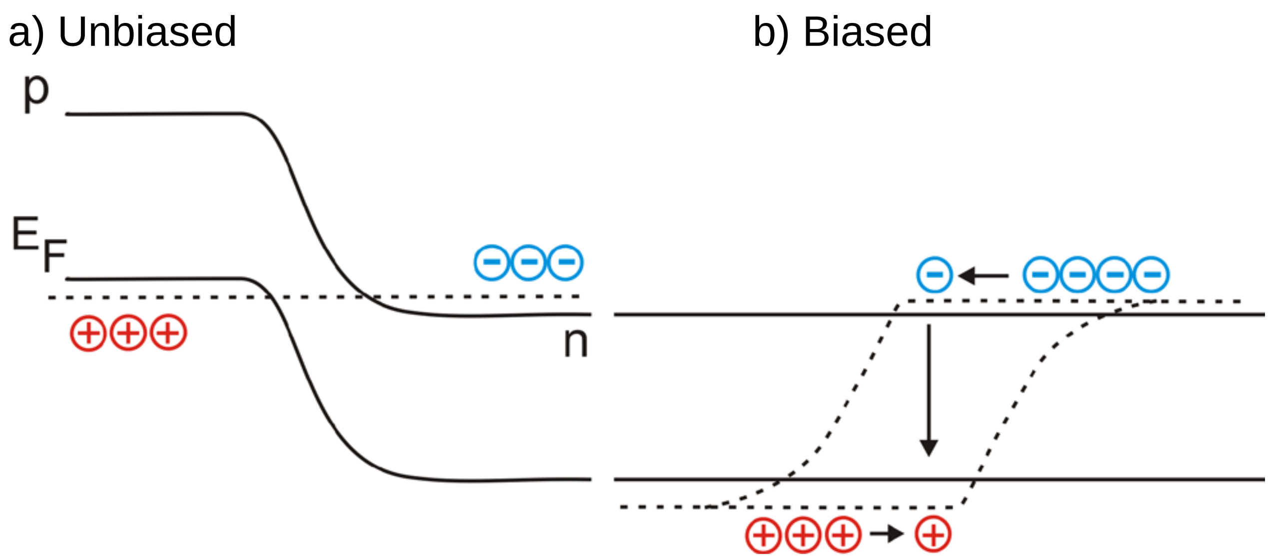

Historically the first laser. Could only be operated at T = 77 K, since this laser has a lot of electrical and optical losses.

Since:
- No waveguide (no optical confinement)
- Enormous optical loss, only photons travelling exactly parallel to the junction are amplified.
- No efficient electrical confinement
- Enormous leakage

Solution: double heterostructure

(Source by Prof H. Kroemer, Nobel price 2000)

The semiconductor laser IV

Solution : double heterostructure enables both

(1) Leakage current ↓ reduction

(2) waveguiding

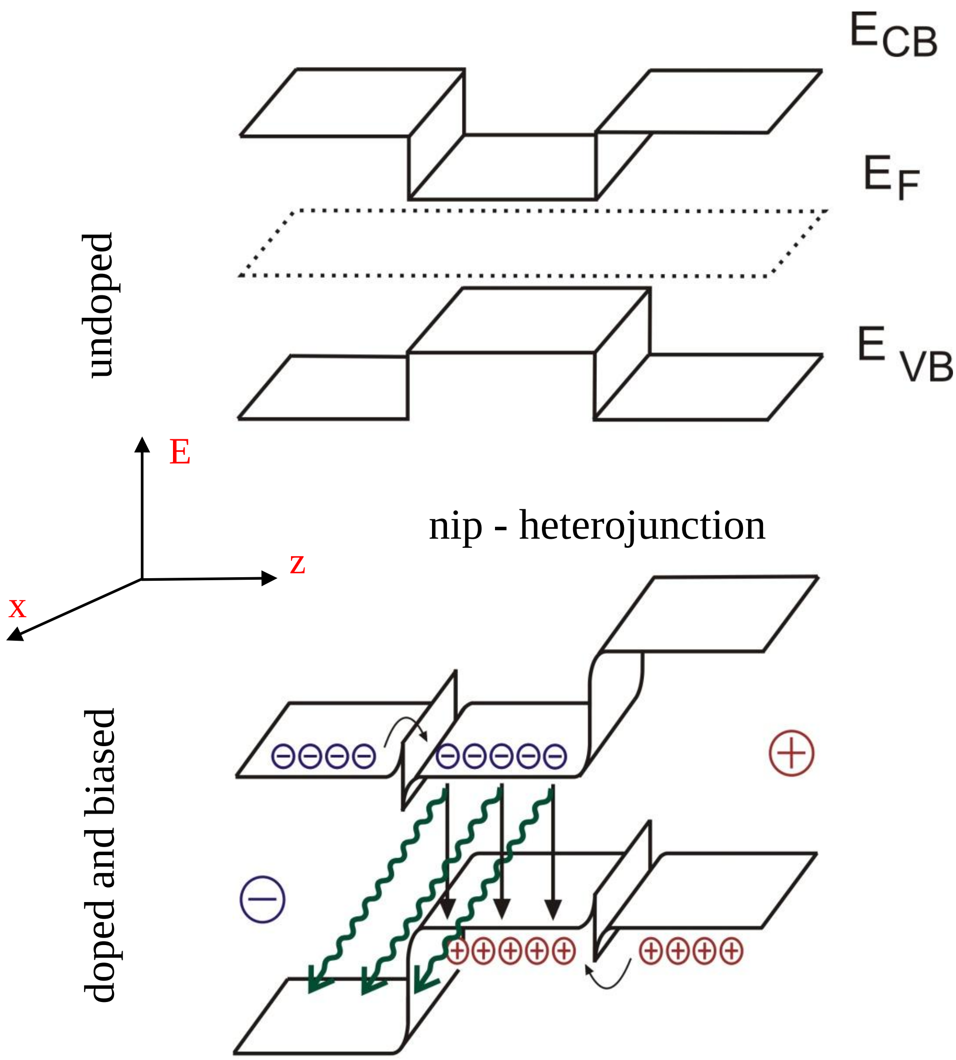

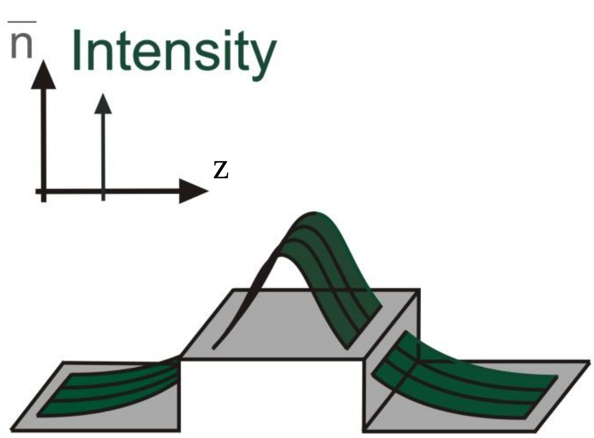

The semiconductor laser structure

pn hetero junction

no electrical and optical confinement

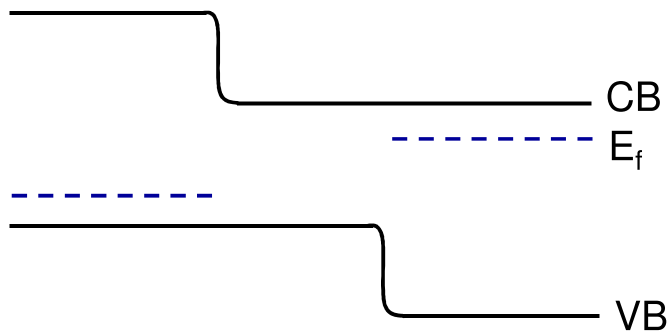

pn heterojunction

electrical and optical confinement

here: active layers = quantum wells

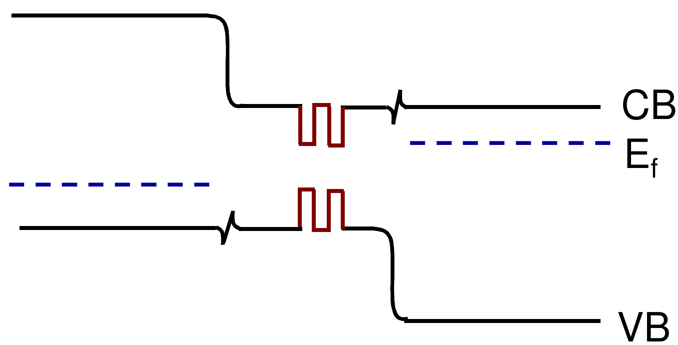

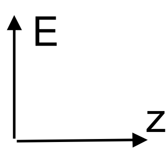

a) SCH – separate confinement heterostructure

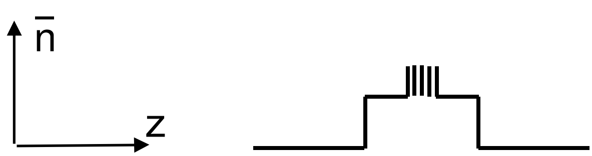

b) GRINSCH – graded index separate confinement heterostructure

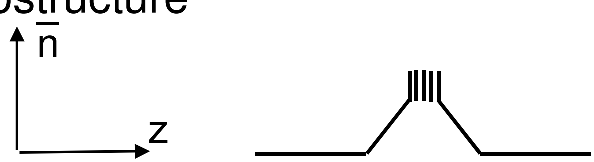

The semiconductor laser V

3. Resonator

A. **Fabry – Perot** cavity:

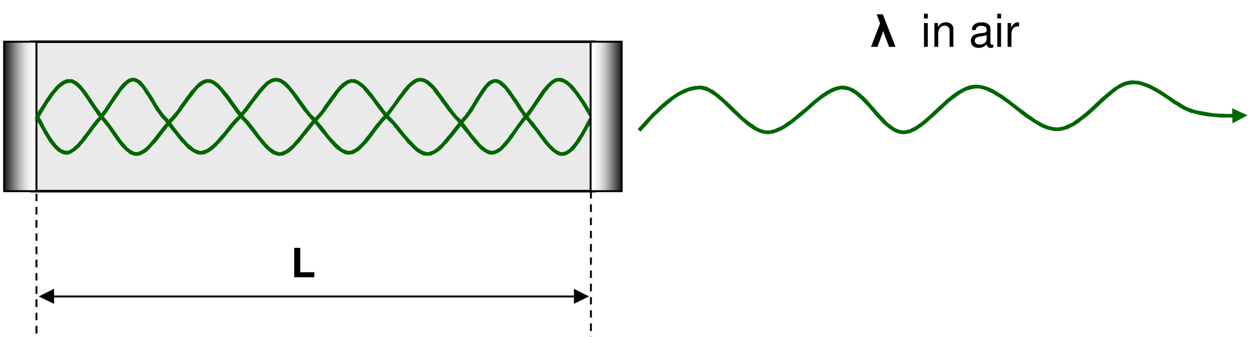

$$L = m \cdot \frac{\lambda / \bar{n}_{eff}}{2}$$

The wavelength in the semiconductor waveguide of effective refractive index $\bar{n}_{eff}$ is $\lambda / \bar{n}_{eff} = \lambda_{Medium}$

material gain and loss

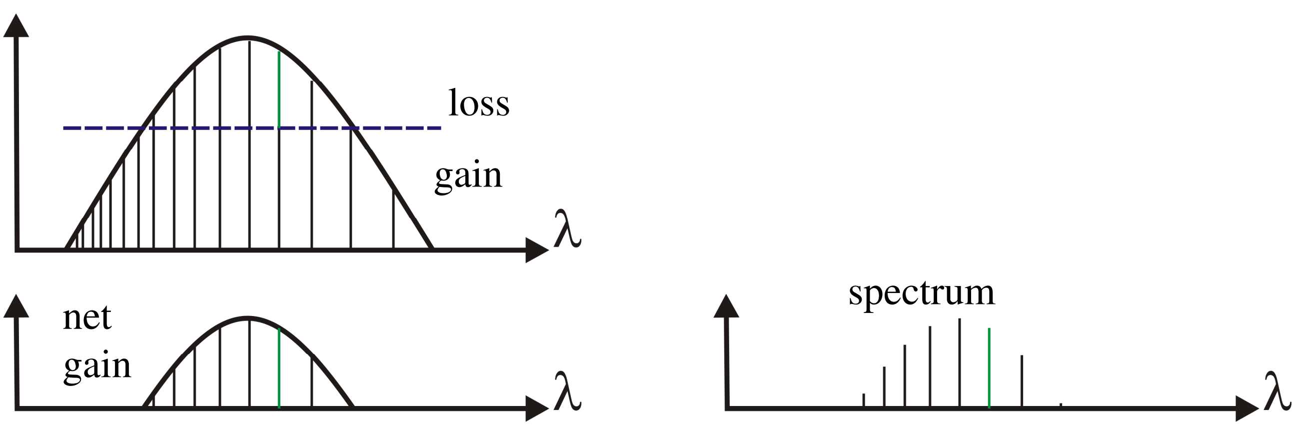

Example: $L = 151\ \mu m$; $\bar{n}_{eff} = 3.31$

active medium is chosen to amplify between 0.95 and 1.05 µm.

→ an individual mode: $\lambda = 1\ \mu m$ corresponds to an order of $m = 1000$
→ $\lambda_{Medium} = 302\ nm$

λ / μm	m
1000	1
500	2
333	3
250	4
200	5
167	6
...	...
...	...
...	...
1,0489	953
1,0478	954
1,0476	955
...	...
...	...
...	...
1,0	1000
...	...
...	...
...	...
0,9566	1045
0,9557	1046
0,9547	1047
0,9538	1048
0,953	1049
0,952	1050
0,9511	1051
0,9502	1052

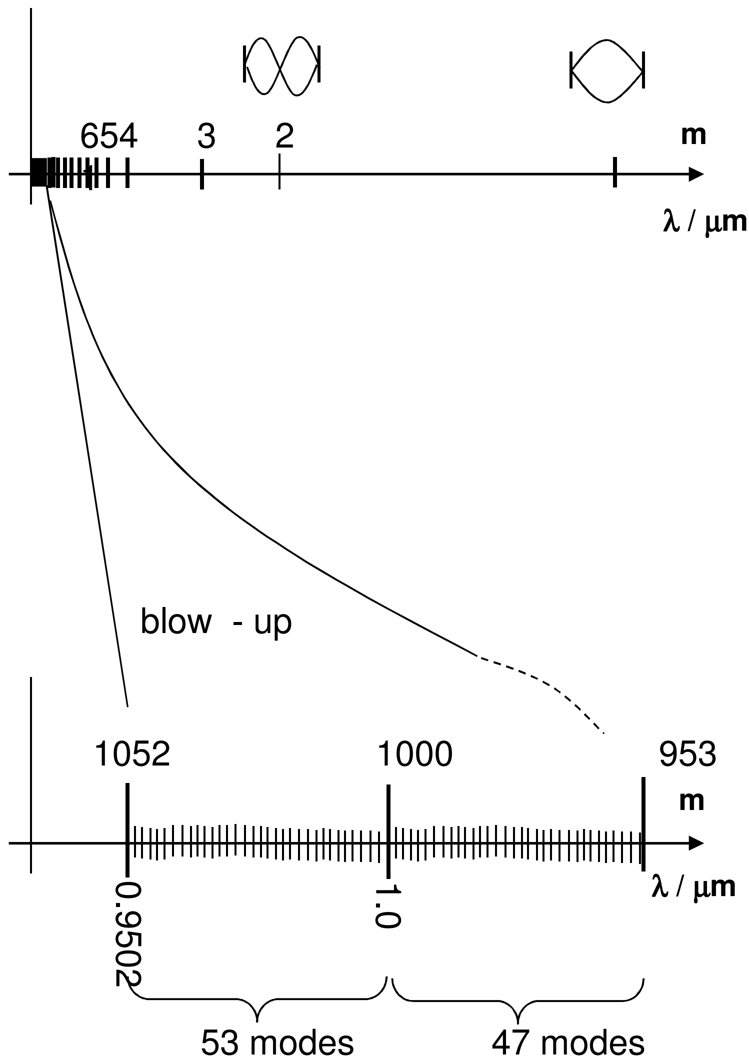

Inside the spectral gain profile of the above example, 100 FP modes are located.

This calculation does not include material dispersion $\overline{n}_{eff} = \overline{n}_{eff}(\lambda)$ which would further make the mode spacing unequidistant!

The modes only seem to be equidistantly spaced, in reality they are not. Due to the optical losses roughly the 10 strongest modes will lase.

<u>FP lasers</u> are multimode in most cases for extremely short cavities: they can be single – mode.

<u>DFB lasers</u> (Distributed feedback laser)

DFB cavity (= resonator type II) can be designed to be single – mode !

Bragg condition:

$$\boldsymbol{\lambda_B} = 2 \cdot \bar{n}_{eff} \cdot \Lambda \cdot \frac{1}{m}$$

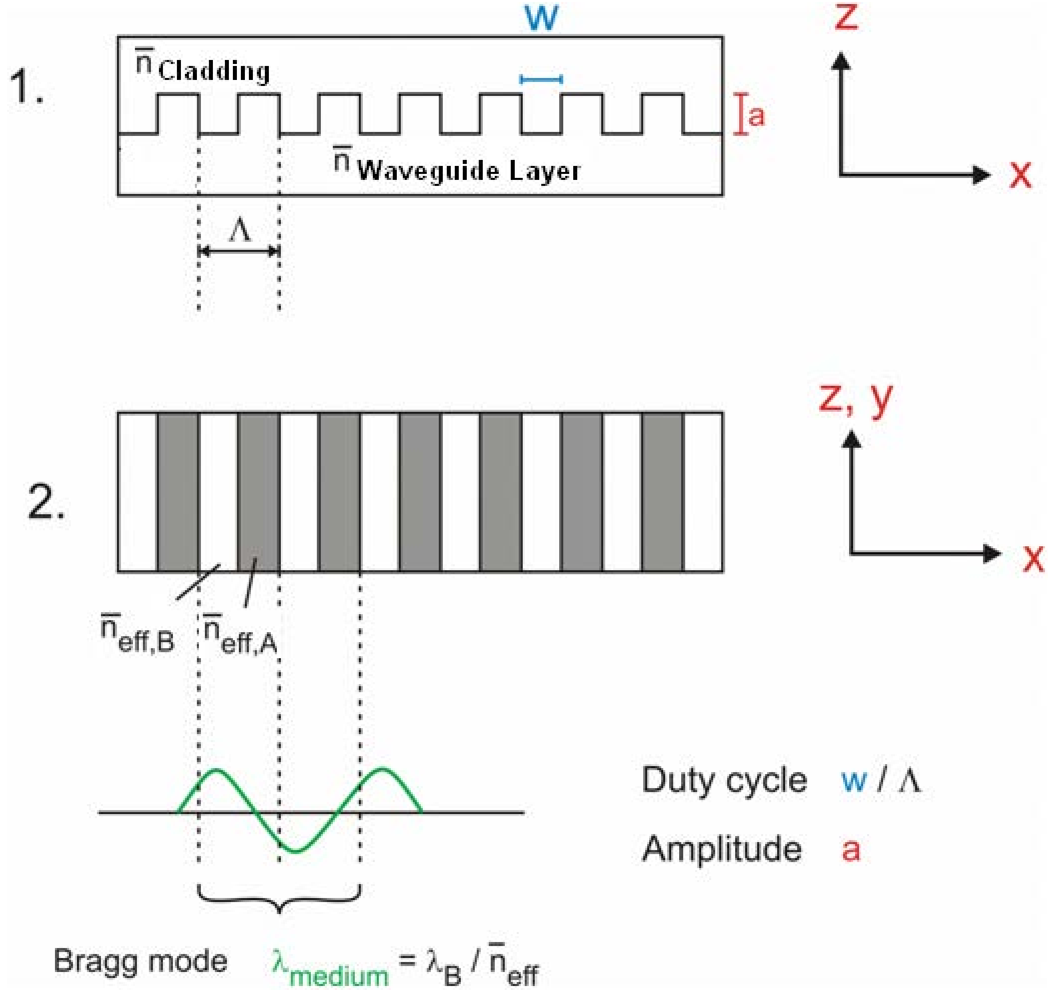

The light propagating in z – direction feels periodic quasi layers of higher ($\bar{n}_{eff,\ A}$) and lower ($\bar{n}_{eff,\ B}$) effective refractive index, as shown in the second diagram

Example: Λ = 228 nm, $\boldsymbol{\lambda_B}$ = 1.55 µm, $\bar{n}_{eff}$ = 3.4 , m = 1

Waveguide with integrated DBR grating

DFB filter (without laser active layer, i. e. without current injection and carrier inversion)

DFB laser (with laser active layer and carrier inversion by current injection)

Classification of important direction

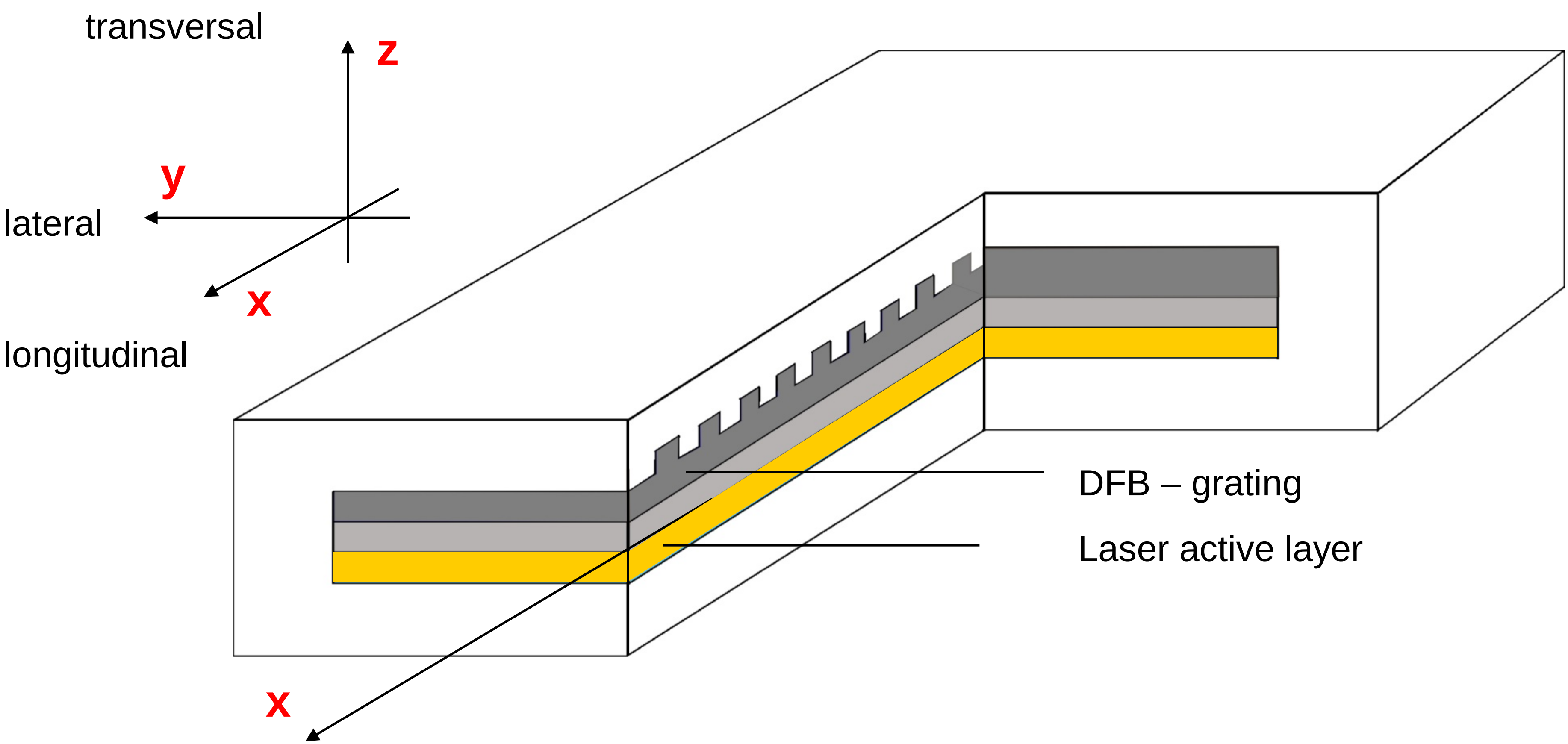

Illustration of the operation of a DFB grating

X-ray diffraction at the atomic planes of a crystal

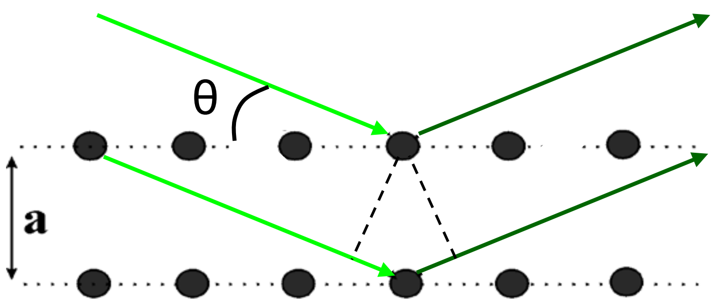

Bragg - condition

$$2a \cdot \sin\theta = m \cdot \lambda$$

m = 1, 2, 3, ...
Lattice constant a ≈ 0.5 nm
wavelength in the X-ray spectrum

Diffraction of light at periodic semiconductor layers e.g. VCSEL

(Vertical-Cavity Surface-Emitting Laser)

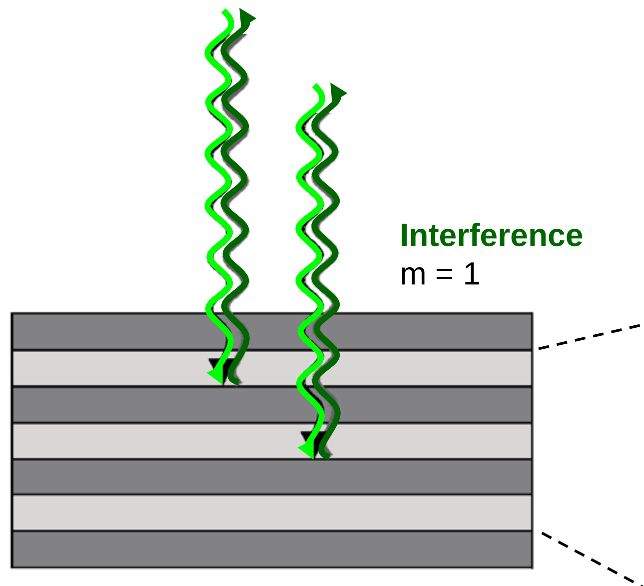

$$\Lambda = \frac{\lambda_B}{\bar{n}_{eff}} \cdot \frac{m}{2}$$

λ_B wavelength of the light in air

Grating period Λ = 100 ... 250 nm
wavelength λ = 800 ... 1600 nm

Technological realization

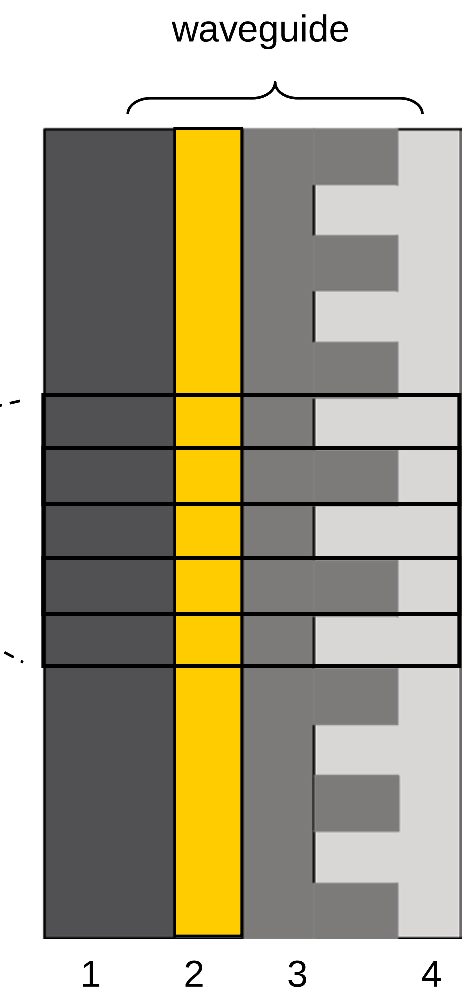

Quasi layers
A, B, A, B, … have effective
refractive indices $\bar{n}_{eff_B}$, $\bar{n}_{eff_A}$

This is a result from solving
Helmholtz - equation
in regions A and B

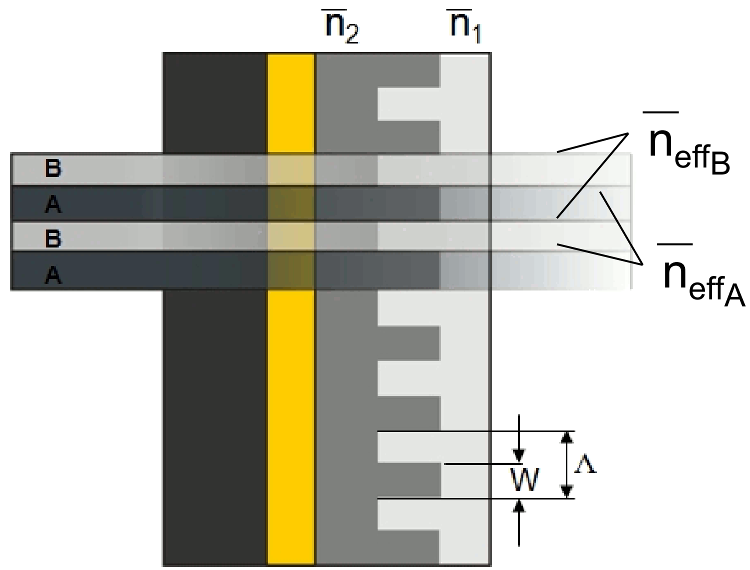

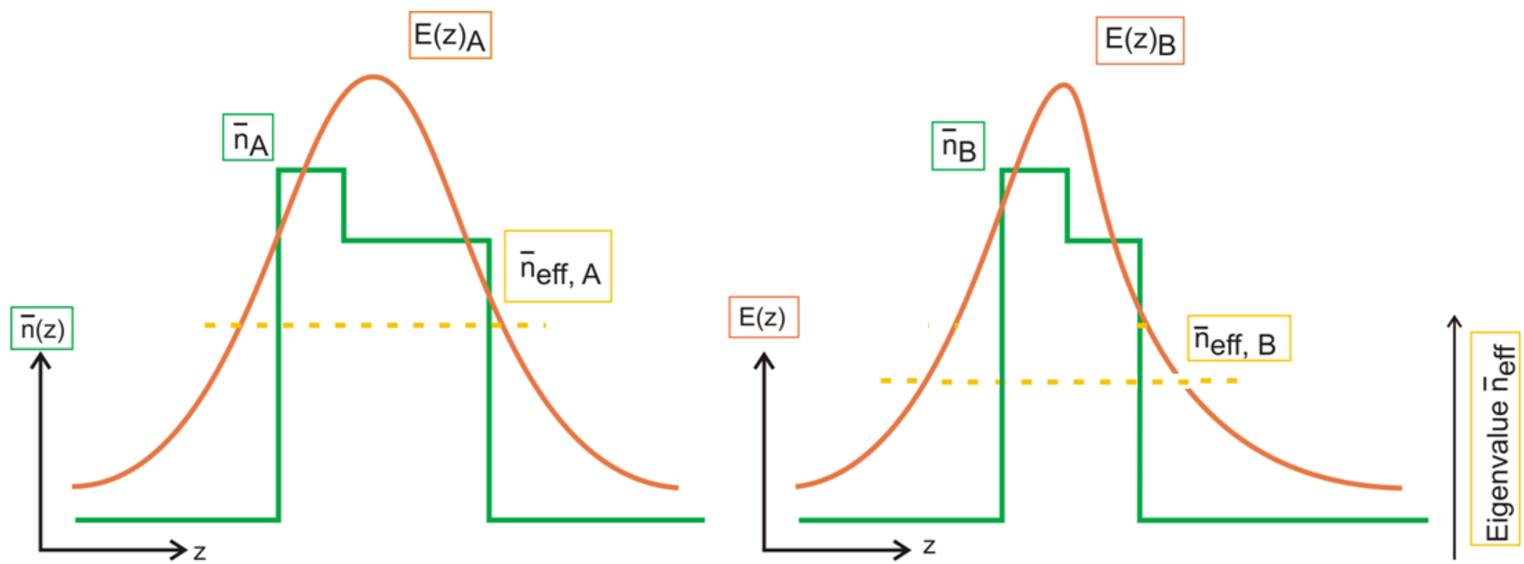

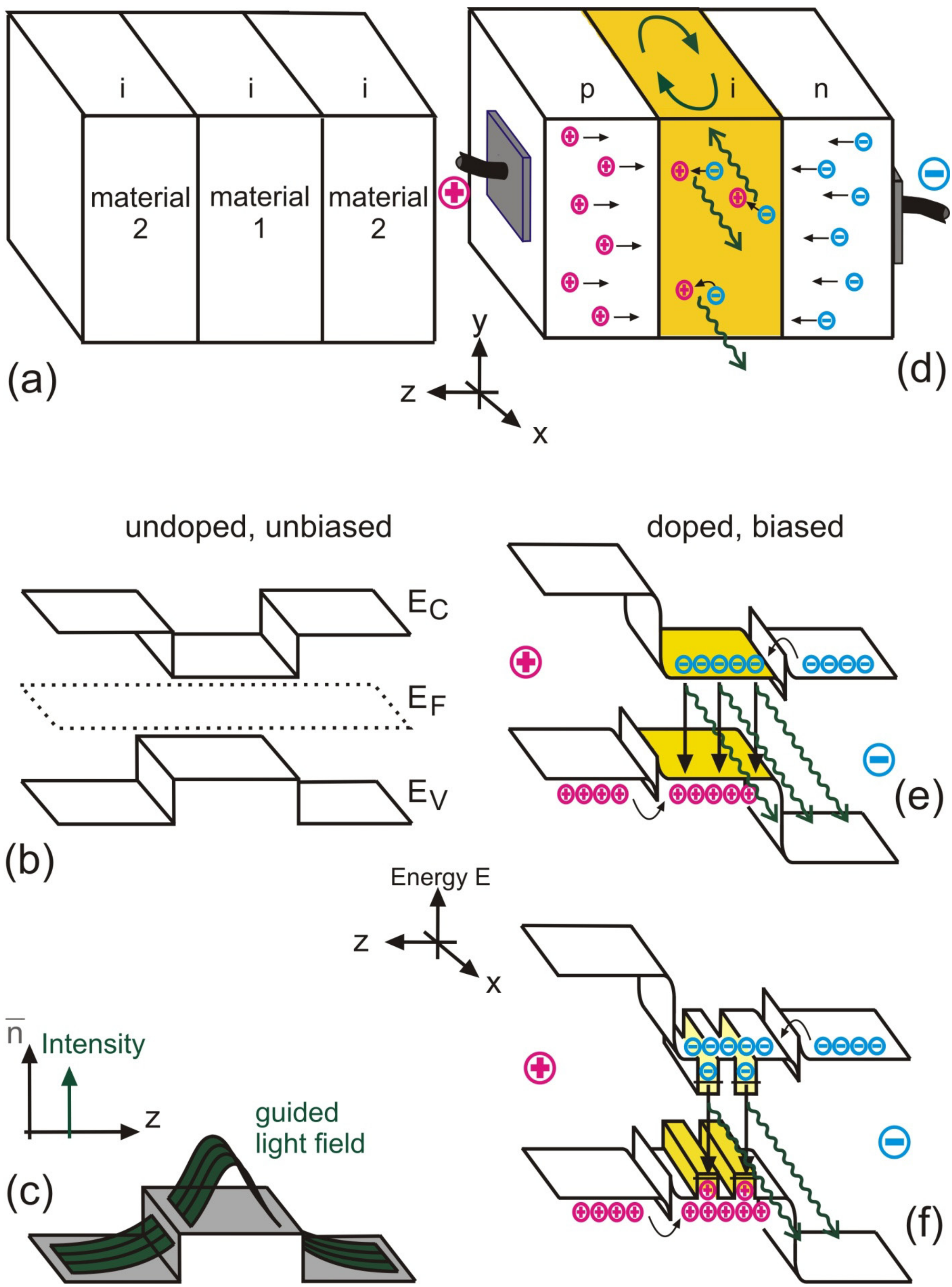
i
i
i
material 2
material 1
material 2
(a)
p
i
n
(d)
y
z
x
undoped, unbiased
E_C
E_F
E_V
(b)
doped, biased
(e)
Energy E
z
x
n
Intensity
z
guided light field
(c)
(f)

The high bit rate optimal transmission of news requires axial single-mode laser, for fiber transmission absportion is minimum at 1.55um

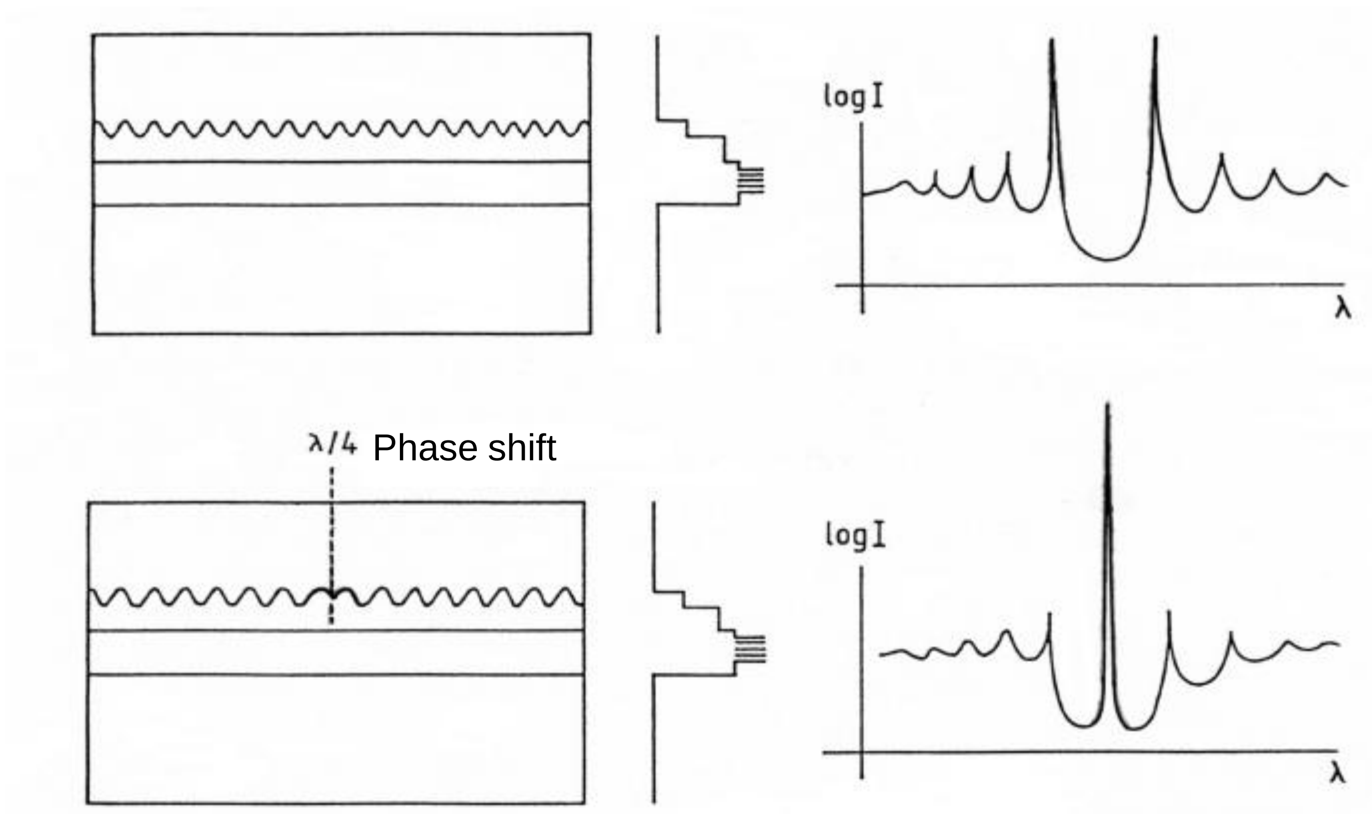

Repealing mode degeneracy

Device cross-sections and corresponding spectra of semiconductor lasers with horizontal and vertical resonator

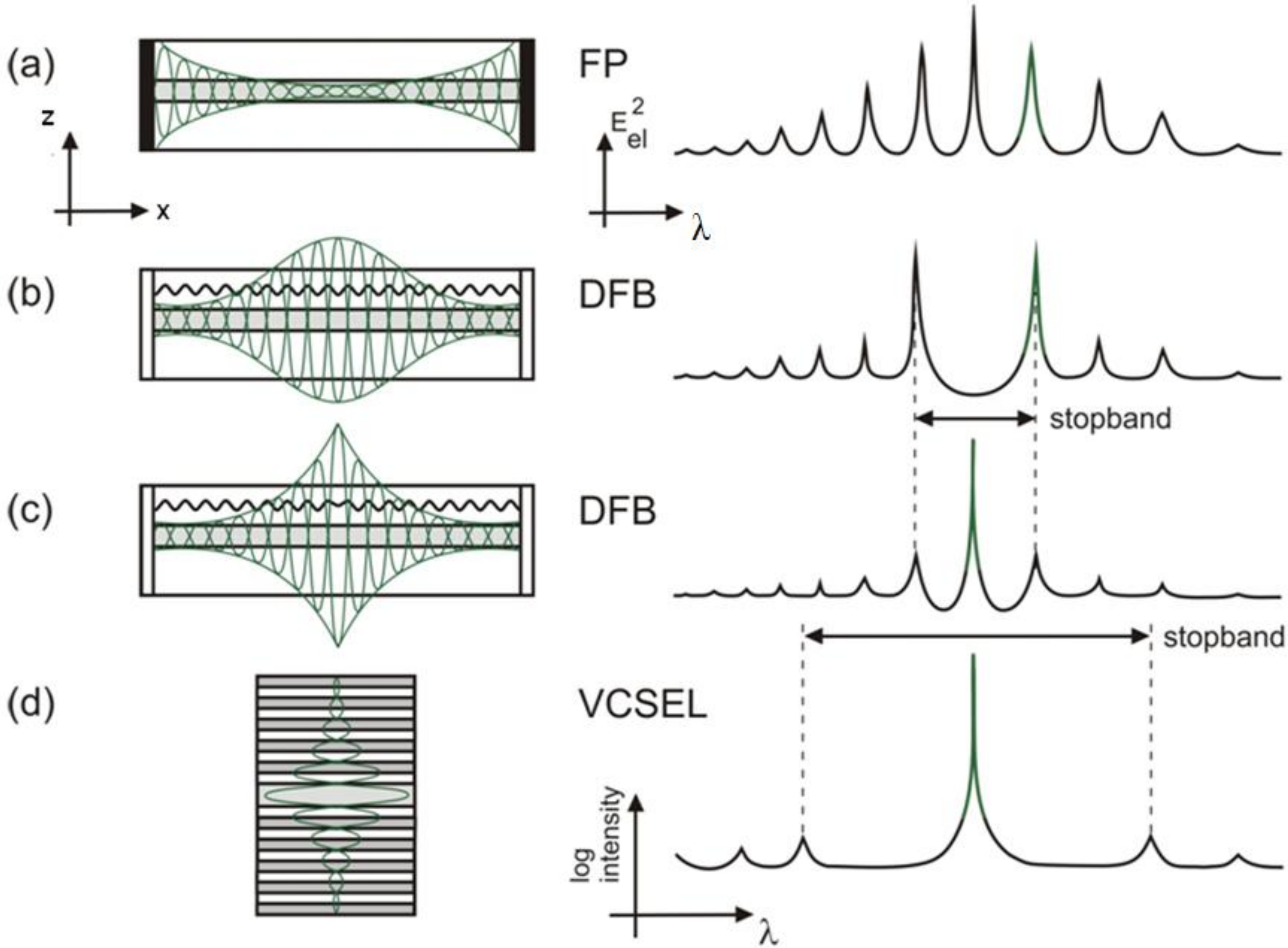

Cross-section of the layeres VCSEL structure with standing wave of the electric field

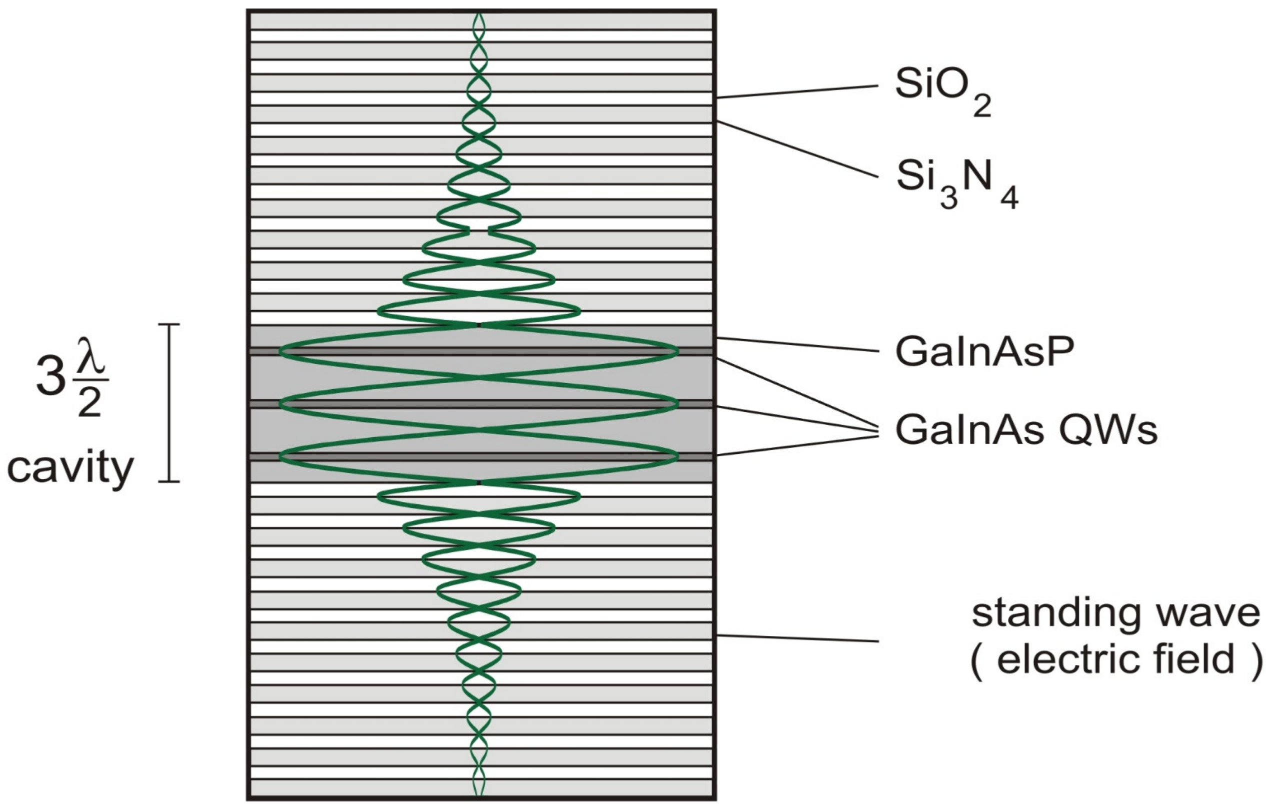

Illustration of the characteristics of a VCSEL Spectrum

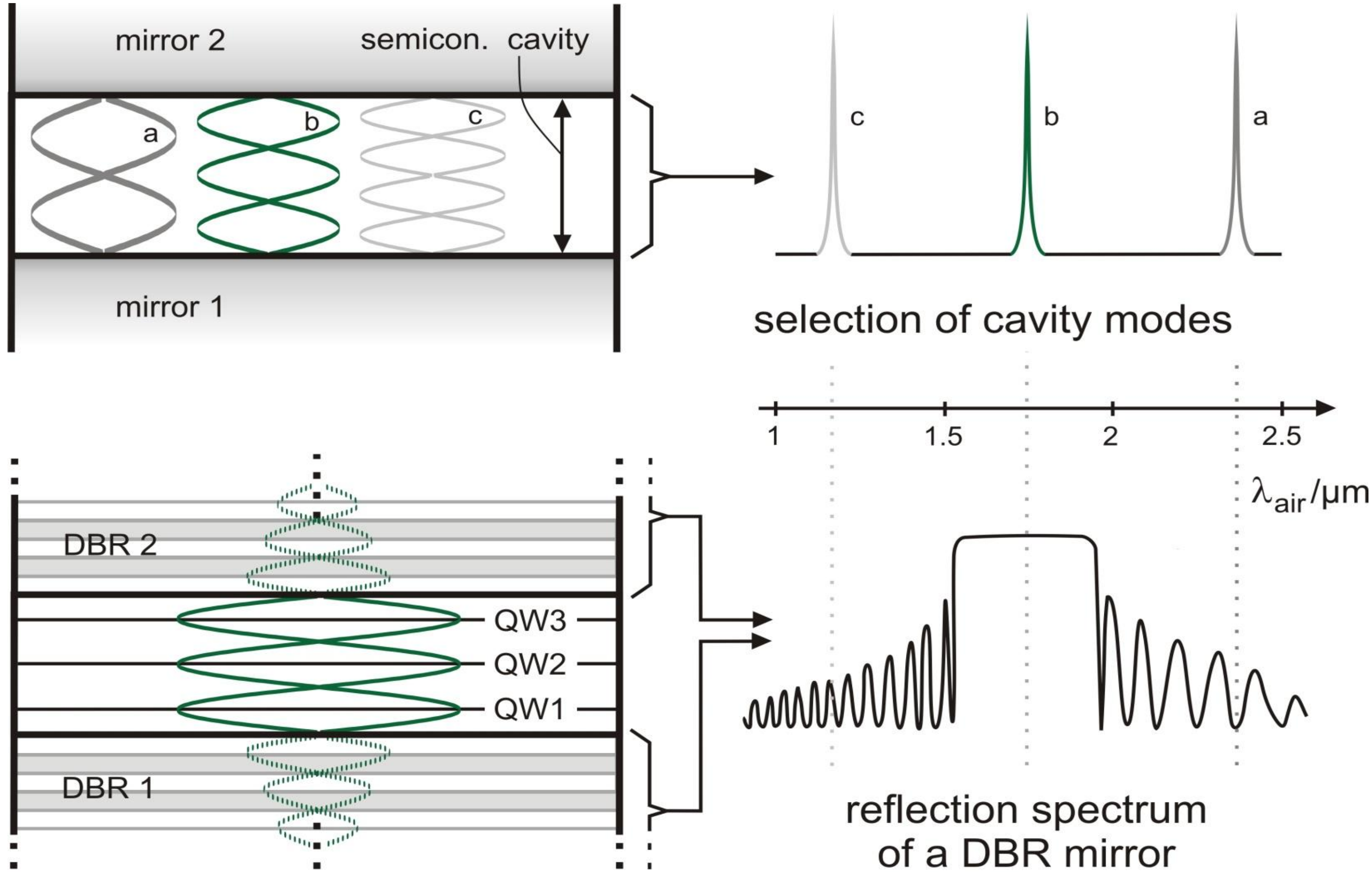

Characteristic spectral components of a VC-resonator. Three standing waves in the cavity (top left) cause the formation of the Fabry-Perot modes (top right) – made clear by right brace.

DBR mirror (bottom left) are characterized by reflection spectra (bottom right) – indicated by the two right braces.

For a short cavity length there‘s only single Fabry-Perot mode inside the stopband.

Long - wavelength VCSELs: Material aspects

Now: Long-wavelength (LW) VCSELs much more difficult to be implemented compared to 840 nm GaAs VCSELs

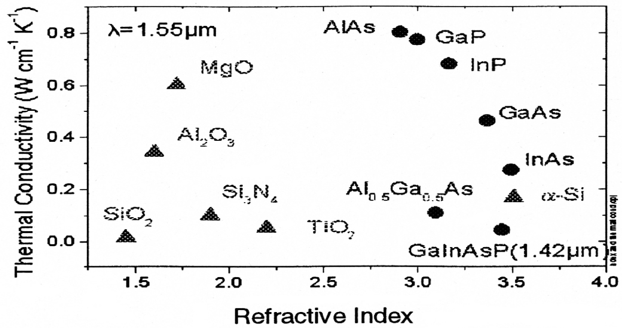

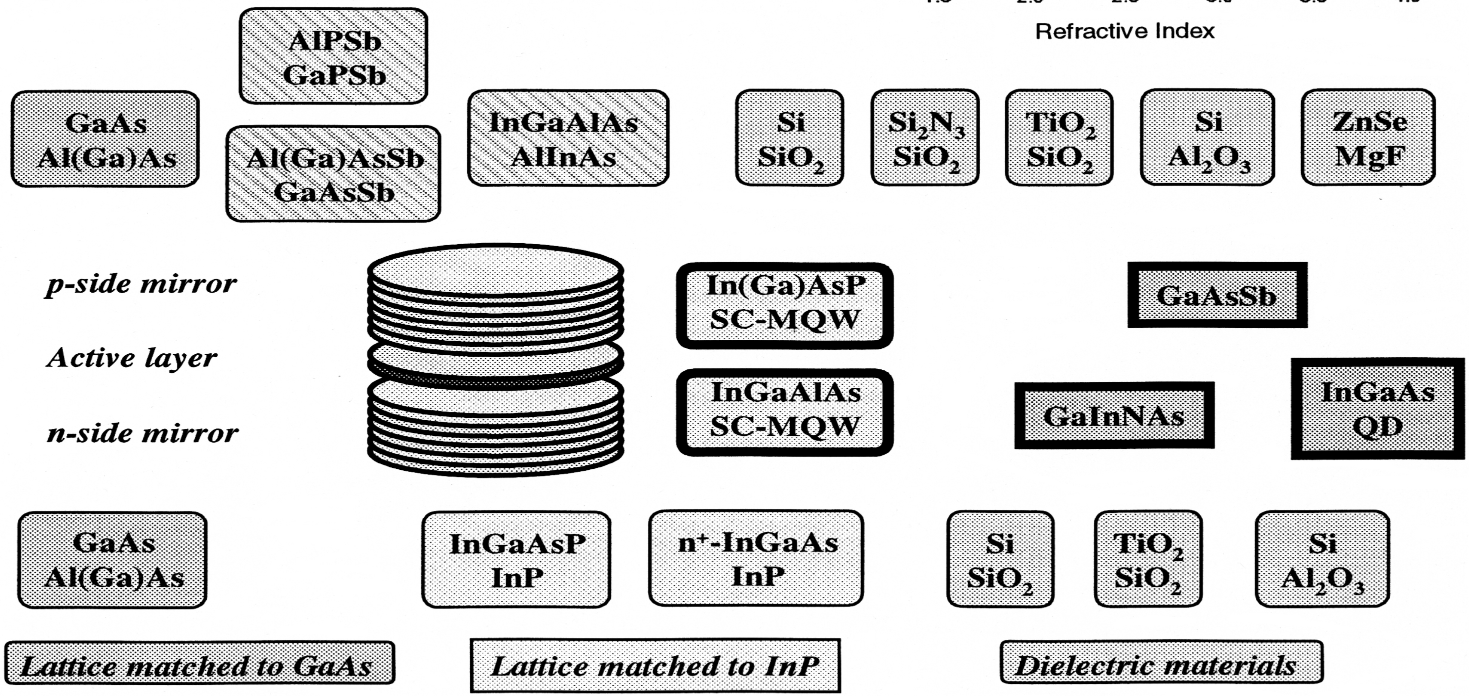

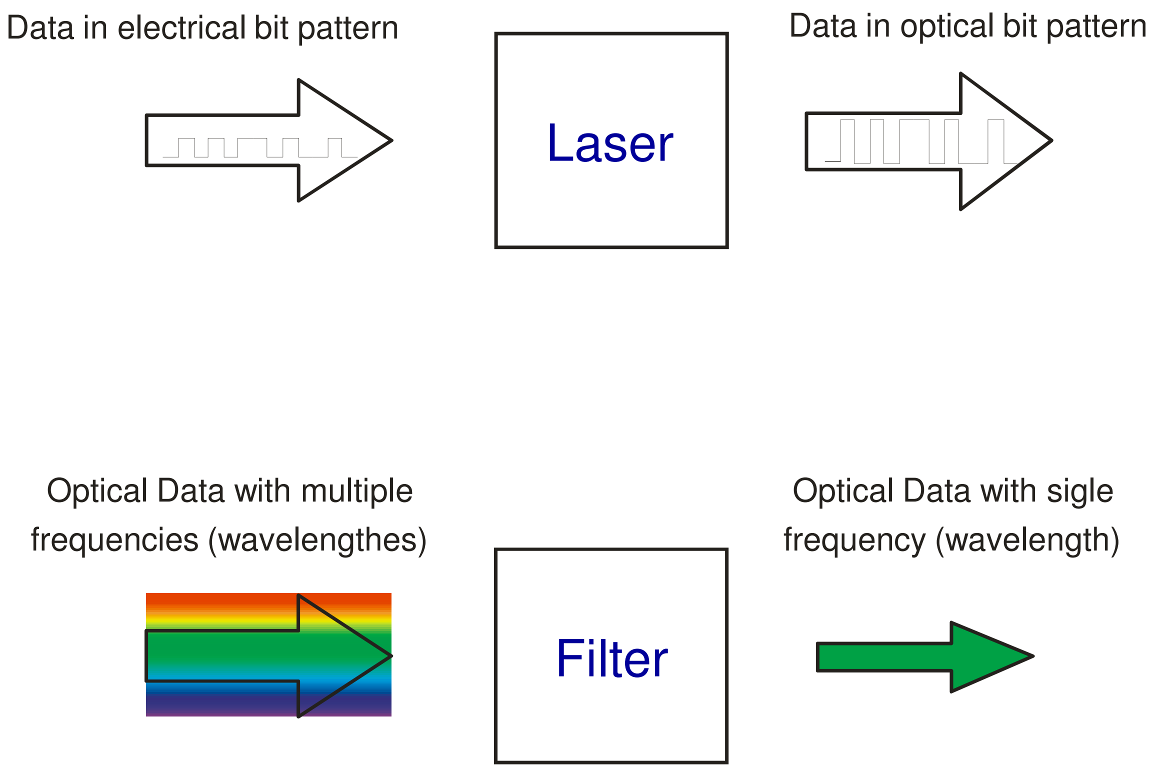
Data in electrical bit pattern
Laser
Data in optical bit pattern
Optical Data with multiple frequencies (wavelengthes)
Filter
Optical Data with sigle frequency (wavelength)

Dense Wavelength Division Multiplex (DWDM) system

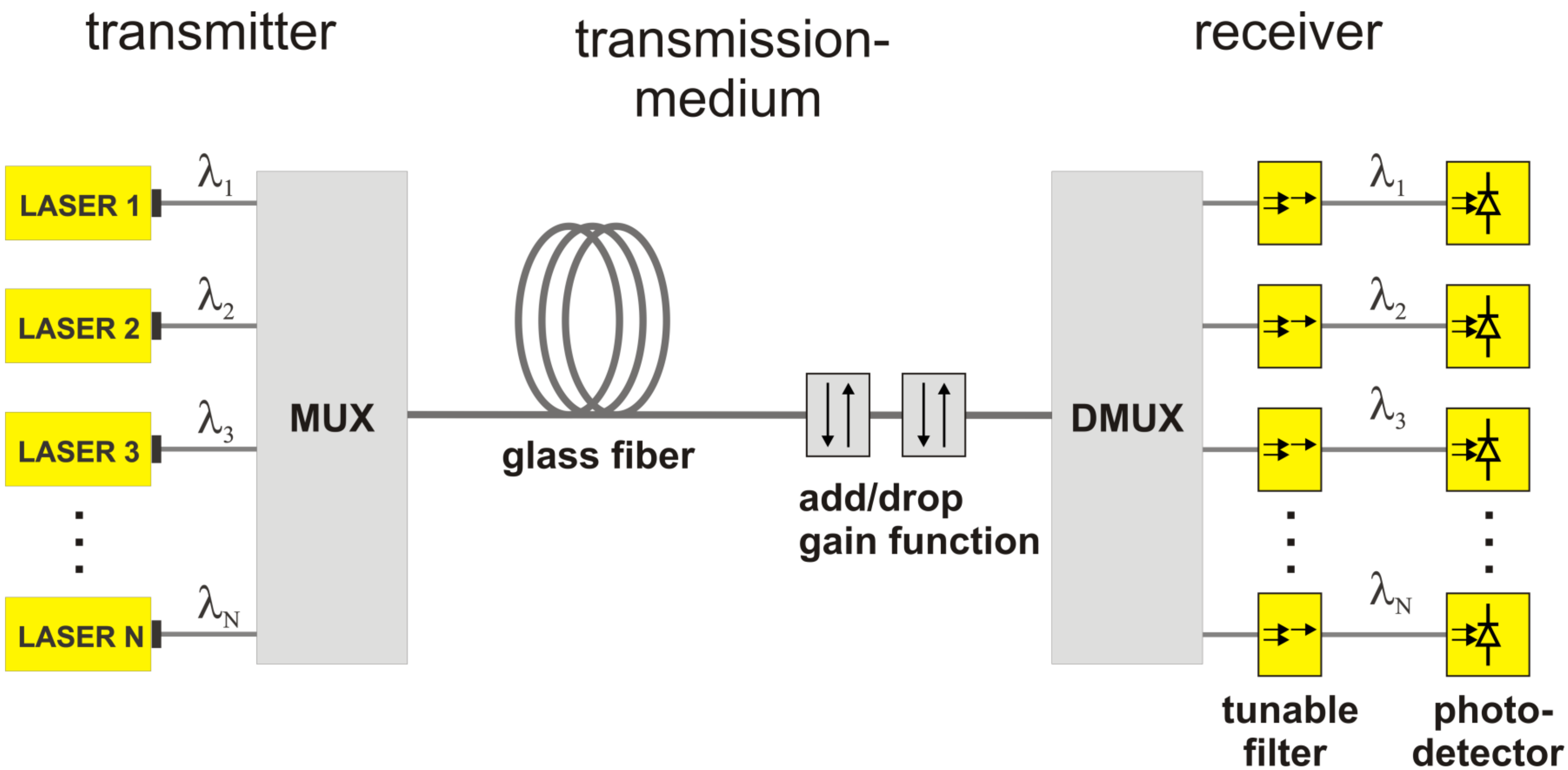

Chapter 8

Introductions to LEDs

LEDs

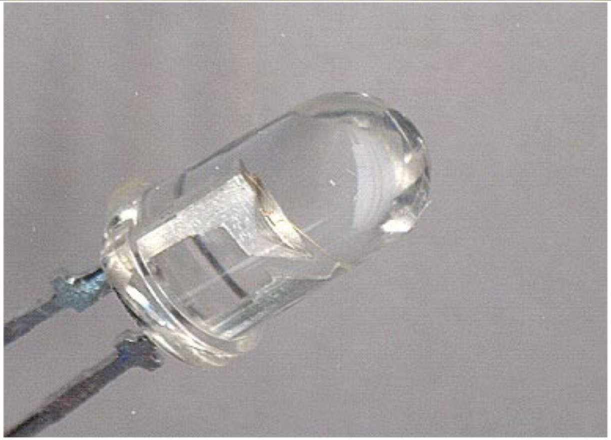

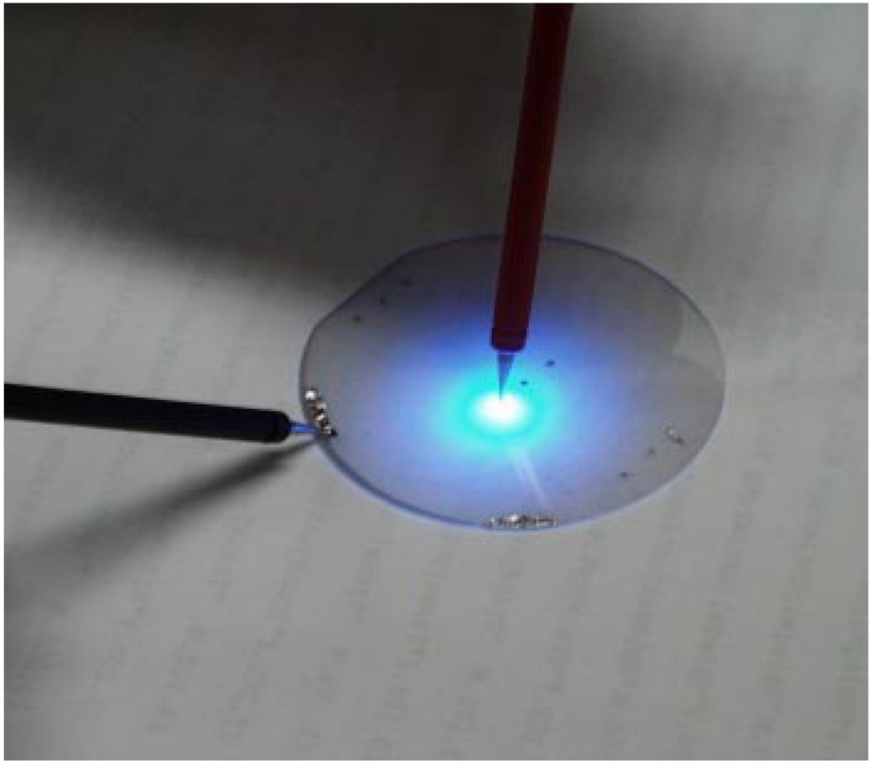

material systems

red: Al Ga As, Ga In P

yellow: Al Ga In P, Al Ga In N

green: Ga P, Al Ga In N, Al Ga In P, Zn Cd Se / Zn S Se

blue: Ga In N / Al Ga In N, Zn Cd Se / Zn S Se

white: blue LED with white fluorescent conversion coating, luminescence – conversion LED

allowes full color display

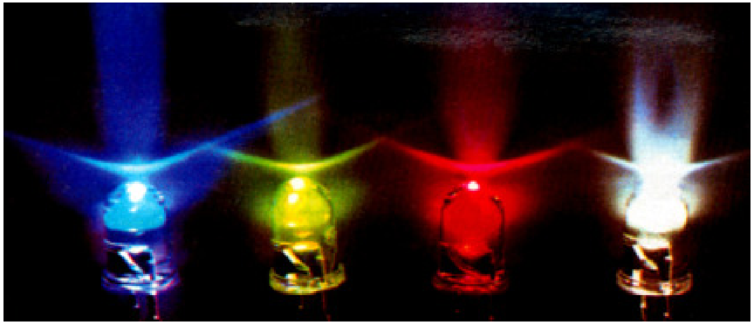

(Siemens)

(Nichia Japan)

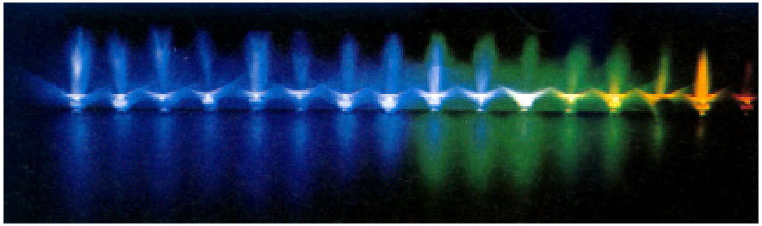

LED colour palette on the basis of nitride compound semiconductors

Traditionally classic light source

thermal emitters

temperatures in between 1500 and 3000 K.

- white light yield around 5%
- lifetime incandescent lamps around 1000h

specification:

Planck's radiation law

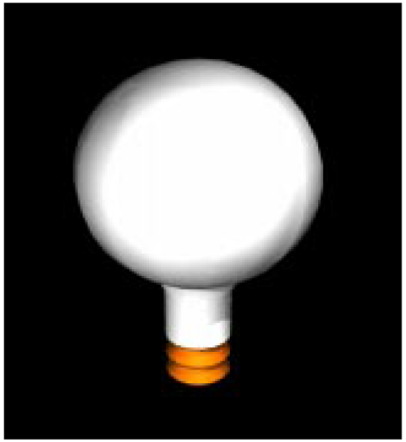

The best classically light source: fluorescent lamp

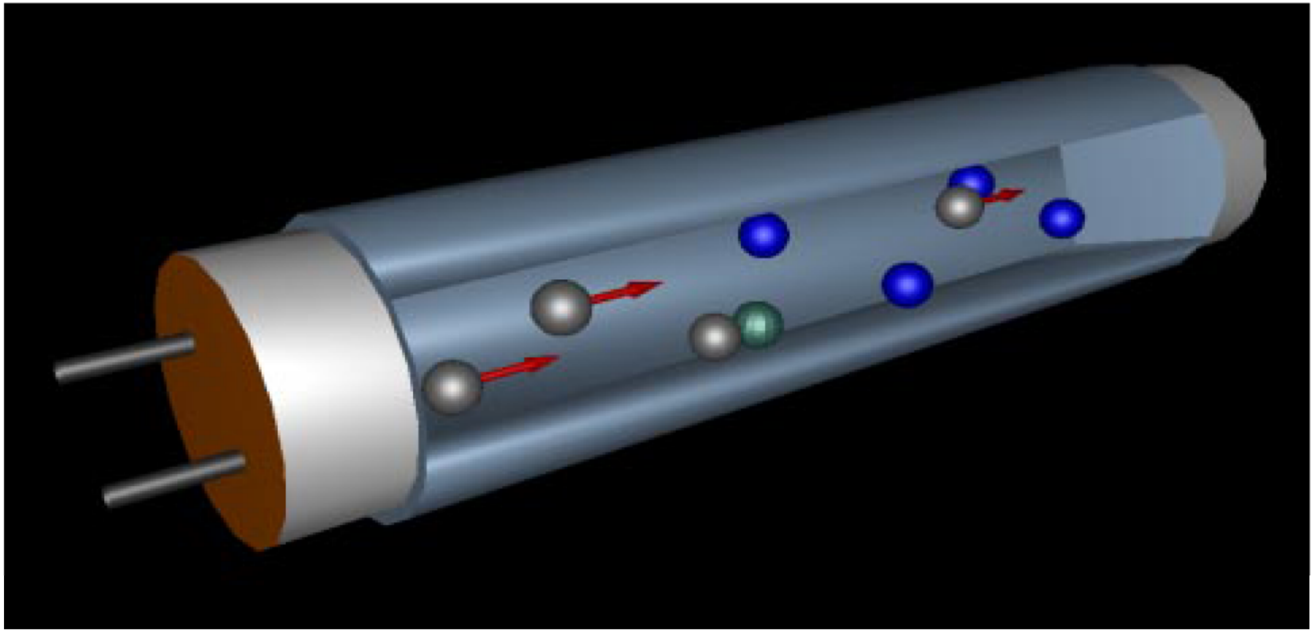

principle: gas discharge, means excitation of atoms by collisions

→ ultraviolet light

conversion in visible light (layer of a phosphor at the wall)

Spectral power distribution: thermal emitter

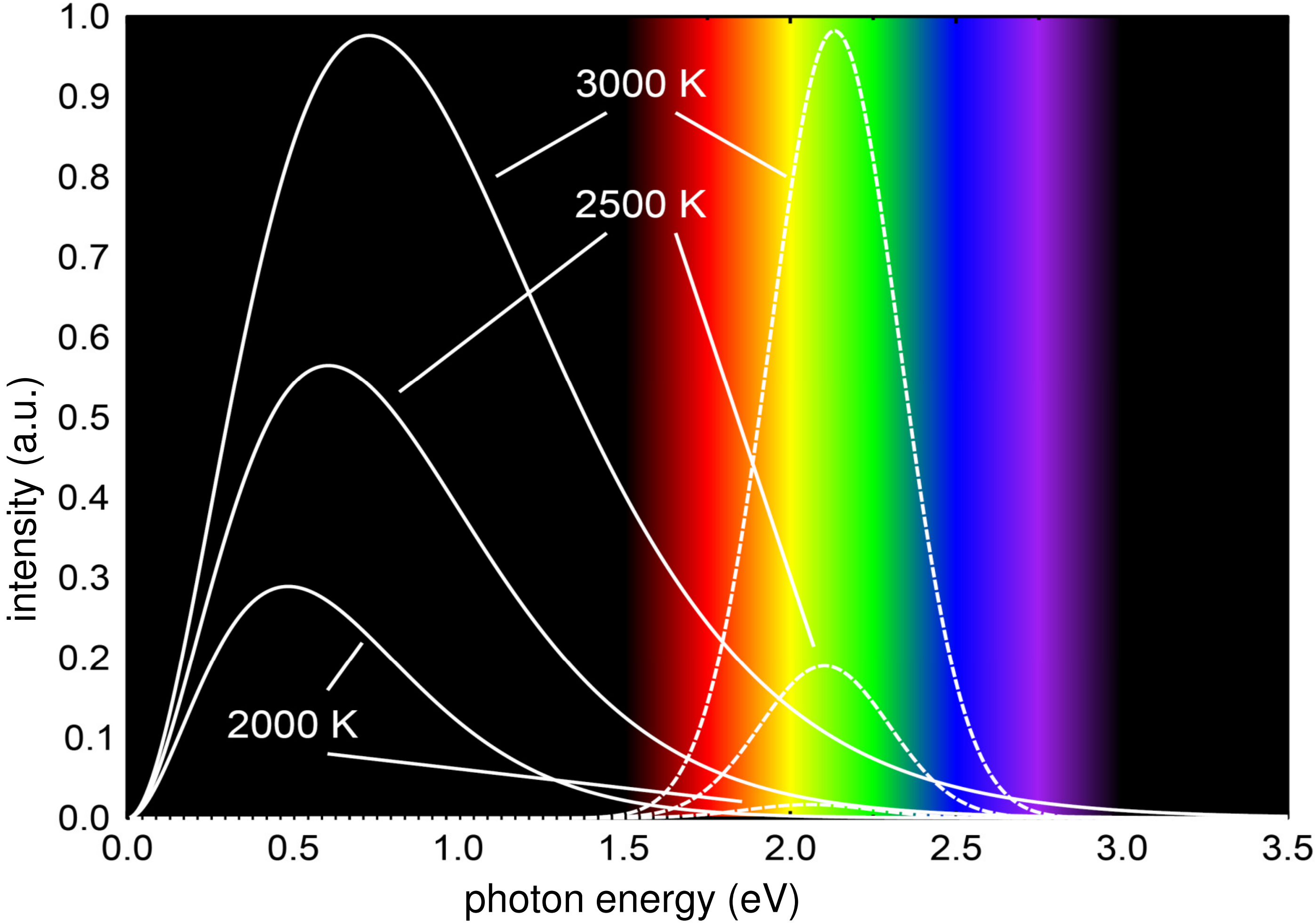

Map of III – V – semiconductors

optoelectronic devices

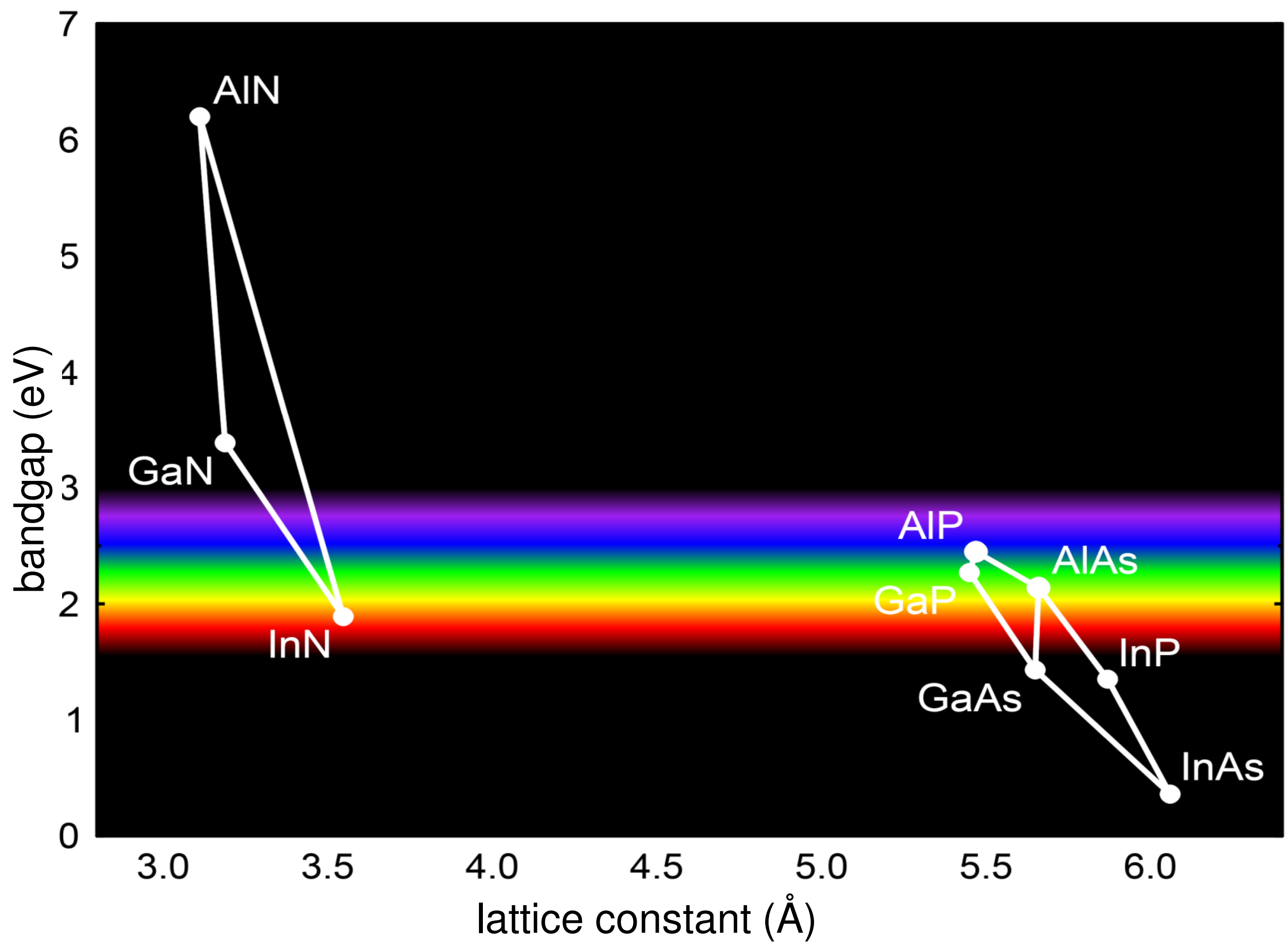

Brightness development for visible LEDs

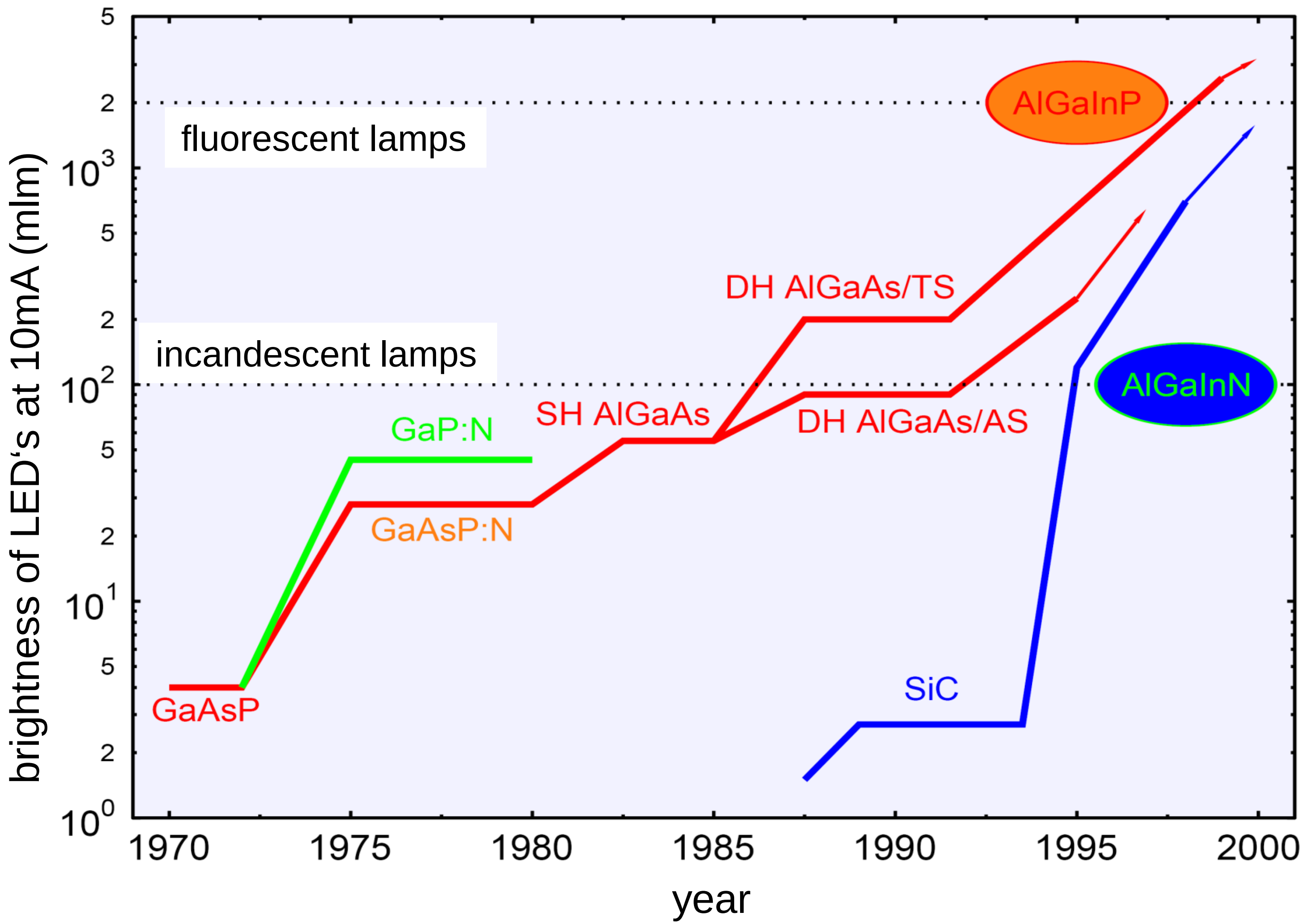

Brightness development for visible LEDs

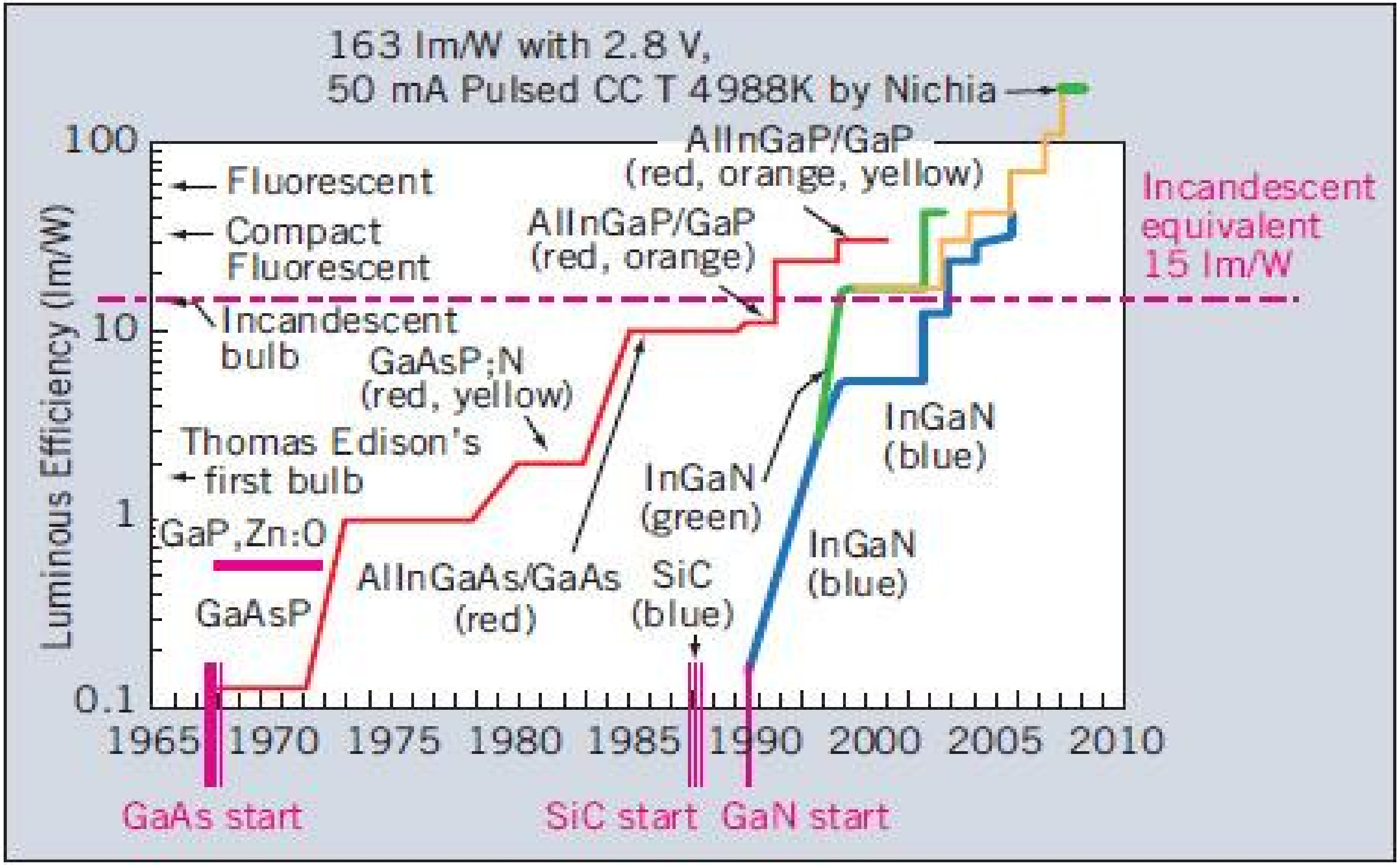

2013 > 200 lm/W

2016 > 300 lm/W

optoelectronic devices

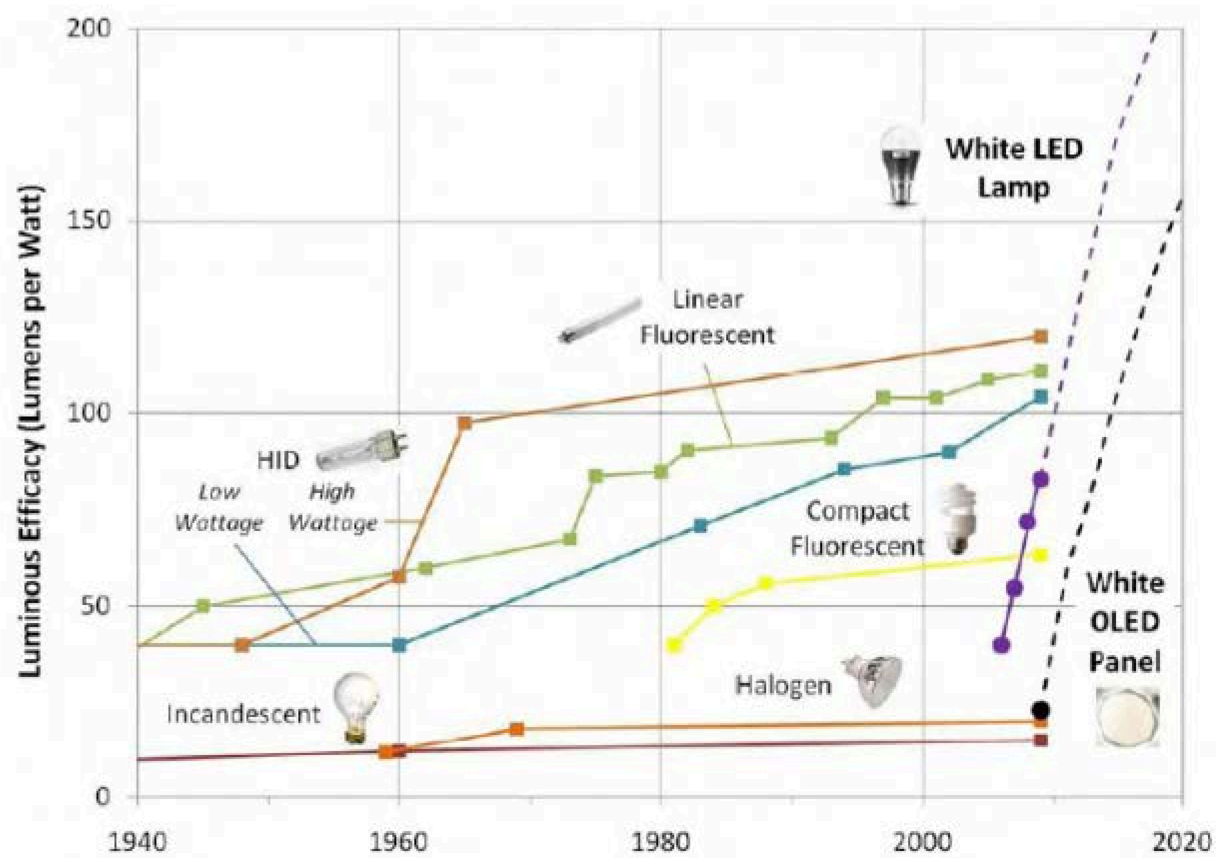

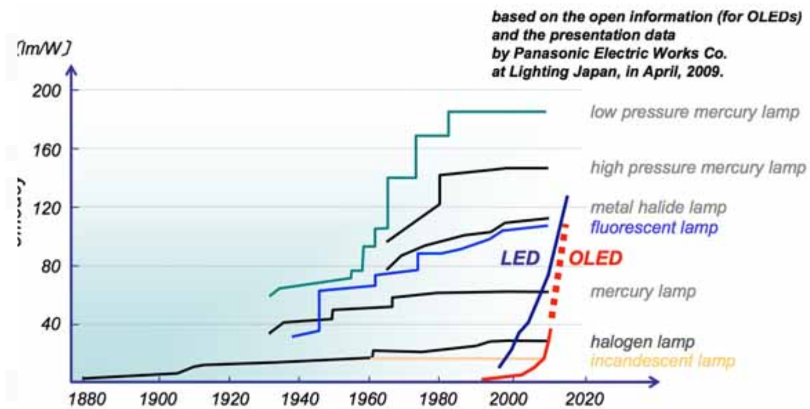

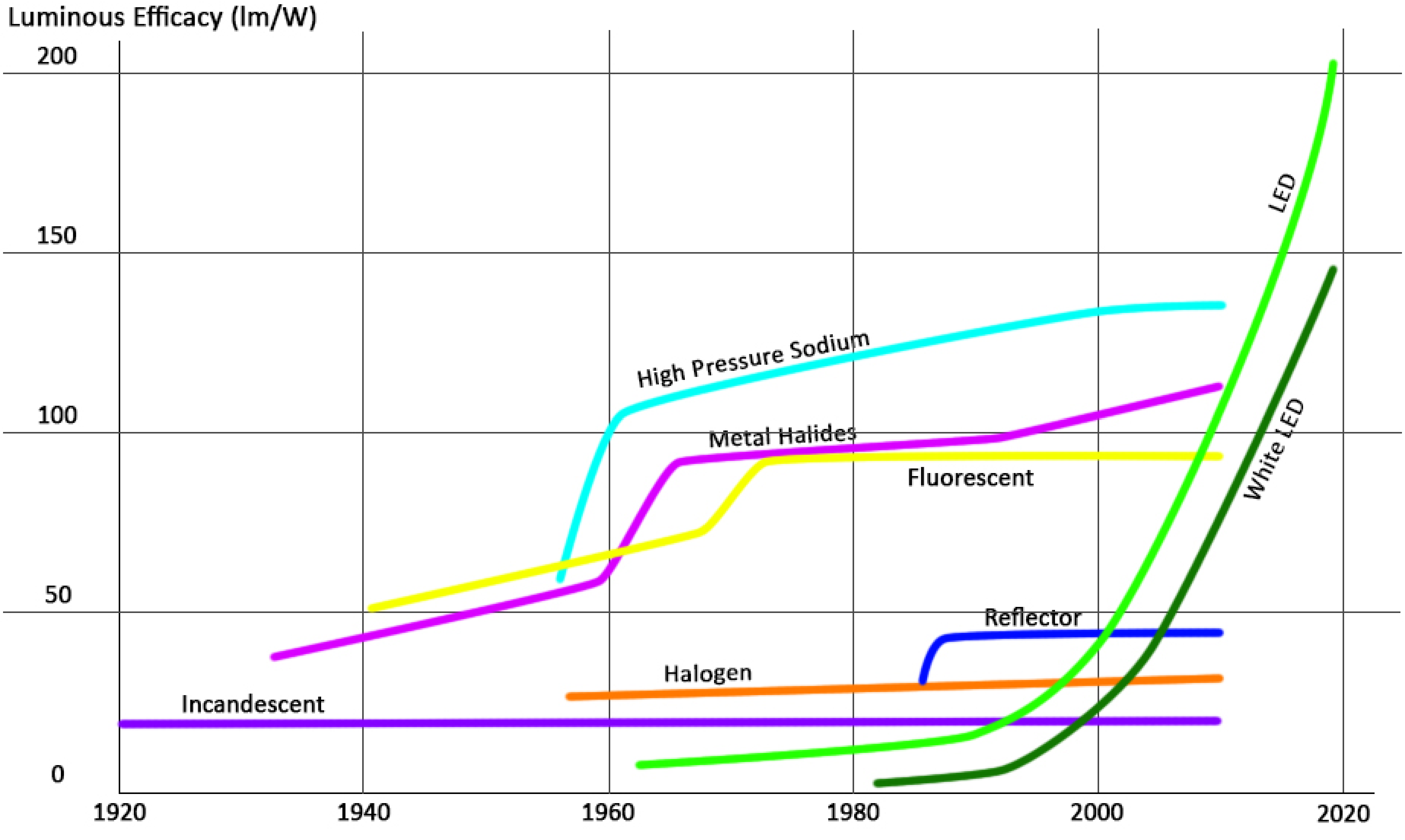
Luminous Efficacy (lm/W)
200
150
100
50
0
1920
1940
1960
1980
2000
2020
LED
White LED
High Pressure Sodium
Metal Halides
Fluorescent
Reflector
Halogen
Incandescent

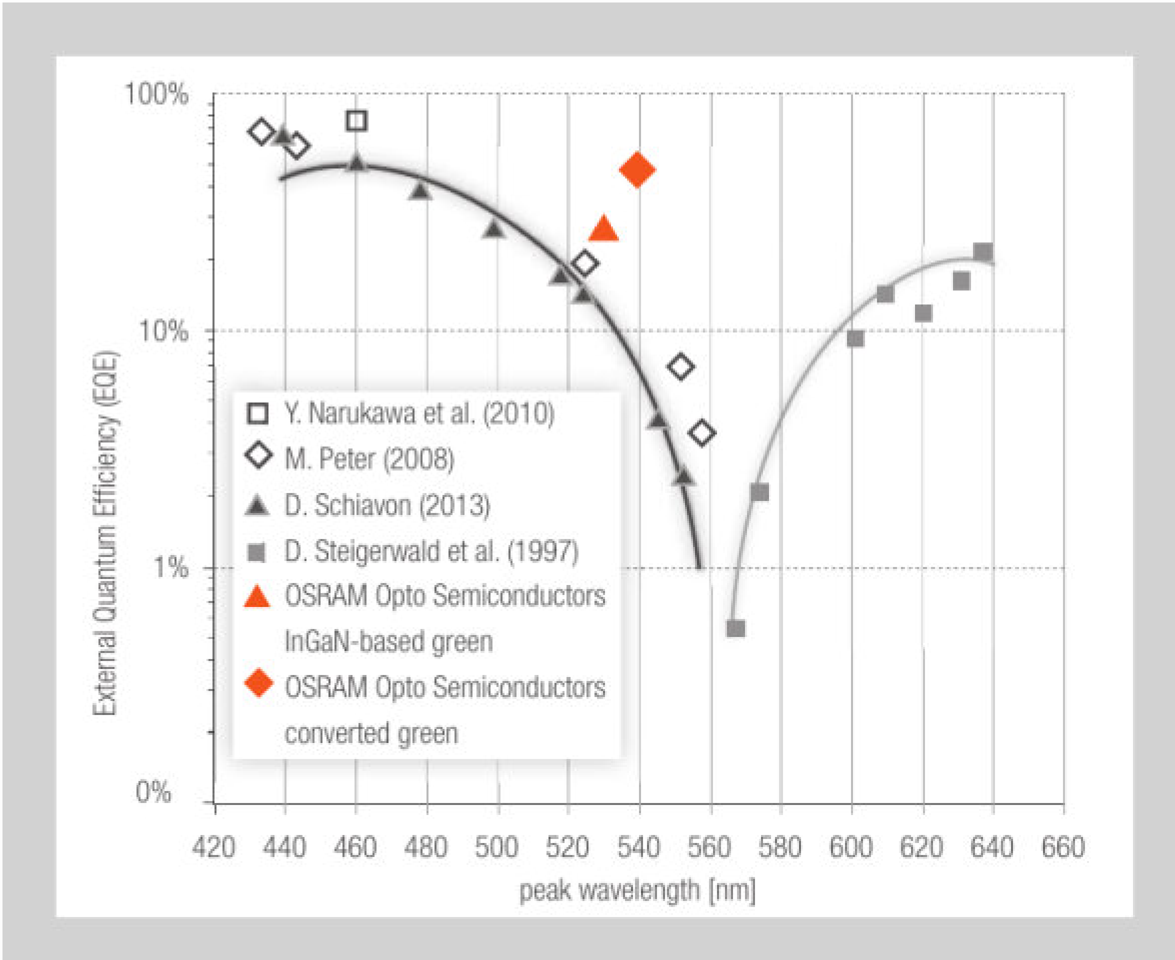
100%
10%
1%
0%
External Quantum Efficiency (EQE)
Y. Narukawa et al. (2010)
M. Peter (2008)
D. Schiavon (2013)
D. Steigerwald et al. (1997)
OSRAM Opto Semiconductors InGaN-based green
OSRAM Opto Semiconductors converted green
420 440 460 480 500 520 540 560 580 600 620 640 660
peak wavelength [nm]

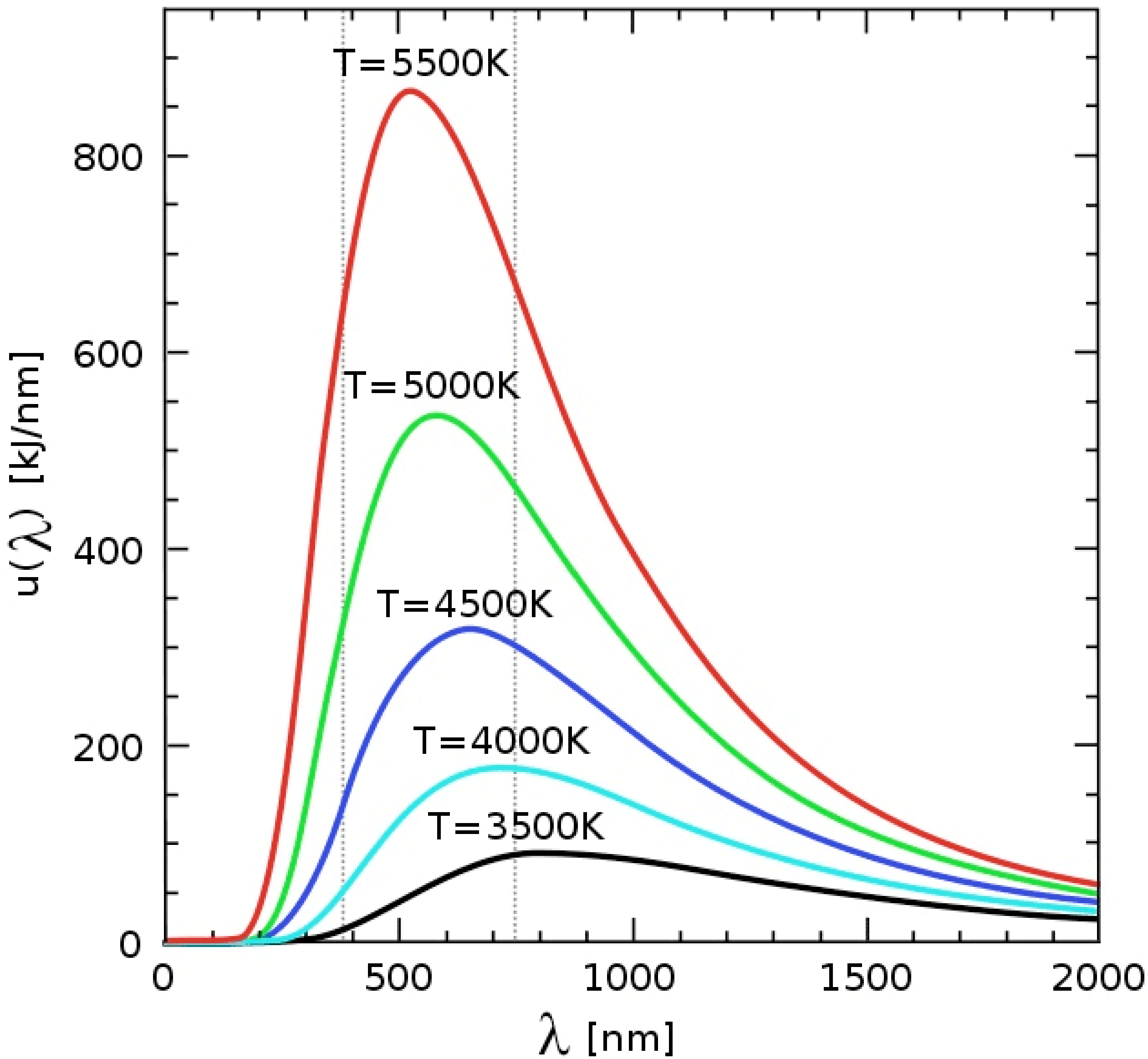
T=5500K
T=5000K
T=4500K
T=4000K
T=3500K
800
600
400
200
0
0
500
1000
1500
2000
u(λ) [kJ/nm]
λ [nm]

Semiconductor materials for optoelectronics

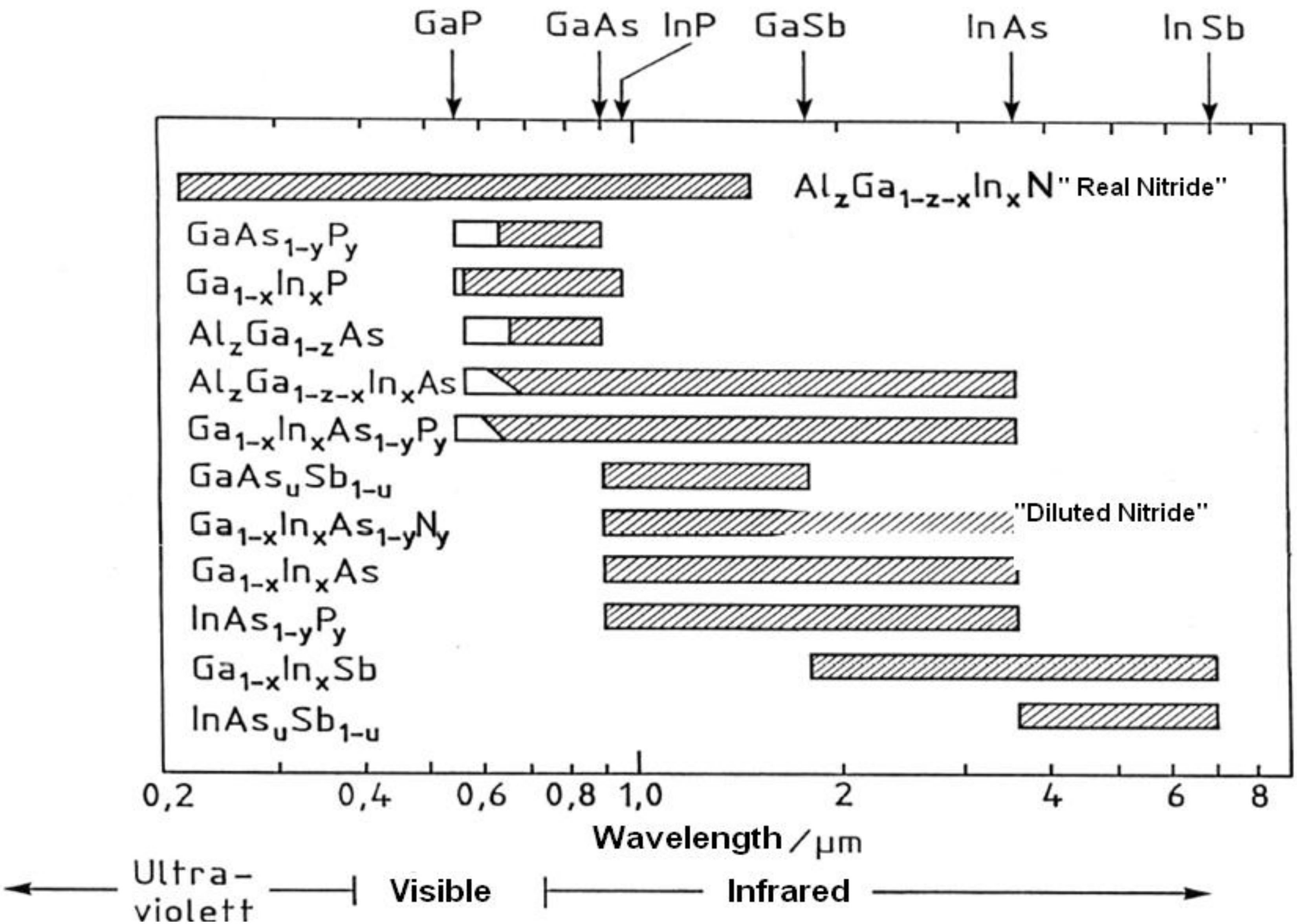

LEDs and lasers for the visible spectral range

Red : AlGaAs, GaInP

Yellow : AlGaInP, AlGaInN

Green : GaP : N, II / IV semiconductors, polymers, AlGaInN

Blue : GaInN / AlGaInN, polymers, II / IV semiconductors, ZnCdSe / ZnSSe, SiC

White : blue LED with a conversion layer which produces white fluorescence (luminescence conversion LED)

Applications :

- full colors displays (10 x 20 m) for e.g. advertisement, screen
- traffic lights
- self-illuminating panelling and route signs
- white light sources (extremely large market)
- blue lasers for optical storage - smaller focus due to the smaller λ $\rightarrow$ higher storage densities
- data communication

Bandgap of the light-active layer determines the emission wavelength of the LED or the laser !

(AlGaIn)N – based violet, blue and green LEDs

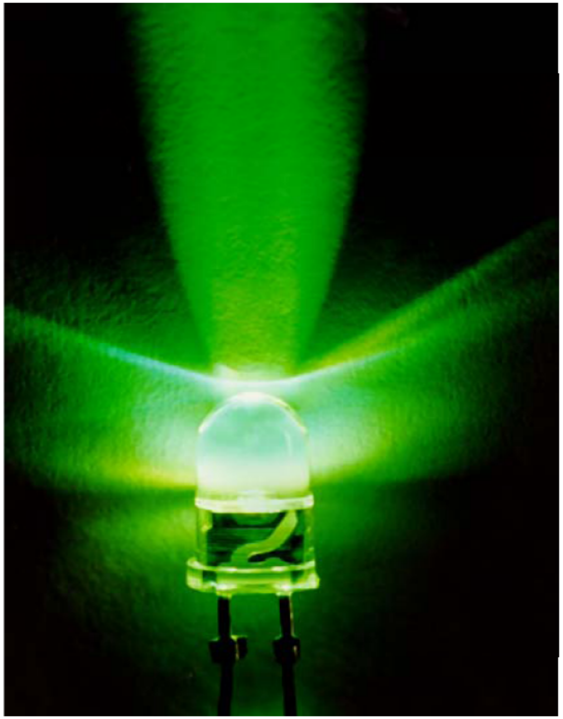

First - generation single - chip white LEDs

Advantages:

- relatively easy to implement
- high overall efficiency as only one luminescence conversion step necessary

Drawbacks:

- limited color tuning
  (only cold bluish hues of white possible)
- limited color rendering
  (particularly in the red)
- color impression dependent on viewing angle

applications

colored LEDs

- color displays
- selfilluminated signage (buildings, traffic)
- traffic lights

white LEDs

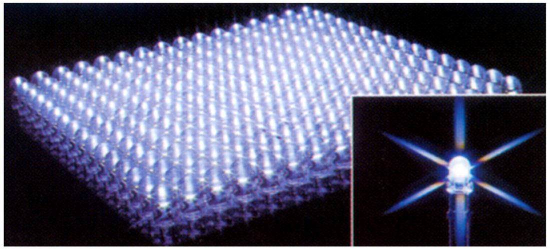

- white light source (extremly large consumer market, substitute for incandescent lamps, halogen lamps and fluorescent tubes)
- signage, color displays

blue LEDs

- optical memory with high storage density by λ ↓

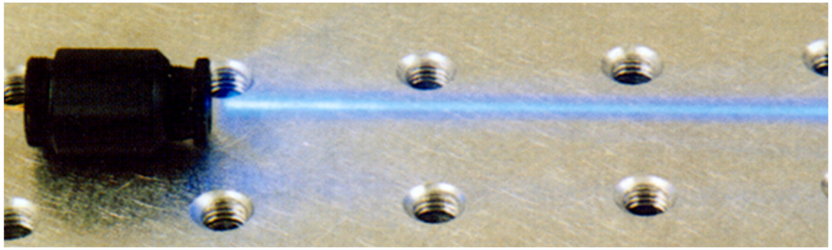

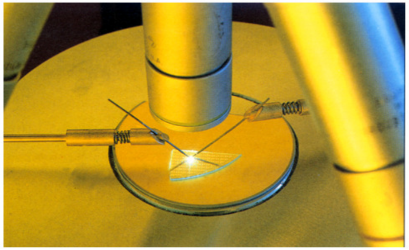

(Nichia, Japan)

White LEDs / products

14 days permanent use with a single battery set conventional torch requires 114 batteries in that period (considerably smaller efficiency)

Lucido®
cool light

First single - chip white LED in 1996 / 97

- **Blue emitting (AlGaIn)N based LED-chip as primary light source**
- **Generation of complementary color by luminescence conversion of part of the primary light in a yellow-emitting YAG:Ce phosphor**
- **White light via additive color mixing of primary light and converted emission**

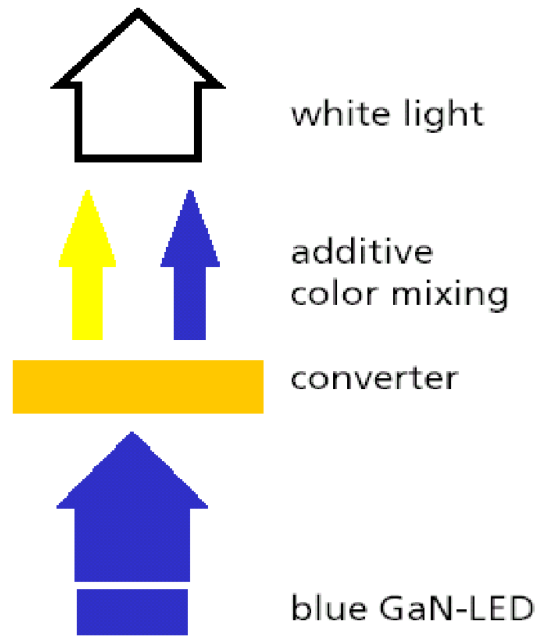

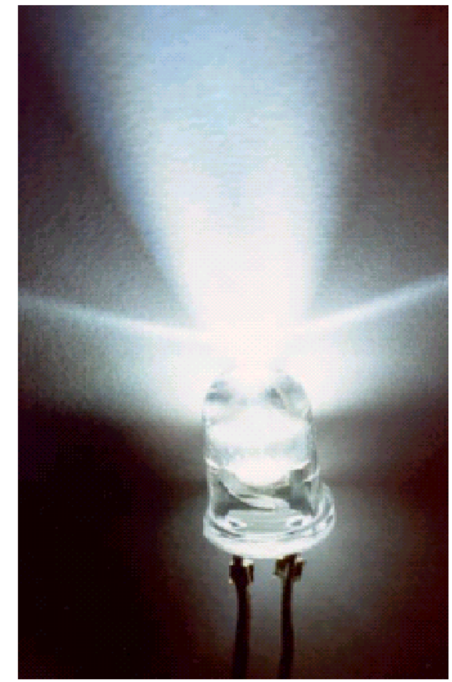

(Fraunhofer IAG, Freiburg)

Spectrum of a Single – Chip White LED

Spectrum of a Single-Chip White LED

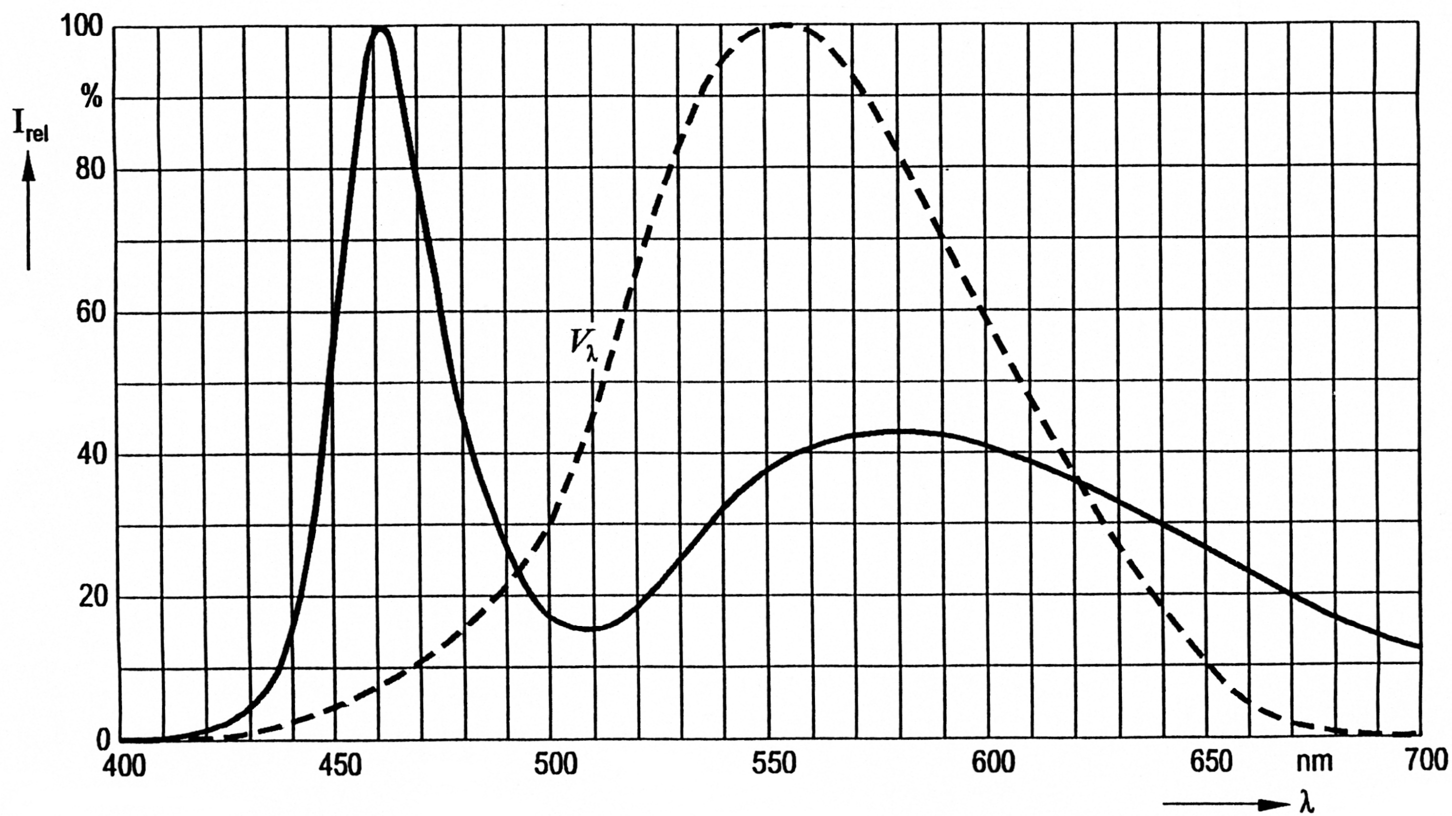

Color temperature ~ 6500 K

Relative Spectral Emission $I_{rel} = f(\lambda)$, $T_A = 25$ °C, $I_F = 20$ mA
V(λ) = Standard eye response curve

Emission spectrum and CIE color coordinates

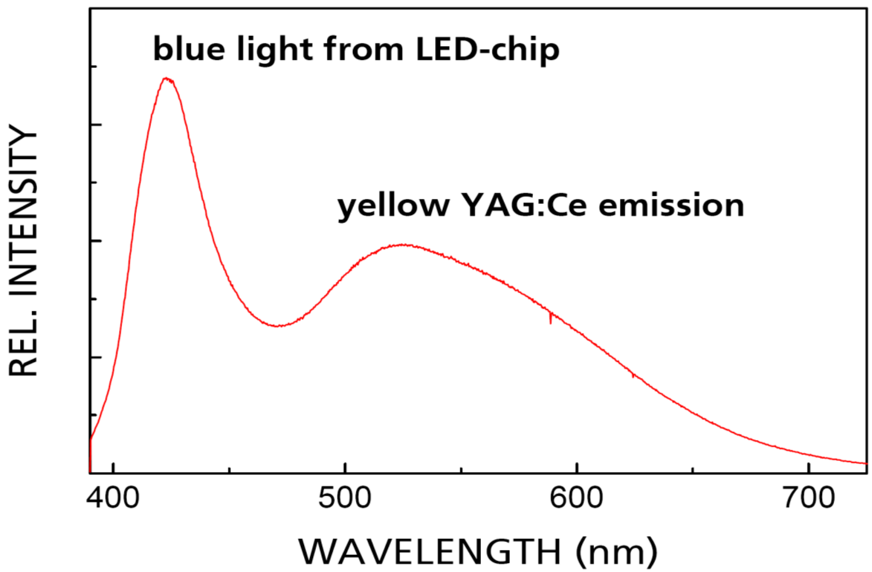

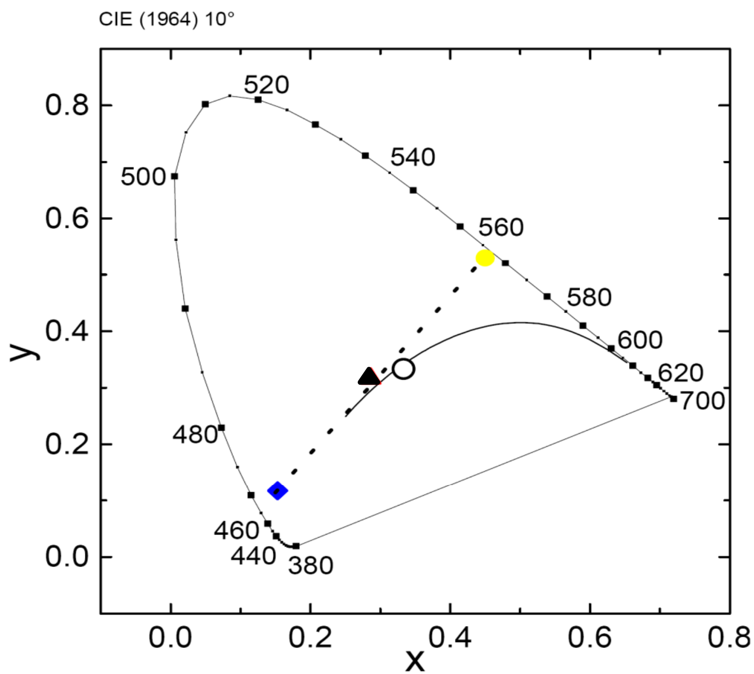

Improved concepts (1): two - band conversion

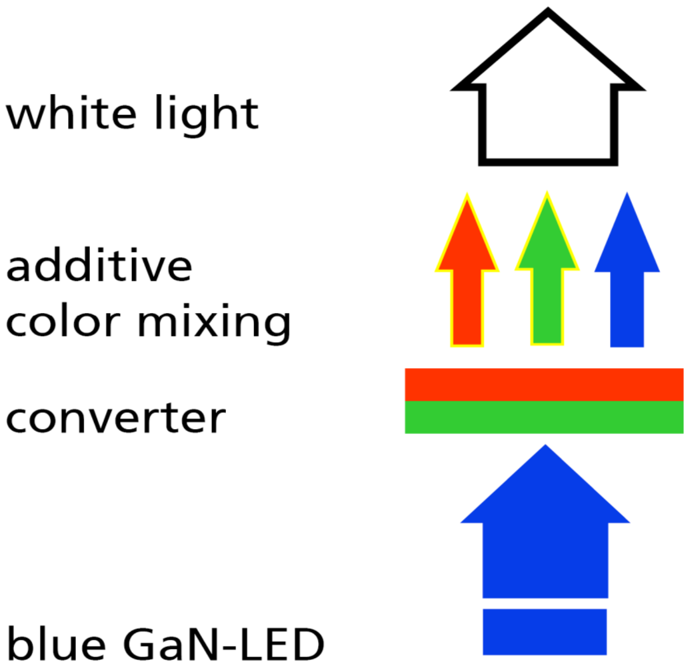

With blue emission from the LED chip as well as green and red emission from the luminescence converting phosphors available, improvements can be made on both

- color tunability and

- color rendering

UV LED plus RGB phosphors replicating fluorescence lighting

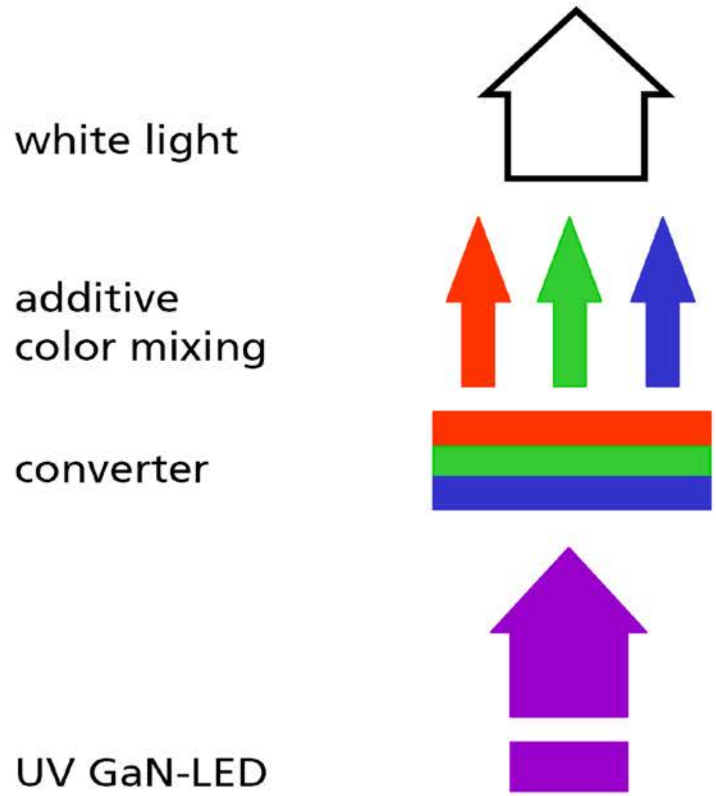

Emission spectrum optimized LED

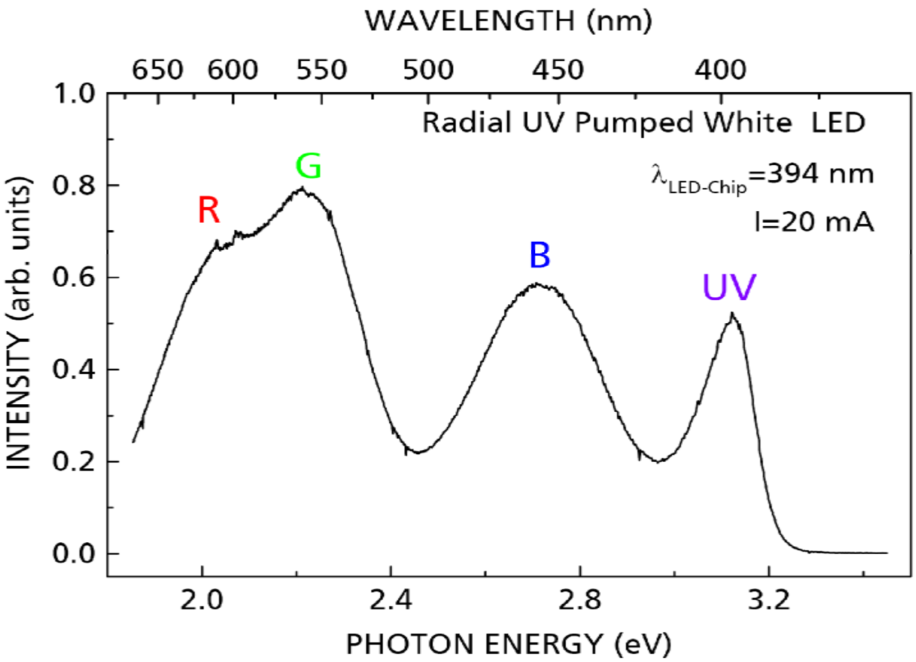

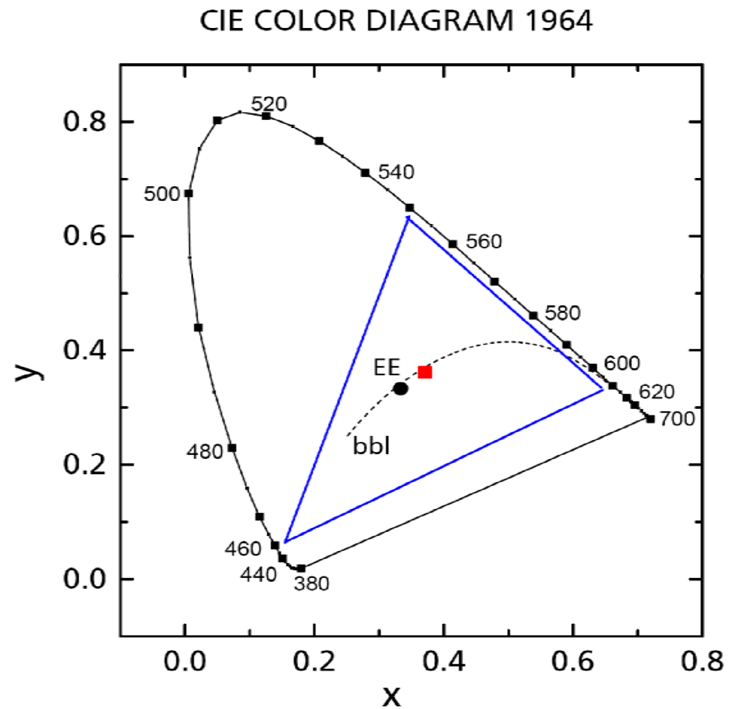

CIE color coordinates: x=0.365, y=0.359, color temperature 4300 K, CRI=78

Efficiencies of AlGaInN and AlGaInP LEDs in the visible spectral range

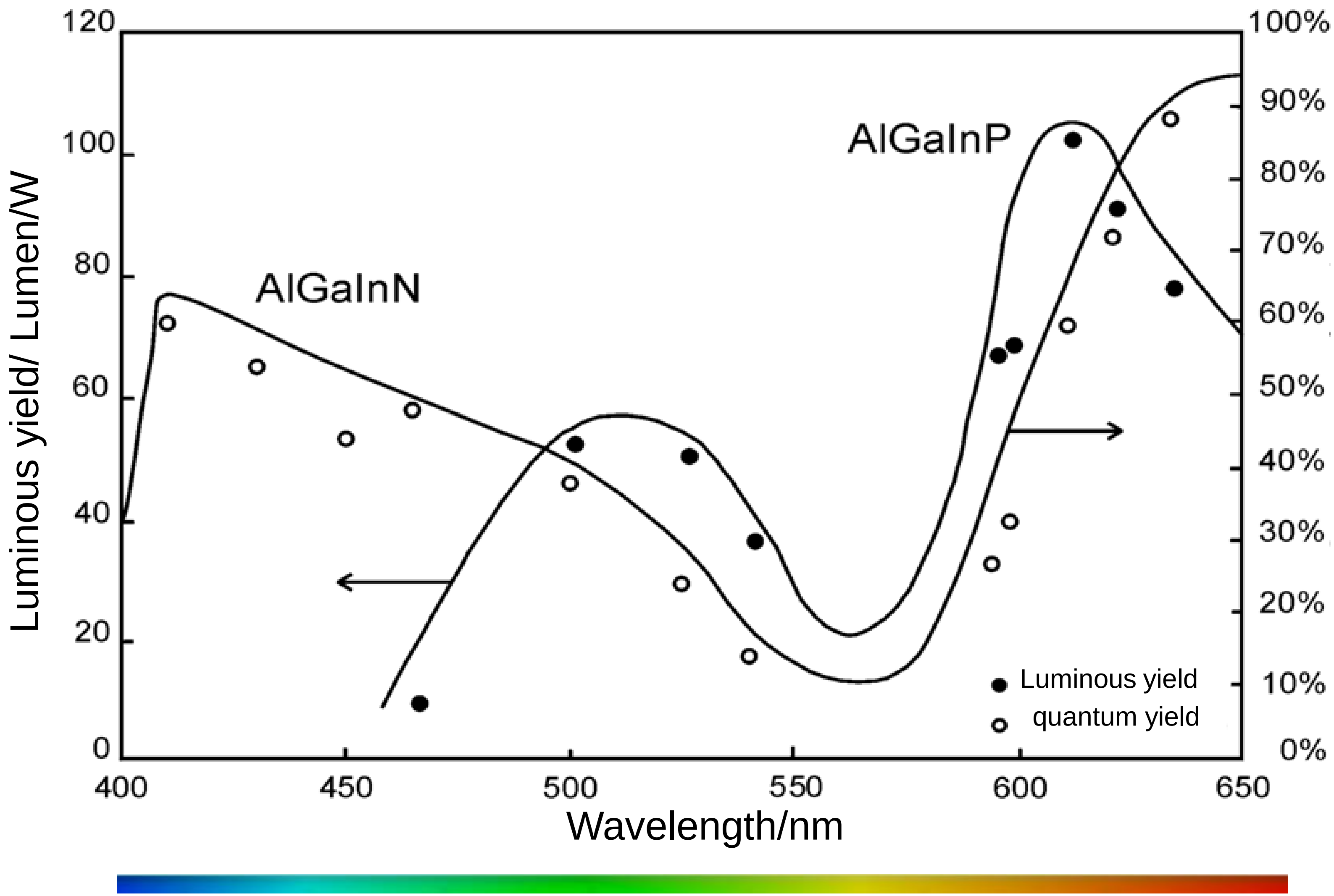

Luminous yield and internal quantum yield as function of the central emission wavelength for AlGaInN and AlGaInP LEDs

Blue AlGaInN LED

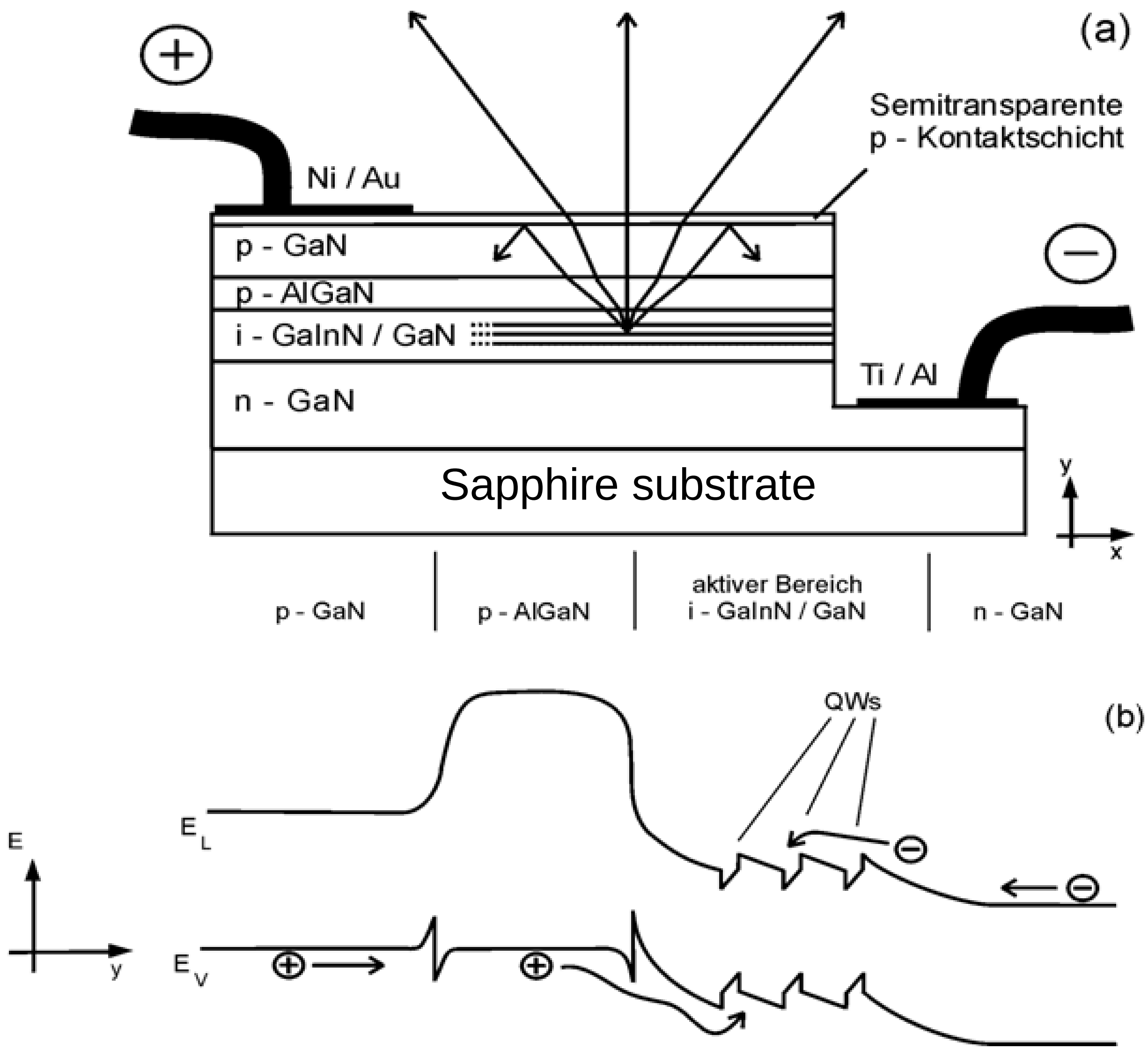

Schematic view of a blue AlGaInN LED (top) and band structure (bottom)

Efficient light coupling into free space

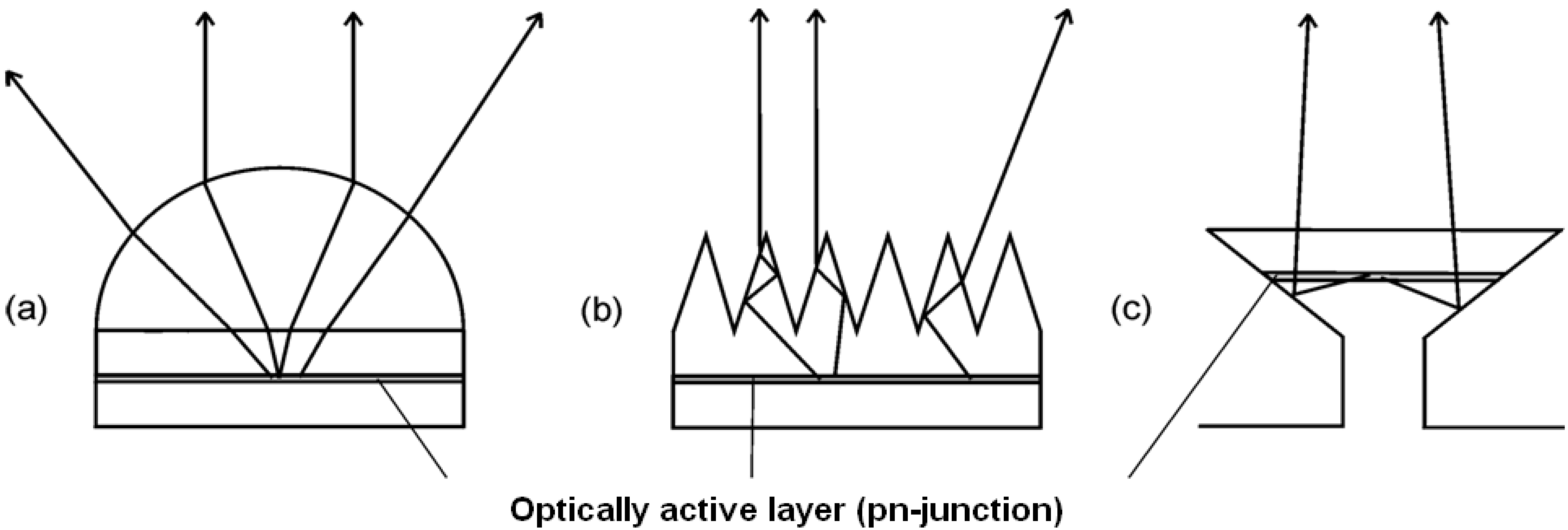

Possibilities for increase the external efficiency in LEDs due to more efficient light extraction

High Power AlInGaP LEDs

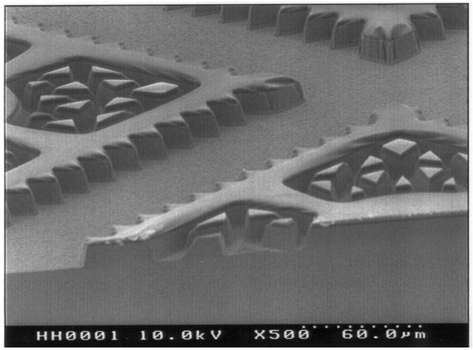

Surface texturing by RIE
(INA Kassel)

top view:

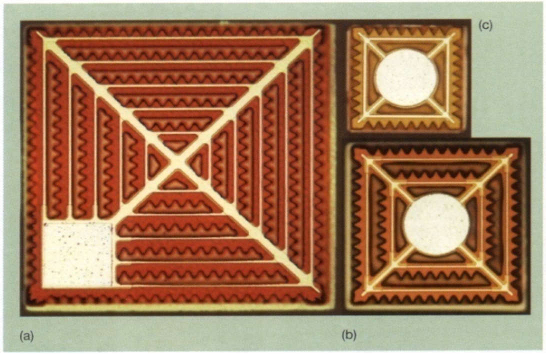

Light extraction modes

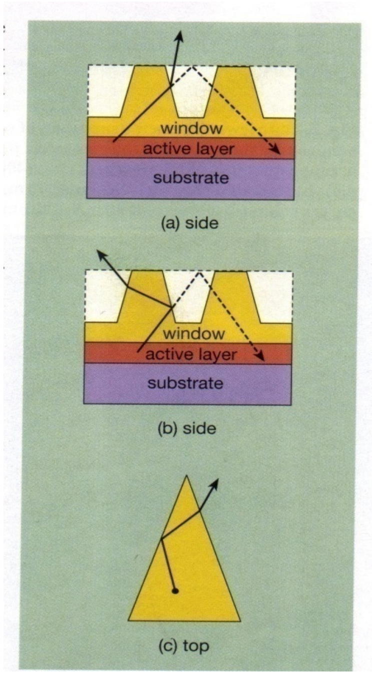

(AlGaIn)N LED: band edge profile and device layout

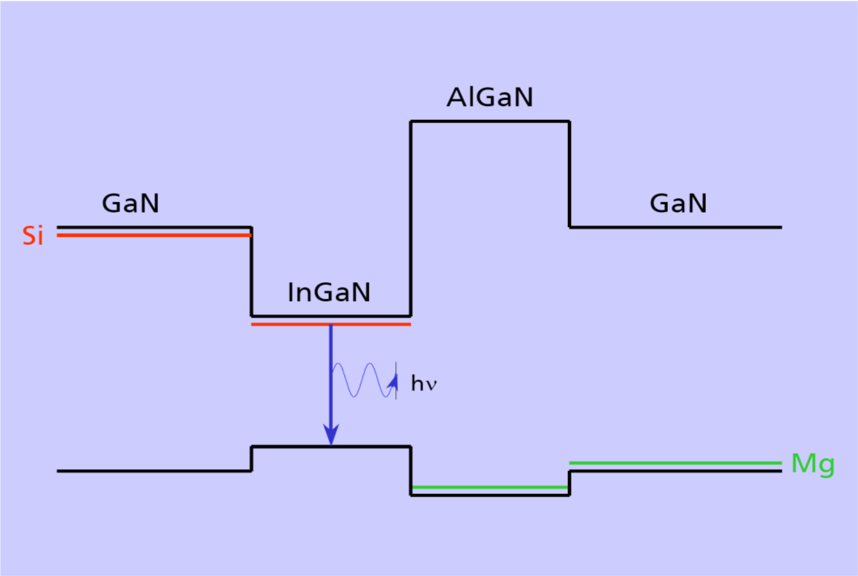

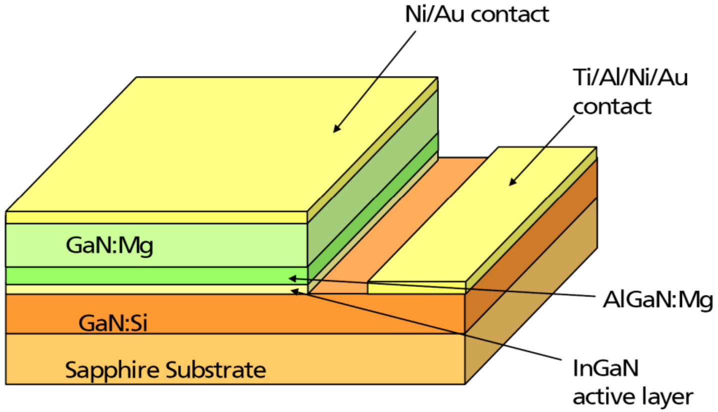

„Conventional“ InGaN LEDs

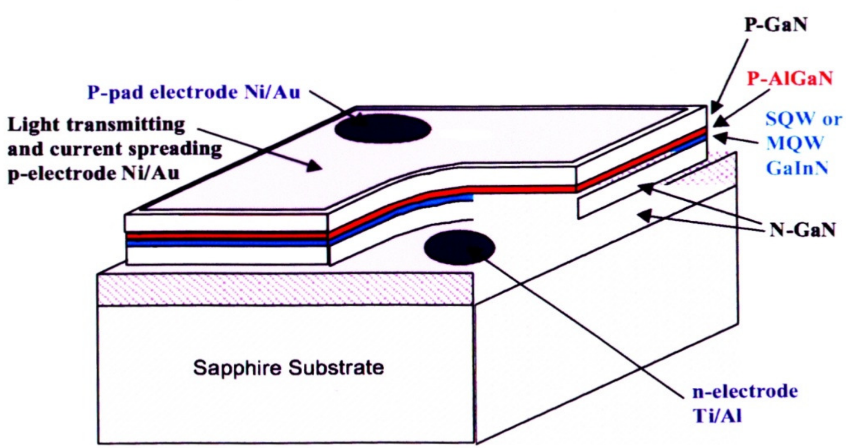

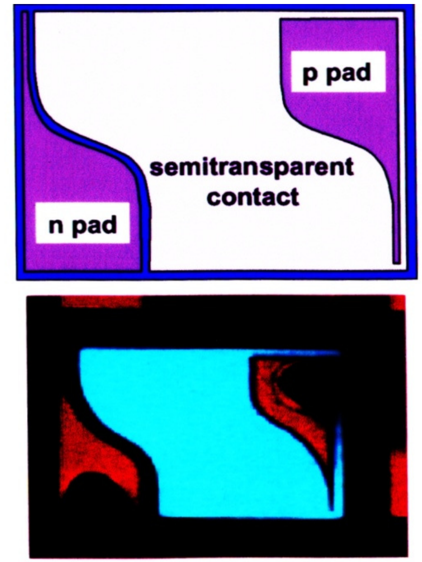

- InGaN LEDs were “born” with a transparent substrate!
- Current-spreading is a challenge.
- Absorption in “semi-transparent” metal is significant.

LUMILEDS

Comparison of LED & LD

	SC LED	SC Laser
max. bitrate (lab conditions)	10 Gb/s	50 Gb/s (direct modulation) >100 Tb/s (OTDM)
energy consumption for data transmission	0.25 fJ/bit	0.5 pJ/bit
min. linewidth with modulation	1-2 nm	<< 0.1 nm (phase modulation) ≈ 0.1 nm (direct modulation)
WDM	☑	☑
dense WDM	–	☑

Chapter 9

Light detecting / absorbing devices

Photodiodes and Solar Cells

Photodiode

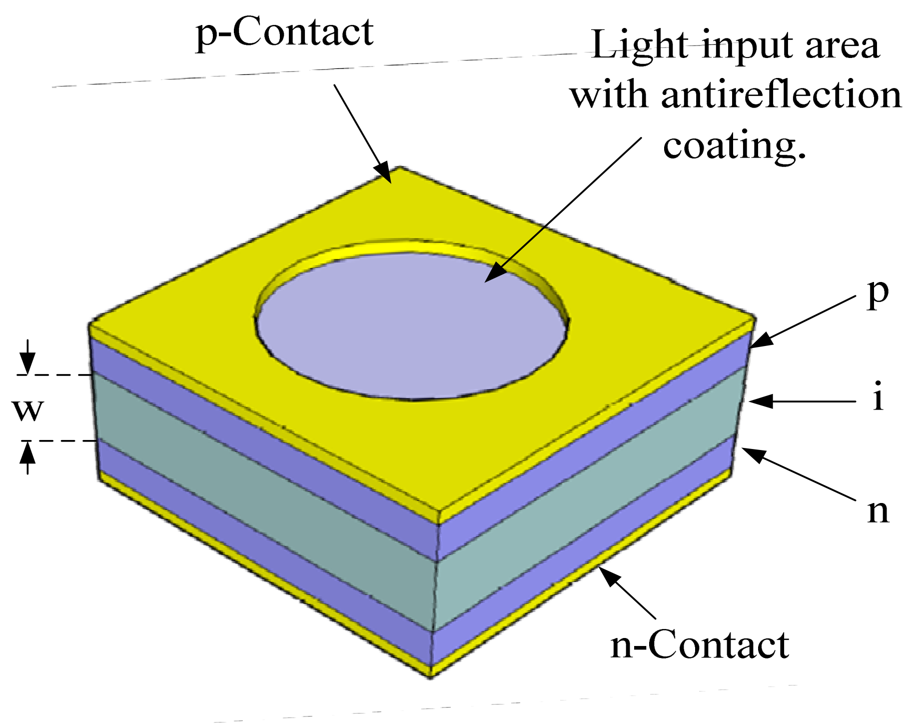
p-Contact
Light input area
with antireflection
coating.
p
i
n
w
n-Contact

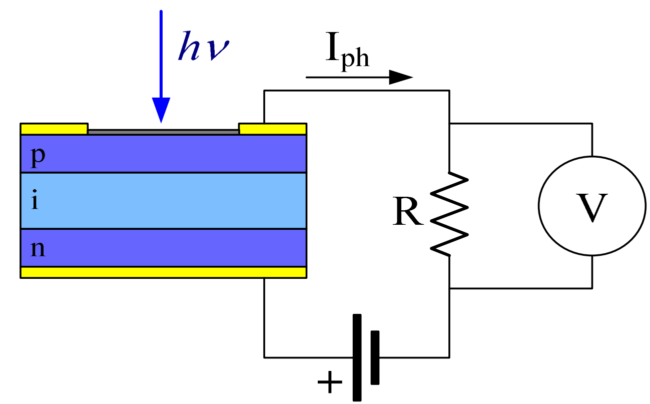
hν
I_ph
p
i
n
R
V
+

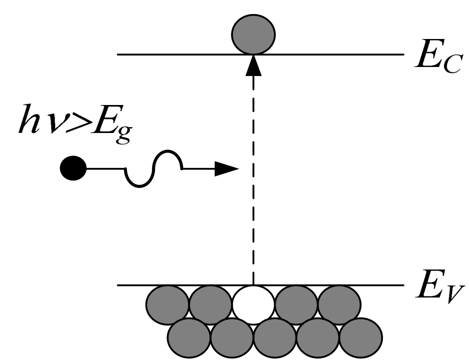
E_C
hν>E_g
E_V

Photodiodes and Solar Cells

Each photon (hf > E_g) which is absorbed generates an electron-hole pair. This pair is separated in the strong internal electrical field (due to the space charge in the depletion region) or by diffusion. Thus, this operation principle is just reverse to that of semiconductor lasers or LEDs.

All pairs which are absorbed in a distance from the depletion region which is larger than the diffusion length are not separated and do not contribute to the generated electric signal or power.

1. Reverse biased pn-junction → photodiodes
2. Unbiased → solar cells

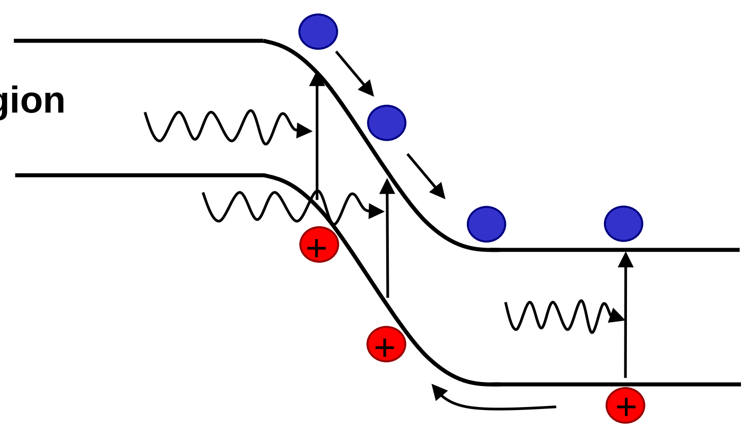

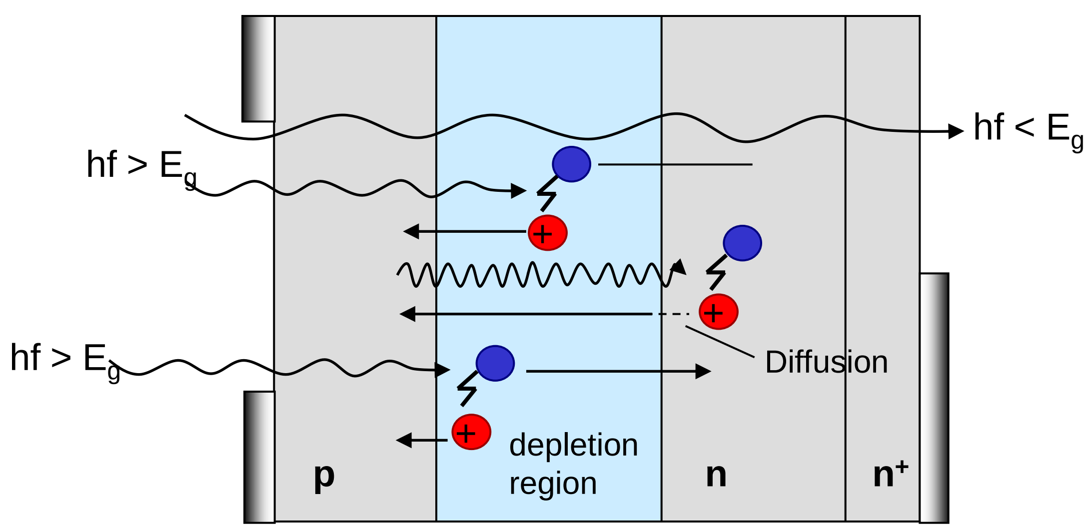

Materials: Si, Ge and compound semiconductor (e.g. InGaAs or InSb) and amorphous Si for solar cells

Types of solar cell arrays

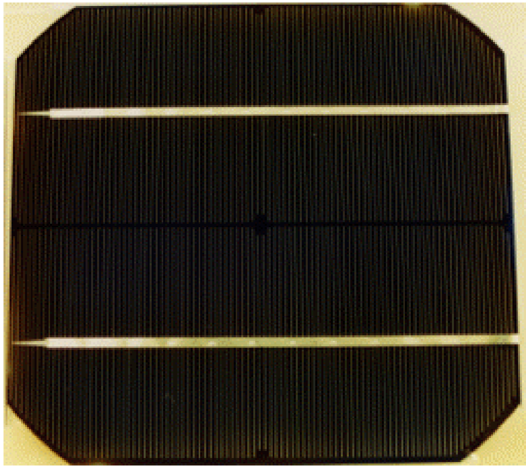

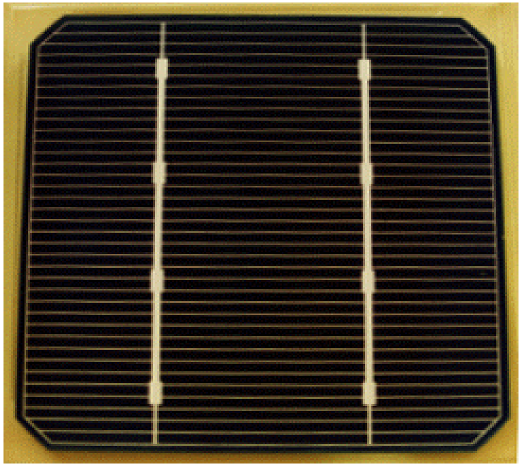

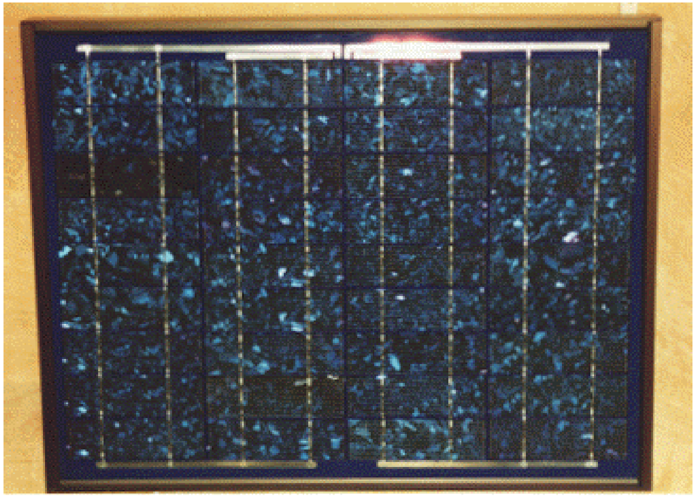

Arrays of solar cells: applications II

applications in space : energy souce of satellites

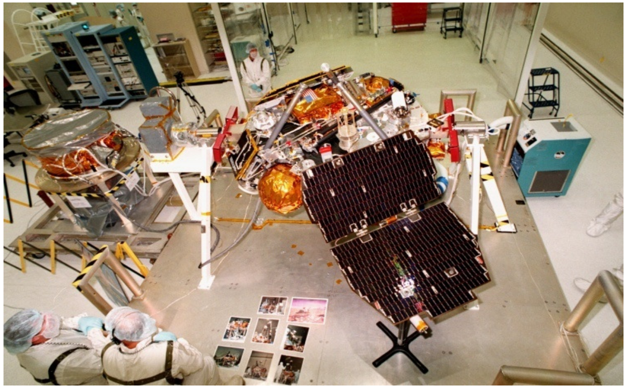

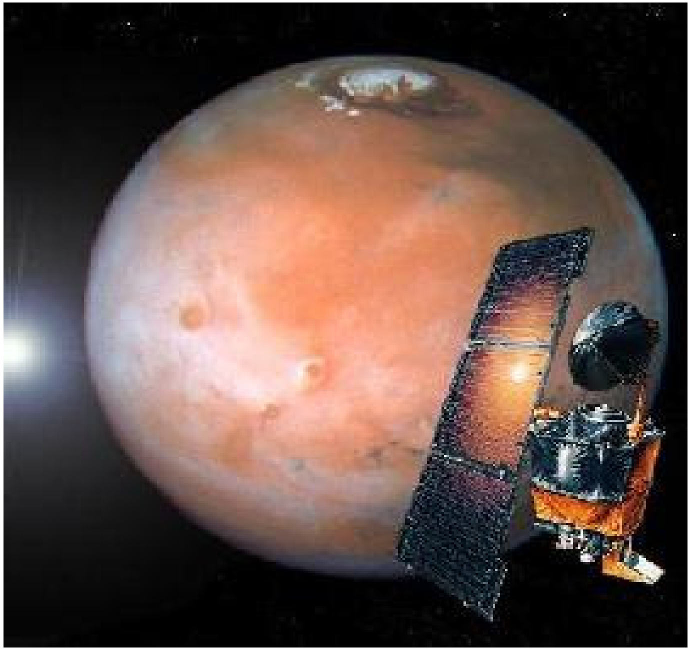

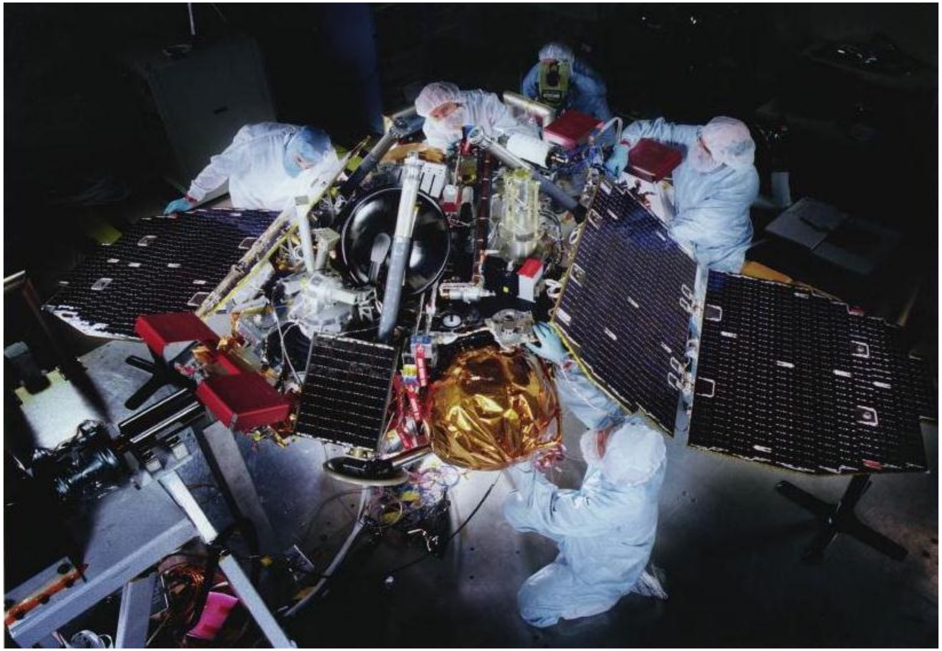

Material classes of solar cells

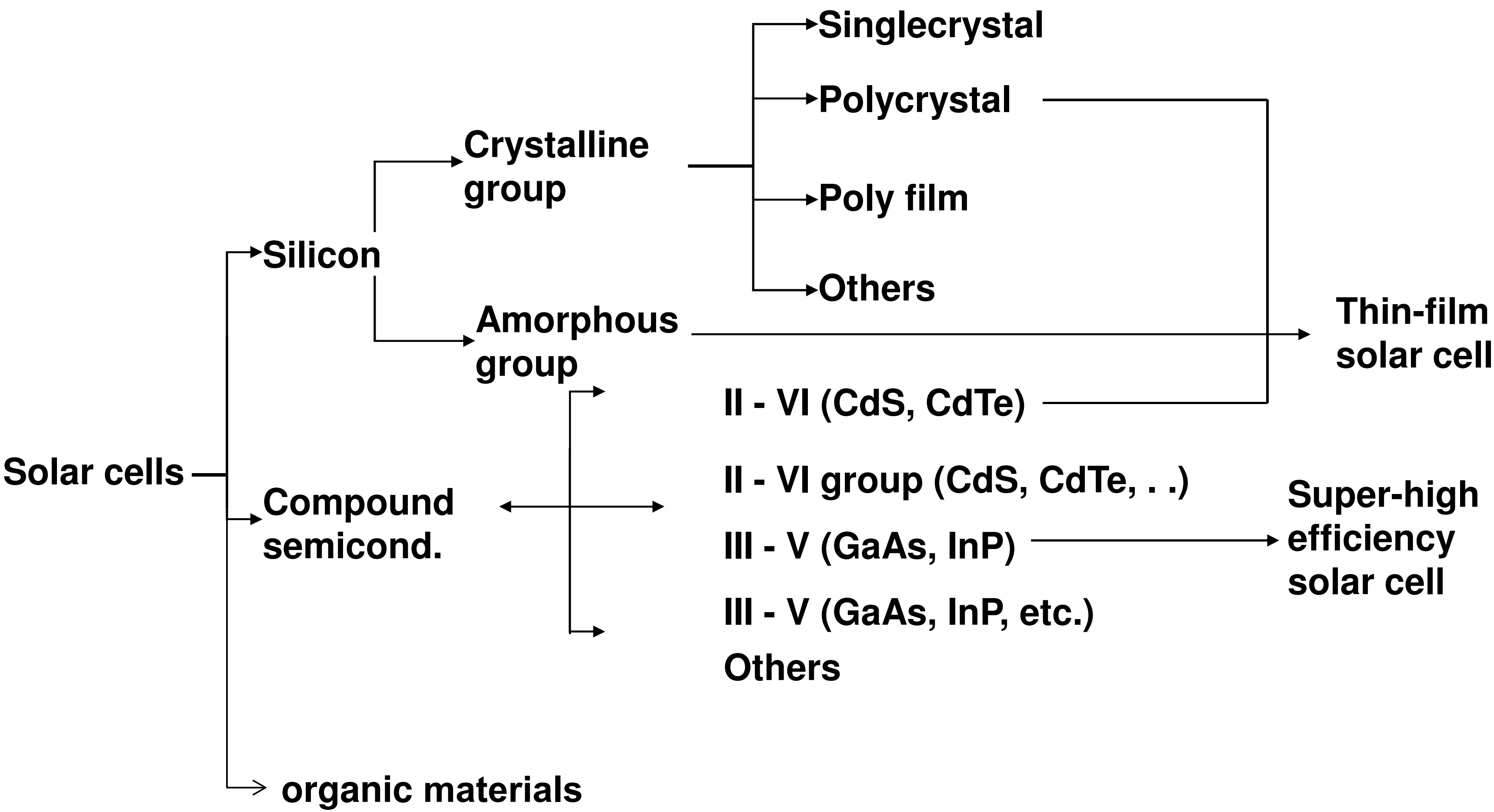

Comparison of Solar Cells

	inorganic	organic
max. efficiency	20 - 40 %	8 %
max. module efficiency	20 %	3.5 %
substrate	semiconductors (Si, GaAs, CdTe, …)	glass, steel (heavy) polymer film
thickness of light sensitive layer	1 – 300 µm	100 nm
deposition temperature	200 – 900 °C	150 °C (from solution)
energy pay back time	2 – 8 years	1.3 – 2 years

Operation principles of solar cells

$$I = I_s (e^{V/V_t} - 1) - I_{ph}$$

$$\text{Fill Factor} = I_m V_m / (I_{sc} V_{oc})$$

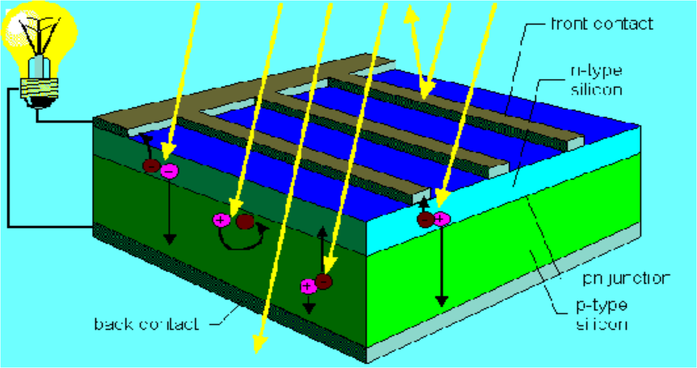

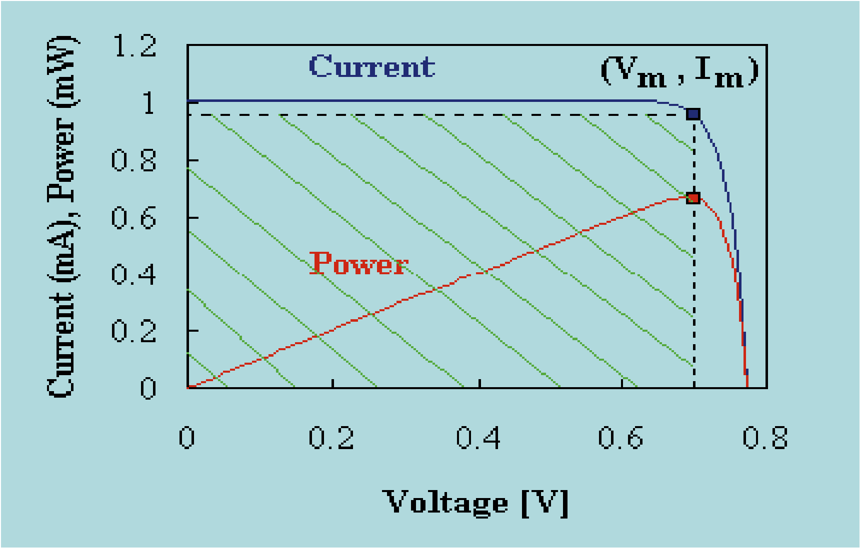

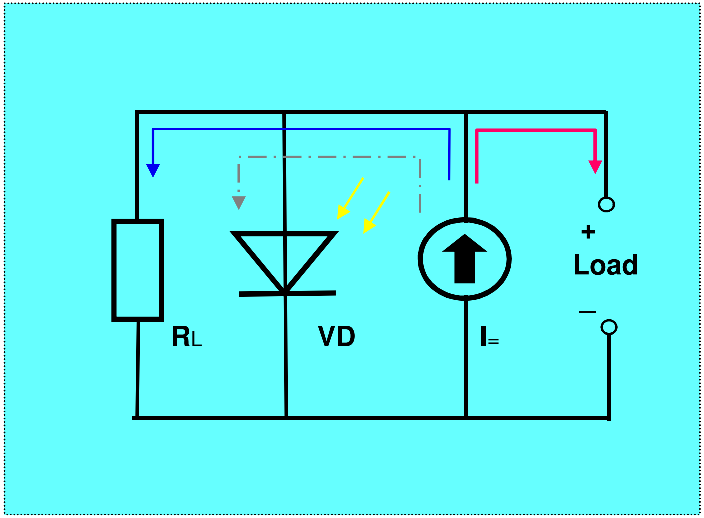

Advantages / disadvantages of photovoltaic (PV)

Renewable energy source

+ Sunlight: clean energy, available nearly everywhere

+ PV generators: small maintenance, no pollution during operation, silent, safe, modularity

+ PV Power is generated at a fixed rate of efficiency, direct or diffuse light.

+ No liquids, corrosive chemicals or moving parts.

+ Very attractive far from electricity networks

- Dependence on cloud coverage
- Restriction to daytimes
- Dependence on position on earth
- Non-economic where in competition

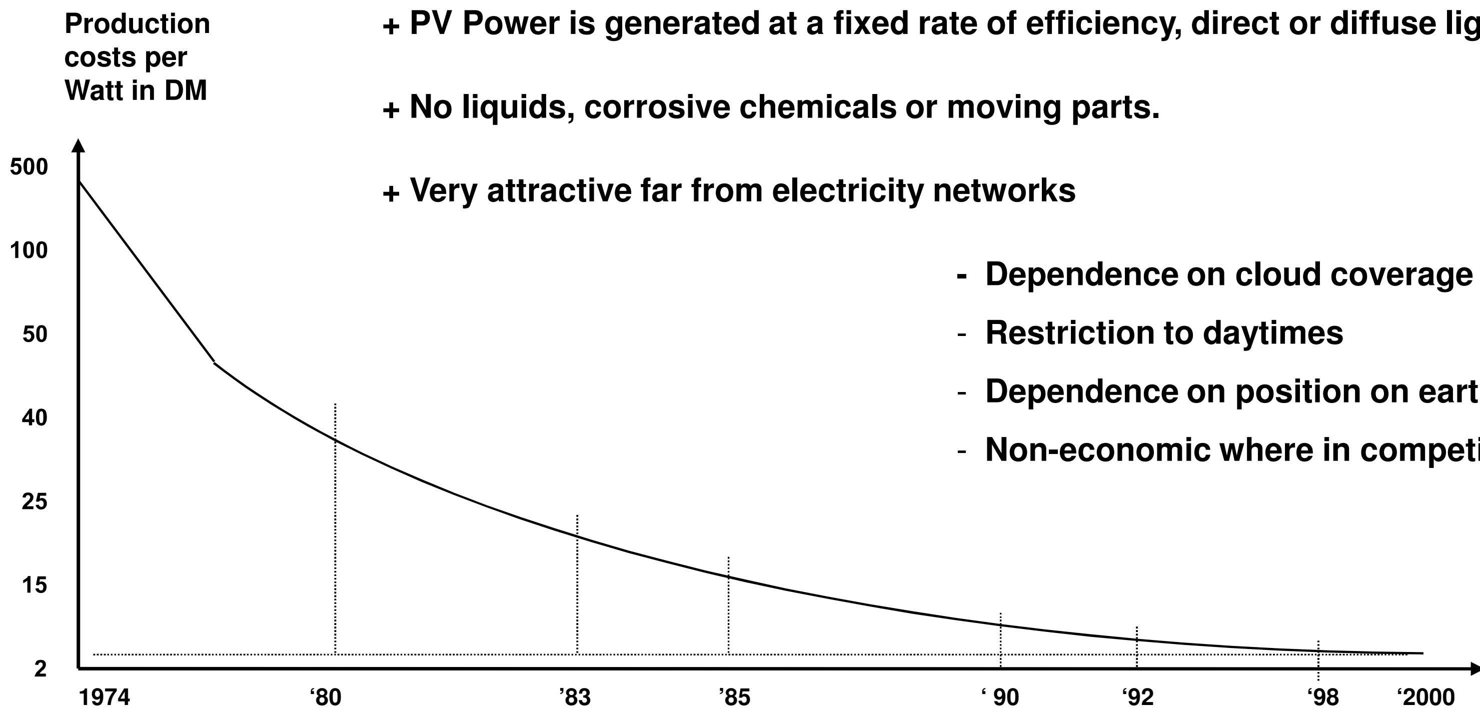

Arrays of solar cells: applications I

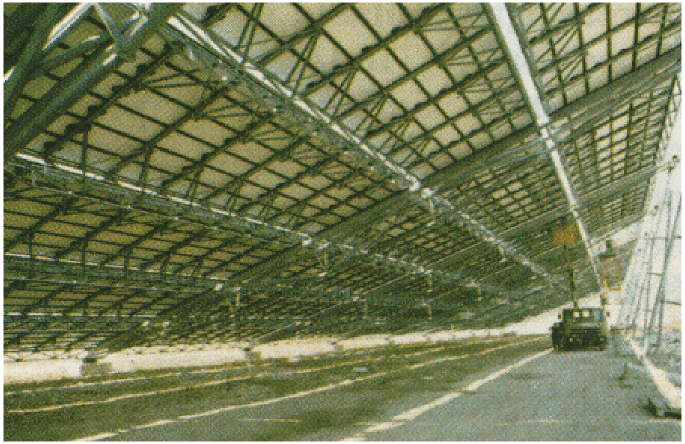

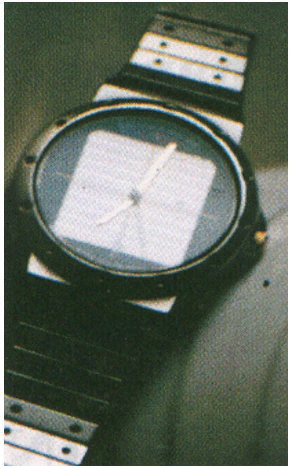

Multi - layer thin - film Silicon solar cells

optoelectronic devices

High-efficiency multi-layer thin-film silicon solar cells deposited by CVD (chemical vapour deposition) on electrically inactive p^{++}-type CZ silicon substrates.

V_{oc} of 664.2 mV, J_{sc} 32.9 mA/cm^{2}, FF of 82.5%, Energy-conversion efficiency 17.6%

High Energy-Conversion Efficiency ~17.6%,

High Open-Circuit Voltage V_{oc} 660 mV . . . 664.2 mV

High Fill-Factor > 80% .

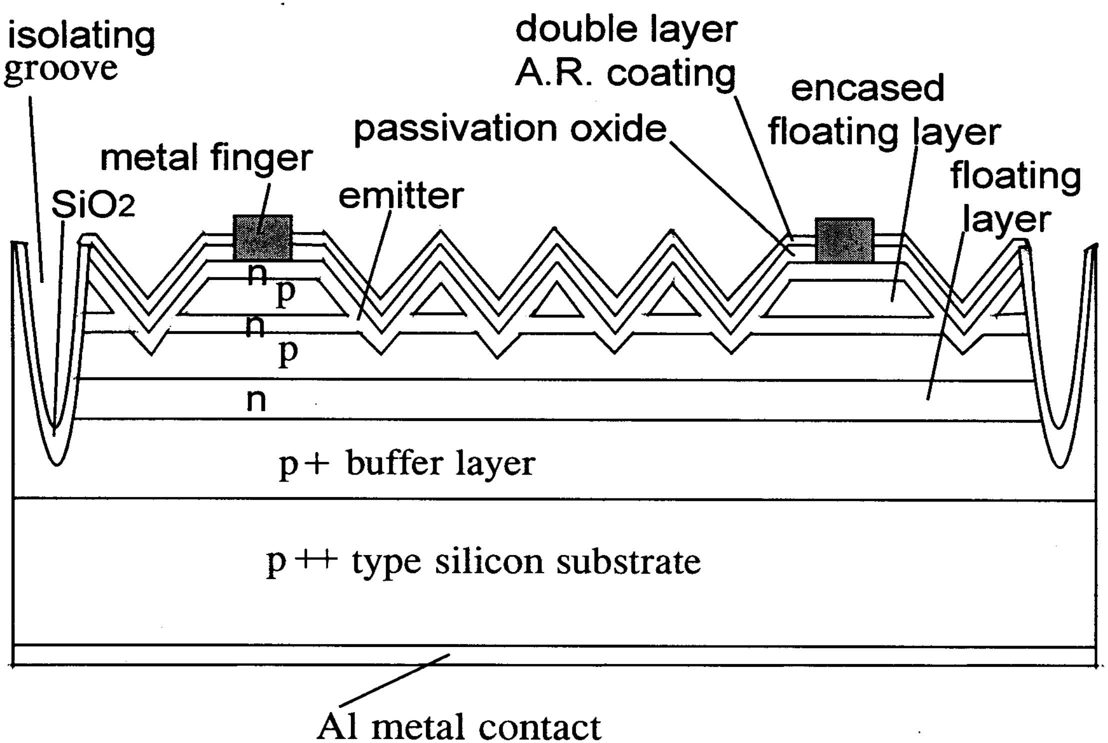

Thinned Multi-Layer Cell Performance:

1. Higher Cell Performance increased J_{sc} by 16%, V_{oc} by 2%, FF by 0.1%, Eff.by 17.3%.

2 Higher Spectral Response

High efficiency solar cells PERL (24%) optoelectronic devices

1. The cell is made on a very pure single crystal of silicon

2. The top surface of the cell is textured to form inverted pyramids, thereby reducing reflection.

3. An antireflection coating (like on spectacles or camera lenses) is deposited on the top surface to further reduce reflection.

3. To minimise shading of the top surface, the fingers forming the top electrode are thinner than a human hair.

They are also spaced very close together and made from silver to minimise the cell's series resistance.

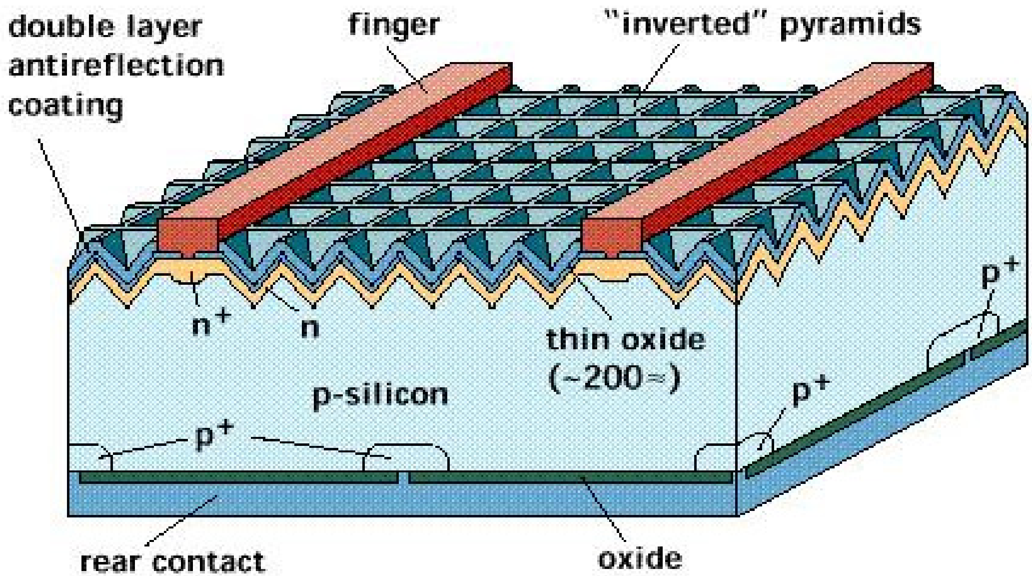

Photovoltaic Research Center at the University of New South Wales

4. A very thin layer of silicon oxide is grown on the top and bottom surfaces of the silicon. Surfaces behave like defects in the crystal and can therefore reduce the cell's efficiency. Growing this oxide reduces the effect of these surfaces on the cell's efficiency, a technique known as "passivation"

5. Since current cannot pass through silicon oxide, small holes are made in the oxide to enable contact to be made between the metal and silicon.

6. To improve the electrical contact between the metal and silicon and reduce the cell's series resistance, small areas of silicon near each of the holes in the oxide are heavily doped (locally diffused)

FLATCON – Concentrator - Technology

Solarcells on the basis of III/V compound semiconductors

FLATCON – Concentrator - Technology

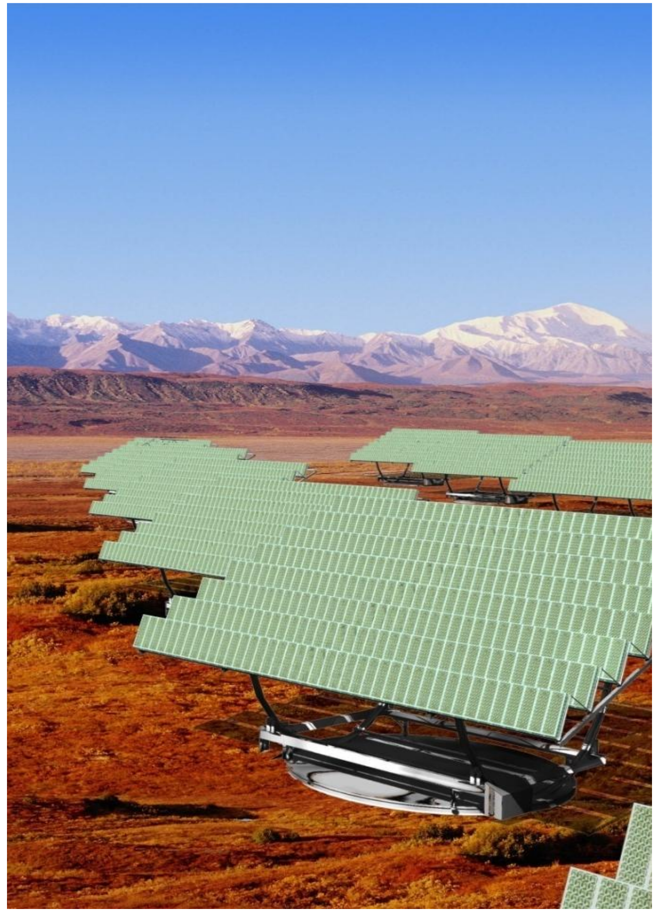

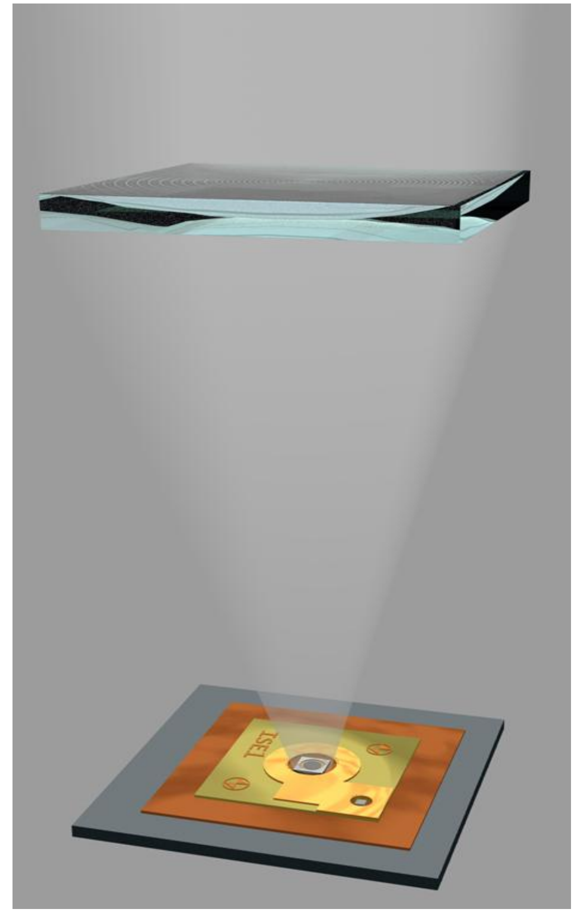

Fraunhofer ISE, Freiburg

III/V solarcells are much efficient but also much more expensive than Si solarcells.
Therefore, light concentration is highly efficient to reduce system costs

FLATCON – Concentrator - Technology

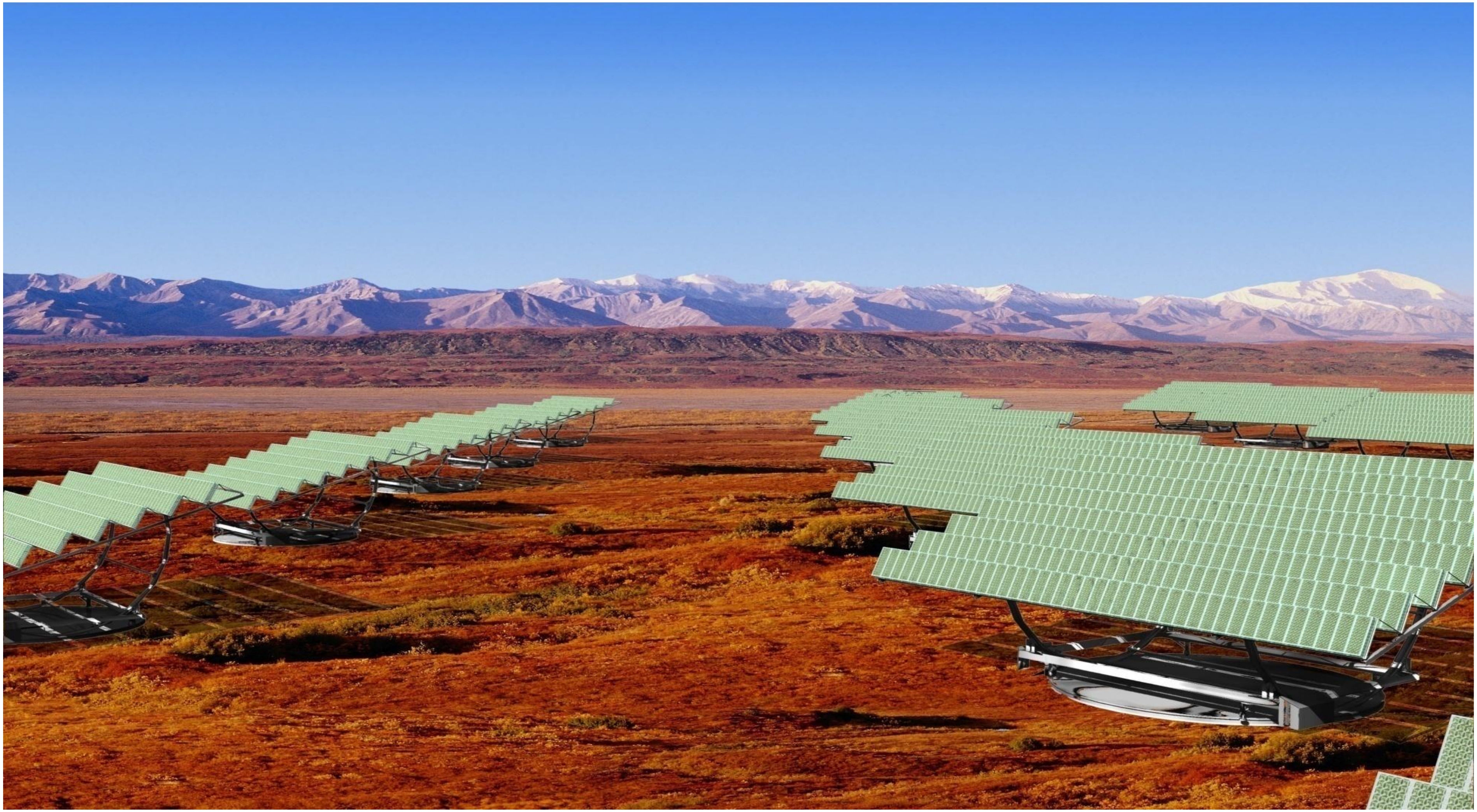

Chapter 10

Micro optics

microooptics microelectronics micromechanics microfluidics

common technology platform

features:

miniaturisation
integration
compatibility

technology	**processing techniques**	**mounting techniques**
classical optics (“macrooptics”)	grinding, polishing, diamond turning	fine mechanics
“miniature optics”	grinding, polishing, gradient index optics, LIGA process (components), fiber pulling	miniaturized mechanics, micromechanics
“microoptics”	lithographic: optical, electron beam, X-ray, LIGA non-lithographic: diamond turning, microjet printing	micromechanics, integration on single substrate bonding techniques

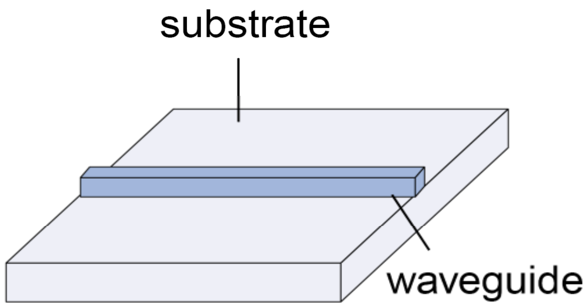

waveguide optics

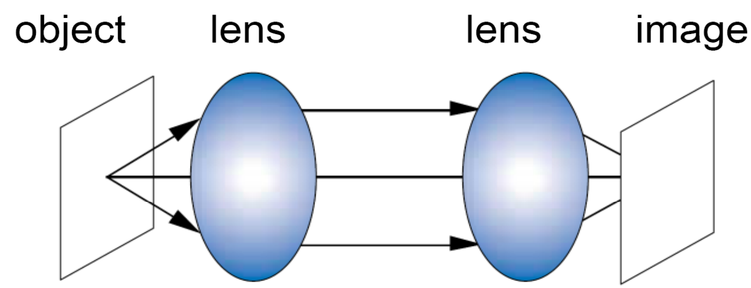

free-space optics

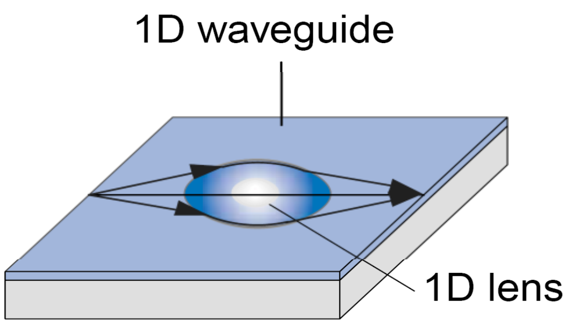

waveguide and free-space optics

Classification of optical components

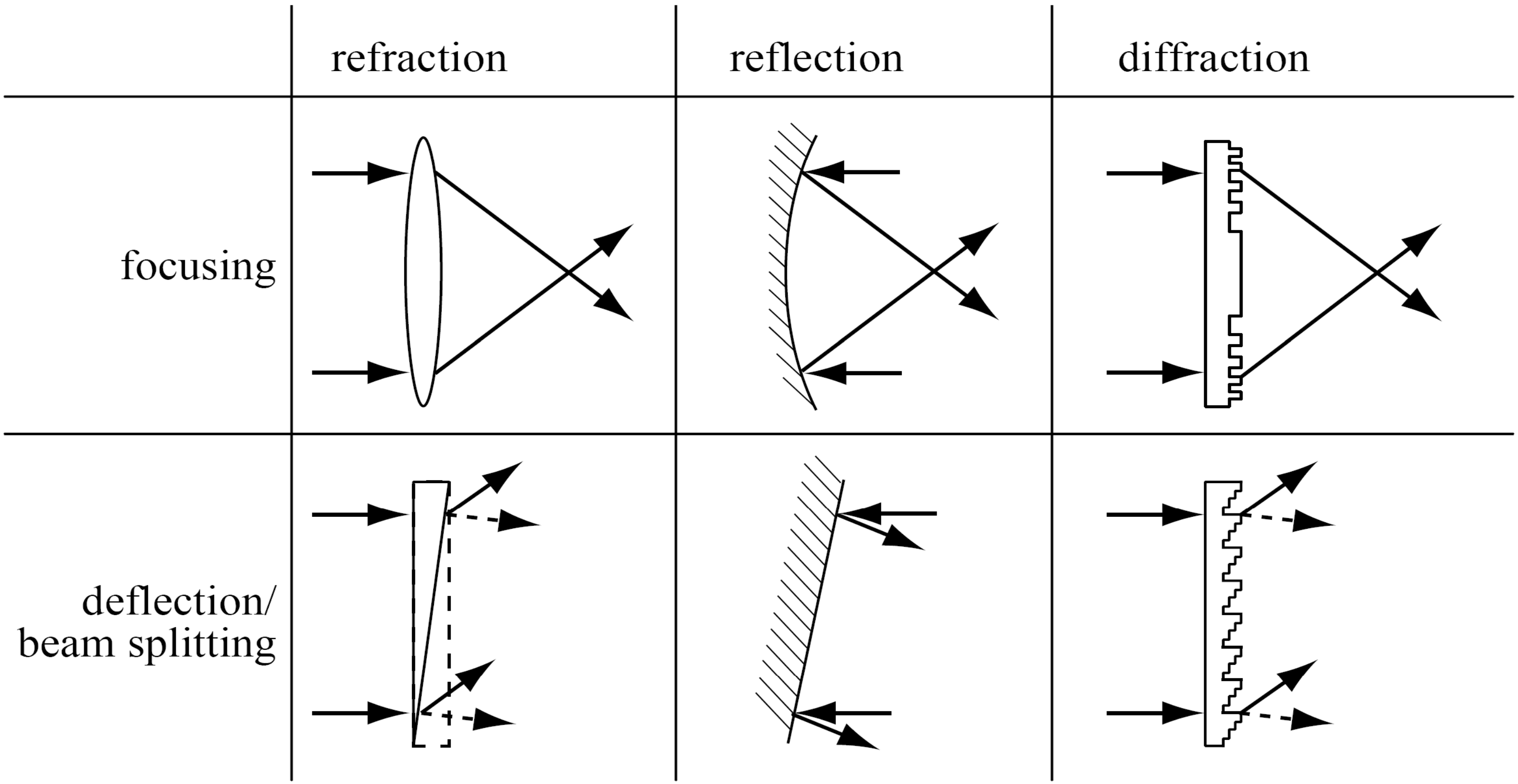

Refractive micro optics

refractive optical elements (ROEs)

- gradient index elements (GRIN)
  - GRIN-rod lenses
  - planar GRIN elements
- surface profile elements
  - distinction through fabrication process e.g. reflow lenses

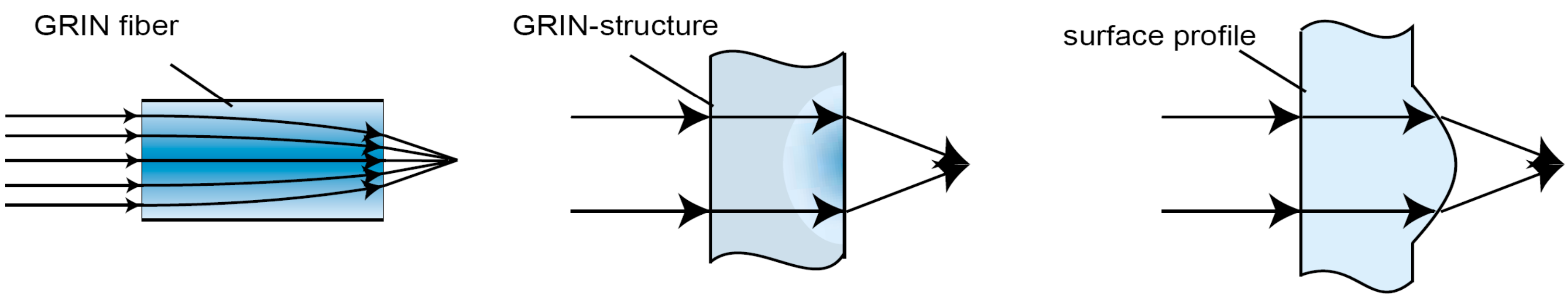

Diffractive micro optics

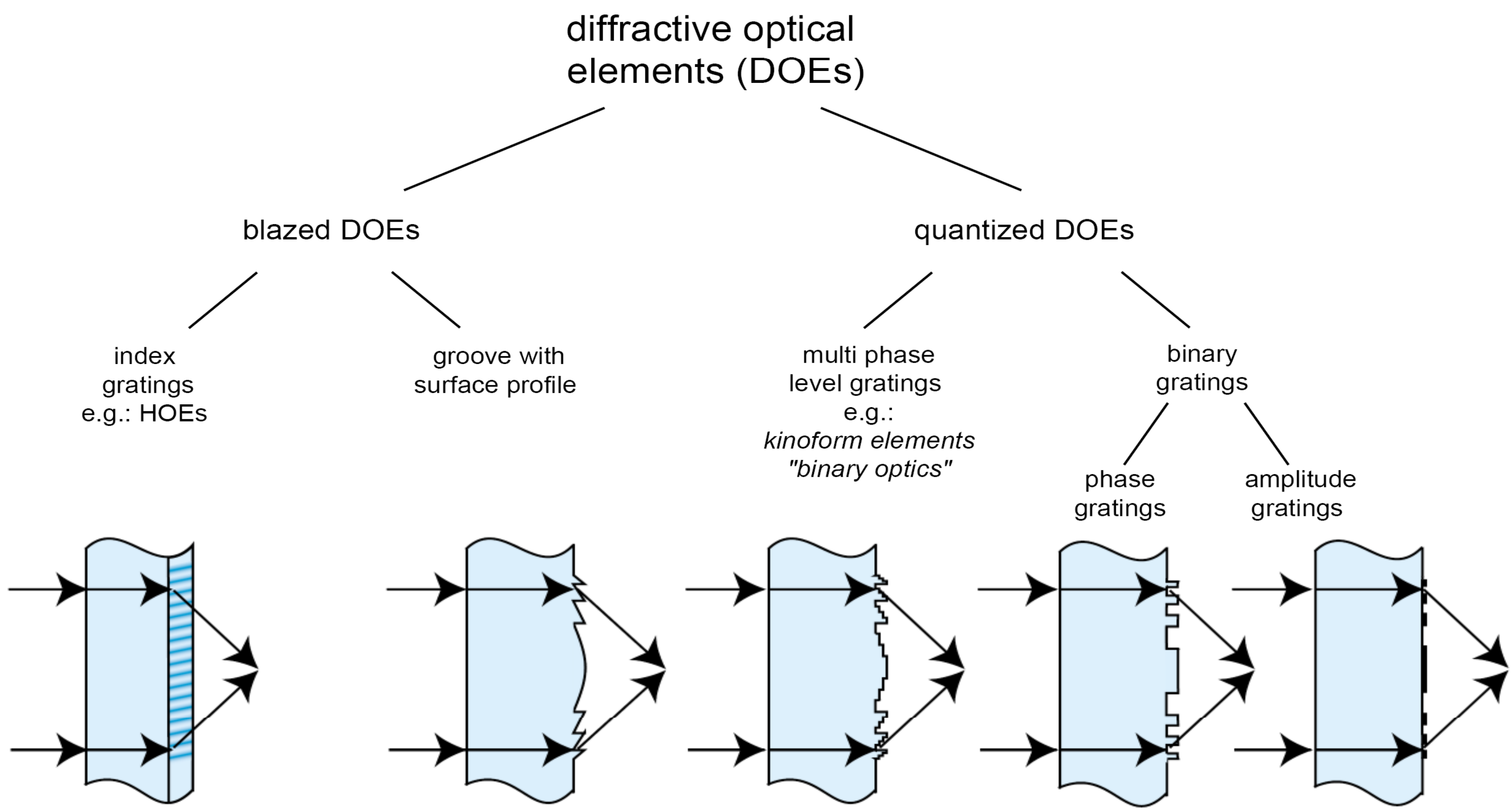

Technology

Optical and e-beam lithography;
analog and binary lithography;
etching and micromachining.

structuring

pattern transfer

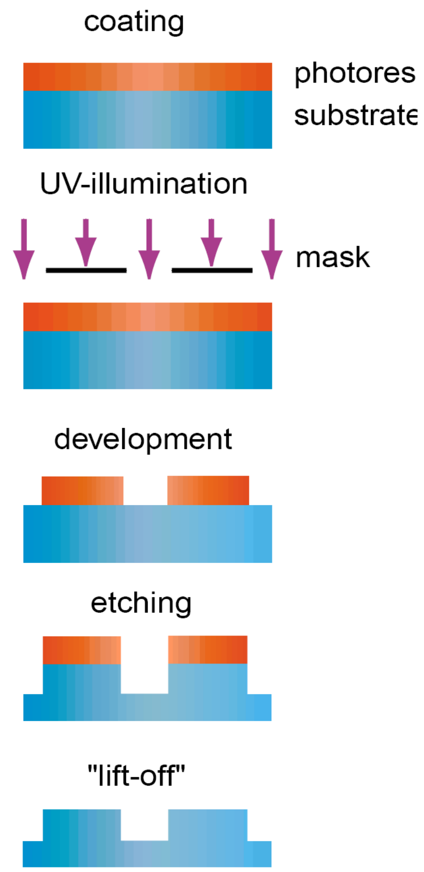

Mask and scanning lithography

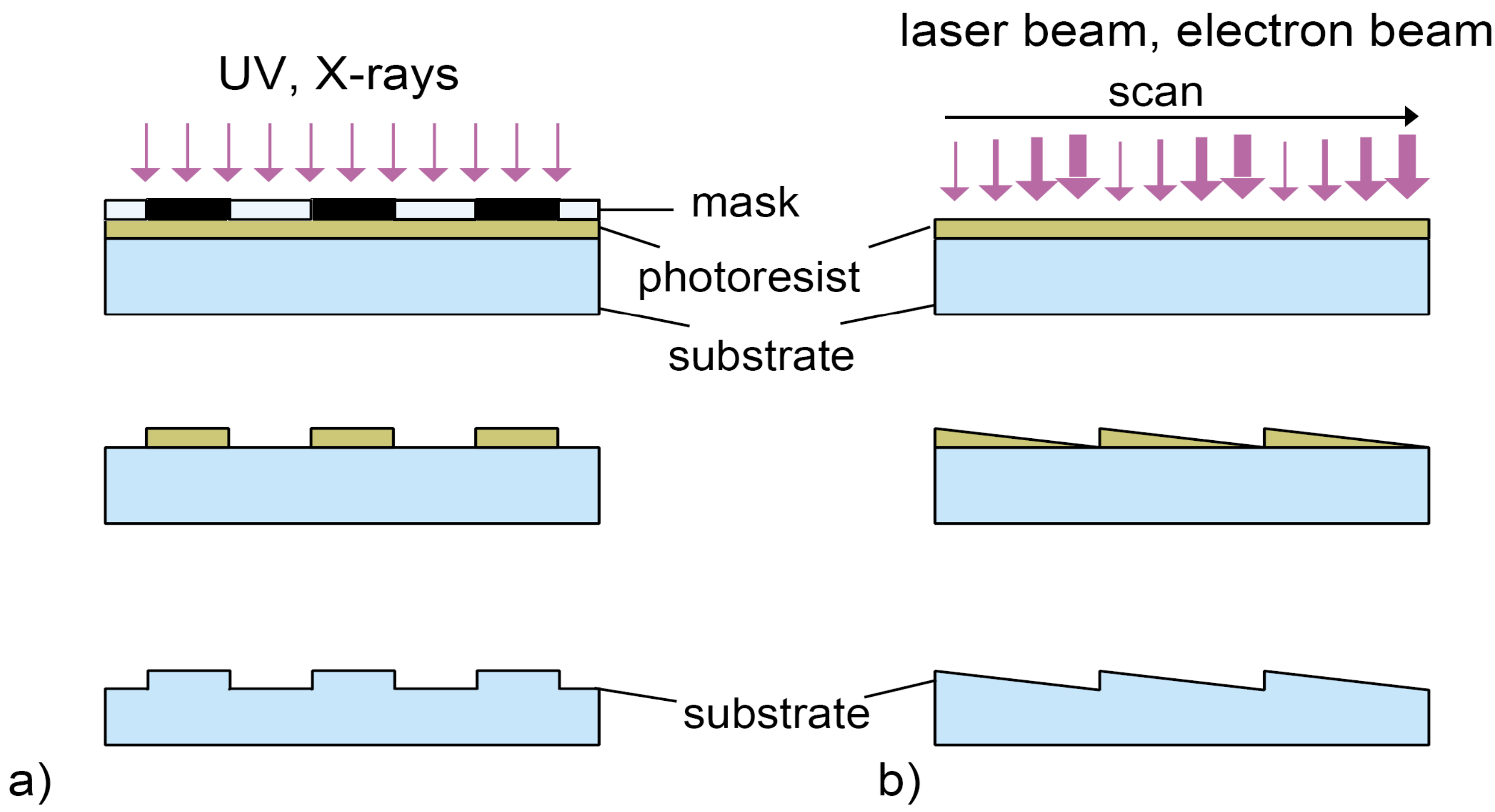

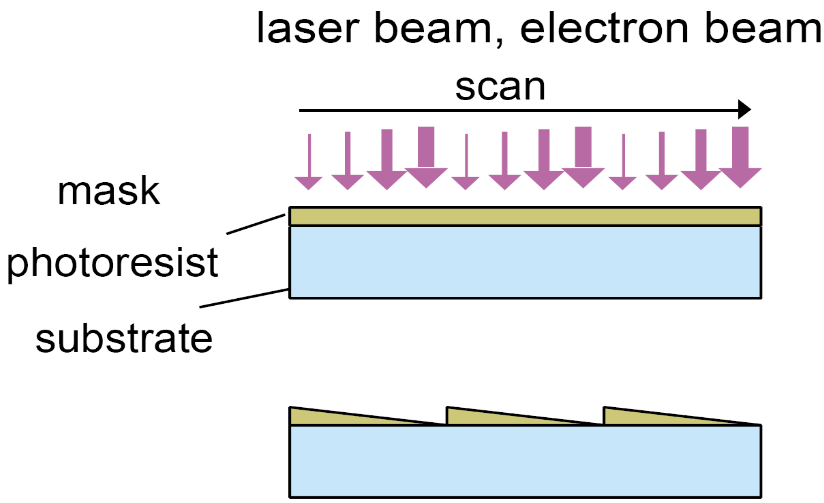

structuring in

- thick photoresist (*shown here*)
- high-energy-beam-sensitive (HEBS) glass

HEBS glass for grey – scale mask

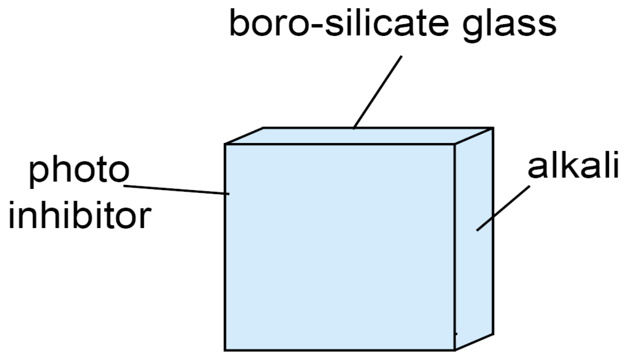

ion-exchange process

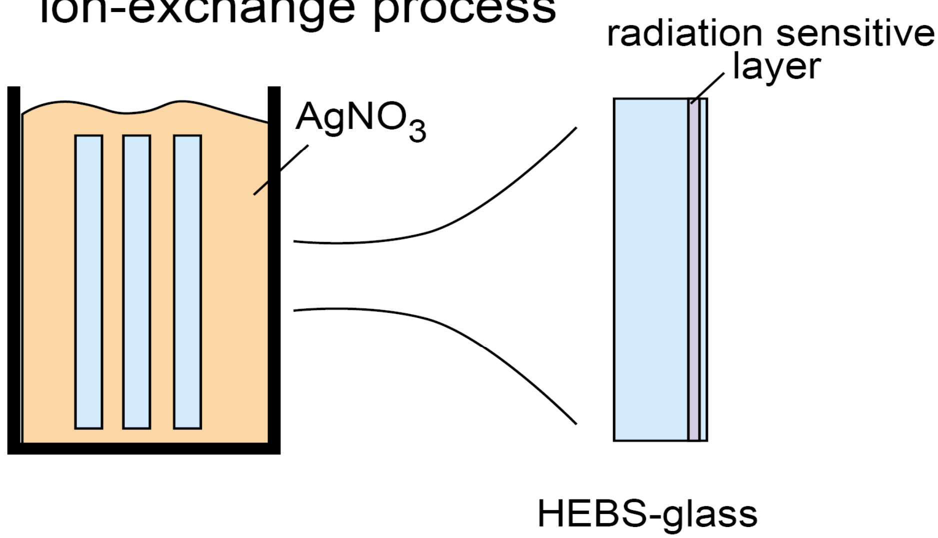

Grey – scale mask in HEBS glass

e-beam illumination

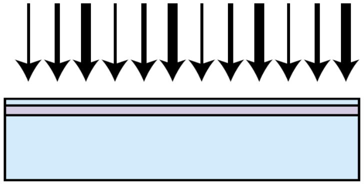

variable dose writing of grey scale masks

Example of a HEBS mask
for the fabrication of microprisms

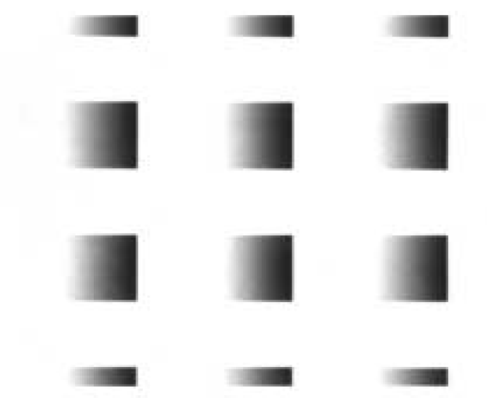

Microoptical components fabricated using HEBS grey-scale masks

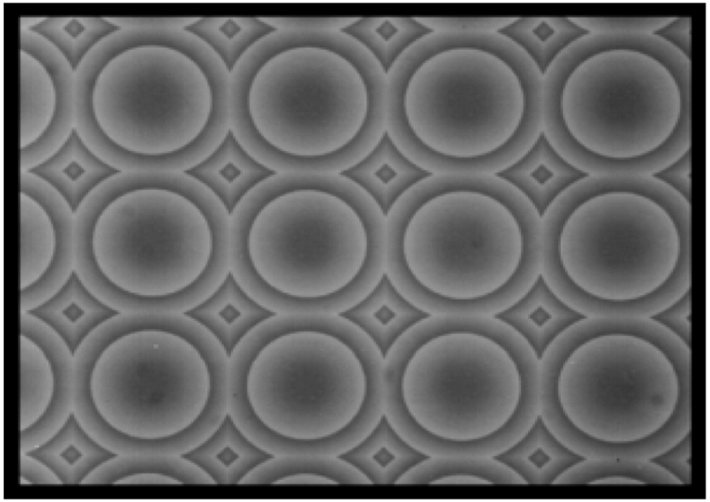

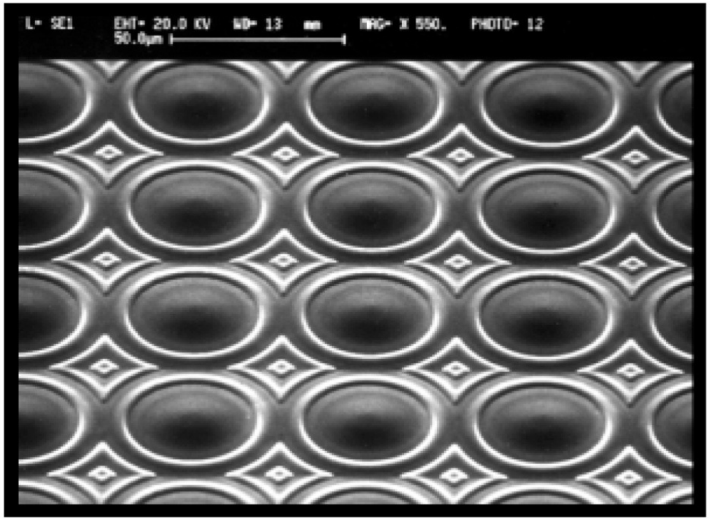

Mask lithography – the illumination process

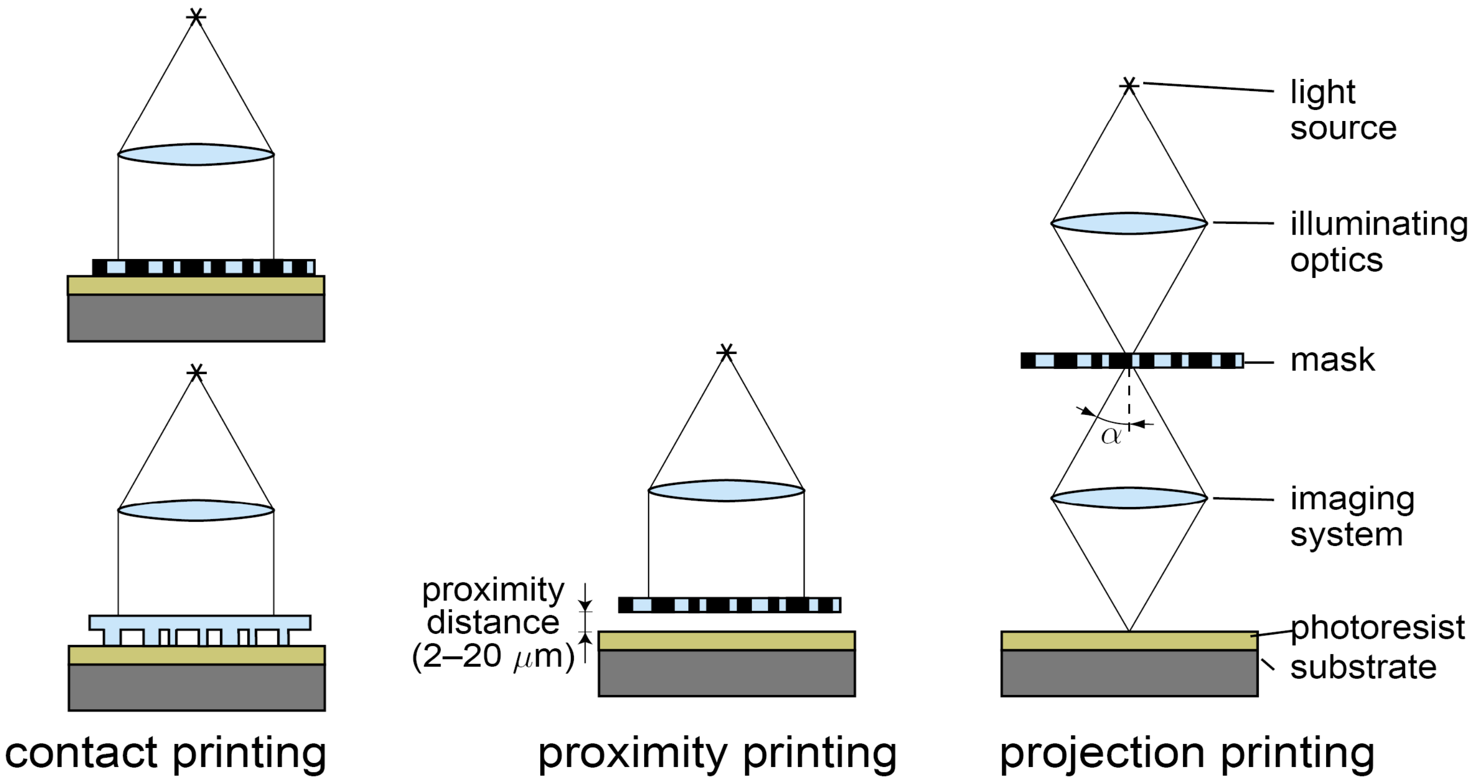

Multimask processing

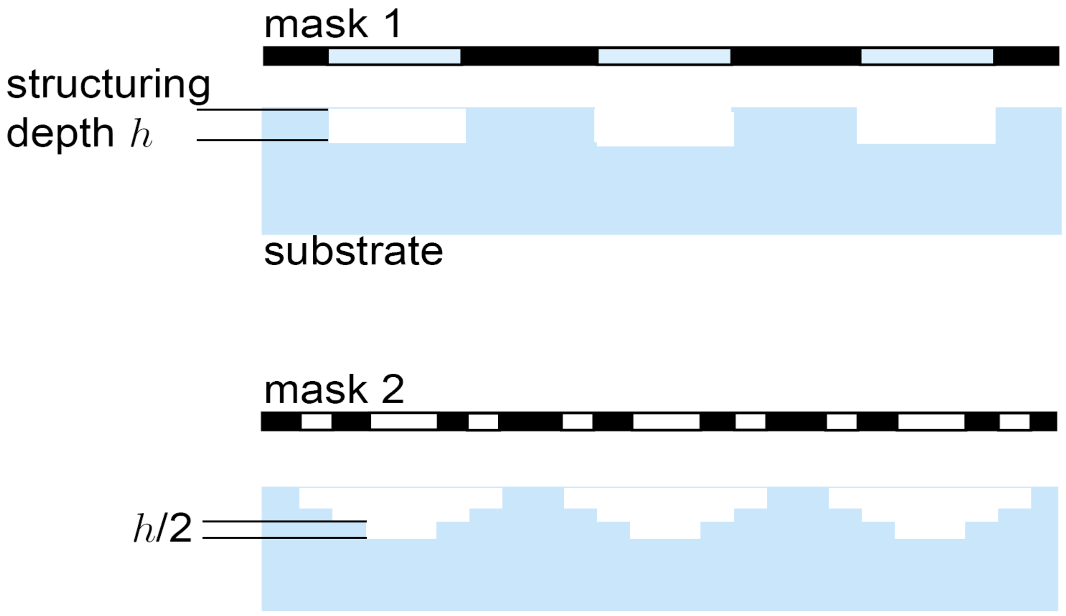

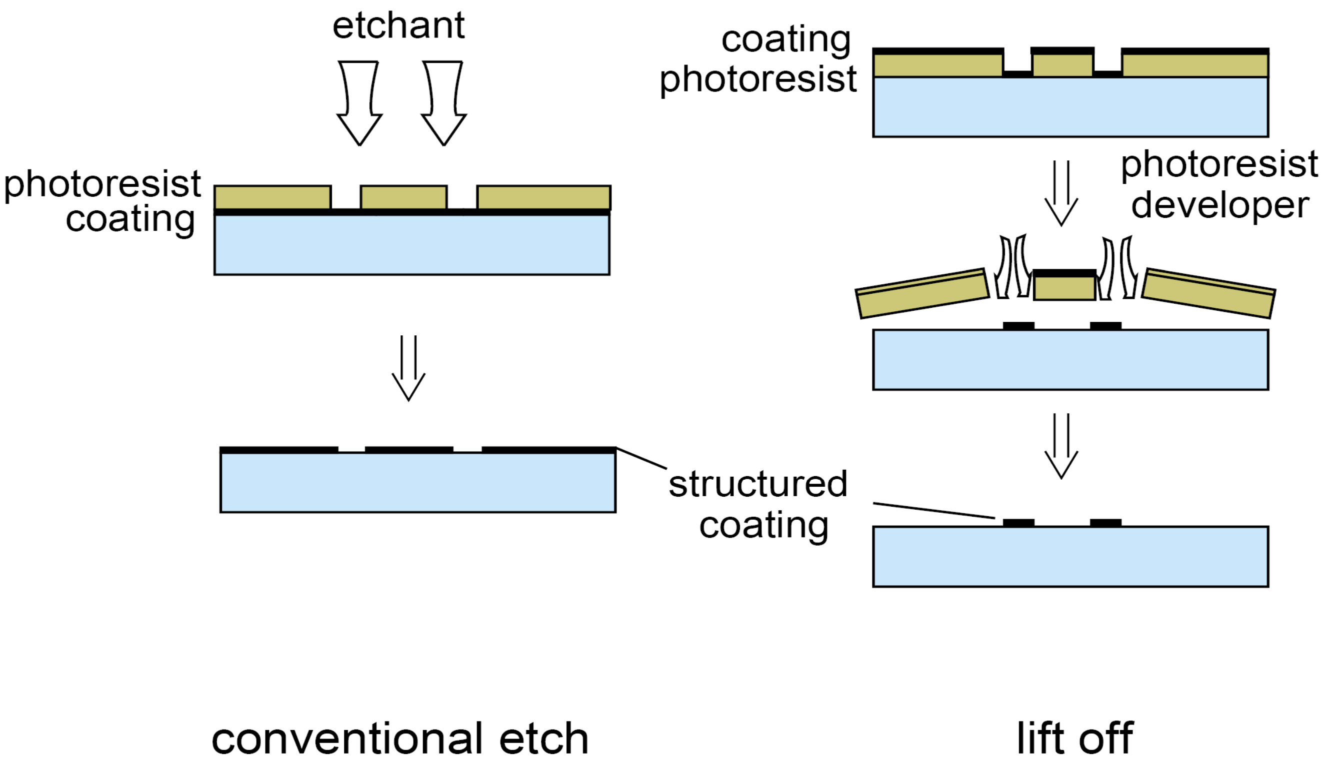
etchant
photoresist
coating
structured
coating
coating
photoresist
photoresist
developer
conventional etch
lift off

Isotropic and anistropic etching

isotropic etching

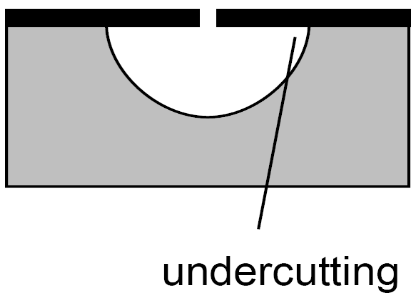

anisotropic etching

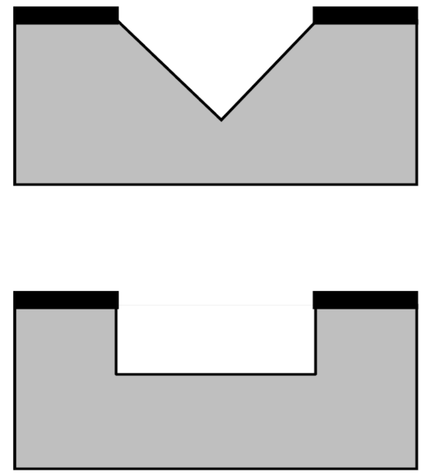

etch rate identical in all directions
(chemical etching)

etch rate in depth >> etch rate in lateral direction
(reactive ion etching)

Differential etching

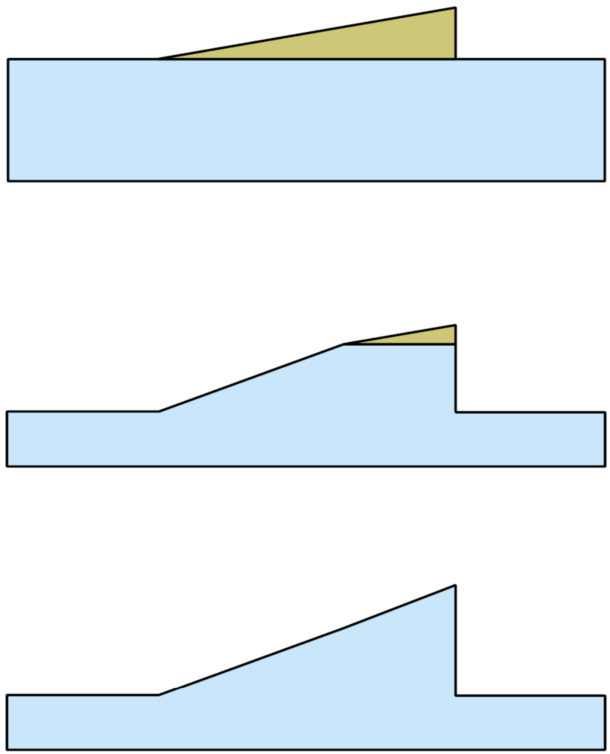

etchants:

O_2 for photoresist
CCl_2F_2 for SiO_2 or Si

(relative pressures
determine relative etch ratio)

Replication of surface relief microstructures

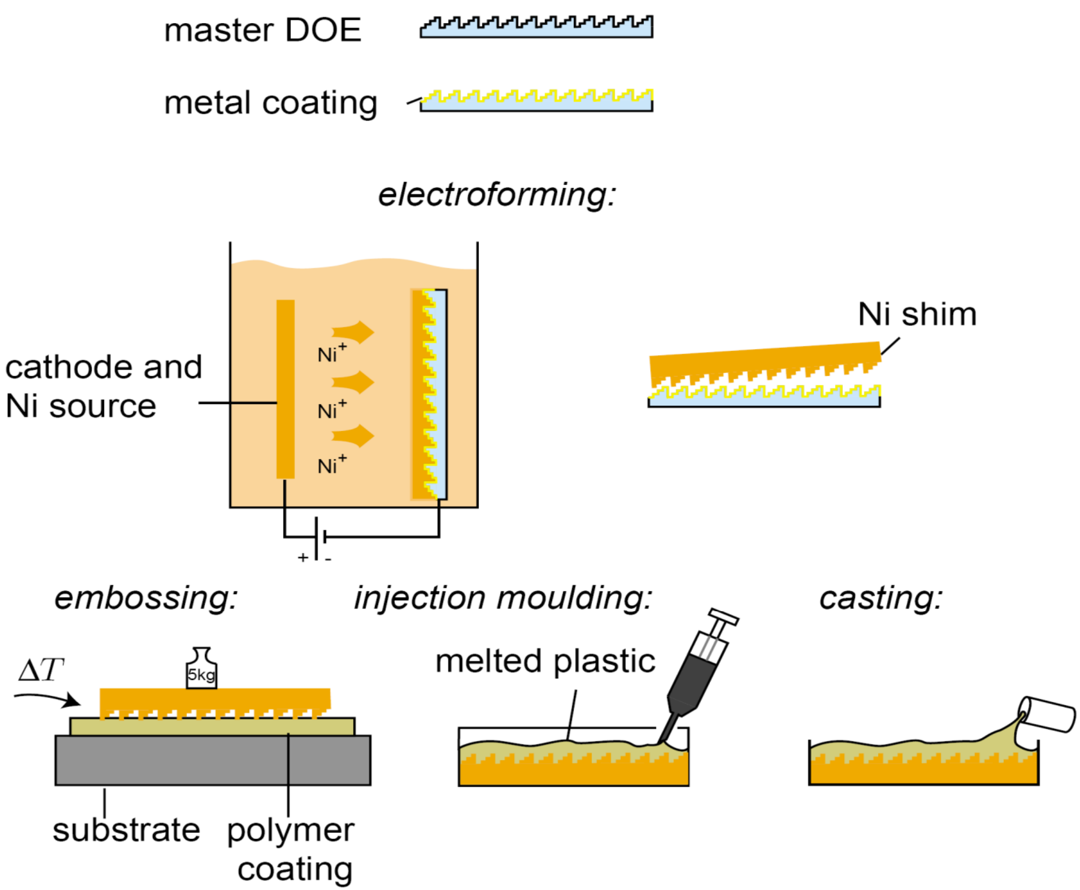

The LIGA process – deepn lithography

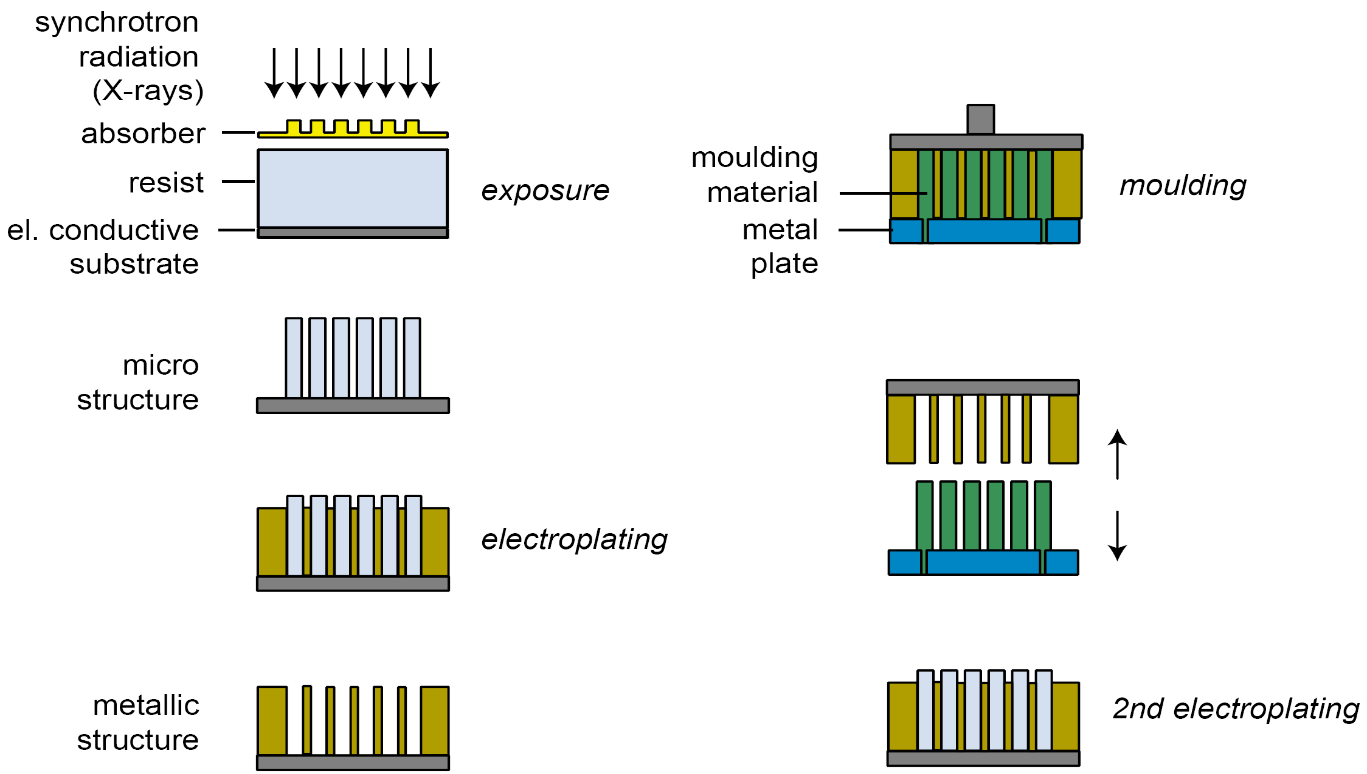

- extreme structure heights (up to 1000 µm)
- minimum lateral feature size: 0.5 µm
- large aspect ratios (>100)

refractive optics;

diffractive optics.

Implementation of optical components

continuous surface profile

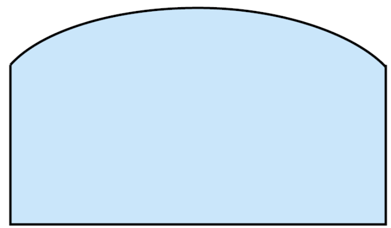

diamond turning,
melting of photoresist,
direct laser or e-beam writing,
dispensing, swelling.

index distribution

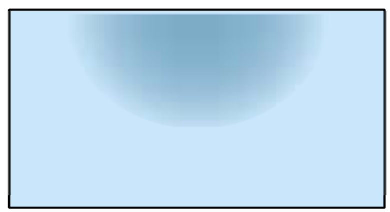

ion exchange,
diffusion

diffractive surface profile

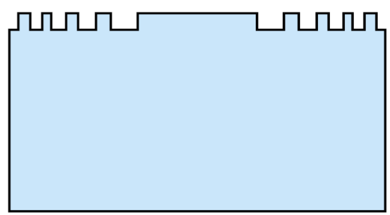

diamond turning,
optical or e-beam lithography.

Reflow micro lenses - example

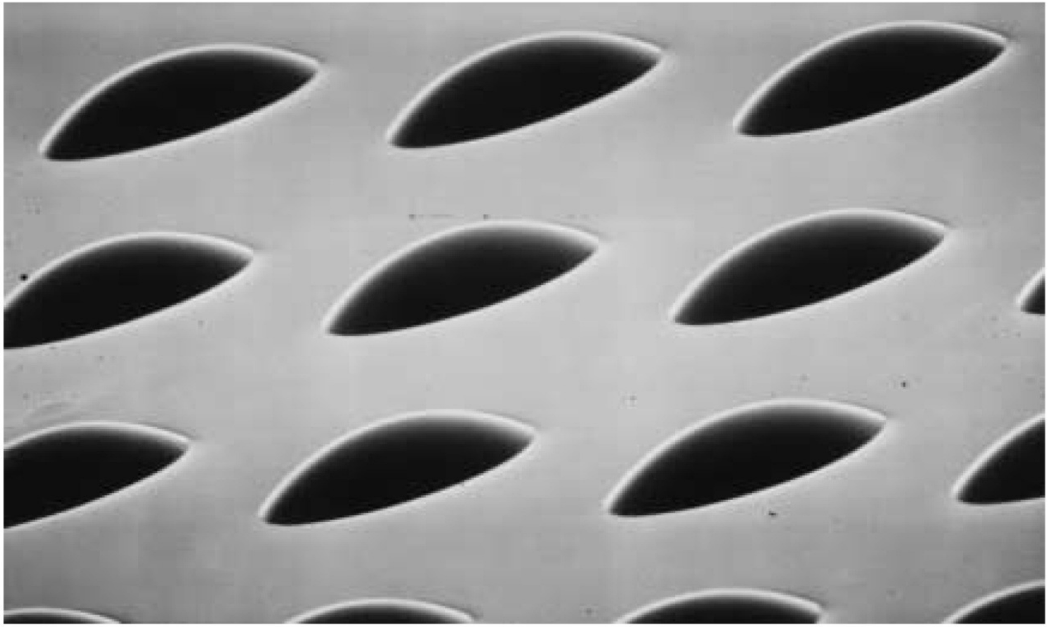

REM photograph of an array of melted photoresist microlenses (diameter: 100µm)

Reflow micro lenses - preshaping

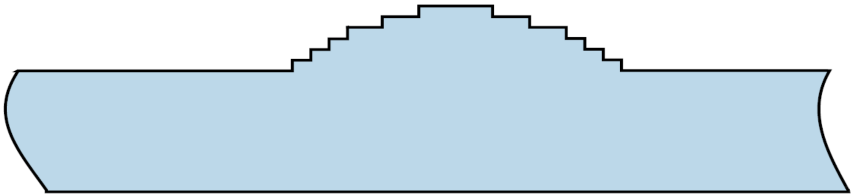

a)

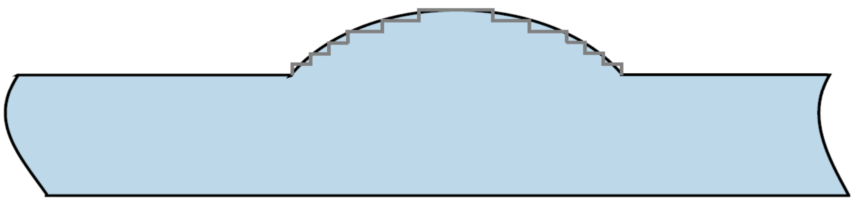

b)

Micro lenses in photosensitive glass

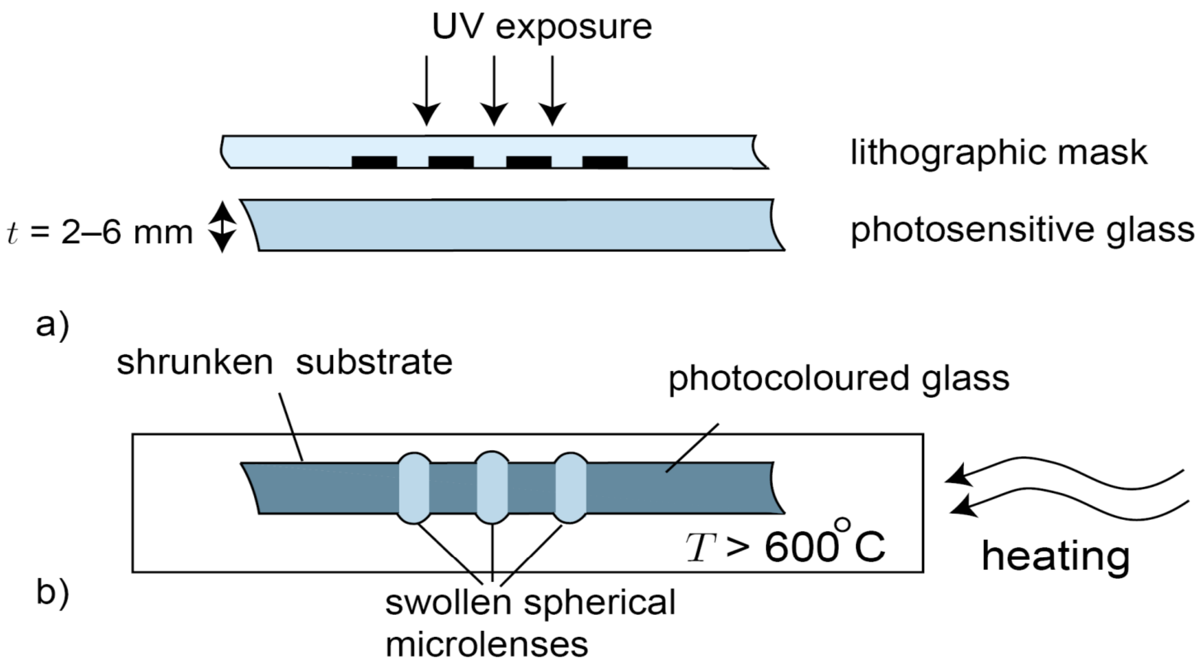

Micro lenses by volume growth in PMMA

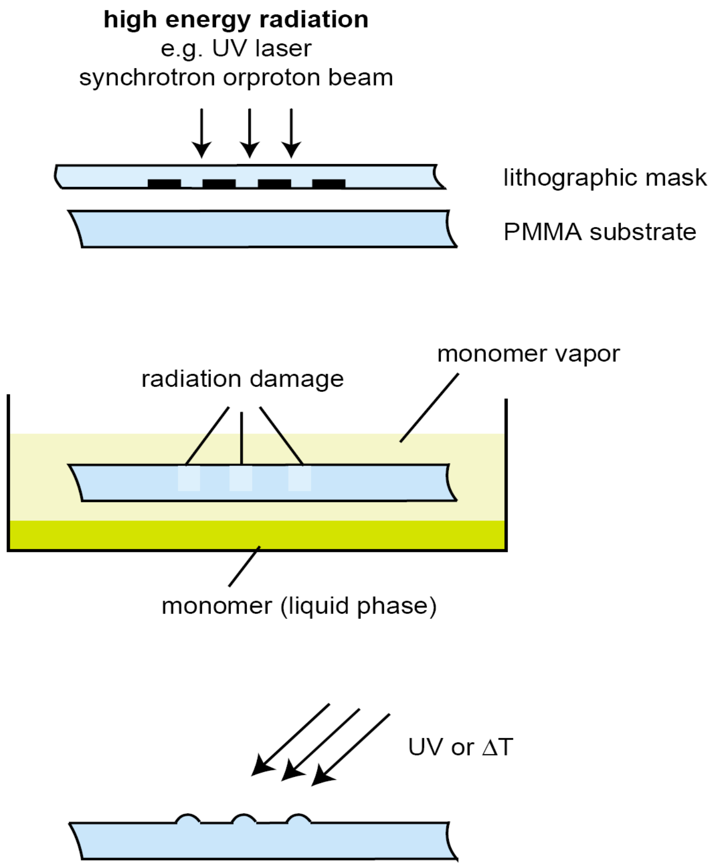

Dispensed micro lenses

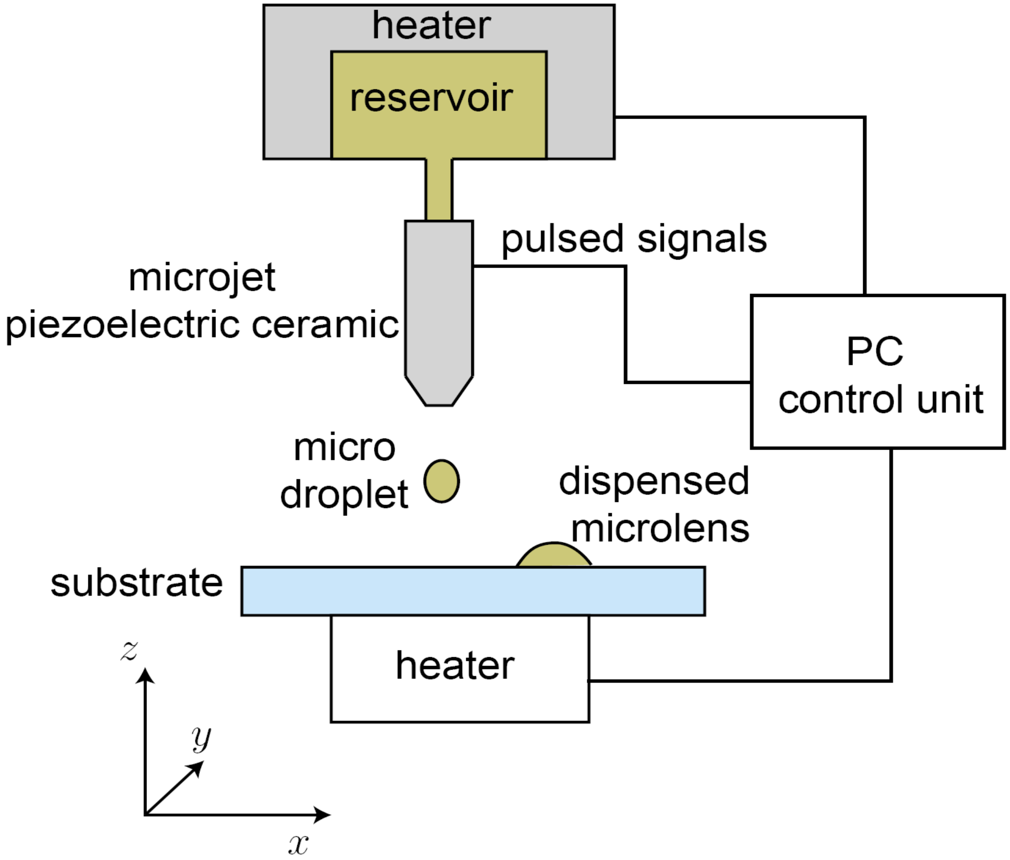

Gradient index micro optics

2-D profile with
radial symmetry

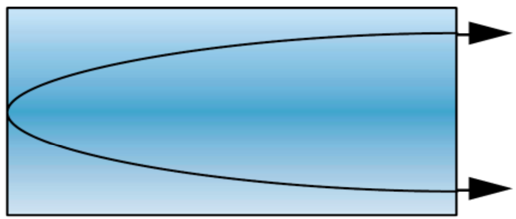

Example: SELFOC™

3-D profile with
point symmetry

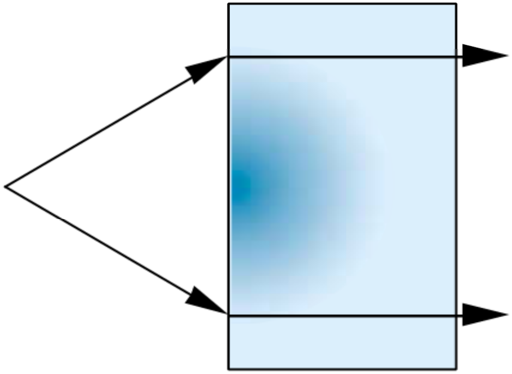

Fabrication of planar GRIN lenses

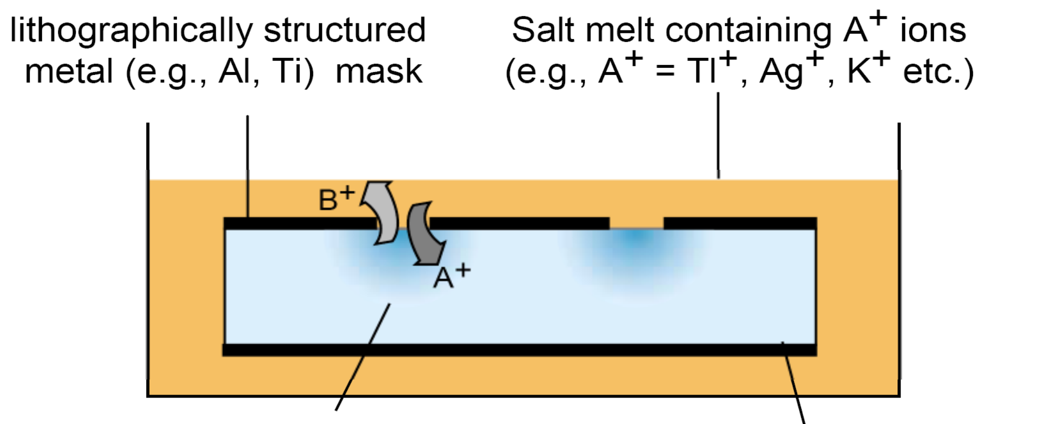

a)

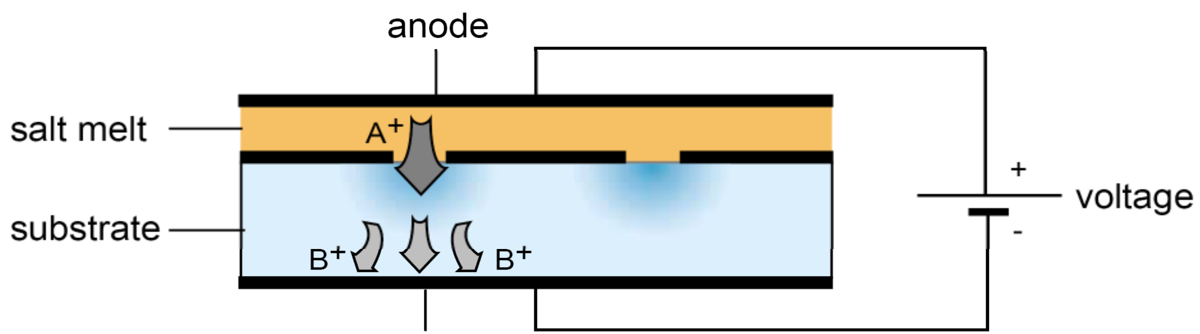

b)

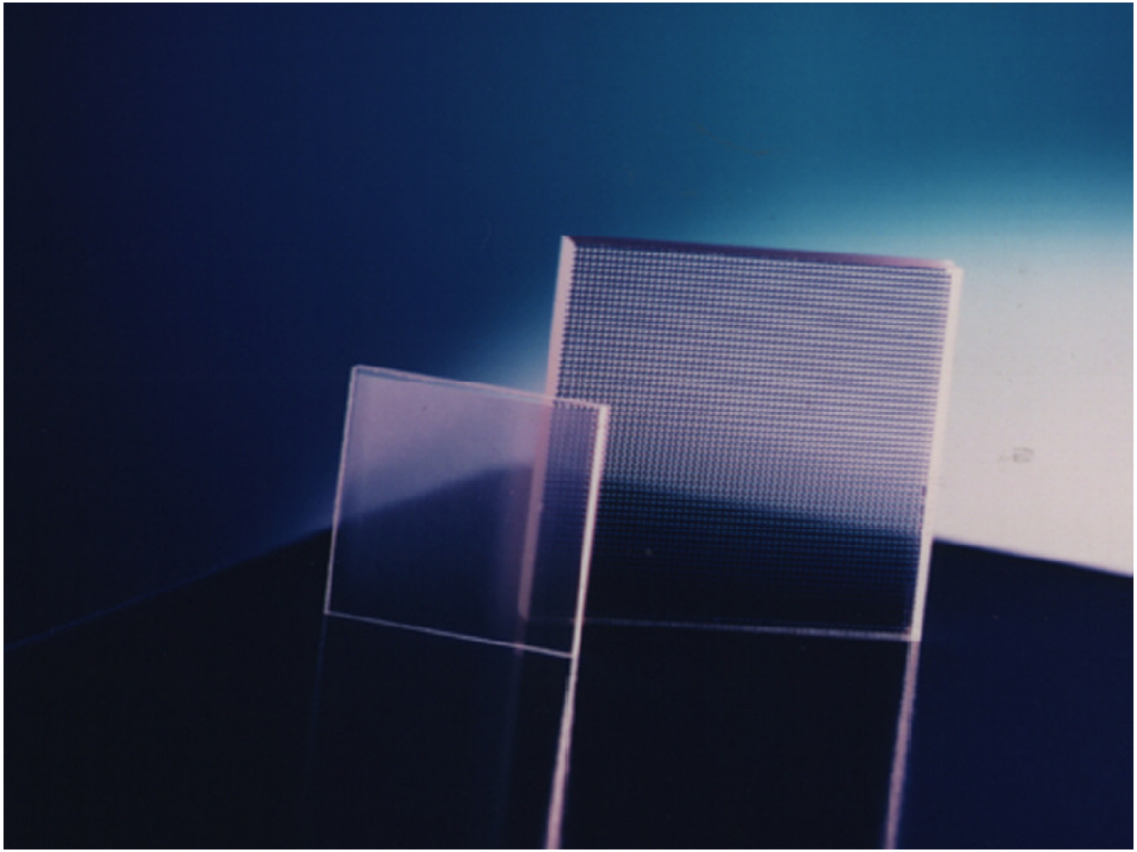

Micro prisms

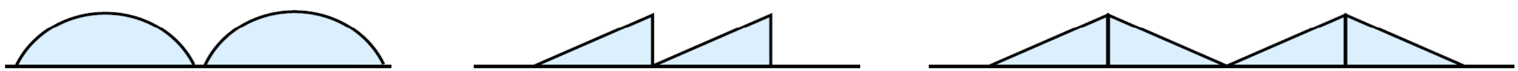

a) b) c)

Micro prisms fabrication by grey-scale lithography

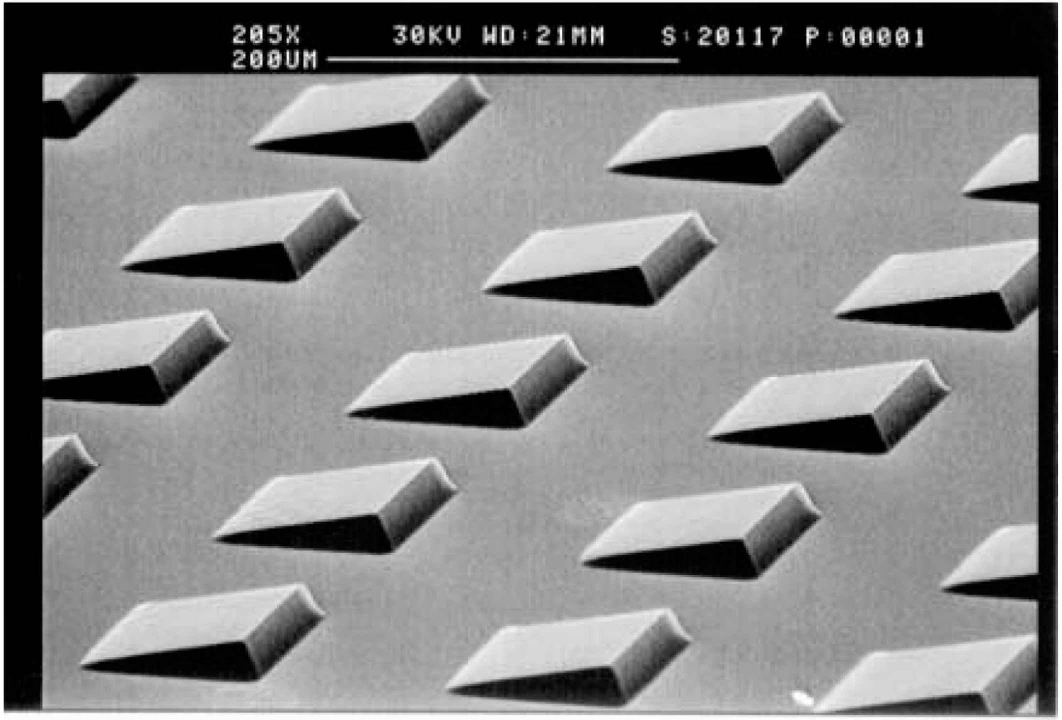

Micro prisms fabrication by mass transport

optoelectronic devices

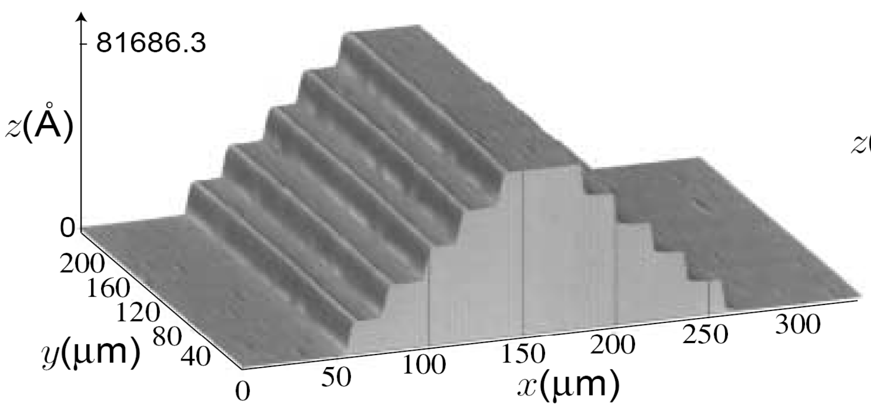

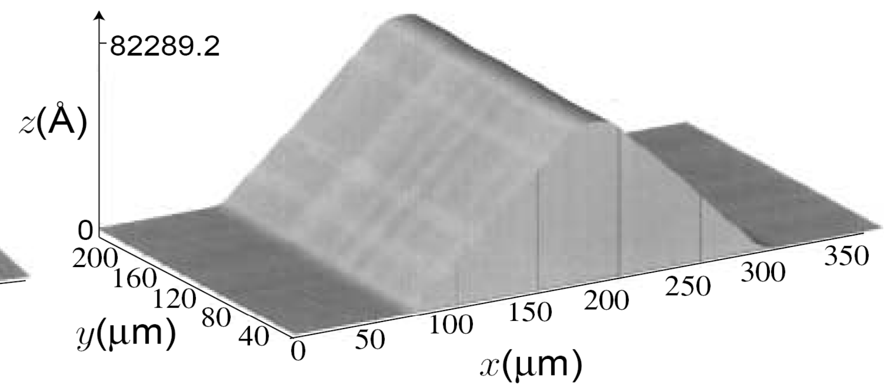

Diffractive optics

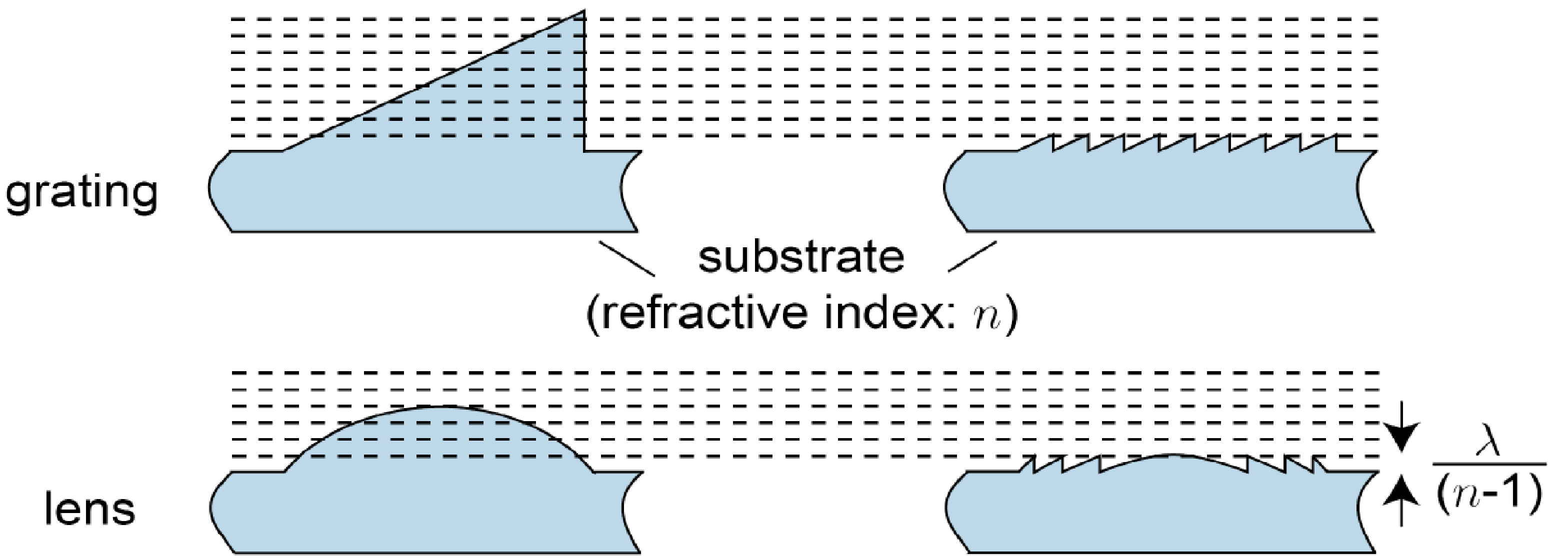

Phase quantization

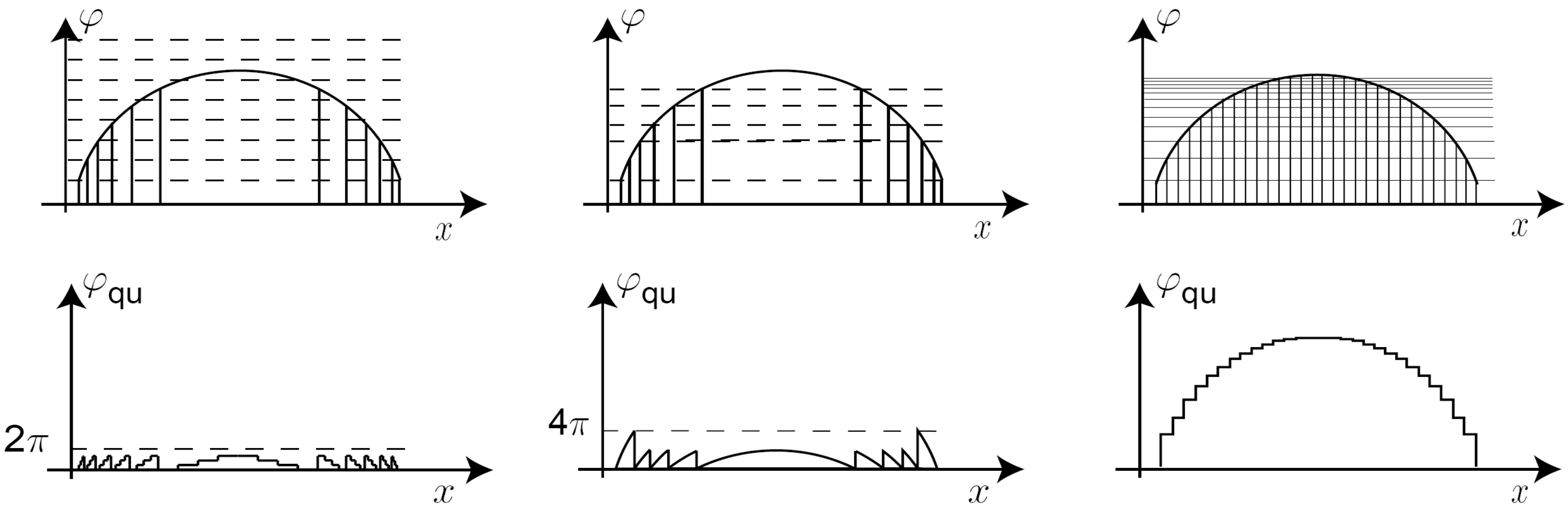

conv. quantization   superzone quantization   phased array quantization

DOE examples

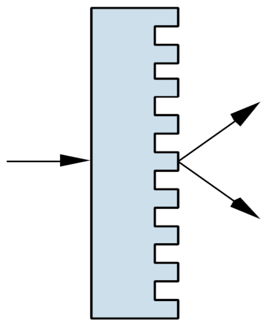

1X2 beamsplitter

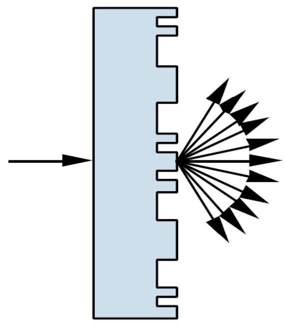

1XN beamsplitter

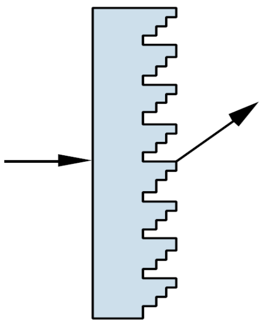

beam deflector

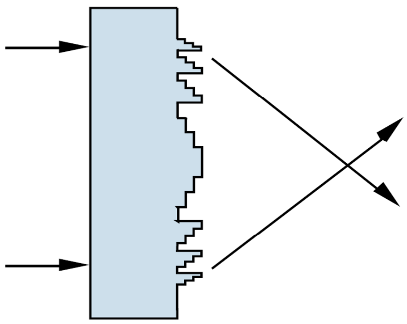

diffractive lens

4 phase level microlens array

8 phase level microlens + beam splitter

Fabrication errors

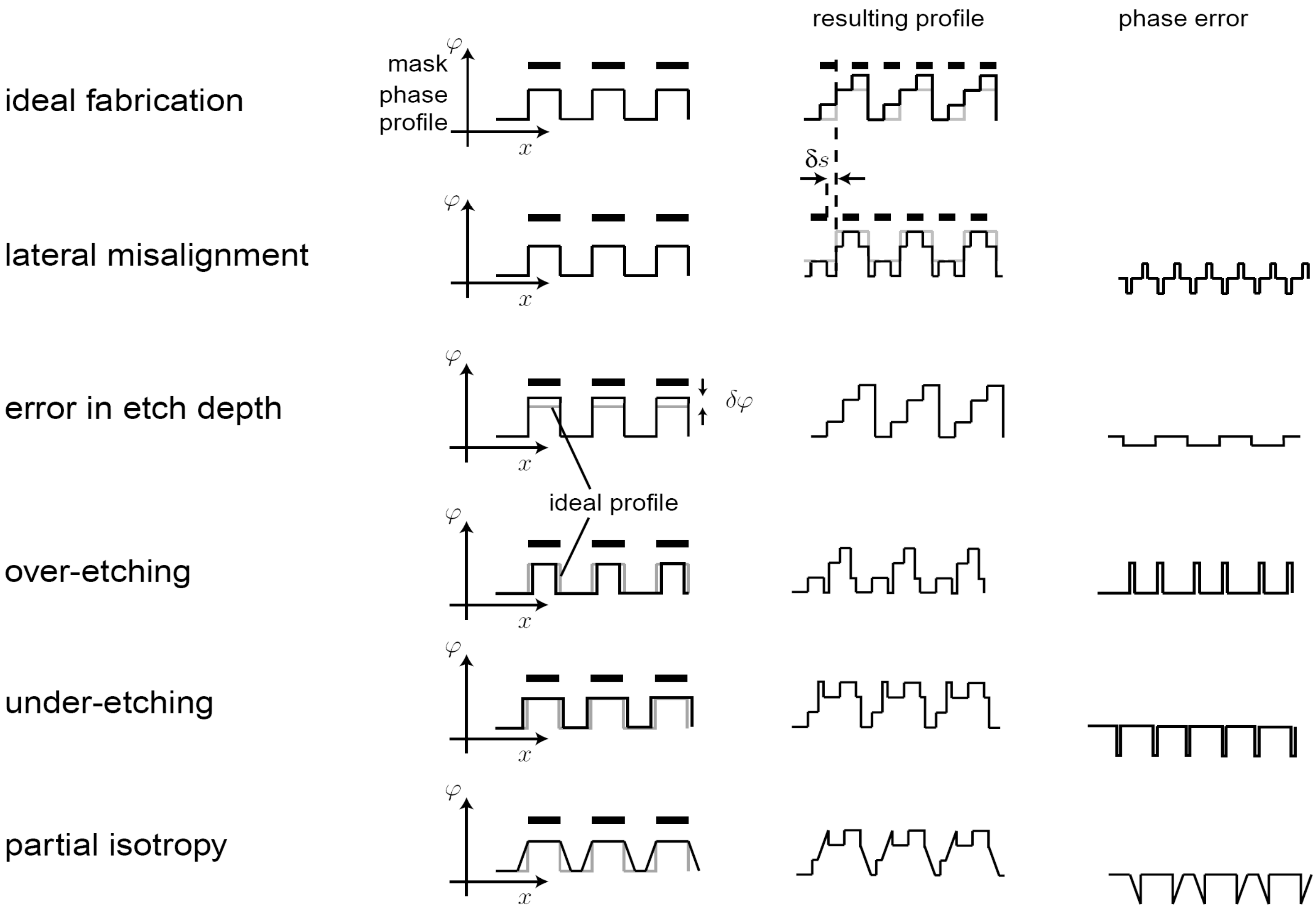

Diffraction efficiency

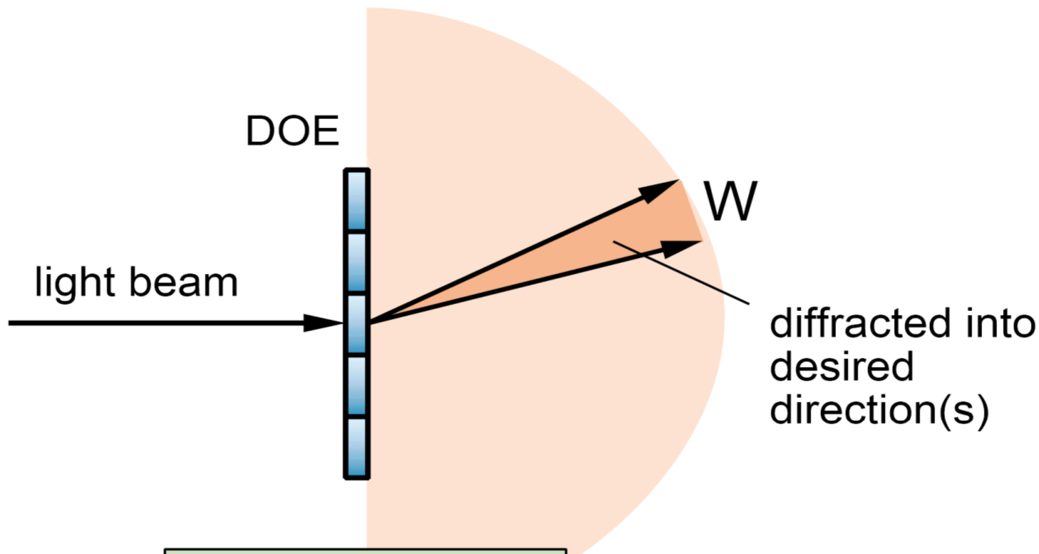

$$\eta = I_W / I_{total}$$

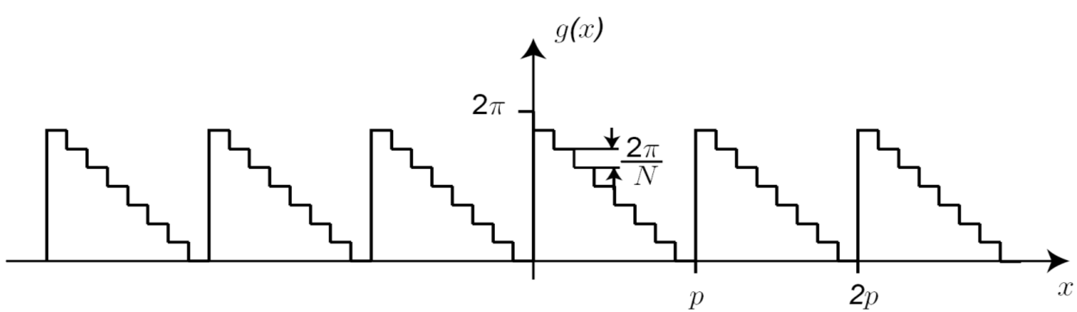

Diffraction at a kinoform grating

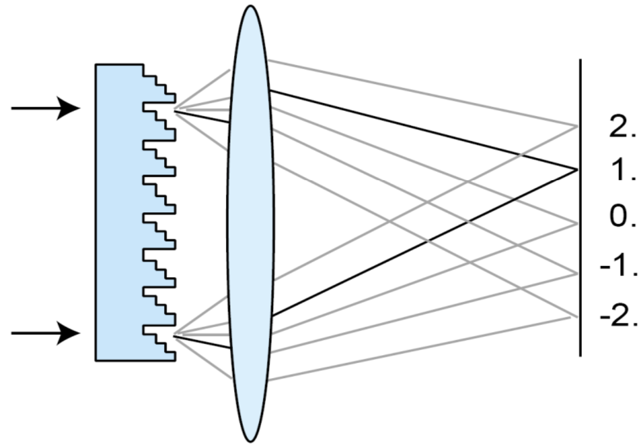

$$\eta = I_1 / \sum_m I_m$$

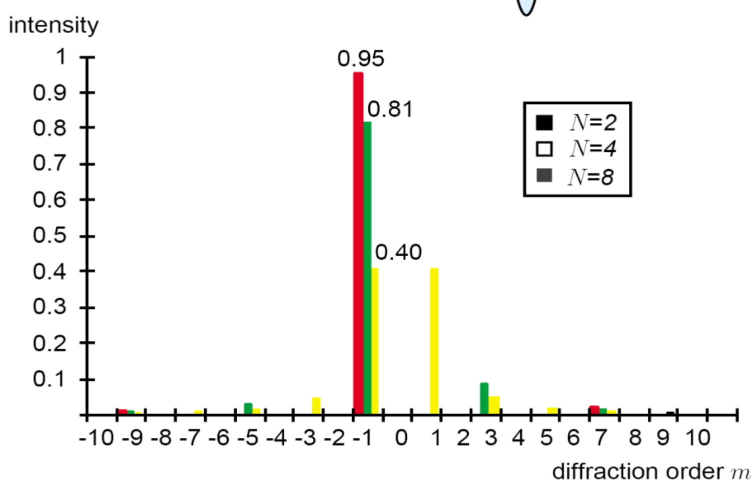

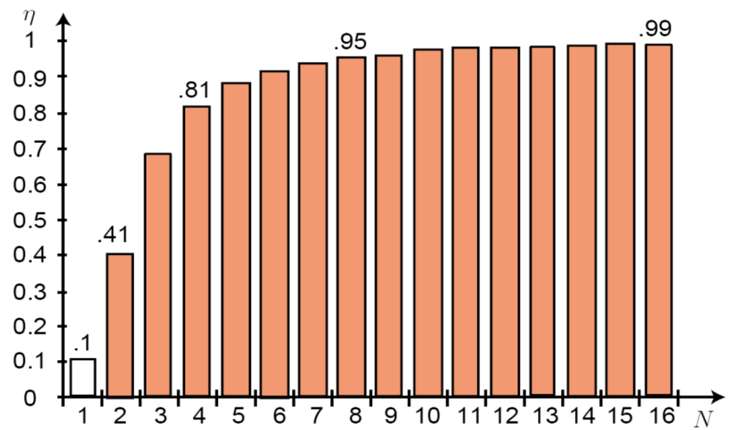

Diffractive lenses

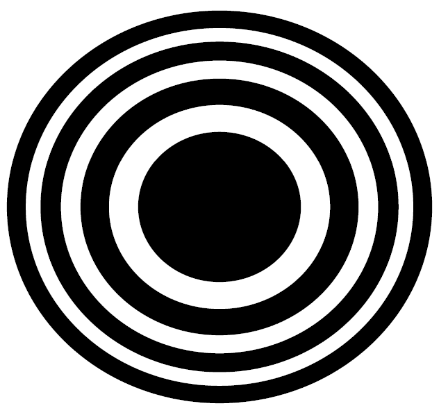

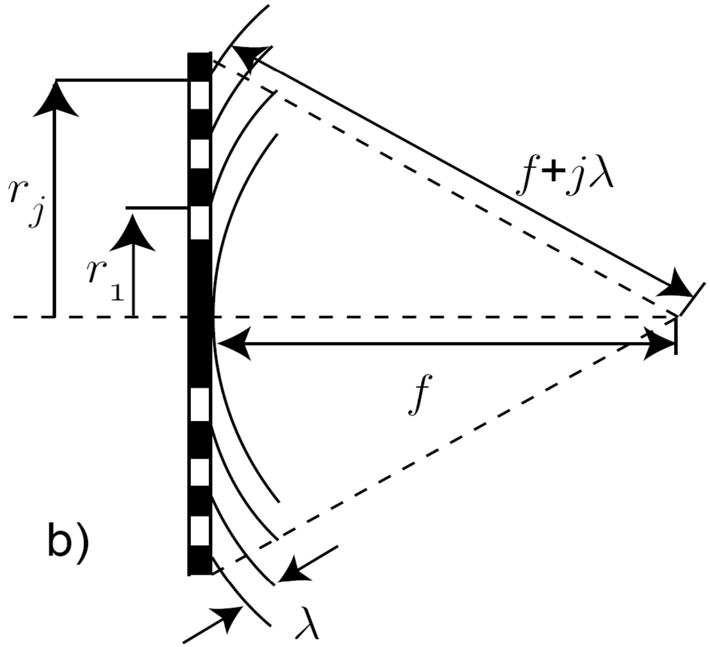

$$f \cong \frac{r_1^2}{2\lambda}$$

multiple beam splitters;

imaging systems;

scaling of optical lenses;

microoptical systems integration;

hybrid integration.

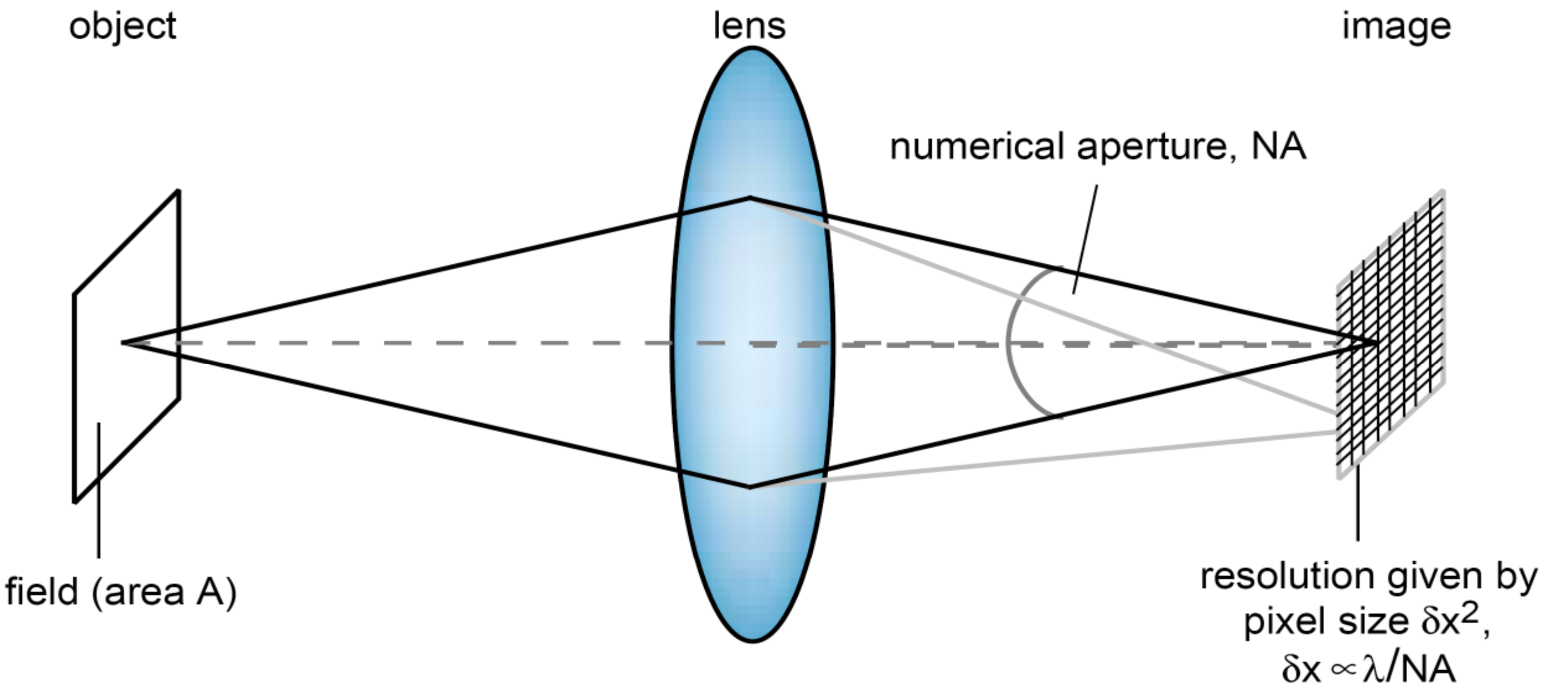

space-bandwidth product: $\mathrm{SBP} = \dfrac{\text{field area}}{\text{pixel area}} = \dfrac{A}{\delta x^2}$

Scaling behaviour of lenses

Photographic scaling:

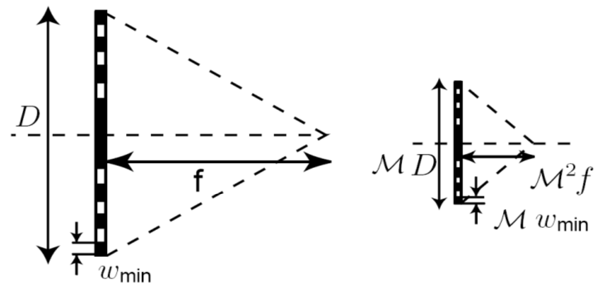

Microscopic scaling:

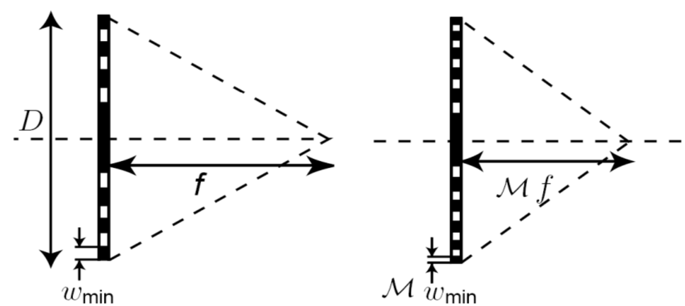

Constant f/# scaling:

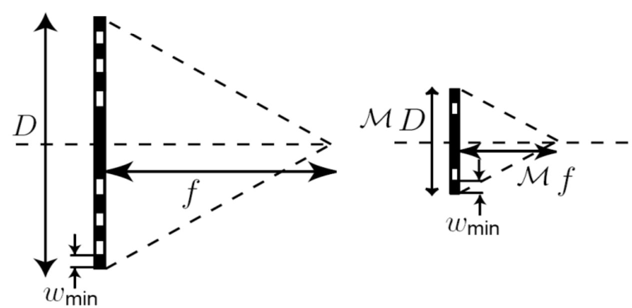

Constant f / # - Scaling

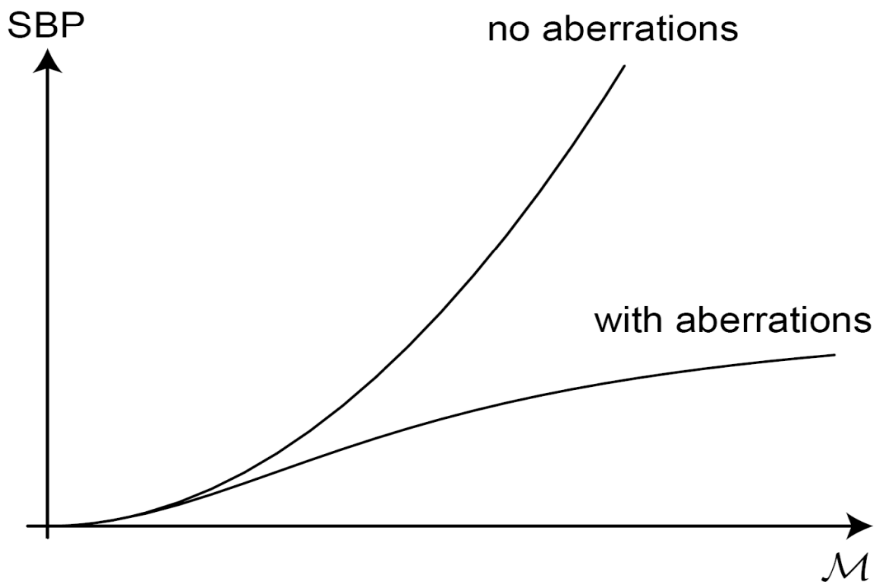

Imaging setups

conventional imaging

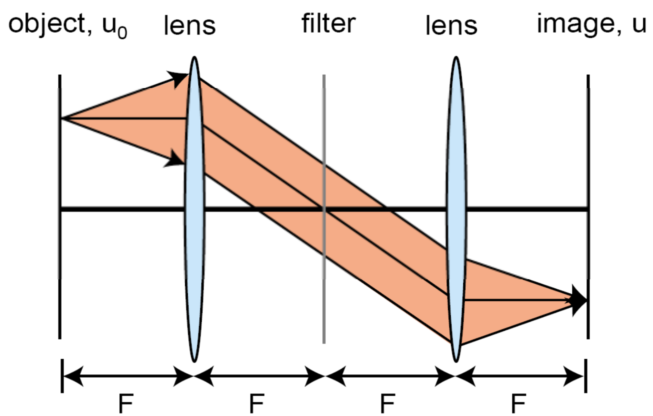

array imaging

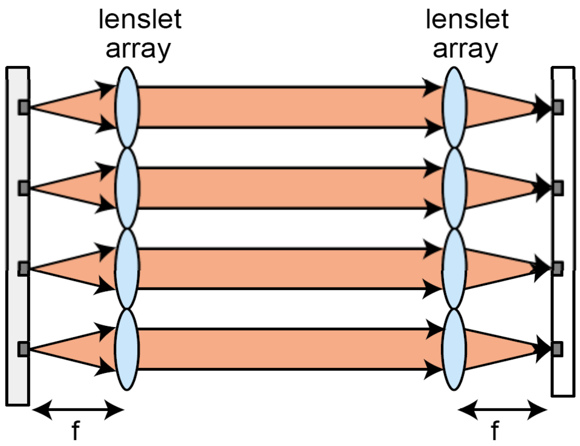

confocal imaging

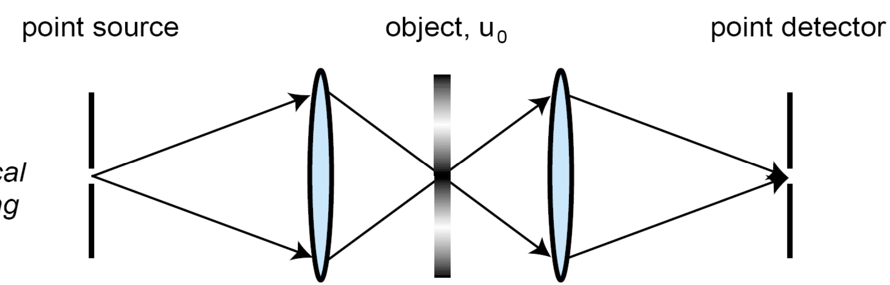

Array optics : imaging of discrete objects

optoelectronic devices

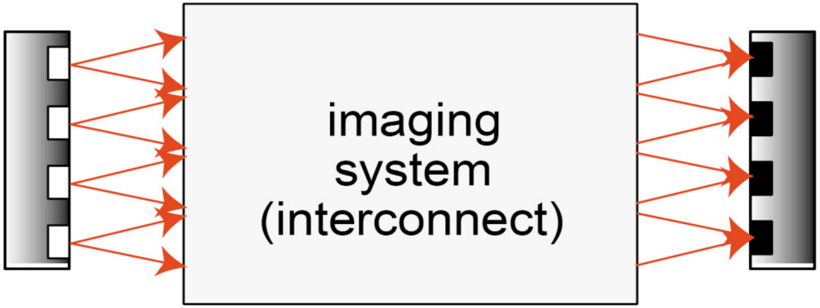

emitter/detector arrays

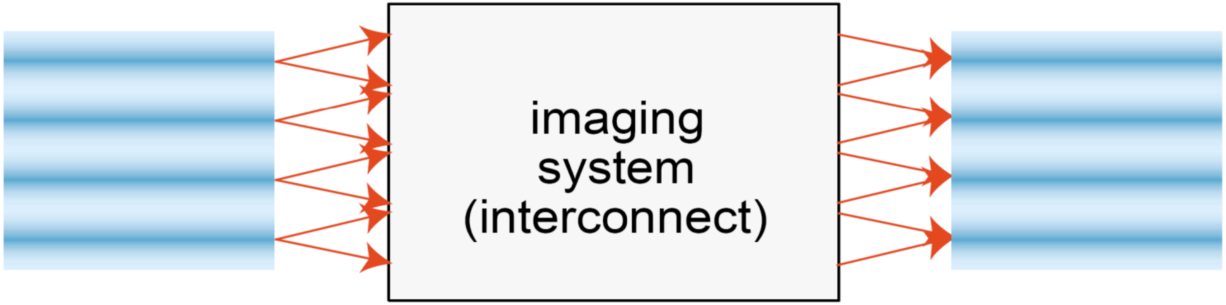

fiber bundles

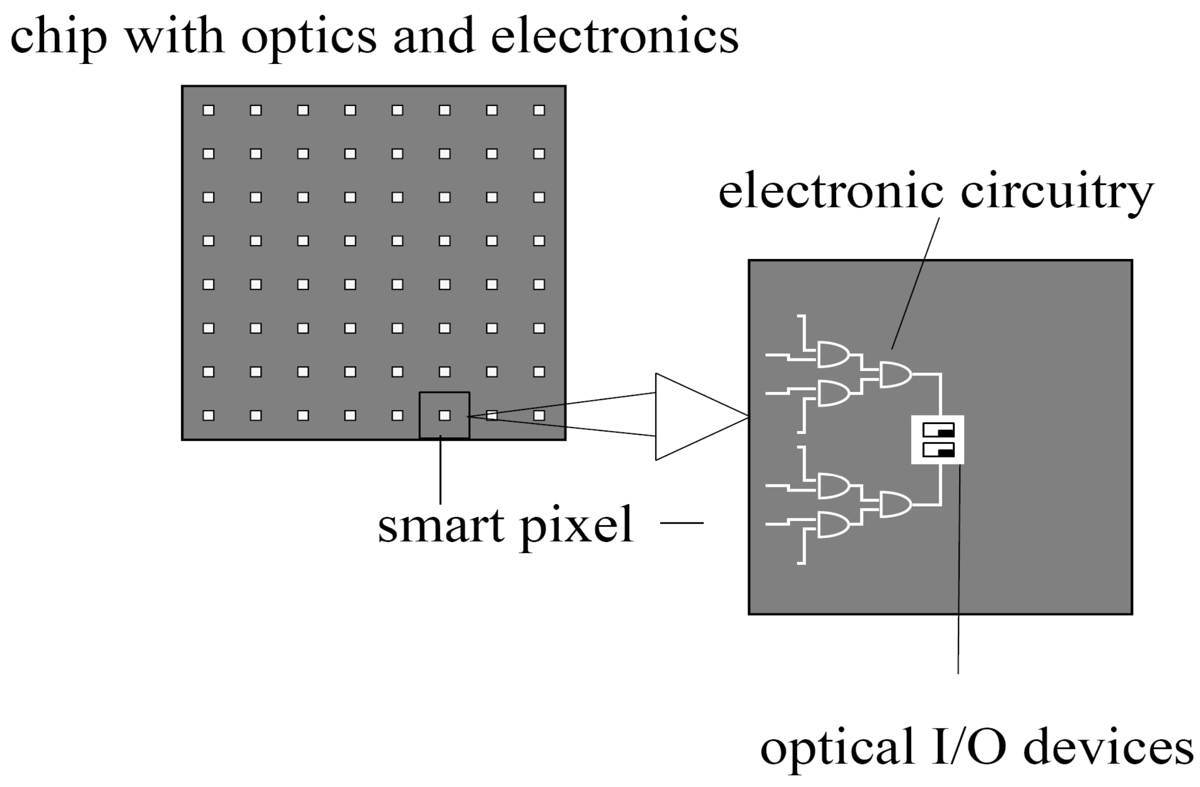
chip with optics and electronics
electronic circuitry
smart pixel
optical I/O devices

micro-optomechanics;

stacked optics;

planar optics

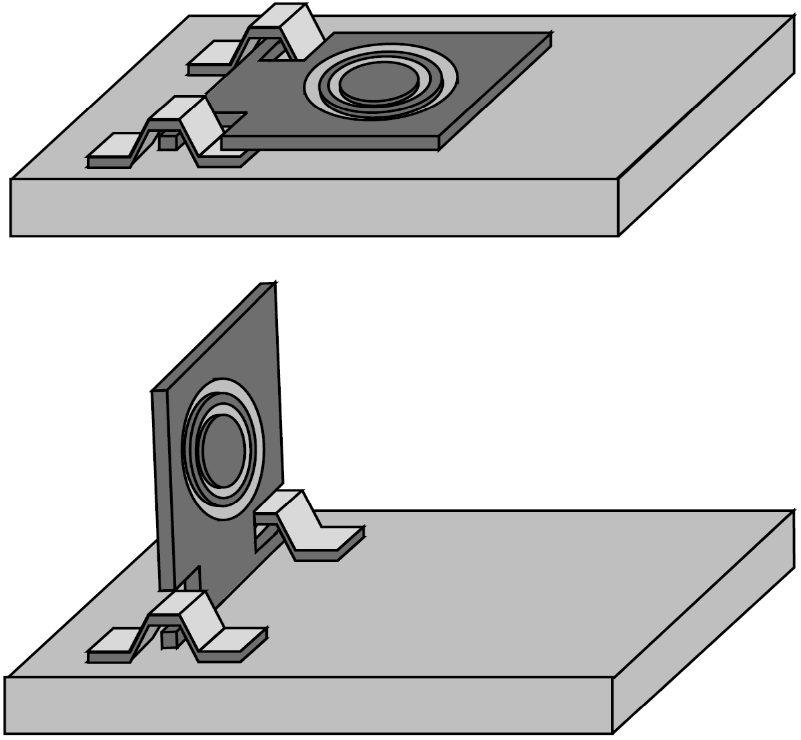

a)

b)

Micromechanical switches for fibre optics

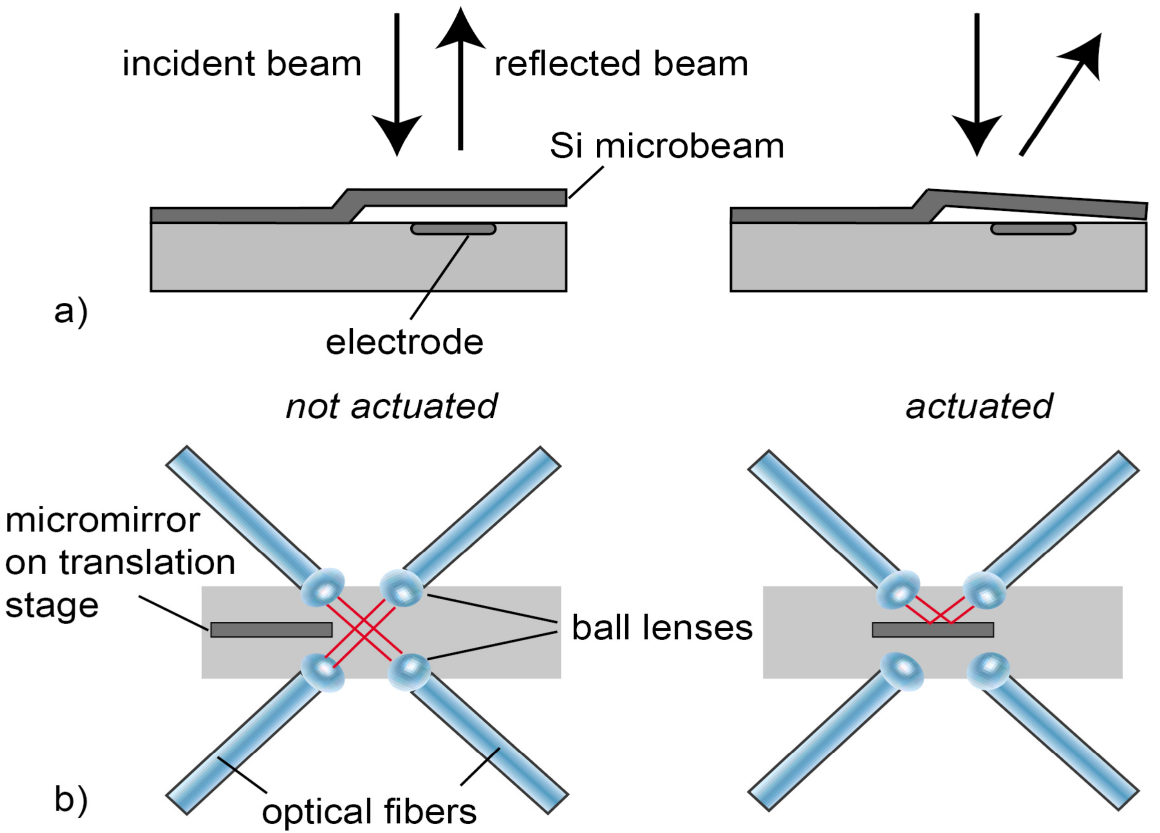

Examples of the micromechanical optical bench **optoelectronic devices**

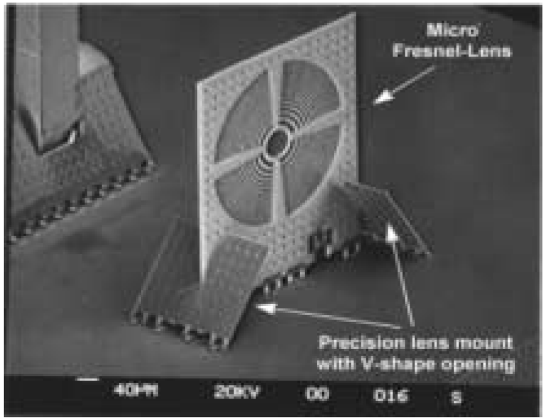

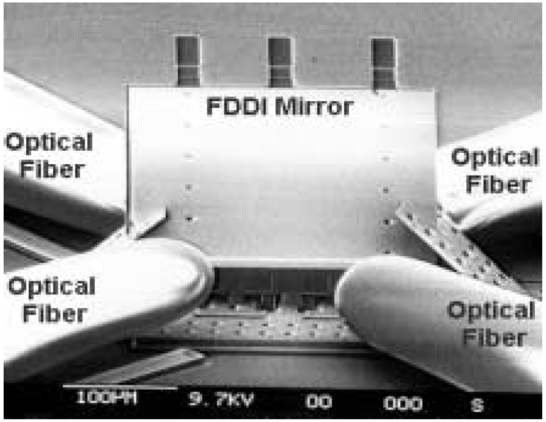

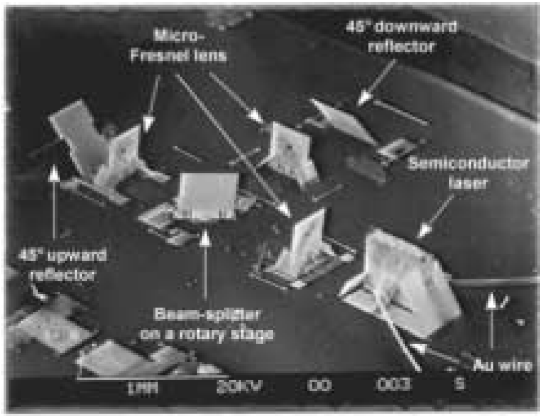

M. C. Wu, Proc. IEEE, **85** (1997), 1833.

Stacked micro optics

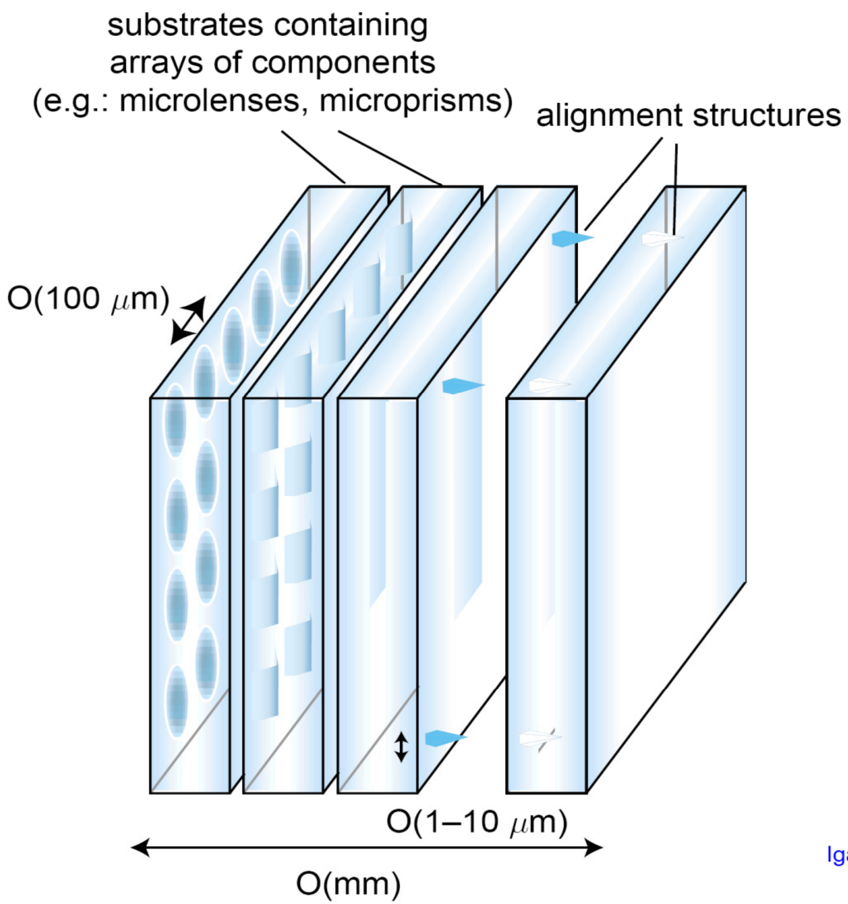

Iga et al., Appl. Opt. 1982

Planar integrated free – space optics

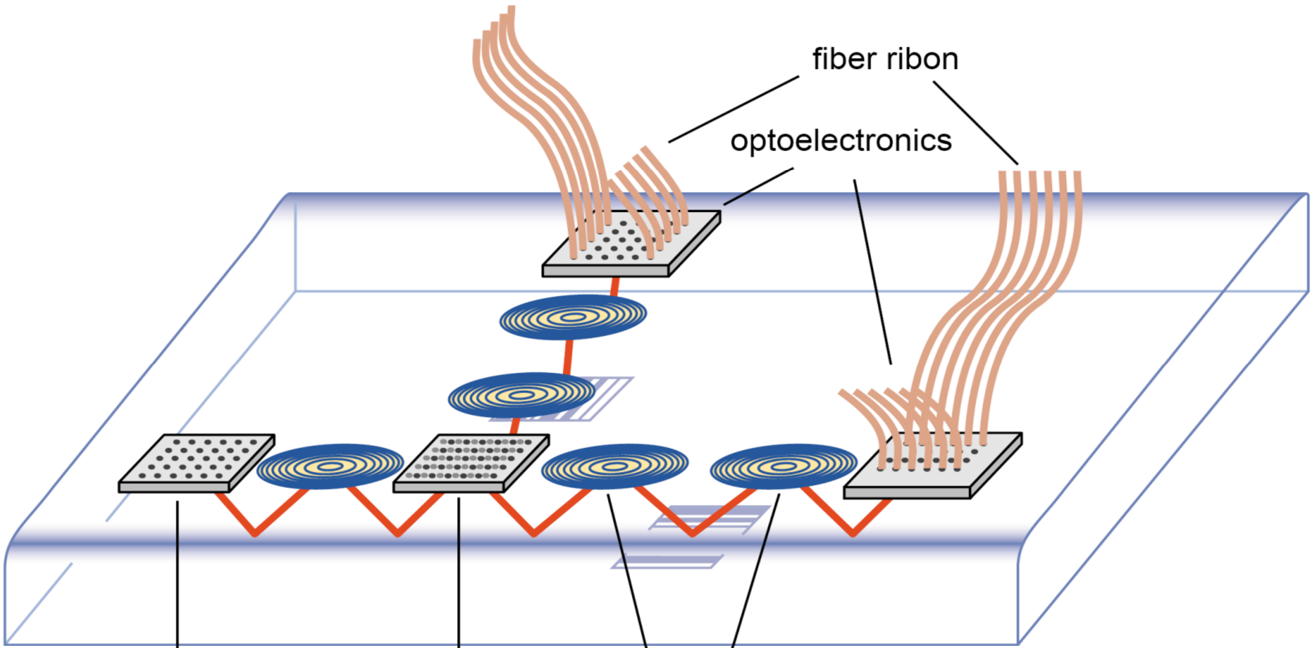

Jahns, Huang, Appl. Opt. 1989
Gruber, Sinzinger, Jahns, Appl. Opt. 2000

Planar optics: general considerations

CONVENTIONAL OPTOMECHANICS

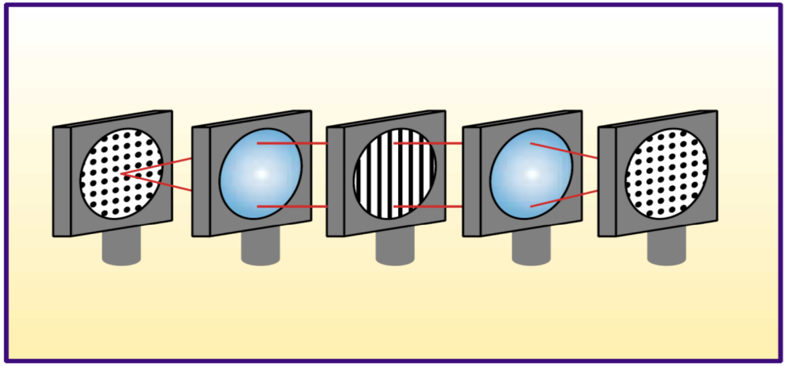

• discrete components
• 3-D layout
• bulky
• alignment-critical

PLANAR INTEGRATED OPTICS

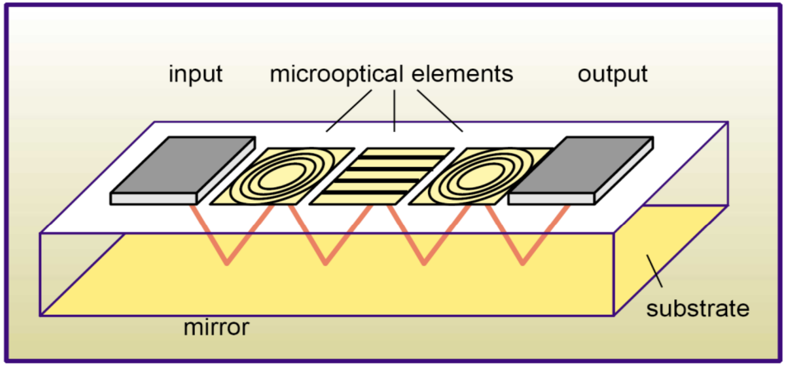

• no optomechanics
• 2-D layout
• lithographic precision
• monolithic integration of passive optics
• hybrid integration with optoelectronics
• surface-mounting
• stable, rugged, small

optoelectronic devices

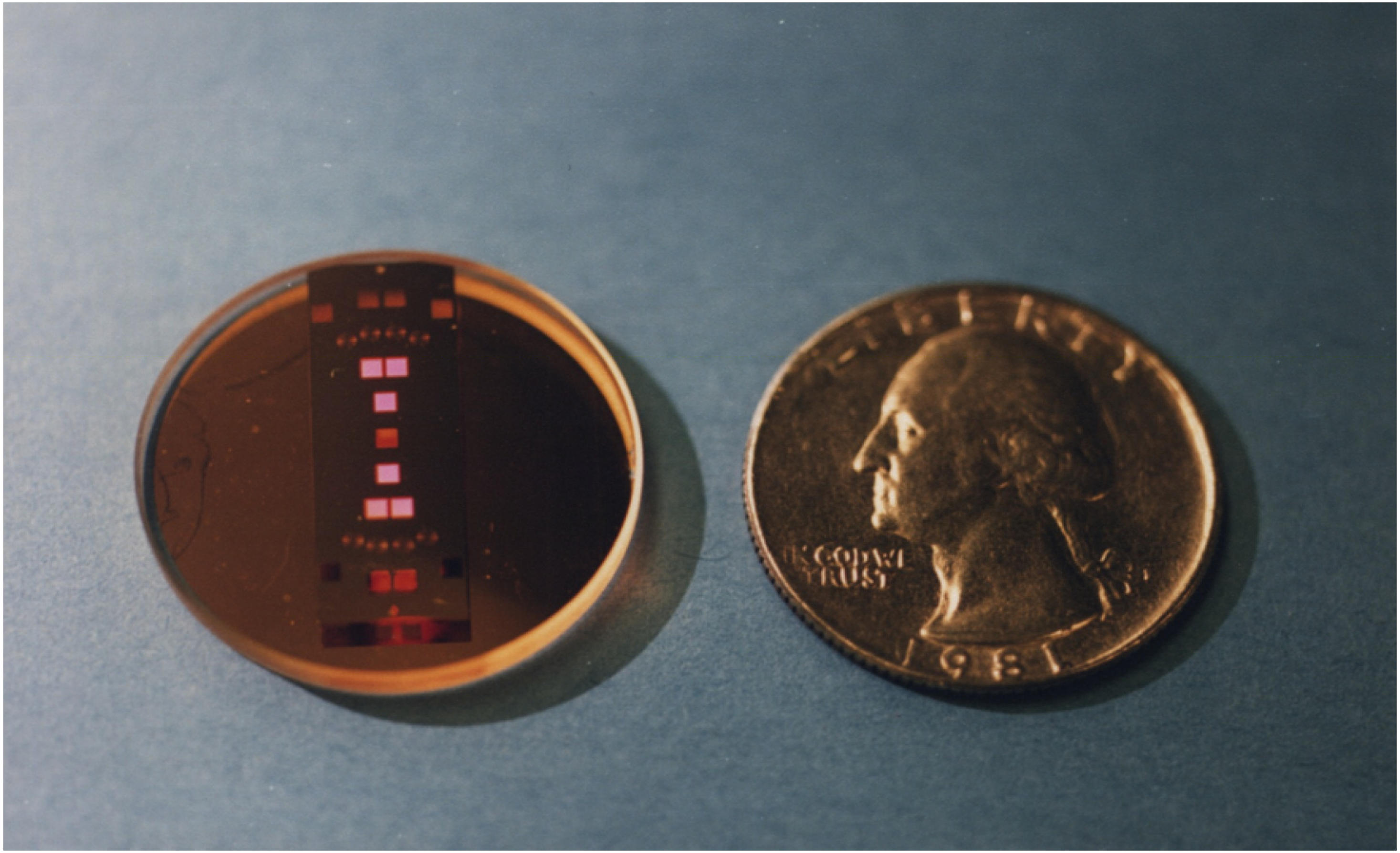

Integrated hybrid imaging setup

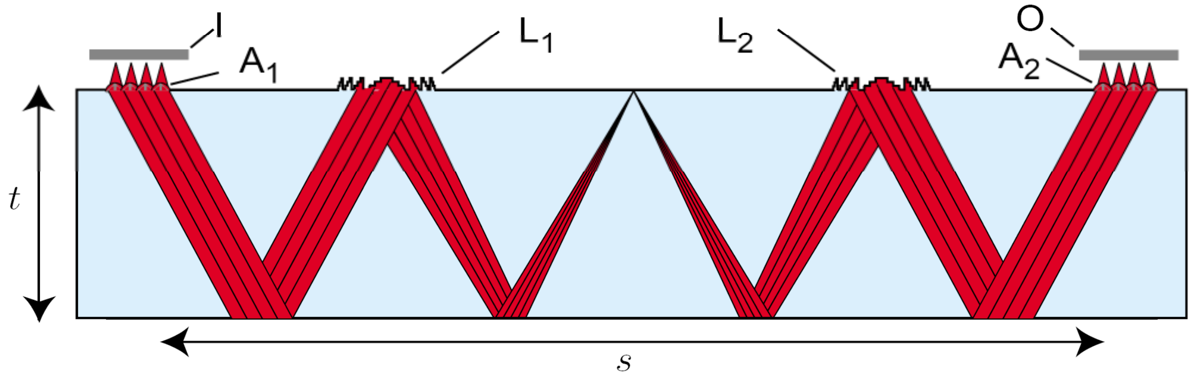

a)

b)

32x32 channels in 1.6mmx1.6mm
Jahns, Acklin, Opt. Lett. 1994

Hybrid integration with input / output devices

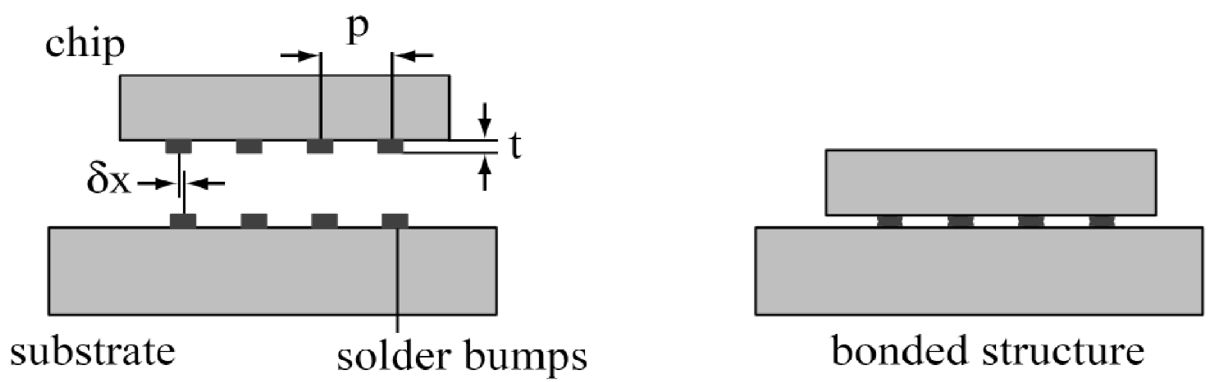

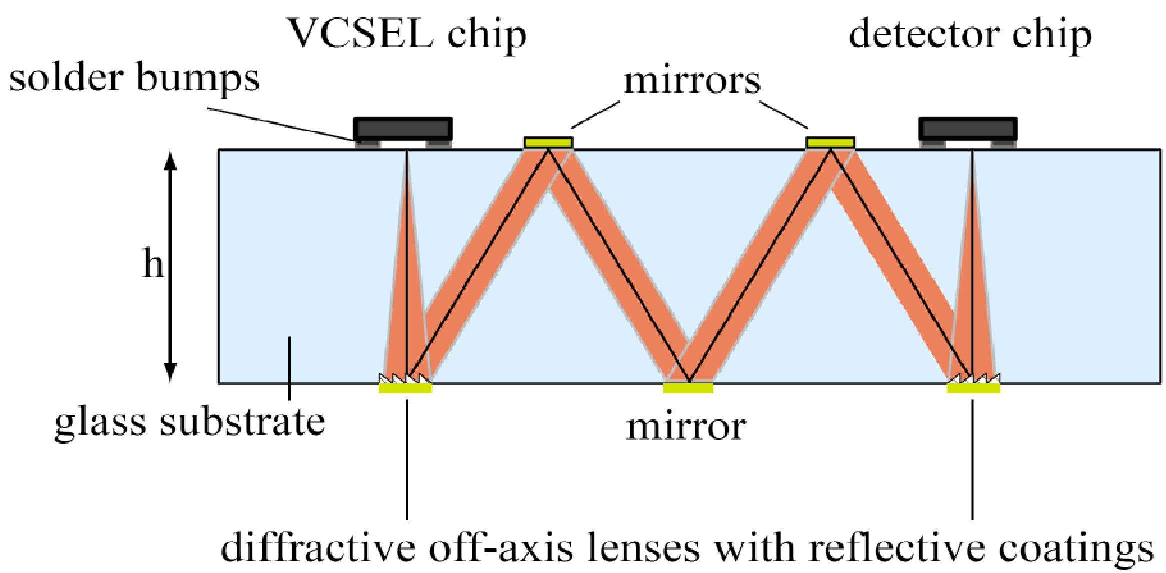

optical interconnects

optical data storage

optical sensors

microlens lithography

laser beam shaping

laser beam relaying

beam steering

Optics as an interconnection technology

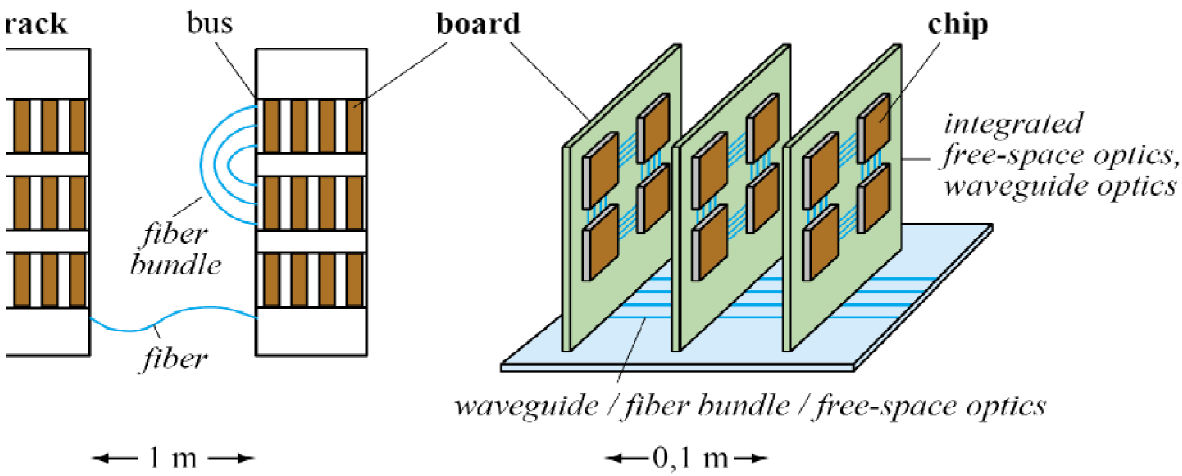

3D-Topology of free-space optics

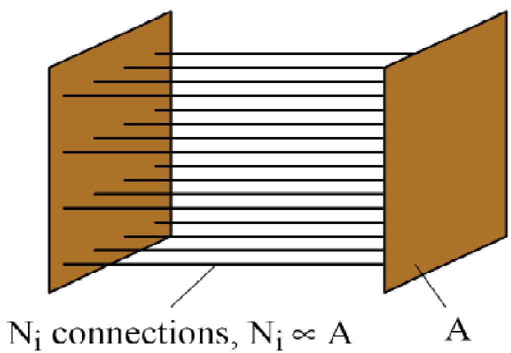

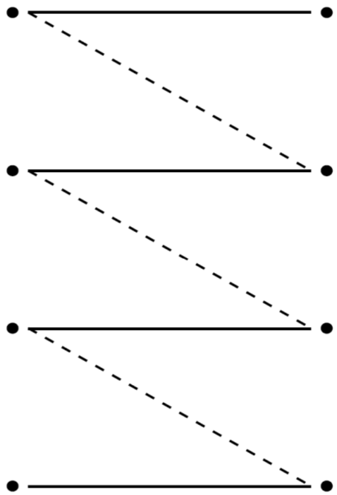

"imaging"

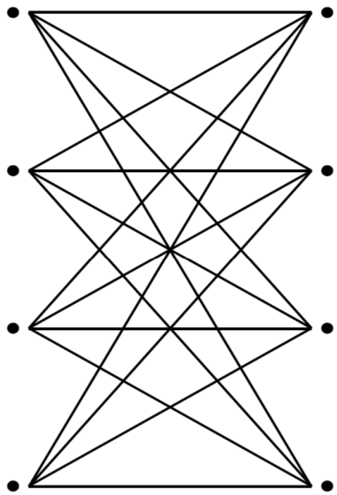

"cross-connection"

Micro optical correlator for kinegram verification

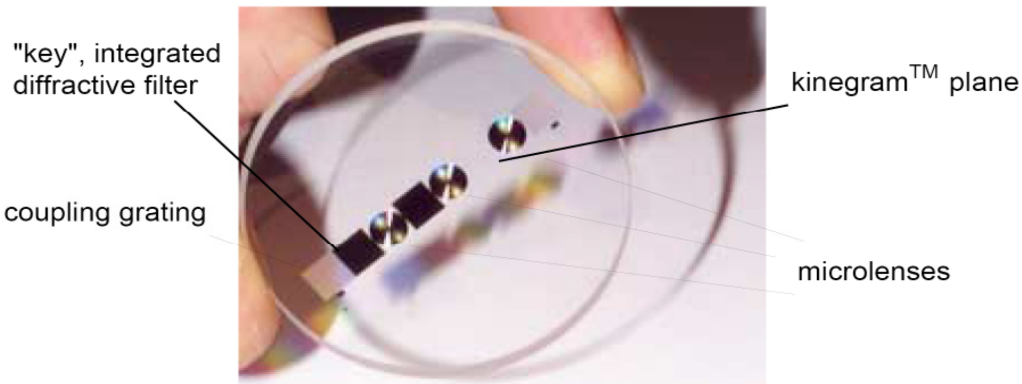

Implemented filters: Fourier plane

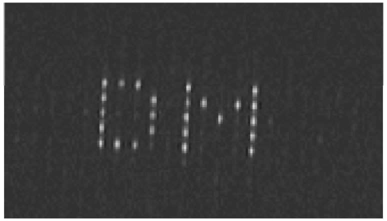

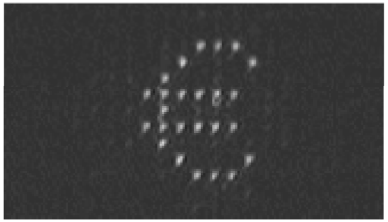

Correlation

Crosscorrelation

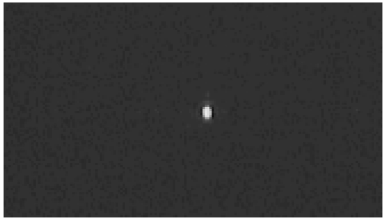

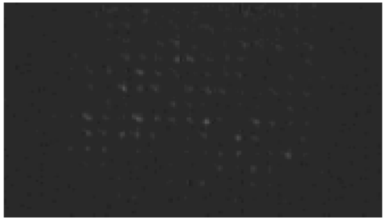

Implementations of interconnection networks

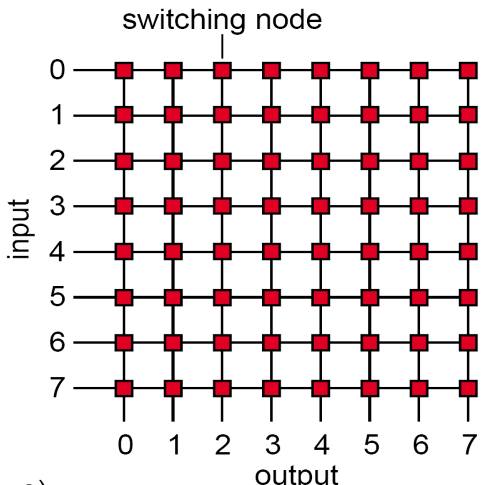

a)

crossbar interconnect

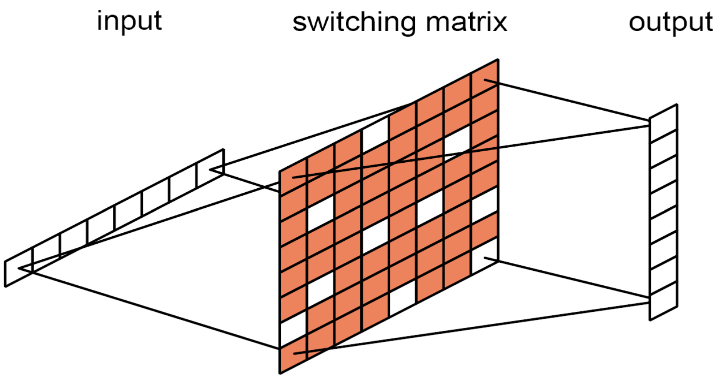

b)

vector-matrix multiplier

Optical realisation of a crossbar switch

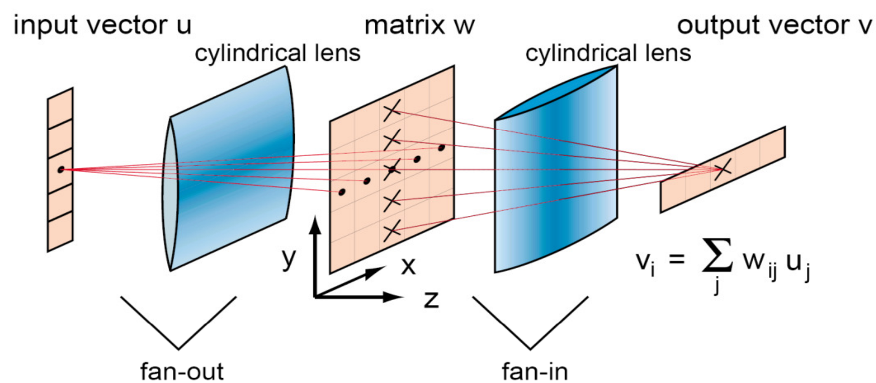

planar integrated system

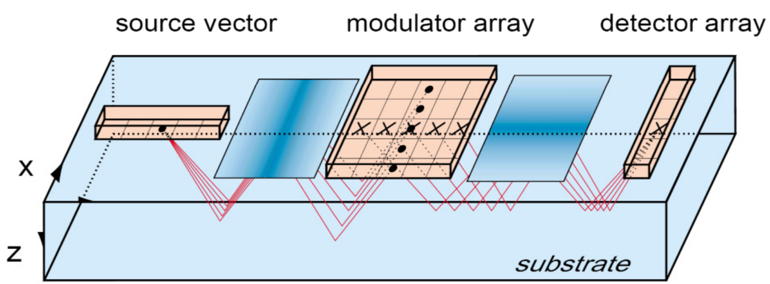

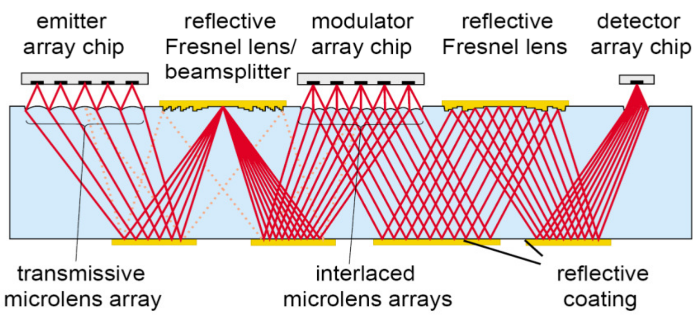

Micro optical realisation of a crossbar switch

fan-out

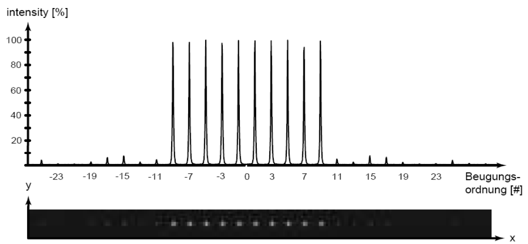

signals in the plane of the matrix

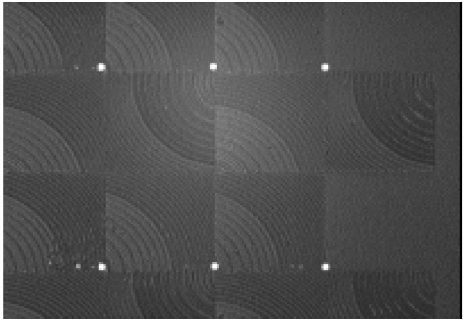

fan- in

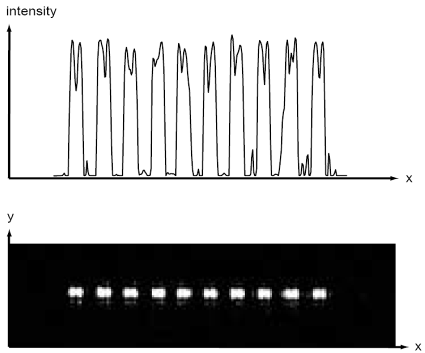

photograph of the integrated system

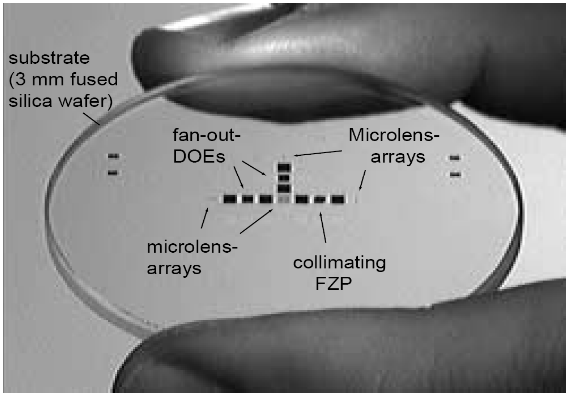

Gruber, Jahns, Sinzinger, Appl. Opt.39 (2000) 5367.

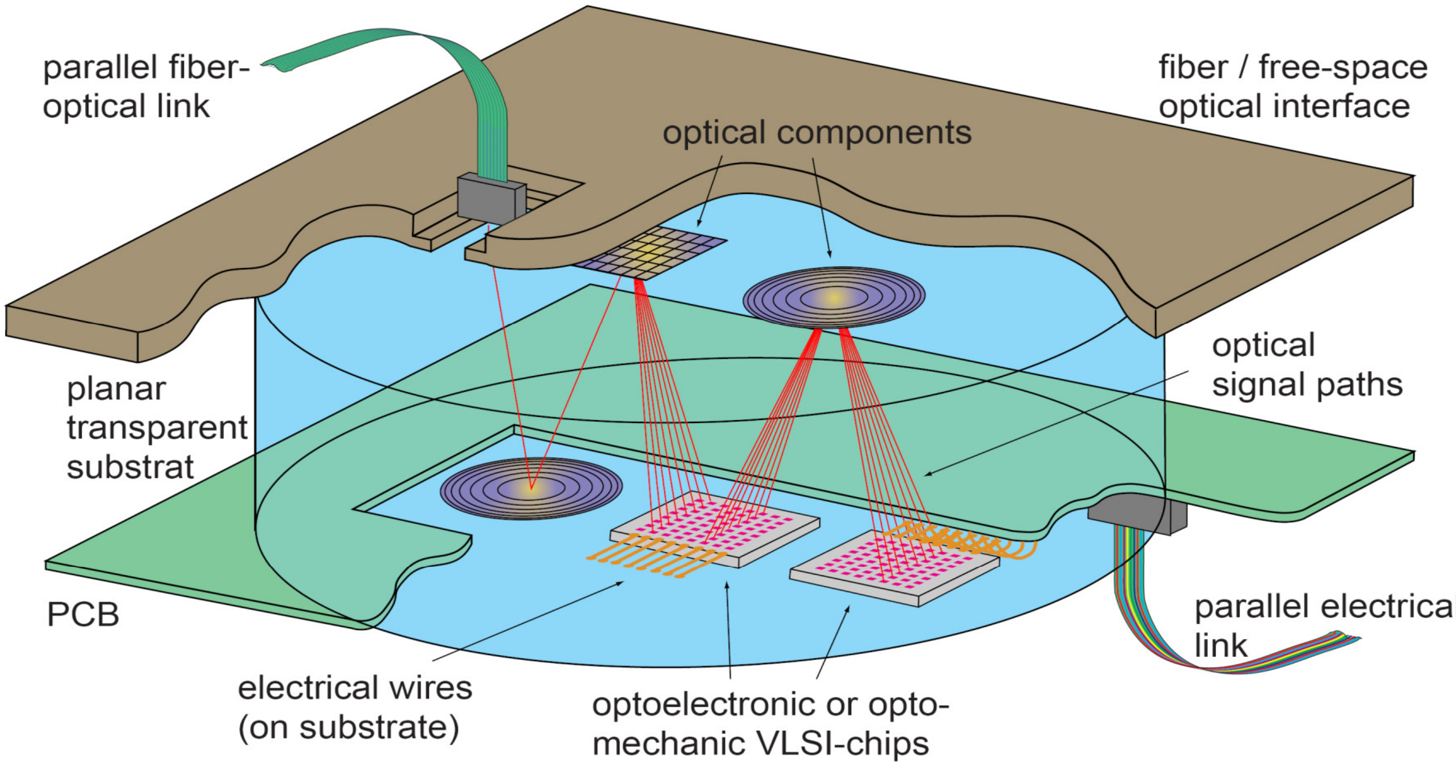
parallel fiber-optical link
fiber / free-space optical interface
optical components
planar transparent substrat
optical signal paths
PCB
parallel electrical link
electrical wires (on substrate)
optoelectronic or opto-mechanic VLSI-chips

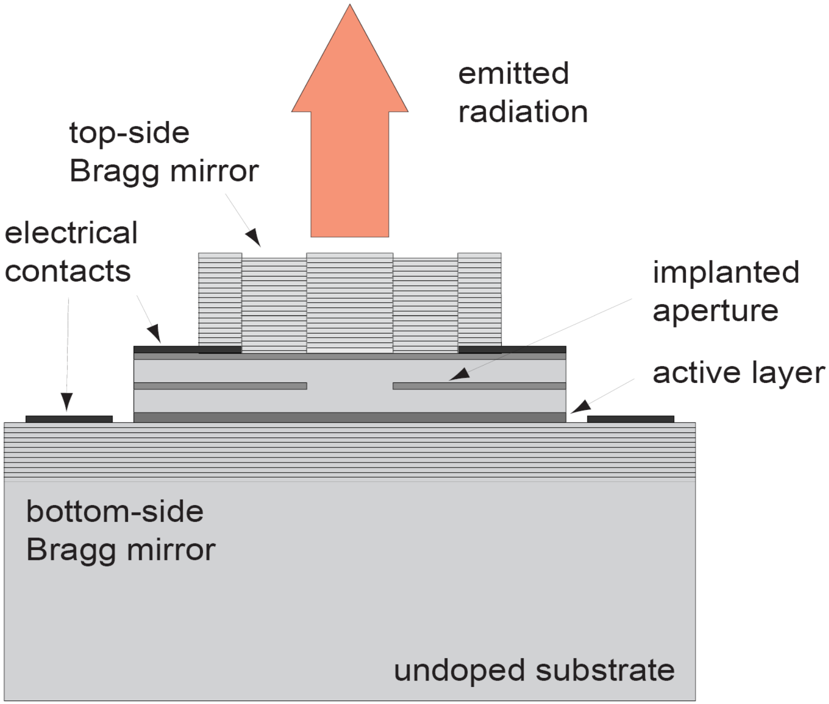

VCSEL: schematic setup

Advantages over edge emitting LD's:

- lower threshold current
- lower power consumption
- higher modulation bandwidth
- good control over characteristics of emitted radiation (wavelength, longitudinal / transversal modes)
- favorable beam characteristics

Favorable properties of VCSEL for planar systems **optoelectronic devices**

- perpendicular emission of light

- small (lateral) size

- perfectly matches 3-D approach of planar integrated systems

- high packaging densities possible (array pitch of 50 µm already achievable now)

Example: CO-OP foundry run

OE-VLSI chips with 2-D array layout

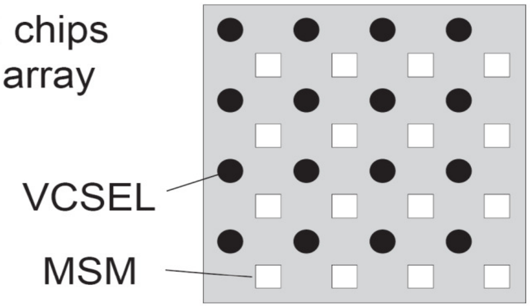

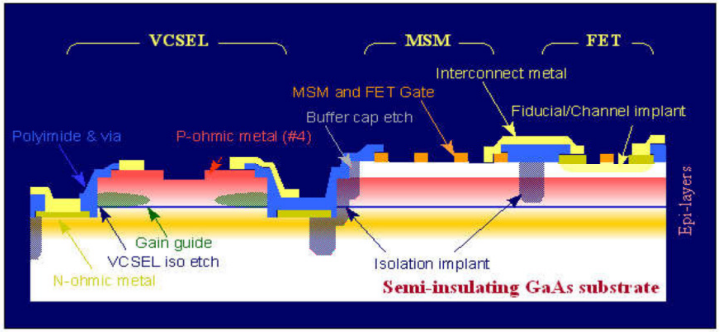

source: http://co-op.gmu.edu

Ultra-thin silicon-on-sapphire CMOS technology — optoelectronic devices

Example: 12 x 1 VCSEL array flip-chip bonded to UTSi-CMOS-chip

view of VCSEL array through sapphire

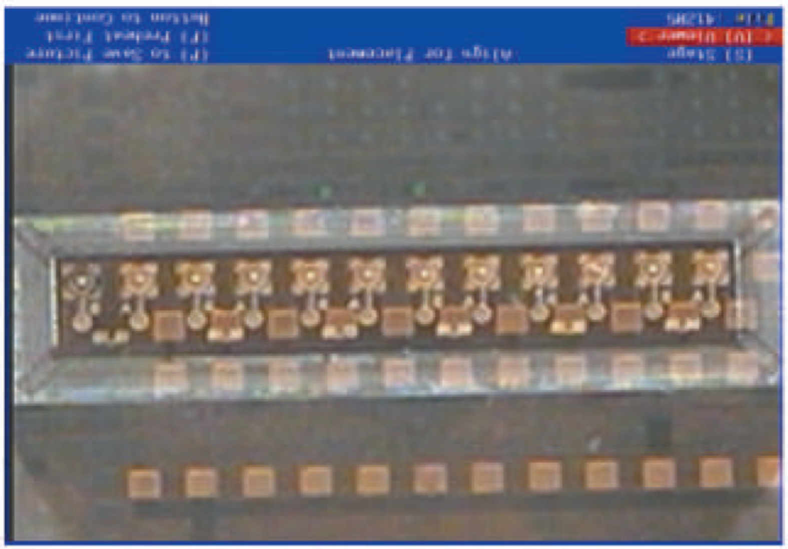

close-up

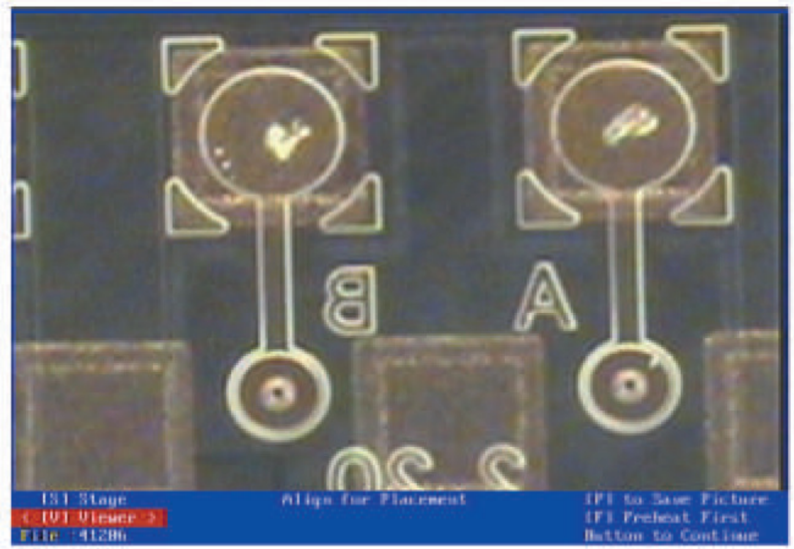

source: Peregrine Semiconductor Corp.
http://www.peregrine-semi.com

- Can be a building block for MOEMS
- Optimally supplements and supports current trends in VLSI
- Is well suited for massively parallel interconnections
- ... *and many other applications!*